UNIVERSITÁ POLITECNICA DELLE MARCHE

DOCTOR OF PHILOSOPHY IN

"BIOMEDICAL SCIENCES"

Coordinator: Prof. Andrea Giacometti

Chemopreventive effects of Manuka and Strawberry tree honey on human colon cancer HCT-116 and LoVo cells: a focus on molecular targets

Ph. D. dissertation by
Sadia Afrin, B.Sc., M.Sc.

Supervisor: Prof. Maurizio Battino

Co-supervisor: Dr. Francesca Giampieri

XXX Triennial Academic Cycle 2014-2017

To my beloved parents & my husband

TABLE OF CONTENTS

ABSTRACT

Despite the major advances in colon cancer treatment, including postoperative care, recurrence and mortality rates remain high; hence the urgent need to complement the current therapies. Numerous investigations have been made on plant bioactive compounds and colon cancer prevention in the recent decades. Honey is a natural food product known to modulate several biological activities including cancer. The main objective of the present work was to evaluate the anticancer potential of Manuka and Strawberry tree honey on *in vitro* colon cancer models targeting different molecular aspects.

Manuka and Strawberry tree were used for phytochemical characterization and total antioxidant capacity. The phenolic compounds were indentified and quantified by HPLC assay. The growth inhibitory effects of Manuka and Strawberry tree honey on human colon adenocarcinoma cells (HCT-116) and Dukes' type C, grade IV, colon metastasis cells (LoVo) were observed by cell viability, cell cycle, apoptosis and intracellular reactive oxygen species (ROS) production assay. The oxidative stress were assessed through the determination of lipid peroxidation, protein carbonyl content and DNA damage, as well as the antioxidant enzyme activities on cells lysates. The expression of proteins related to inflammation, apoptotic, endoplasmic reticulum (ER) stress and EGFR signalling was determined by western blotting. Bioenergetic characterization was evaluated by observing several parameters of mitochondrial respiration (oxygen consumption rate) and glycolysis (extracellular acidification rate) in both cell lines. Anti-metastasis effects were observed through migration and colony formation assay, and the expression of invasion, epithelial mesenchymal transition (EMT) and metastasis markers were observed by western blotting. Finally, the synergistic or addictive effects of Manuka and Strawberry tree honey on 5-fluorouracil (5-FU) chemotherapy were evaluated in both colon cancer cell lines.

Manuka and Strawberry tree honey represent a good source of phenolic compounds, flavonoids and antioxidant capacity. Both types of honey exhibited profound inhibitory effects on the growth of human colon cancer cells, without showing any toxic effect on normal non-cancer cells. At different concentrations, a strong induction of cell cycle arrest, apoptosis and oxidative stress was observed after the treatments since they increased the accumulation of ROS and elevated the damage of protein, lipid and DNA of the HCT-116 and LoVo cells. Anti-inflammatory effects were observed through the suppression of NFκB, p-IκB-α and other pro-inflammatory cytokines expression, while the suppression of p-Akt indicated anti-proliferative effects; at the same time the increased levels of p-

p38MAPK and p-Erk1/2, after honey treatments, indicated the up-regulation of apoptosis rate. Furthermore, suppression of Nrf2 dependent antioxidant enzyme expression (superoxide dismutase (SOD), catalase and hemeoxygenase 1) and the activity of catalase, SOD, glutathione peroxidase, reductase and transferase enzymes were observed in both cell lines after honey treatments. The ER stress was also inducted, as suggested by the elevation of ATF6 and XBP1 protein expression. In HCT-116 and LoVo cells, both honeys decreased mitochondrial function that is correlated with cell survival potential and concurrently, decreased the extracellular acidification rate (glycolysis). Moreover, the expressions of p-AMPK/AMPK, PGC1α and SIRT1 were suppressed after the treatments which were involved in the survival of HCT-116 and LoVo cells under metabolic stress condition. In addition, the migration and colony formation abilities were reduced, as well as the invasion abilities were suppressed by both types of honey through the expression of matrix metallo-proteinases (MMPs). Expressions of EMT markers, such as E-, N-cadherin and β-catenin and tumor metastasis promoting factor CXCR4 and NF-κB, were also down-regulated by Manuka and Strawberry tree honey treatments.

Both honey varieties potentiate the anticancer effects of 5-FU chemotherapy on human colon cancer cells at less concentration compared to single dose of 5-FU. In the presence of Manuka or Strawberry tree honey, 5-FU induced synergistic effects by suppressing the expression of inflammation markers, EGFR pathways and antioxidant enzyme activities, while it increased MAPK pathway and ROS production at less concentration of 5-FU alone compared to IC_{50} values. Moreover, additive effects were observed by arresting cell cycle and increasing lipid peroxidation, protein carbonyl content and ER stress. All the parameters of mitochondrial respiration and glycolysis function were decreased in a similar way after all the treatments, while the expression of AMPK pathway was suppressed more after the combination treatments compared to single doses of 5-FU. In addition, anti-metastasis effects of 5-FU also increased when it was combined with Manuka and Strawberry tree honey by decreasing the migration ability, as well as suppressing the expression of MMP-2, MMP-9, E-cadherin, NFκB and CXCR4 proteins.

The above findings indicate that Manuka and Strawberry tree honey induce growth inhibitory effects of HCT-116 and LoVo cells, while the anticancer potential of 5-FU chemotherapy is enhance in the presence of both honey varieties at less doses. These preliminary results are interesting and suggest a potential chemopreventive action which

could be useful for further studies in order to develop chemopreventive agents for colon cancer treatment.

ITALIAN SUMMARY

Il cancro al colon rappresenta una delle principali cause di morbosità e mortalità per neoplasia in tutti i Paesi occidentali. Nonostante i numerosi progressi ottenuti nei trattamenti pre- e postoperatori, i tassi di recidiva rimangono ancora elevati; da qui l'urgente necessità di integrare le attuali terapie convenzionali. Negli ultimi decenni numerose ricerche hanno valutato l'effetto dei composti bioattivi naturali nella prevenzione del cancro del colon. In questo contesto, il miele rappresenta un prodotto alimentare naturale noto per modulare diverse attività biologiche e prevenire alcune patologie, tra cui il cancro. L'obiettivo principale del presente lavoro è stato valutare *in vitro* il potenziale antitumorale del miele di Manuka e del miele di corbezzolo su due diversi modelli cellulari di cancro al colon, che differiscono tra loro per l'espressione di alcuni geni di metastatizzazione.

I due mieli sono stati analizzati per determinare la composizione fitochimica, mediante analisi di HPLC, e la capacità totale antiossidante. Gli effetti antitumorali esercitati dal miele di Manuka e di corbezzolo sono stati valutati indue linee di adenocarcinoma del colon (HCT-116 e LoVo), attraverso la determinazione della vitalità cellulare, del tasso di apoptosi e dei livelli intracellulari di specie reattive dell' ossigeno (ROS). Lo stress ossidativo è stato misurato mediante la determinazione della perossidazione lipidica, del contenuto di gruppi carbonili e del danno del DNA, nonché mediante la valutazione delle attività degli enzimi antiossidanti nei lisati cellulari. I livelli di espressione delle proteine correlate all'infiammazione, all'apoptosi, allo stress del reticolo endoplasmatico (RE) e alla via molecolare dell' EGFR sono stati determinati attraverso saggi di Western blot. La caratterizzazione bioenergetica è stata analizzata valutando diversi parametri di respirazione mitocondriale (tasso di consumo di ossigeno) e glicolisi (velocità di acidificazione extracellulare) in entrambe le linee cellulari. Gli effetti anti-metastatici sono stati osservati attraverso il saggio di migrazione cellulare e di formazione delle colonie; l'espressione di marcatori di invasione, transizione mesenchimale epiteliale (EMT) e metastatizzazione è stata osservata mediante Western blot. Infine, sono stati analizzati gli effetti sinergici del miele di Manuka e di corbezzolo con il chemioterapico 5-fluorouracile (5-FU) in entrambe le linee cellulari.

I risultati hanno dimostrato che il miele di Manuka e di corbezzolo rappresentano una buona fonte di composti fenolici, flavonoidi e possiedono una notevole capacità antiossidante. Entrambi i tipi di miele hanno dimostrato profondi effetti inibitori sulla

crescita delle cellule tumorali, senza mostrare, al tempo stesso, alcun effetto tossico in cellule sane non cancerose. Nello specifico, dopo il trattamento con il miele, è stata evidenziata una forte induzione dell'arresto del ciclo cellulare, dell'apoptosi e dello stress ossidativo con un significativo aumento di ROS e del danno a carico di proteine, lipidi e DNA in entrambe le linee cellulari. Gli effetti antinfiammatori sono stati osservati attraverso la riduzione di NFκB, p-IκB-α e di altre citochine pro-infiammatorie, mentre la soppressione della proteina p-Akt ha evidenziato effetti antiproliferativi; allo stesso tempo, l'incremento dei livelli di p-p38MAPK e p-Erk1/2, dopo il trattamento con il miele, ha indicato l'induzione dell' apoptosi. Inoltre, è stata osservata la riduzione dell'espressione degli enzimi antiossidanti (superossido dismutasi (SOD), catalasi ed eme-ossigenasi 1) dipendenti da Nrf2, così come l'attività della catalasi, SOD, glutatione perossidasi, reduttasi e transferasi in entrambe le linee cellulari. Il trattamento con il miele ha indotto anche lo stress del RE, come suggerito dall'incremento dell' espressione di ATF6 e XBP1. E' stata evidenziata anche una riduzione della funzionalità mitocondriale, correlata con il potenziale di sopravvivenza cellulare, e, contemporaneamente, una diminuzione del tasso di glicolisi. Inoltre, il trattamento con il miele ha ridottoi livelli di espressione di p-AMPK/AMPK, PGC1α e SIRT1 coinvolte nella sopravvivenza delle cellule HCT-116 e LoVo in condizioni di stress metabolico. Inoltre, è stata evidenziata una diminuzione delle abilità di migrazione cellulare e di formazione delle colonie, cosi come delle capacità di invasione e metastatizzazione, come dimostrato dalla riduzione dell'espressione delle metallo-proteinasi, delle E-, N-caderine, delle β-catenine e di CXCR4 e NF-κB.

Infine, è stato riscontrato che entrambe le varietà di miele sono in grado di potenziare gli effetti antitumorali del chemioterapico 5-FU. In presenza dei mieli, infatti, il 5-FU ha soppresso l'espressione dei marcatori di infiammazione, dell' EGFR e le attività degli enzimi antiossidanti, mentre ha stimolato le MAPK e la produzione di ROS, ad una concentrazione minore rispetto a quando utilizzato da solo. Inoltre, sono stati osservati effetti additivi nell'arresto del ciclo cellulare e nell'induzione della perossidazione dei lipidi, nel contenuto di carbonili e nello stress del RE. Il trattamento combinato ha inoltre ridotto tutti i parametri di funzionalità mitocondriale e glicolitica e l'espressione delle proteine coinvolte nella via dell' AMPK, delle MMP-2, MMP-9, E-cadherina, NFκB e CXCR4 .

Questi risultati indicano che il miele di Manuka e di corbezzolo sono in grado di esercitare effetti inibitori sulla crescita delle cellule HCT-116 e LoVo ed effetti sinergici con il

chemioterapico 5-FU; queste interessanti scoperte, sebbene preliminari, suggeriscono una potenziale azione chemiopreventiva che potrebbe risultare utile per sviluppare agenti chemiopreventivi per il trattamento del cancro al colon.

LIST OF ABREVIATIONS

A

Annexin binding buffer, ABB; 2,2′-azino-bis(3-ethylbenzothiazoline-6-sulfonic acid), ABTS; acetyl-CoA carboxylases, ACC; ACF, aberrant crypt foci; activate metalloproteases in the disintegrin and metalloprotease, ADAM; artificial honey, AH; Akt, protein kinase B; adenosine monophosphate, AMP; AMP-activated protein kinase, AMPK; *adenomatous polyposis coli*, APC; activator protein-1, AP-1; antioxidant response element, ARE; apoptosis signal-regulating kinase , ASK; activating transcription factor, ATF; American type culture collection, ATCC.

B

B-cell lymphoma 2 associated death promoter, Bad; B-cell lymphoma 2 associated X protein, Bax; B-cell lymphoma, Bcl; B rapidly accelerated fibrosarcoma, BRAF; bovine serum albumin, BSA.

C

(+)-catechin equivalents, CAE; complementary and alternative medicine, CAM; cyclin-dependent kinase inhibitor 2A, CDKN2A; 1-chloro-2,4-dinitro benzene, CDNB; caudal type homeobox transcription factor 2, CDX2; CCAAT-enhancer-binding protein homologous protein, CHOP; combination index, CI; CpG island methylator phenotype, CIMP; chromosomal instability, CIN; cyclooxygenase 2, COX-2; colorectal cancer, CRC; C-X-C chemokine receptor type 4, CXCR4.

D

Diode array detector, DAD; 2-Deoxy-D-glucose, 2-DG; DNA methyltransferase 1, DNMT1; dinitrophenylhydrazine, DNPH; 2,4-dinitrophenol, 2,4-DNP; 2,2-diPhenyl-1-picrylhydrazyl, DPPH.

E

Eukaryotic translation initiation factor 4E-binding protein 1, 4E-BP1; extracellular acidification rate, ECAR; epidermal growth factor, EGF; epidermal growth factor receptor, EGFR; eukaryotic initiation factor 2 alpha, eIF2α; epithelial–mesenchymal transition, EMT; endoplasmic reticulum, ER; extracellular-signal-regulated kinase 1/2, Erk 1/2.

F

Familial adenomatous polyposis, FAP; first apoptosis signal, FAS; cellular Fos proto-oncogene, c-Fos; ferric reducing antioxidant power, FRAP; 5-fluorouracil, 5-FU.

G

Glyceraldehyde-3-phosphate dehydrogenase, GADPH; gallic acid equivalents, GAE; guanosine diphosphate, GDP; G-protein-coupled receptors, GPCRs; glutathione peroxidase, GPx; glutathione reductase, GR; glucose-regulated protein-78, GRP-78; glycogen synthase kinase 3-β, GSK-3β; glutathione transferase, GST; guanosine triphosphate, GTP.

H

Human dermal fibroblast, HDF; human epidermal growth factor receptor, HER; hairy-enhancer-of-split, Hes; helicase like transcription factor, HLTF; hereditary non-polyposis colorectal cancer, HNPCC; hemeoxygenase 1, HO-1; high-performance liquid chromatography, HPLC; harvey rat sarcoma viral oncogene homolog, HRAS.

I

Inflammatory bowel disease, IBD; 50% inhibitory concentration, IC_{50}; insulin-like growth factor-binding protein 7, IGFBP7; inhibitor of kappa B, IκB; interleukin, IL; inducible nitric oxide synthase, iNOS; inositol requiring kinase-1, IRE-1; integrin alpha-4 precursor, ITGA4.

J

Jun N-terminal kinase, JNK; Jun, Jun proto-oncogene.

K

Kirsten rat sarcoma virus oncogene homolog, KRAS.

L

L-Leucine equivalents, LE; lymphoid enhancer factor, LEF; liver kinase B1, LKB1.

M

Mitogen-activated protein kinase, MAPK; mitogen-activated protein kinase kinase, MAPKK; mitogen-activated protein kinase-activated protein kinase, MAPKAPK; malondialdehyde, MDA; myocyte enhancer factor-2, MEF2; O^6-methylguanine DNA methyltransferase, MGMT; Manuka honey, MH; MutL Homolog, MLH; mismatch repair, MMR; matrix metalloproteinases, MMP; mitogen-activated protein kinase interacting protein kinase, MNK; maximal respiration rate, MRC; MutS homologs, MSH; mitogen- and stress-activated protein kinase, MSK; microsatellite instability, MSI; 3-(4,5-Dimethyl-2-thiazolyl)-2,5-diphenyl-2H-tetrazolium bromide, MTT; mammalian target of rapamycin complex 1, mTORC1; Myc proto-oncogen, c-Myc.

N

Nicotinamide adenine dinucleotide phosphate, reduce form, NADPH; blue tetrazolium, NBT; nuclear factor kappa B, NFκB; Notch intracellular domain, NICD; nuclear related factor 2, Nrf2.

O

Oxygen consumption rate, OCR; 8-Oxoguanine DNA glycosylase, OGG1; oxidative phosphorylation, OXPHOS.

P

Poly (ADP-ribose) polymerase, PARP; plating efficiency, PE; protein kinase-like ER kinase, PERK; peroxisome proliferator activated receptor gamma coactivator 1-alpha, PGC1α; prostaglandin E2, PGE2; propidium iodide, PI; phosphatidylinositol 3-kinase, PI3K; phosphatidylinositol-4,5-bisphosphate, PIP2; phos-phatidylinositol-3,4,5-triphosphate, PIP3; ribosomal protein S6 kinase beta-1, P70S6K; picomoles per minute, pmole/min; p38-regulated/ activated protein kinase, PRAK; protein patched homolog 1, PTCH1.

R

Rapidly accelerated fibrosarcoma, RAF; RBPJ-associated module, RAM; reactive nitrogen species, RNS; rat sarcoma virus oncogene, RAS; reactive oxygen species, ROS; retention time, RT; receptor tyrosine kinases, RTKs.

S

Standard deviation, SD; secreted frizzled related protein, SFRP; sirtuin 1, SIRT1; superoxide dismutase, SOD; solid-phase extraction, SPE; spare respiratory capacity, SRC; signal transducer and activator of transcription, STAT; strawberry tree honey, STH.

T

Total antioxidant capacity, TAC; thiobarbituric acid, TBA; thiobarbituric acid-reactive substances, TBARS; Tris HCl buffered saline with Tween 20, TBST; trichloroacetic acid, TCA; T-cell factors, TCF; Trolox equivalents, TE; trolox equivalent antioxidant capacity, TEAC; total flavonoid content, TFC; transforming growth factor beta, TGF-β; tumor necrosis factor alpha, TNF-α; total polyphenol content, TPC; 2,4,6-tripyridyl-S-triazine, TPTZ; tuberous sclerosis, TSC.

V

Vascular endothelial growth factor, VEGF.

X

X-box-binding protein one, XBP1.

CHAPTER 1. INTRODUCTION

1.1. General overview on colorectal cancer

1.1.1. Epidemiology of colorectal cancer

Globally, colorectal cancer (CRC) is the third most widespread cancer in both men and women, while over 1 million new cases are diagnosed each year accounting for 9.7% of all cancers apart and consequently more than 693,933 deaths per annum corresponding to 8.5% of the total number of cancer deaths (Ferlay et al., 2015). In the United States, colon cancer is the second most prevalent cause of death from cancer in men and women after lung cancer; in 2017, an estimated 71,420 men and 64,010 women new cases of colon cancer and 27,150 men and 23,110 women deaths were reported (Siegel et al., 2017a). In Europe, CRC is the second most common cancer, with almost 500,000 new cases diagnosed accounting for 13.0% of all cancers apart and 214,866 death which correspond to 12.2% of the total number of cancer deaths in 2012 (Ferlay et al., 2015).

The incidence rate of CRC gets higher with increasing age. At the time of diagnosis greater number of patients affected with sporadic cancer are more than 50 years of age, with 75% of patients with rectal cancer and 80% of patients with colon cancer being more than 60 years of age. The age standardized incidence rate of CRC is higher in men (20.6 per 100,000 individuals) than in women (14.3 per 100,000 individuals) (Kuipers et al., 2015). The incidence of CRC mostly varies on geographic distinctions worldwide, with almost 55 % of the cases occurring in more developed countries (Figure.1.1). These geographic variations may be attributable to diverse dietary and environmental revelations that are imposed upon a background of genetically determined susceptibility. The age standardized mortality rate of CRC is higher in men (10.0 per 100,000) than in women (6.9 per 100,000) which reflects disease incidence (Kuipers et al., 2015). In 2012, the cumulative risk of CRC in persons aged under 75 was 1.95% worldwide (2.36% in men, 1.57% in women) and 3.51% in Europe (4.48% in men, 2.73% in women) (Ferlay et al., 2013). In developed countries, such as Australia, Canada, United States, New Zealand and European countries etc. higher mortality rates exits compared to developing countries, such as Africa, Central America, Japan, China, Singapore and Korea etc. in the recent years (Siegel et al., 2016). Mortality rate also depends on the stage of diagnosis, which is motivated by the availability of a population screening program and by the level of care in each country (Kuipers et al., 2015).

Like the incidence and mortality, survival rates vary by biological and sociological factors (Jackson-Thompson et al., 2006). Most of the marked global and regional disparity in

survival is likely due to differences in access to diagnostic and treatment services (Boyle and Langman, 2000). The prevalence rate of CRC after 5 years was estimated at 3,543,582 worldwide (68.2 CRC survivors per 100,000 population) and 1,203,943 in Europe (192.3 CRC survivors per 100,000 population) in 2012 (Ferlay et al., 2013). On the global economy, CRC has a great impact on the medical care. By 2020, CRC is estimated to exceed $17 billion in healthcare system only in the USA (Mariotto et al., 2011).

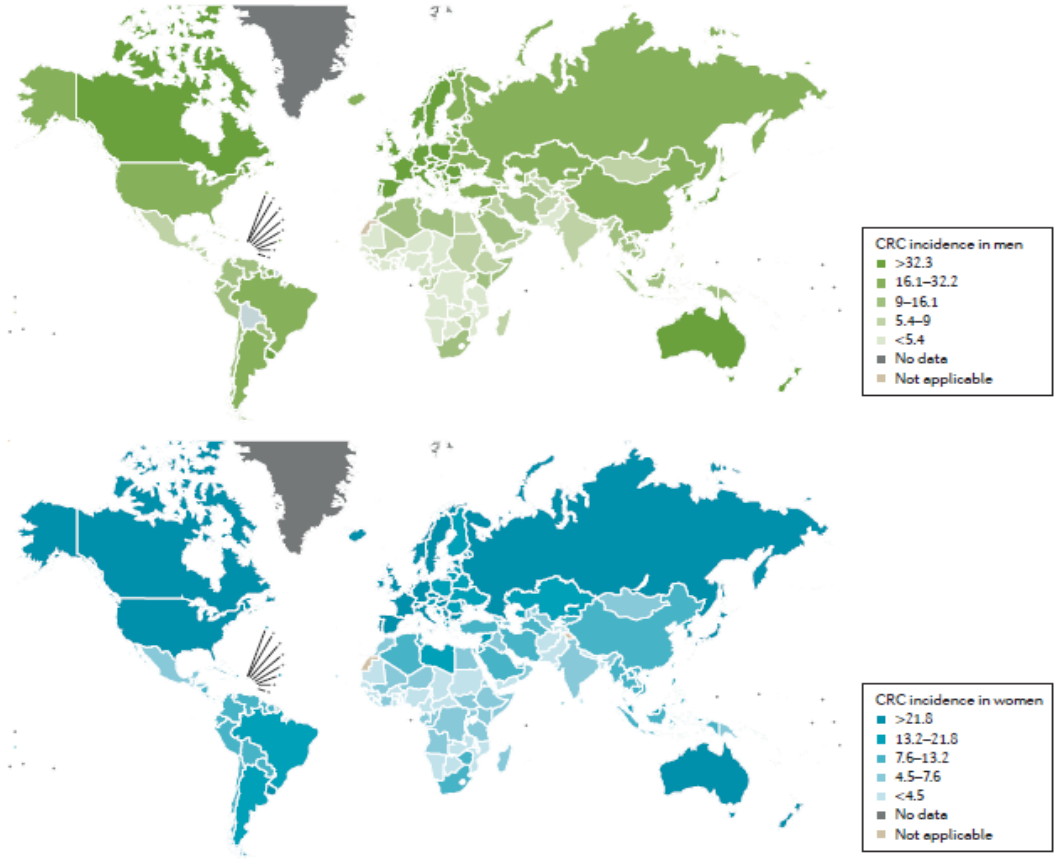

Figure 1.1. Geographical variations in colorectal cancer (CRC) rates. Data from the WHO demonstrating the high incidence of CRC in westernized countries in men and women (Ferlay et al., 2013).

1.1.2. Risk factor and etiology of CRC

Multiple factors are associated with the development of CRC (Figure 1.2). The incidence of CRC is rising in the age group. An individual's risk of CRC increases with advancing age, with the livelihood of cancer diagnosis increasing after 40 years of age and rising progressively after 50 years of age. According to the WHO and the center for disease control, obesity and cancer are two main epidemics in current century, and prevalence has significantly increased in the last few decades. High consumption of processed foods,

animal fat, and a high calorie diet are risk factors for CRC development (Vucenik and Stains, 2012).

In the last 20 years, a benefit of physical activity on cancer etiology has been growing interest. Several evidences support that the prevention strategies with convincing data that physical activity decreases CRC risk (Winzer et al., 2011). Diet has an essential function in the development of CRC. Calcium, fiber, milk, and whole grains have been related with a lower risk of CRC, while high content in fat and/or red meat and processed meat have been connected with an increased risk (Song et al., 2015).

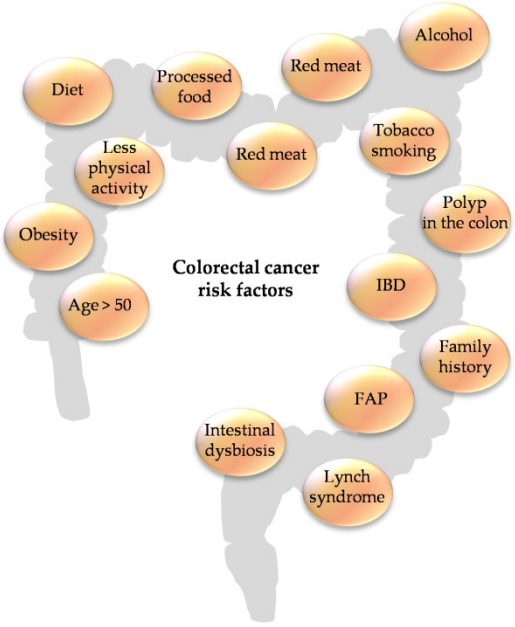

Figure 1.2. Several risk factors associated for CRC development.

Other environmental factors including cigarette smoking are associated with 20% while alcohol abuse is associated with 60% of greater risk to the CRC development (Derry et al., 2013). Furthermore, chronic inflammatory bowel disease (IBD) increased the incidence of ulcerative colitis and Crohn's disease, which contributed the CRC progression (Terzić et al., 2010). Insulin resistance, metabolic consequences of obesity (Meyerhardt et al., 2003), intestinal dysbiosis (Gao et al., 2015) and circadian clock alter digestion (Derry et al., 2013) could also influence the CRC.

CRC can be developed through the mutation of specific gene related to the tumor suppressor, oncogene and DNA repair mechanism. About 70% of CRC cases occur sporadically due to transformation of specific morphological changes starting from adenoma to carcinoma state, 5% are related to inherited (familial adenomatous polyposis (FAP), hereditary non-polyposis colorectal cancer (HNPCC) or Lynch syndrome and MUTYH-associated polyposis) and the rest of the 25% of CRC are associated with familial, only a few are known with high microsatellite instability, with DNA mismatch repair (MMR) deficiency (Stoffel and Kastrinos, 2014).

In the colonic epithelial cells, the environmental and genetic factors cause CRC progression by promoting the acquisition of characteristic behaviors of CRC (Figure 1.3).

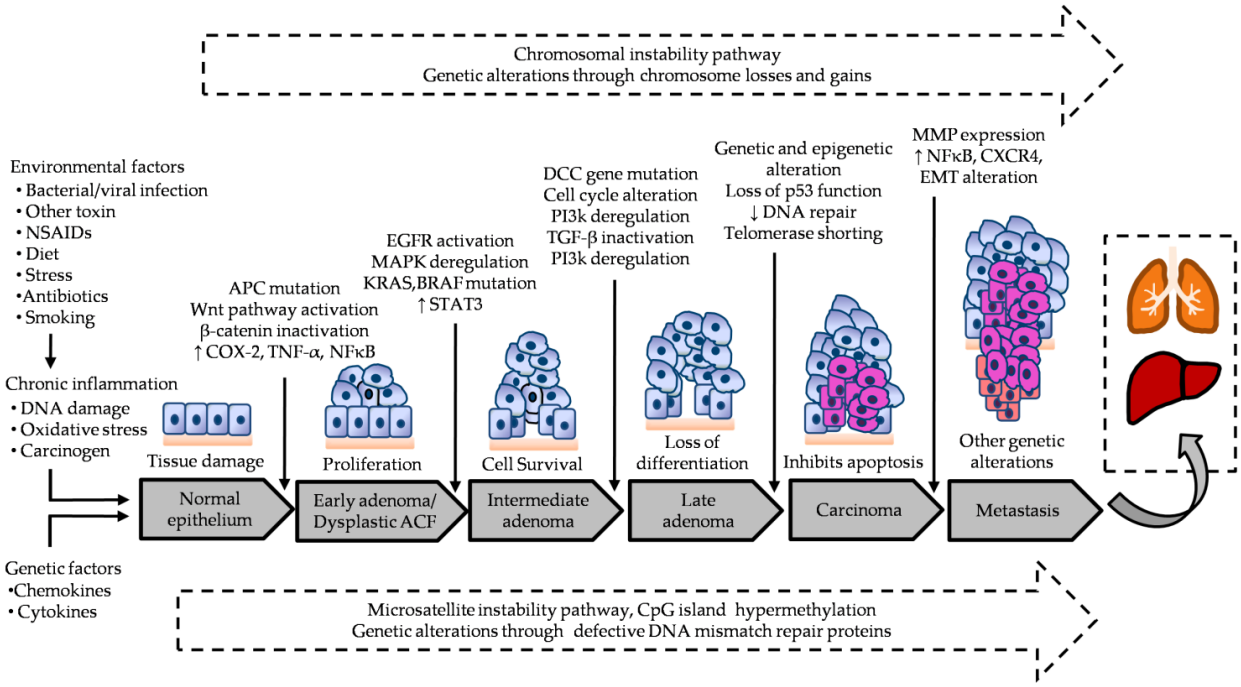

Figure 1.3. Genetic alterations during CRC development.

Several genetic and epigenetic alterations may increase the accretion of mutation and epigenetic changes of oncogenes and tumor suppressor genes, and alteration several signaling pathways which drive the malignant transformation from early neoplastic lesions (aberrant crypt foci (ACF), adenomas and serrated polyps) to cancer progression sequence (Vogelstein et al., 1988).

1.1.2.1. Inflammation and CRC

Even through the physiologic levels of inflammation are preventive and encourage tissue repair, extreme inflammation is harmful and lies at the origin of IBD that is eventually connected to the expansion of CRC (Clevers, 2004). Genetic alteration could also be promoted by inflammation in the intestinal tract by generating pro-inflammatory cytokine, chemokine, reactive oxygen species (ROS) and reactive nitrogen species (RNS) (Munkholm, 2003). Continuous production of cytokines and other mediators are associated with the progression of colitis-associated tumors by generating a microenvironment favoring colonic epithelial proliferation, survival and invasiveness (Munkholm, 2003) (Figure 1.4).

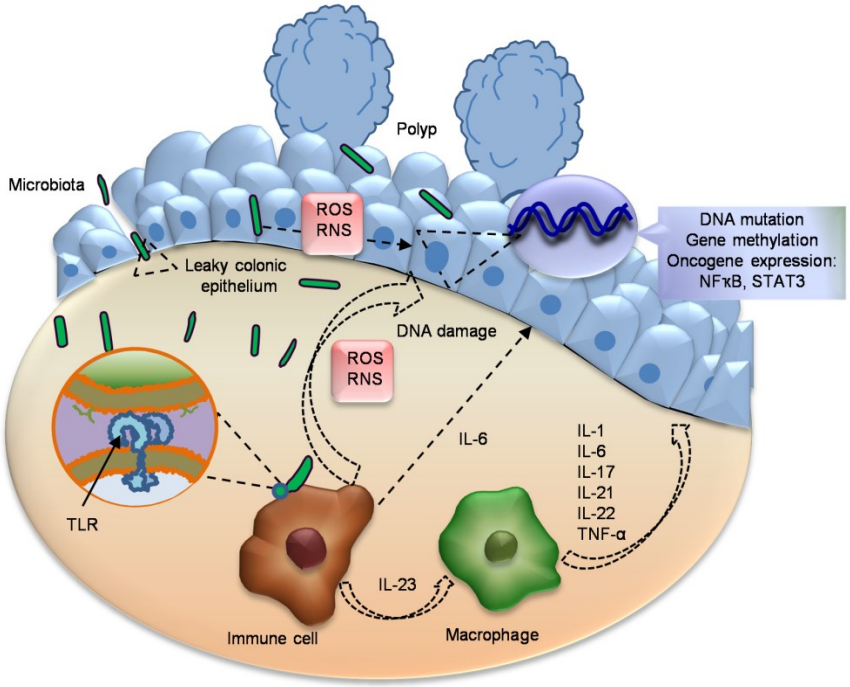

Figure 1.4. Inflammation and oxidative stress induces CRC.

Tumor necrosis factor alpha (TNF-α) activated from this course form macrophage and T-cells and induced DNA damage, angiogenesis and nuclear factor kappa B (NFκB) activation. Activated NFκB also observed by the intestinal bacteria breaches the colonic epithelial barrier by the Toll like receptors (TLRs) (Abreu, 2010). It helps to increase other pro-inflammatory cytokines (interleukin (IL)-1β and IL-6) and mediators (inducible nitric oxide synthase (iNOS), cyclooxygenase 2 (COX-2) and prostaglandin E2 (PGE2)) (Klampfer, 2011) to progression of CRC development by increasing chromosomal instability, mutations of adenomatous polyposis coli (APC) gene, elevating the levels of DNA methyltransferase 1 (DNMT1). DNMT1 enzyme is overexpressed in IBD and stimulates tumor promotion, angiogenesis and inhibits apoptosis (Foran et al., 2010). Additionally, the stimulation of a number of oncogenic signaling pathways, Wnt/β-catenin, kirsten rat sarcoma virus oncogene homolog (KRAS), phosphatidylinositol 3-kinase (PI3K)/ protein kinase B (Akt) and signal transducer and activator of transcription (STAT3) has been observed for development of inflammation associated CRC (Ullman and Itzkowitz, 2011).

1.1.2.2. Oxidative damage and CRC

In oxidative stress, there is an imbalance between production of ROS or other oxidants and their abolition by defensive mechanisms of antioxidant enzymes. In the carcinogenic pathway oxidative stress has the potential impact to enhance the malignant transformation and proliferation of initiated CRC cells (Figure 1.4) (Li and Martin, 2016). Disorder in the redox equilibrium, such as increased production of ROS and nitrogen species, hampers immune system and may lead to damage of lipids, proteins and DNA (Nogueira and Hay, 2013).

ROS play an important role to modulate multiple signal transduction pathways, such as NFκB, PI3K/Akt, heat shock proteins and mitogen-activated protein kinase (MAPK), which is associated with inflammation, proliferation, growth, differentiation and apoptosis. In cancer cells, there are an unbalanced ROS level due to the defective cell metabolism and it acts as a pro-tumorigenic (Nogueira and Hay, 2013). The helpful or destructive role of ROS depends on their concentrations on the cells. The high ROS content in cancer cells renders them more susceptible to oxidative stress-induced cell death, and can be exploited for selective cancer therapy.

ROS initiates lipid peroxidation by a chain of reaction that produces free radicals and other substances (malondialdehyde (MDA), hydroperoxides, lipoperoxides, and toxic aldehydes), which facilities membrane permeability and increases inflammation (Mena et al., 2009). Additionally, lipid peroxidation may act as a signal transducer for cells proliferation and modulates gene expression in the DNA bases which may contribute to CRC (Marnett, 1999). ROS restrain proteolytic system by oxidizing structural proteins and accretion of damaged proteins in cancer cell, which acts as an inhibitor of the proteasome (Grune et al., 2003). This process induces accumulating misfolded and damaged proteins and affects the lysosomal system, which hampers protein turnover and gradually leads to further structural and functional alteration for promoting cancer initiation (Brunk and Terman, 2002). Reproducing cells are highly sensitive against DNA damage by arresting cell cycle or induction of transcription, replication error, initiation of signaling pathways and genomic alteration, all of which associated with CRC progression (Valko et al., 2006).

1.1.2.3. Alteration of oncogene and tumor suppressor gene

The development of the CRC from initiation to progression depends on a serious of well-characterized histopathological changes from mutation of several oncogenes and tumor suppressor genes. At least four chronological genetic changes require ensuring CRC development, such as oncogene, KRAS, as well as the tumor suppressor genes APC, Smad4 and TP53, are the main targets of these genetic changes. Mutations of APC gene can promote the destruction of β-catenin and therefore activate of the wingless-type (Wnt) pathway, a common mechanism for initiating polyp to cancer progression (Vogelstein et al., 1988). p53 (transcriptional factor) that controls cell cycle, apoptosis and DNA repair mechanisms. Mutation of this gene is one of the familiar genetic changes in the development of CRC (Rodrigues et al., 1990). In addition, mutations of oncogenes, KRAS or B rapidly accelerated fibrosarcoma (BRAF) proto-oncogene, occur in approximately 55% to 60% of CRCs, aberrantly activating the MAPK signaling pathway (Samowitz et al., 2005). Multiple additional genetic alterations contribute to carcinoma formation and metastases by altering cellular growth, metabolism, migration and invasive capabilities, and angiogenesis. Major signaling pathways have been described in the below following part which is modulated at the alteration of oncogene and tumor suppressor gene.

1.1.2.3.1. Wnt signaling

Activation of the Wnt signaling pathway through the mutation of the APC gene is a crucial incident in the development of colon cancer. Inactivation of the APC gene is the single gene defect responsible for FAP, and about 90% of sporadic colon cancers harbor activating mutations within the Wnt pathway; most of these mutations destroy APC function (Miyaki et al., 1994). On the basis of the biological activity of Wnt over expression, it has been classified into two types: canonical (β-catenin-dependent) and non-canonical (β-catenin-independent) (Figure 1.5).

APC gene encodes the APC protein that combines and degrades the downstream signaling component cytoplasmic β-catenin. Cytoplasmic β-catenin is arrested by a destruction complex composed of APC, glycogen synthase kinase 3-β (GSK-3β), Axin, and other components. In the absence of functional APC, the distraction of the destruction complex discharges β-catenin and allows it to accumulate in the nucleus along with lymphoid enhancer factor/ T-cell factors (LEF/TCFs). As nuclear concentrations increase, LEF/TCFs recruit β-catenin to target genes transcription, such as Myc proto-oncogen (c-Myc), Axin2 and LEF1 which leading to constitutive activation of the Wnt signaling pathway. A similar effect can arise via mutations in β-catenin and Axin2, however, these are significantly less recurrent mutations than in APC (Najdi et al., 2011). At the same time, Wnt pathway activation evidently helps to the development of adenomas by activation of other additional signaling pathways, such as those mediated by the proto-oncogene KRAS, which is necessary for optimal nuclear localization of β-catenin to the nucleus and promotion of the carcinoma program (Najdi et al., 2011). For the development of the precancerous adenomas by the alteration of APC/ β-catenin gene, canonical dependent Wnt signaling is the main focus. Furthermore, recently non-mutational Wnt signal activation has been observed for the development of cancer by the non-canonical pathway.

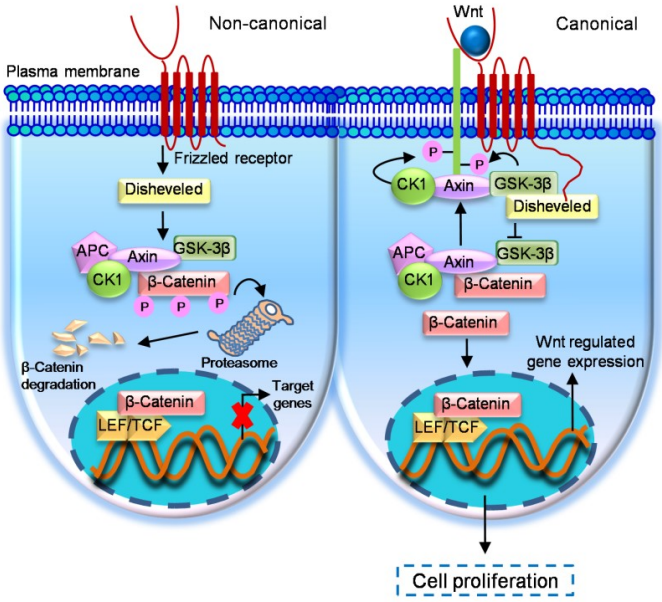

Figure 1.5. Wnt signaling pathway in CRC.

1.1.2.3.2. MAPK signaling

The MAPK are serine/ threonine (proXser/ThrPro) kinases and they can convert various extracellular signals into intracellular responses through serial phosphorylation cascades. When mitogen binds to the kinase it activates guanosine triphosphatase (GTPase) by converting its guanosine diphosphate (GDP) to GTP and then phosphorylates the downstream of MAPK. The major MAPK families containing of extracellular-signal-regulated kinase 1/2 (Erk1/2), Jun N-terminal kinase (JNK), and p38 MAPK, are known to

relay, amplify and integrate signals from a diverse range of stimuli in controlling cellular proliferation, differentiation, cell cycle, inflammatory responses, apoptosis, invasion and angiogenesis (Zhang and Liu, 2002). In CRC, dysregulated Erk1/2, p38MAPK and JNK pathway have been found which are associated with the destruction of the normal mechanism of colonic epithelial cells (Figure 1.6).

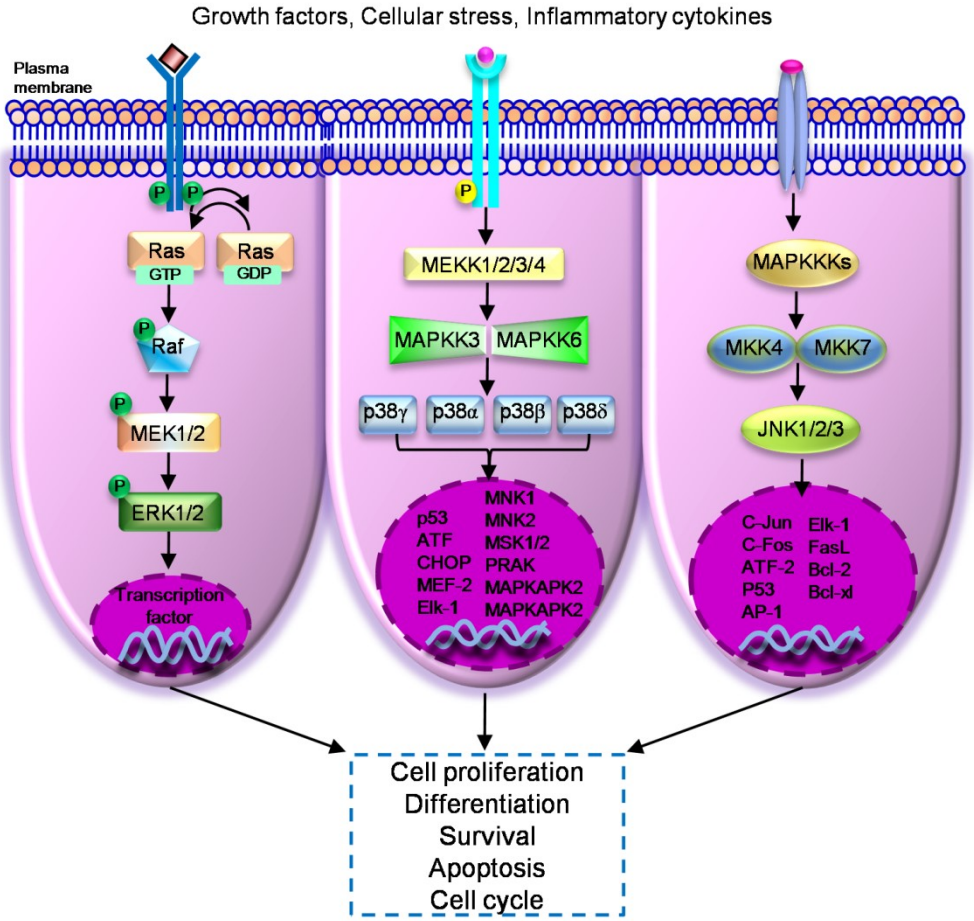

Figure 1.6. MAPK signaling pathway in CRC.

The Erk1 and Erk2 module are activated upon phosphorylation by MEK1 and MEK2 which are activated when phosphorylated by BRAF. Erk1/2 signaling is a particular consequence to CRC and activated by numerous extracellular stimuli and growth factors. In this pathway, ligand-mediated activation of receptor tyrosine kinases triggers GTP loading of the rat sarcoma virus oncogene (Ras) GTPase which can then recruit rapidly accelerated fibrosarcoma (RAF) kinases to the plasma membrane for activation. Mutation of the KRAS and BRAF genes is observed in the early step of CRC, which leads to constitutive activation of Erk1/2 signaling cascade and increases the cell proliferation (Dhillon et al., 2007). Additionally, this signaling pathway is also involved in the

metastasis process through increasing epithelial to mesenchymal transition, migration and invasion (Urosevic et al., 2014). Conversely, the Erk1/2 pathway is connected to the activation of apoptosis because they are often stimulated in response to different cellular stress and growth factors (Jeon et al., 2005).

In mammals, four genes have been identified that encode p38αMAPK, p38βMAPK, p38γMAPK and p38δMAPK. Several extracellular stimuli can activate p38MAPK pathways and allow cells to respond properly by generating a plethora of diverse biological effects such as inflammation, cell proliferation differentiation, and apoptosis in a tissue-specific and signal-dependent manner. A variety of combination of upstream kinases control the activation of p38 isoforms by activating mitogen-activated protein kinase kinase (MAPKK)3 and MAPKK6 which are activated by their upstream kinases MEKK1/2/3/4 and the apoptosis signal-regulating kinase 1 (ASK1) and another way that is MAPKK independent. Non-phosphorylated p38MAPK is inactivated and become activated by phosphorylation of two Thr-Gly- Tyr motifs. Phosphorylated p38 proteins can activate several transcription factors, such as activating transcription factor 1/2/6 (ATF 1/2/6), CCAAT-enhancer-binding protein homologous protein (CHOP)-1, myocyte enhancer factor-2 (MEF-2), p53, and Elk-1 and a variety of kinases, including mitogen-activated protein kinase interacting protein kinase (MNK)1, MNK2, mitogen- and stress-activated protein kinase (MSK)1, MSK2, p38-regulated/ activated protein kinase (PRAK), mitogen-activated protein kinase-activated protein kinase (MAPKAPK)2 and MAPKAPK3 are involved in regulating cytoplasmic or nuclear signaling networks and response to growth factors, cytokines, toxins and pharmacological drugs (Grossi et al., 2014). In colon cancer, p38 MAPKs can play a dual role: they can either mediate cell survival or promote cell death through different mechanisms. According to the previous evidence, it was suggested that the p38α can act as a tumor suppressor by suppressing the inflammation associated colon tumor, negatively regulate the malignant transformation by mutation of harvey rat sarcoma viral oncogene homolog (HRAS) and increased apoptosis through upregulation of first apoptosis signal (FAS), B-cell lymphoma 2 associated X (Bax) and downregulation of Akt survival pathway. Conversely, aberrant activation of p38MAPK has been observed in high grade of CRC and IBD (Grossi et al., 2014; Gupta et al., 2014).

The JNK proteins are encoded by three genes, JNK1, JNK2 and JNK3, each of which has 2 to 4 isoforms and can be activated by the upstream MKK4 and MKK7 kinases kinases via dual phosphorylation of the Thr-Pro-Tyr motif. The activated JNK can not only regulate a

variety of transcription factors such as c-Jun (cellular Jun proto-oncogene), c-Fos (cellular Fos proto oncogene), ATF-2, activator protein-1 (AP-1), p53 and Elk but also phosphorylate many cytoplasmic substrates such as cytoskeletal proteins, mitochondrial proteins like B-cell lymphoma (Bcl)-2 and Bcl-xl. In colon cancer, the oncogenic role of JNKs is based on their aptitude to phosphorylate Jun and to activate AP-1 that controls cell survival, cell cycle, apoptosis and metalloproteinases, while tumour suppressor functions of JNK are correlated to their pro-apoptotic activity (Ogunwobi and Beales, 2007; Wagner and Nebreda, 2009).

1.1.2.3.3. PI3K/Akt signaling

The PI3K/Akt signaling pathway can be activated by several growth factors and by G-protein-coupled receptors (GPCRs) upon stimulation with phospholipids and chemokines which can activate the signals for cell survival and proliferation, cell cycle and anti-apoptotic effects leading to CRC carcinogenesis (Huang and Chen, 2009). The growth induced activation of PI3Ks that are recruited to receptor tyrosine kinases (RTKs) consists of two subunits: catalytic subunit p110 and regulatory subunit p85. In the case of GPCRs induced activation, p110 PI3K subunits directly bind to the αβγ-trimeric G protein. Binding and activation of PI3K to membrane-bound RTKs stimulate the conversion of phosphatidylinositol- 4,5-bisphosphate (PIP2) to phosphatidylinositol-3,4,5-triphosphate (PIP3) that in turn phosphorylates Akt which thereby becomes activated (Figure 1.7).

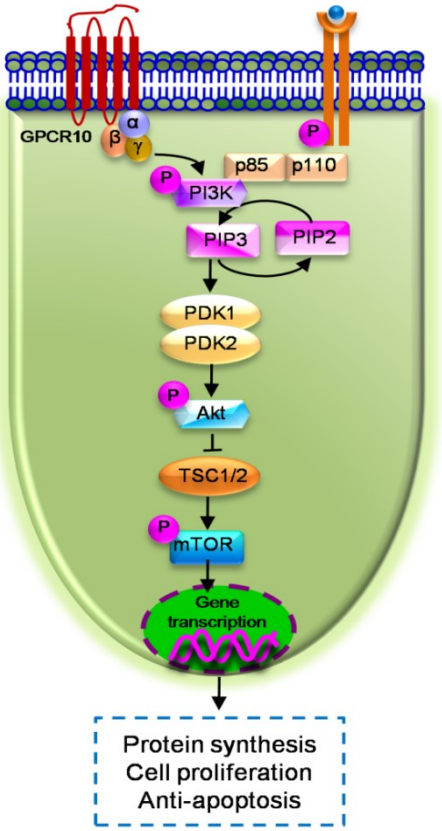

Figure 1.7. PI3K/Akt signaling pathway in CRC.

Activated Akt inhibits apoptosis through preventing cytochrome c release, phosphorylating B-cell lymphoma 2 associated death promoters (Bad) and increasing NFκB. Additionally, Akt stimulates cell proliferation through blocking kinase activity by reducing GSK3β which decreases Cyclin d1 degradation and elevates β-catenin accumulation. Furthermore, AKT-mediated phosphorylation of tuberous sclerosis (TSC) 2 releases TSC-inhibition of

the GTPase, which activates mammalian target of rapamycin complex 1 (mTORC1) kinase. Activated mTORC1 phosphorylates eukaryotic translation initiation factor 4E-binding protein 1(4E-BP1) and ribosomal protein S6 kinase beta-1 (P70S6K) which allows protein translation initiation and elongation (Zhang et al., 2013a).

1.1.2.3.4. EGFR signaling

Gene amplification of the epidermal growth factor receptor (EGFR) gene encodes for a transmembrane glycoprotein involved in signaling pathways that affect cell growth, differentiation, proliferation, and angiogenesis. EGFR is over-expressed in up to 60 to 80% of CRC and high tumor EGFR overexpression is related with worse prognosis (Goldstein and Armin, 2001).

EGFR belongs to the ErbB family of receptor which includes ErbB1 (EGFR or human epidermal growth factor receptor (HER) 1), ErbB2 (HER2), ErbB3 (HER3), and ErbB4 (HER4)). The EGFR signaling can be activated by numerous ligands, such as epidermal growth factor (EGF), transforming growth factor, heparin-binding EGF, epiregulin (EREG), and betacellulin binding to the receptor dimerization with another EGFR monomer (homodimerization) or with a monomer of another ErbB family member. Several tyrosine residues in the intracellular domain are phosphorylated creating a series of high-affinity binding sites for various transducing molecules. The two major signaling pathways RAS–RAF–MAP and PI3K-Akt pathway are activated by EGFR signaling (Saletti et al., 2015). These mechanisms are relevant because of the availability of pharmacologic agents that can influence these signaling pathways and affect cell growth.

1.1.2.3.5. TGF- β signaling

Transforming growth factor beta (TGF-β) signaling pathway has the potential to control a range of biological processes such as cell growth, differentiation, apoptosis, extracellular matrix modeling, and immune response. TGF-β signaling pathway acts as a tumor suppressor and alterations in this pathway promote CRC cell growth, migration, invasion, angiogenesis and metastasis (Ramamoorthi and Sivalingam, 2014).

Once activated, the TGF-β ligands regulate cellular processes by binding to three high-affinity cell surface receptors- the type 1 TGF-β receptor (TβRI), the type 2 TGF-β receptor (TβRII), and the type 3 TGF-β receptor (TβRIII) serine/ threonine kinases- on the cell surface and induce heterotetrameric receptor complexes. In the early stage of CRC,

TGF-β signaling acts as a tumor suppressor and it encourages colon cancer cell growth, migration, invasion, angiogenesis and metastasis in later stages (Ramamoorthi and Sivalingam, 2014). There is a lack of function of TβRI and TβRII receptors which are accountable to alter the TGF-β induced growth inhibition in colon cancer. Over expressed TGF- βI is observed in the primary stage of CRC, while TGF-βII expression is higher in advanced stage of CRC which promotes colon cancer progression and metastasis. Similarly, the expression of TβRI, TβRII, Smad4 and Smad7 is not so much increased in early stage but in advanced stage, Smad7 is overexpressed while Smad4, TGF-β1 and TβRII expression is reduced. The overexpression of TβRIII is increased TGF-β signaling pathway through phosphorylation of Smad 2/5/8 and p38 and downregulation of p21 and p27 levels and thus enhances proliferation of colon cancer cells (Zhang et al., 2013a).

1.1.2.3.6. NFκB signaling

Aberrant NFκB activation has been detected in more than 50% of colorectal and colitis-associated tumors (Kojima et al., 2004). The transcription factor, nuclear NFκB pathway, plays a leading to inflammation to carcinogenesis by modulating several genes responsible for the generation of pro-inflammatory mediators and cytokines (Figure 1.8).

In presence of multiple pro-inflammatory stimuli, inhibitor of kappa B (IκB) is rapidly degraded by the ubiquitin-proteasome pathway. The degradation of IκB induces the translocation of NFκB subunits into the nucleus, and the NFκB subunits bind to the promoter regions of target genes, including iNOS, COX-2, TNF-α and IL-1β, and stimulate transcription genes which encode cytokines, growth factors, chemokines, and anti-apoptotic factors. Furthermore, activated NFκB pathway also increases cell proliferation, anti-apoptosis, genomic instability, glycolysis and drug resistance in colon cancer cells (Sakamoto et al., 2009).

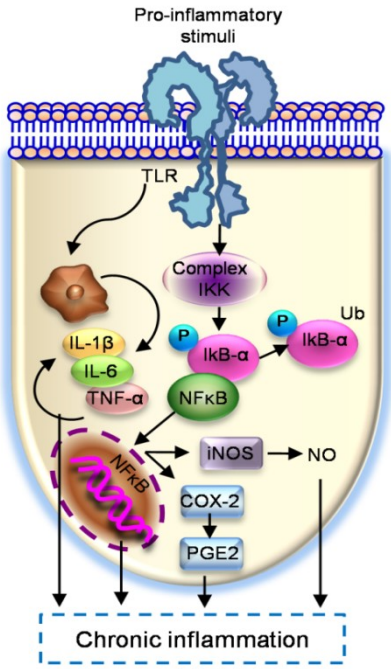

Figure 1.8. NFκB signaling pathway in CRC.

1.1.2.3.7. Nrf2 signaling

Nuclear related factor 2 **(**Nrf2) transcription factors play a vital role in cellular protection by regulating many antioxidant and detoxification enzyme genes via the antioxidant response element (ARE). In the presence of oxidative stress, Nrf2 translocates to the nucleus and binds to ARE sequences to regulate the transcription of several types of genes. Nrf2 downstream genes are involved in intracellular redox-balancing, metabolism, autophagy and apoptosis. Depending on the function of the genes, activated Nfr2 protects the stressed cells form toxic exposure (Menegon et al., 2016).

Previously, Nrf2 has been considered as a tumor suppressor for its cytoprotective effects which are believed to the main cellular protection mechanism against exogenous and endogenous insults, including xenobiotics and oxidative stress. Conversely, several recent studies revealed that hyperactivation of the Nrf2 signaling creates a favorable environment for survival of malignant cells, protecting them against oxidative stress, chemotherapeutic agents and radiotherapy (Menegon et al., 2016). In CRC, the cytoprotective effects are associated by inhibiting Nrf2 repressor Keap1, which maintains Nrf2 expression at the basal levels and decreases the risk of CRC. Conversely, after inhibiting Nfr2 signal, protection of other external signal disappears and increases the risk of CRC. However, overexpressed Nfr2 also increases the risk of CRC by arising Nrf2 mediated inflammation and chemotherapy resistance (Gonzalez-Donquiles et al., 2017).

1.1.2.3.8. Notch signaling

Notch signaling is important for maintaining the cellular proliferation, differentiation, apoptosis, angiogenesis and migration of cancer cells (Schroeter et al., 1998). The activation of Notch signaling is concerned in colon carcinogenesis due to the initiation of pro-survival signaling in colonic epithelial cells. Overexpression of Notch elements, such as receptors, ligands and downstream target genes, is connected with promoting progression, metastatic potential, recurrence and poor prognosis and clinical outcome in various cancers including CRC (Suman et al., 2014).

The activation of Notch signaling depends on cell to cell communication in which Notch ligands bind to Notch receptors, which is present on a neighboring cell and activate metalloproteases in the disintegrin and metalloprotease (ADAM) family, resulting in the cleavage of the extracellular domain (Figure 1.9). Consequently, activated γ-secretase

breaks within the transmembrane domain of Notch receptors, resulting in the release of the Notch intracellular domain (NICD), translocates to the nucleus and binds via its RBPJ-associated module (RAM) and ankyrin domains to the DNA-binding transcription factor CSL (CBF1, Suppressor of Hairless, Lag-1). Once created, this complex displaces the co-repressors and binds to the transcription factors, recruits transcriptional co-activators and induces the expression of target genes, such as hairy-enhancer-of-split (Hes-1) and Hes-related protein gene families, that subsequently implement pro-survival functions (Suman et al., 2014).

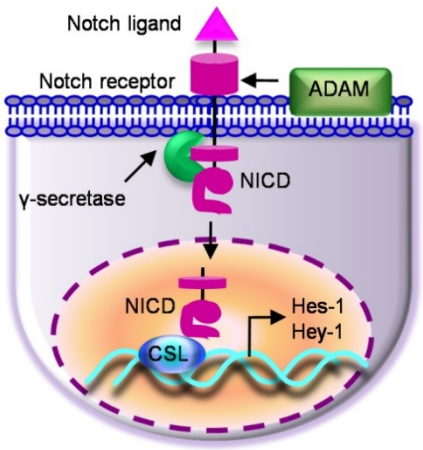

Figure 1.9. Notch signaling pathway in CRC.

1.1.2.3.9. JAK/STAT3 signaling

The Janus kinase/ signal transducers and activators of transcription (JAK/STAT) signaling pathway is important in cytokine mediated immune responses, proliferation, apoptosis and migration. In the CRC, JAK/SATA3 signaling is one of the important pathways for colonic tumorigenesis and has a critical function in different aspects together with initiation, promotion and progression (Slattery et al., 2013). The JAK family consists of four non-receptor protein tyrosine kinases, JAK1, JAK2, JAK3 and TYK2, ubiquitously expressed in the mammals cells (Figure 1.10).

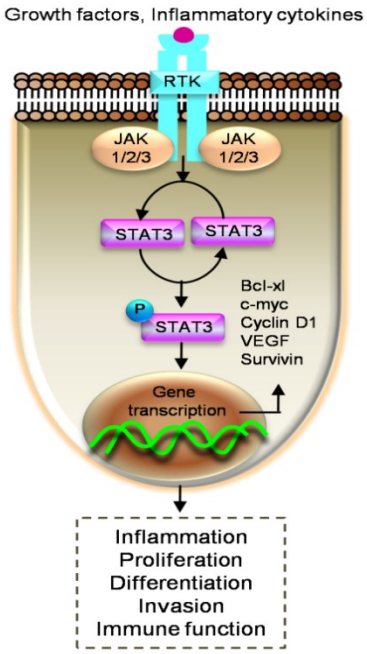

Figure 1.10. JAK/STAT3 signaling pathway in CRC.

In the presence of growth factors and cytokines, RTK promotes activation of JAKs. Activated JAKs auto-phosphorylate and recruit signal transducers and activators of transcription factor STATs. Five additional STATs have been identified: STAT3, STAT4, STAT5A, STAT5B, and STAT6, and in CRC STAT3 is more activated. Activated STAT3 complex then translocates from the cytoplasm to the nucleus where they initiate transcription of STAT3 targets genes by combining with DNA consequence elements, such as BcI-xL, c-Myc, cyclin D1, vascular endothelial growth

factor (VEGF) and survivin, which are involved in CRC cells inflammation, proliferation, differentiation, invasion and immune function (Wang and Sun, 2014).

1.1.2.4. The role of endoplasmic reticulum stress in CRC

The endoplasmic reticulum (ER) is the main intracellular organelle responsible for protein folding, translocation and post-translation modification of secreted and membrane proteins, maintenance of calcium homeostasis and lipid biosynthesis. Accretion of unfolded proteins and disorder of calcium homeostasis within ER causes ER stress (Kim et al., 2008b). Targeting ER stress has gained a great deal of attention as the molecular pathway that can lead to the cell death through apoptosis intrinsic or extrinsic-mediated pathways to eliminate the damaged cells as well as enhance the sensitivity of tumor towards chemotherapeutic agents (Kim et al., 2008b).

In various stressful conditions, ER stress may restore homeostasis and make favorable environment for colon cancer cells survival and proliferation by activating unfolded protein response. Three ER transmembrane proteins: protein kinase-like ER kinase (PERK), ATF6, and inositol requiring kinase-1 (IRE-1) primary regulate the ER stress response and play key role for colon tumorigenesis (Figure 1.11). These three proteins remain inactive and bound to the ER-resident chaperone glucose-regulated protein-78 (GRP-78) in normal conditions. In the period of ER stress, GRP-78 separates from these proteins complex and autophosphorylation of detached PERK and IRE-1 and transcolation of ATF6 to the Golgi apparatus where is sequentially cleaved by protease for making active nuclear ATF6. These variations cause activation of their downstream signaling pathways. Activated PERK then phosphorylates eukaryotic initiation factor 2 alpha (eIF2α) to attenuate protein translation and decrease ER protein overload, while expanded ER stress induces apoptosis by increasing CHOP expression. This is one the therapeutic targets for the ER stress inducing cancer cell death. Furthermore, activated IRE-1 acts as an endonuclease to enhance the X-box binding

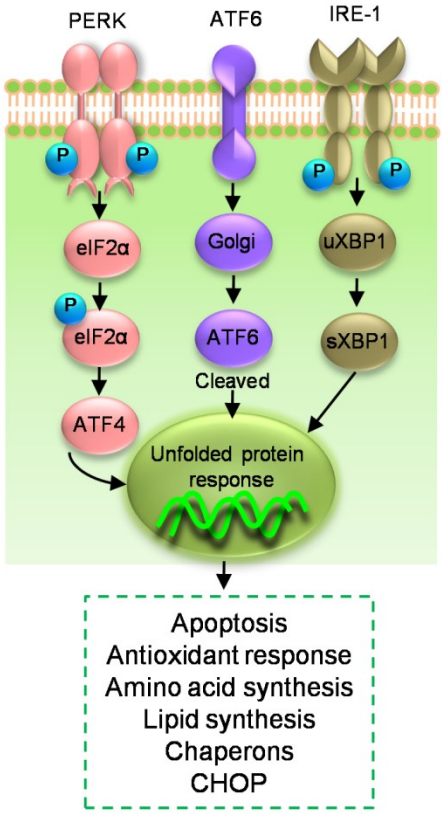

Figure 1.11. Unfolded protein response signaling pathway in CRC.

protein 1 (XBP1) splicing, thereby leading to upregulation of genes for cell survival during ER stress (Yadav et al., 2014). Interestingly, elevated levels of the unspliced form of XBP1 increase the apoptosis of cancer cells (Davies et al., 2008).

1.1.2.5. The role of AMPK signaling in CRC

Adenosine monophosphate (AMP)-activated protein kinase (AMPK) is an evolutionarily conserved serine/threonine kinase that is a master regulator of metabolic and energy homeostasis in tumor cells in energy stress environments by promoting both glycolytic and mitochondrial metabolism (Chaube et al., 2015). AMPK consists of a catalytic α subunit and regulatory β and γ subunits, each of which has at least two isoforms; the activation of this pathway happens by binding of AMP to the γ subunit, and phosphorylation of Thr172 in the activation loop of the α catalytic subunit by upstream kinases, such as liver kinase B1 (LKB1). The activated AMPK acts as a tumor suppressor because this signaling network contains a number of tumor suppressor genes including LKB1, p53 and TSC2, while LKB1 is an upstream activator of AMPK, and p53 and TCS2 are direct AMPK substrate (Hardie, 2011; Mihaylova and Shaw, 2011). Under nutrient depletion, mTOR regulates the cancer cells growth and proliferation, while AMPK directly inhibits mTOR through phosphorylating raptor, one of the molecules of TOR complex (Laplante and Sabatini, 2012).

However, recent evidence recommended that AMPK activation is necessary to regulate oxidative stress and enhance cancer cell proliferation in metabolic stress microenvironment (Chaube et al., 2015; Jeon, 2016; Li et al., 2015). In cancer cells under energy diminution condition, AMPK induces metabolic adaptation by initiating signaling cascade resulting in the reduction of ATP consuming pathways with concomitant stimulation of biochemical reactions that generate ATP (Figure 1.12).

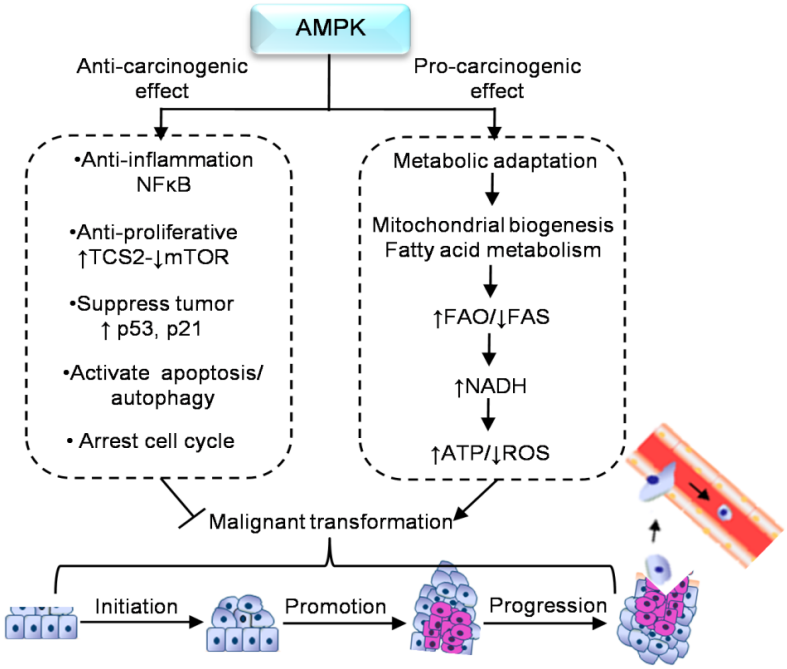

Figure 1.12. Role of AMPK signaling pathway in cancer. Figure slightly modified form Jeon (2016).

Under stress condition, nicotinamide adenine dinucleotide phosphate in its reduced form (NADPH) generate by pentose phosphate pathway is damaged but AMPK initiates alternative pathway to inhibit cancer cell death by maintains NADPH. The suppression of the acetyl-CoA carboxylases (ACC) 1 and ACC2 by AMPK sustains NADPH levels by reducing NADPH consumption in fatty-acid synthesis and elevating NADPH production in fatty-acid oxidation. Therefore AMPK, in addition, maintaining in ATP homeostasis has an another role in NADPH maintenance, which is vital for cancer cell survival under energy stress conditions (Chaube et al., 2015; Jeon, 2016; Jeon et al., 2012; Li et al., 2015). Additionally, in gastric cancer cells, AMPK activation protects the anticancer drugs induced cell death by diminishing apoptosis (Kim et al., 2008a).

Activation of AMPK increases the expression of downstream targets peroxisome proliferator activated receptor gamma coactivator 1-alpha (PGC1α), and its associated genes for cancer cells survive under energetic stress conditions (Chaube et al., 2015). PGC-1α is a major transcription co-activator and it encourages oxidative, mitochondrial and fatty acid metabolism to enhance cancer cell proliferation (Jones et al., 2012) and metastasis (LeBleu et al., 2014). Sirtuin 1 (SIRT1) is another downstream target of AMPK, depending on nature and phase of the tumor; it acts as a tumor suppressor and an oncoprotein (Chalkiadaki and Guarente, 2015). In CRC patients, elevated levels of SIRT1 expression promote carcinogenesis and are associated with a poor prognosis (Chen et al., 2014).

1.1.2.6. The role of matrix metalloproteinases in CRC

Matrix metalloproteinases (MMPs) play an important role for maintaining extracellular homeostasis by sharing proteolytic activity against other extracellular matrix molecules. Several studies investigated that the expression and activation of MMP-2 and MMP-9 in CRC is associated with cancer progression, angiogenesis, invasion and metastasis (Mook et al., 2004). MMP-2 and MMP-9 contain the gelatinase sub-family of MMPs, and though the principal substrates for these enzymes are type IV collagen and gelatin. Integrins are necessary for the cell adhesion, in colon cancer cells MMP-2 degrades the β1 integrins activity for increasing motility and decreasing cell adhesion capability (Kryczka et al., 2012). Gelatinase can activate by multiple signaling pathways. Smad proteins are involved in TGF-β signaling and modulating of colon cancer cell migration by regulating MMP-9 activity. However, in colon cancer cells, overexpression of p38γMAPK has been observed to lead to enhanced c-Jun synthesis, resulting in increased MMP-9 transcription and MMP-9-dependent invasion. Furthermore, MMP-9 is highly expressed in colitis associated colon cancer through modulating Notch and Wnt signaling (Said et al., 2014).

1.1.2.7. The role of epithelial-mesenchymal transition in CRC

The transformation of epithelial cells to mesenchymal cells in a specific pathophysiological condition is known as epithelial-mesenchymal transition (EMT). By modulating several transcriptional regulator, epithelial cancer cells maintain a basal-apical polarity by connecting with several types of junction to undergo various biochemical's changes; these modifications allow them to disrupt cell to cell adherence by losing E-cadherin levels, remodel the cytoskeleton of cells by increasing vimentin levels and obtain mesenchymal characteristics such as increased migration capability, invasiveness, anti-apoptosis activity by enhancing the production of N-cadherin, osteopontin, Snail, slug and other EMT machineries (Boyer and Thiery, 1993). In CRC, EMT plays a vital role in in situ infiltration and distant metastasis by modulating a complex transcriptional regulator (Figure 1.13).

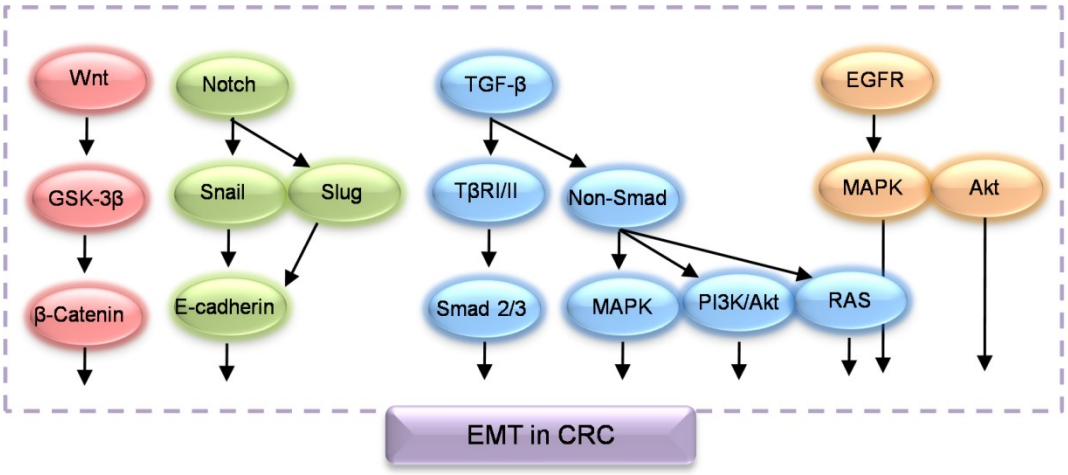

Figure 1.13. Signaling pathways involved in the EMT of CRC. Figure slightly modified form Jin et al., (2015).

A decrease in the expression of E-cadherin and an increases in the expression of vimentin in CRC patients indicate the presence of lymph node associated metastasis, poor tumor differentiation and prognosis (Cao et al., 2015). In the cancer cells, E-cadherin expression is lossed by methylation of the promoter, degradation and phosphorylation of targets protein and enhances the expression of transcriptional repressors such as Snail, Slug, Sip1 and Zed1. Loss of E-cadherin expression can increase β-catenin in the cytoplasm and in the nuclease, bind to transcription factors TCF/LEF and induce the transcription of target genes of Wnt signaling pathways. Therefore, activation of E-cadherin/β-catenin complex and Wnt signaling potentially encourage colon cancer development and metastasis (Jin et al., 2015). Another important EMT mechanism is overexpression of N-cadherin, while E-cadherin is decreased. In this circumstance, epithelial cancer cells are chopping from the primary focal, invade nearby tissues and migrate via lymphatic and blood circulation (Rosivatz et al., 2004).

Furthermore, the progression of CRC are through to undergo in a dynamic process of EMT by developing several signaling routes (Cao et al., 2015), including TGF-β induced activation of Smad dependent and non-Smad dependent signaling, Wnt signaling, Notch signaling and EGFR induced signaling which are already described in the above section.

1.1.2.8. Genetic instability of CRC

One of the basic processes driving the initiation to progression of CRC is the accretion of a diversity of genetic changes in colonic epithelial cells. Chromosomal instability (CIN),

microsatellite instability (MSI), and CpG island methylator phenotype (CIMP) are the main pathways in CRC pathogenesis (Núñez-Sánchez et al., 2015). Most of the CRC occur by CIN due to imbalance in chromosome number (aneuploidy) and loss of heterozygosity, which affects chromosomal segregation, telomere stability and DNA damage response (Pino and Chung, 2010). CIN is observed in 65 to 70% of sporadic CRC, which reflects gain or loss some or whole portion of chromosome that creates karyotyping variability between the cells (Lengauer et al., 1998). This instability affectes the number of oncogenes (BRAF, KRAS, and Smad) and tumor suppressors genes (APC and p53) associated with cell growth. According to the literature data, patients with CIN have less prognostic outcome compared with MSI (Pino and Chung, 2010).

MSI is associated with DNA MMR deficiency due to germline mutation of MutL Homolog (MLH)1, MutS homologs (MSH) 2, MSH6, PMS1 and PMS2 genes (Boland and Goel, 2010). About 15% of all CRC, MSI is detected, within this 3% are caused by Lynch syndrome and 12% are associated with sporadic, obtained methylation of MLH1, which take place in tumors through the CIMP (Hampel et al., 2005). CRC by MSI have characteristic features, including an affinity to begin in the proximal colon, lymphocytic infiltrate, and an inadequately differentiated, mucinous or signet ring appearance (Boland and Goel, 2010). Detection of CRC with MSI has increased alertness of the variety of this cancers and implications for particular management of patients.

The CIMP shows gene silencing due to hypermethylation of CpG islands. Majority of CIMP cancer composes of sporadic MSI of CRC (Poynter et al., 2008) together with a preference for proximal location in the colon, female gender, poor and mucinous histology, and the presence of frequent KRAS and BRAF mutations (Toyota et al., 1999; Weisenberger et al., 2006). There are limited data available to the prognostic marker CIMP tumor. The results from a large study recommend that CIMP is related with a positive prognosis in CRC patients, which is without of MSI and BRAF mutation status (Ogino et al., 2009).

Rarely, these three pathways are overlapping with each other, such as about 25% MSI CRC can show CIN (Sinicrope et al., 2006). Additionally, CIMP CRC are most common for MSI positive or CIN negative CRC, while about 33% CIMP CRC can exhibit a high amount of chromosomal abnormalities (Cheng et al., 2008). On the contrary, about 12% of CIN positive CRC demonstrate high levels of MSI (Shen et al., 2007).

1.1.2.9. Epigenetic alterations in CRC

Epigenetic alterations commonly found in CRC include aberrant DNA methylation, abnormal histone modifications, and altered expression of various noncoding RNAs, including microRNAs (miRNAs). The function of epigenetic alterations in the sequence of normal epithelial cells-polyp-CRC appears by alterations of hundreds to thousands number of genes (Fearon and Vogelstein, 1990). In present situation epigenetic alterations are useful biomarkers for the early detection, diagnosis, prognosis and management of CRC patients.

1.1.2.9.1. DNA methylation in CRC

Aberrant DNA methylation is the most broadly studied epigenetic alteration in CRC. DNA methylation is interceded by DNMTs that make easy the catalytic addition of methyl groups to the cytosine rings of CpG dinucleotides (Herman and Baylin, 2003). We already observed the three different types (CIMP, CIN and MSI) of hypermethylation phenotype of CRCs characterized and within them, a high frequency of DNA hypermethylation have been identified in CIMP (Toyota et al., 2000). Additionally, several varieties of genes, such as integrin alpha-4 precursor (ITGA4), secreted frizzled related protein (SFRP) 2, cyclin-dependent kinase inhibitor 2A (CDKN2A), protein patched homolog 1 (PTCH1), O^6-methylguanine DNA methyltransferase (MGMT) and helicase like transcription factor (HLTF), are hypermethylated in the epigenetic alterations and some of these play an important role in the polyp to progression of CRC (Okugawa et al., 2015). As the same time, when DNA hypermethylation can silence tumor suppressor genes, DNA hypomethylation start to develop CRC by inducing CIN (Chen et al., 1998).

Currently an alternative pathway “serrated pathway” has been recognized that induces CRC by using another route (Jass and Smith, 1992). The common feature of this pathway induces BRAF and KRAS gene mutation, together with CIMP. In addition mutation of BRAF and KRAS induce MAPK activation, serrated polyps develop by methylation-mediated transcriptional inactivation of various genes, such as β-catenin/Wnt pathway (SFRP, mutated in CRC), caudal type homeobox transcription factor 2 (CDX2)), p53 signaling pathway (insulin-like growth factor-binding protein 7 (IGFBP7)), cell cycle control proteins (CDKN2A) and the DNA mismatch repair (MLH1) family (Okugawa et al., 2015).

1.1.2.9.2. Histone modifications in CRC

Chromatin is a complex of macromolecules consisting of DNA, RNA and protein and histone is a primary protein component of chromatin, which control DNA compaction and gene expression.

Dysregulation of histone modifications has been observed in CRC at the initial discovery (Fraga et al., 2005). Histone modification, such as acetylation of histone H3 lysine 56 and di- or tri-methylation of histone H3 lysine 9 and 27, has possible to be prognostic biomarkers in CRC (Tamagawa et al., 2012) but due to the limitation of determining the histone modification in primary cancer tissue the use of this biomarker has been limited.

1.1.2.9.3. The role of microRNAs in CRC

Recent studies demonstrated that a number of miRNAs play a key role in CRC development and progression. Several miRNAs act as an oncogene or tumor suppressor gene in different molecular targets for activating or deactivating different signaling including: miR-135, miR-26b, miR-34a/b etc. in Wnt pathways, miR-143, miR-145, let-7a, miR-181b in KRAS and BRAF gene, miR-143 and miR-145 in Erk pathways, miR-126 in PI3K/Akt pathways, miR-20a, miR-21, miR-25, miR-34a/b/c etc. in Tp53 function destruction and miR-17-5p, miR-20a, miR-21, miR-23b, miR-17-92 cluster etc in TGF-β pathways (Schetter et al., 2012). Numerous studies have demonstrated that miRNA in stool, serum, plasma and tissues shows potential biomarker for screening, diagnosis, prognosis and treatment of CRC (Schetter et al., 2012). For instance, certain 12 miRNAs (such as miR-7, -17, -20a, -21, -92a, -96, -106a, -134, -183, -196a, -199a-3p, and -214) showed higher expression levels in stool samples from CRC patients than in those from healthy controls, whereas eight miRNAs (miR-9, -29b, -127-5p, -138, -143, -146a, -222, and -938) were shown to be downregulated (Ahmed et al., 2013).

1.1.3. Current treatment and management of CRC

Colon cancer is classified into stages I, II, III, and IV, respectively. The cure rate of colon cancer is well connected with cancer stages. Stages I and II, also called early stages (localized cancers usually at the adenoma to carcinoma stage), have a cure rate at 80-95% and 55-80%, respectively. In advanced stages such as metastatic stage IV, the cure rate drops to an unsatisfactory 5-10 % (Simon, 2016).

In the early stage, CRC can be diagnosed by several methods such as fecal occult blood testing, double-contrast barium enema X-ray, flexible sigmoidoscopy, computed tomography colonography and colonoscopy (gold standard) to identify adenomatous polyps, a precursor lesion for colon cancer (Jenkinson and Steele, 2010). The most commonly used biomarkers, such as DNA, RNA, proteins or metabolites in CRC for the determination of MSI, CIN, CIMP, KRAS and BRAF mutations in tumor samples in order to classify the tumor, make a prognosis of the disease and manage therapy (Mármol et al., 2017).

Currently next-generation sequencing applications are being developed for CRC detection, for example, DNA sequencing by ColoSeq^{TM} assay for screening hereditary CRC, miRNA sequencing by RT-qPCR or miRNA microarray assay can differentiate the healthy tissue from CRC tissue and 16S rRNA sequencing can discriminate gut microbiota composition in healthy and CRC tissue (Li and Martin, 2016). Also, a large number of kits are available for determinations of other gene expression profiling are under clinical investigation. Tumor resection is the most common treatment for all stages of CRC. Treatments used for CRC may include some combination of surgery, radiation therapy, chemotherapy and targeted therapy. Depending on the cancer stage and patient's features, several chemotherapies drugs and regimens for CRC management are proposed. The use of various 5-fluorouracil (5-FU) based chemotherapeutics as neoadjuvant or adjuvants such as FOLFOX and FOLFIRI, along or combination with bevacizumab, cetuximab, oxaliplatin or panitumumab depends on the individual patients and tumor characteristics (Schmoll et al., 2012). Even though increasing treatment strategies including surgery and chemo- and radio-therapy have improved the overall survival rates in the early stages of CRC, 40–50% of all patients present metastasis either at the time of diagnosis or as recurrent disease upon intended curative therapy. Most CRC patients with distant metastasis are not appropriate candidates for conventional therapy and exhibit a poor five year survival rate of less than 10% (Siegel et al., 2012). In addition with traditional chemotherapy, monoclonal antibodies or proteins selectively design targeted specific molecules, such as anti-VEGF that blocks VEGF induced angiogenesis, anti-EGFR that is effective in only wild type KRAS gene (Van Cutsem et al., 2014). The affordability and complexity issue jointly with high drug resistance percentage has augmented CRC treatment difficulty worldwide, thus the immediate attention need to complement the existing therapies.

Besides the limitations of current cancer management (surgery, chemotherapy and radiotherapy), available cytotoxic drugs are not easily affordable or available in certain places (especially in developing countries), and their use is also associated with a number of undesirable side and adverse effects (Chidambaram et al., 2011). As a consequence, a large proportion of the population prefers to patronize complementary and alternative medicine (CAM) (Erejuwa et al., 2014). Despite its own limitations, CAM has a number of advantages (such as affordability, availability and lower side effects) compared to synthetic or standard drugs (Mendel, 2004). The use of various natural and synthetic drugs for CRC prevention has indeed attained remarkable attention in recent years, in this context, natural food products may represent a valid alternative, because of their chemopreventive or chemotherapeutic properties against certain diseases, such as cancer (Song et al., 2015).

1.2. Honey as a food

From the centuries honey has been used as a food and medicinal products. *Apis mellifera* (most common) leads to a range of valuable natural products into the beehives, which include pollen, propolis, royal jelly and honey. Honeybees produce the honey that is sugary liquid of flowers, from nectar of blossoms or from exudates of trees and plants giving nectar honey or honeydews. It is created by regurgitation, action of bee enzymes (diastase, invertase and glucose oxidase), and water evaporation and finally store it in wax.

According to the origin, honey can be classified into different categories as follows: (1) blossom honey, obtained predominantly from the nectar of flowers; (2) honeydew honey, produced by bees after they collect “honeydew” which pierce plant cells, ingest plant sap and then secrete it again; (3) monofloral honey, in which the bees forage predominantly on one type of plant and which is named according to the plant; and (4) multifloral honey (also known as polyfloral) that has several botanical sources, none of which is predominant, e.g., meadow blossom honey and forest honey (Alvarez-Suarez et al., 2014).

The relationship between the bee and people begins as early as the Stone Age and from the early period of Homo sapiens, honey has been used as a most favorable natural sweetener, for baking, deserting, preparing special bread, beverage for tea, preparing sauces etc. Honey is a complex product that can be easily digested and absorbed and from the ancient time Egyptians, Chinese, Greeks and Romans used honey together with vegetable or animal fat. For the medicinal properties, in many customs honey has been used as a balm for curing burn, cataracts, ulcers and wound healing (Vandamme et al., 2013). In the recent

years, much attention is being paid on functional foods because of consumer's rising concerns regarding their health, which has encouraged research effort into such foods (Viuda-Martos et al., 2008). Nowadays, honey is classified as a functional food because of its naturally diverse nutritional composition and high antioxidant capacity, which could contribute to the prevention of certain diseases and increase interest of this foodstuff worldwide (Alvarez-Suarez et al., 2013).

According to the latest data FAOSTAT, 1.5 million tons of honey were produced in 2014 worldwide, while the leading producer country was China alone accounting for 31% of the world total and next largest production countries were Turkey, United States, Ukraine and Russia accounted for approximately 22% of the world total, respectively (Table 1.1).

Table 1.1. Leading producers of honeys in the world (FAOSTAT, 2014).

Countries	Production (ton)	% of World production
China	462,028	31%
Turkey	103,525	22%
United States	80,862	22%
Russia	74,686	21%
Ukraine	66,521	20%

The ingestion of honey varies to a great extent from region to region. The major honey exporting country is China that has small annual consumption rates of 100 to 200 g per capita. In developed countries honey consumption rate is higher but the domestic production does not always fulfill the demand of market. The European Union is a major honey importer and producer. The annual consumption differs from 300 to 400 g per capita in Italy, France, Great Britain, Denmark and Portugal and 1 to 1.8 kg per capita in Germany, Austria, Switzerland, Portugal, Hungary and Greece, while in countries such as the USA, Canada and Australia the average consumption is 600 to 800 g per capita (Alvarez-Suarez et al., 2010b).

1.3. Bioactive profile of honey

The bioactive profile of honey is difficult to describe since it is a mixture of approximately 200 compounds, consisting mainly of different types of sugar, proteins, free amino acid, organic acid, essential minerals, water, enzymes, vitamins, volatile compounds, variety of phenolic compounds and pigments (Alvarez-Suarez et al., 2013). The nutritional composition of honey is variable and mainly depends on the floral source and geographical

regions together with some external factors, such as seasonal and environmental factors, processing and storing condition. The range of bioactive compounds is discussed bellow in Figure 1.14 to Figure 1.20, with specific focus on major components.

1.3.1. Chemical composition of honey

1.3.1.1. Sugar in honey

About 75% monosaccharide is present in honey where fructose (~ 40%) and glucose (~30%) are the main sugar components. Additionally, 10 to 15% are disaccharides mainly ~7.20% maltose and ~1.50% sucrose, small amounts of turanose, isomaltose, maltulose, trehalose, nigerose, kojibiose and trisaccharides maltotriose and melezitose (Alvarez-Suarez et al., 2013).

Chemical composition of honey (per 100 g)

Proximates		Minerals		Vitamins	
Water	17.1 g	Sodium	0.0-7.60 mg	Riboflavin (B2)	0.38 mg
Energy	304 kcal	Potassium	13.2-16.8 mg	Niacin (B3)	0.121 mg
Ash	0.2 g	Calcium	4.4-9.20 mg	Pantothenic acid (B5)	0.068 mg
Dietary fiber	0.2 g	Iron	0.06-1.5 mg	Vitamin B6	0.024 mg
Proteins	0.2-1.6 g	Magnesium	1.2-3.5 mg	Folate (B9)	2 mg
Amino acid	1 g	Manganese	0.02-0.4 mg	Vitamin C	0.5 mg
Proline	0.090 g	Phosphorus	1.9-6.30 mg	Choline	2.2 mg
Aspartic acid	0.027 g	Zinc	0.03-0.4 mg	Betaine	1.7 mg
Glutamine	0.018 g	Copper	0.036 mg		
Phenyllamine	0.011 g	Selenium	1.0-2.91 µg		
Leucine	0.010 g	Fluoride	7 µg		
Enzyme (Diastase)	1-8 mg				
Sugar	75-82 g				
Fructose	28-41 g				
Glucose	22-35 g				
Maltose	7.2 g				
Sucrose	1.5 g				
Galactose	3.10 g				
Higher sugar	1.5 g				
Other/ Underminds sugar	3.2 g				
Organic acid	0.57 g				
Free acid as gluconic	0.43 g				
Lactone as gluconolactone	0.14 g				

Figure 1.14. Chemical composition of honey (USDA, 2015a).

According to previous investigations, several types of disaccharides and trisaccharides are identified in various type of honey depending on the analytical technique (Alvarez-Suarez et al., 2010b). Most of the disaccharides and trisaccharides (sucrose and maltotriose) are enzymatically hydrolyzed to monosaccharides. For example, sucrose contains of one molecule of fructose joined with glucose by α-1,4 bonding. An equimolar mixture of hexoses is produced by hydrolyzing with the enzyme invertase (Kamal and Klein, 2011).

Similarly, maltotriose contains three molecules of glucose units which produce maltose by enzymatic hydrolysis. Maltose again converte molecules of glucose by hydrolyzing with the enzyme glucosidase (Soldatkin et al., 2013).

The properties and the concentration of sugars in honey mainly depend on the botanical origin (types of flower used by honeybee), geographical origin (climate factors), and processing and storage conditions (Escuredo et al., 2014). The ratio between the fructose and glucose is a useful marker of the categorization of monofloral honey. In most of the honey fructose is the main carbohydrate present in greatest proportion, except in some honey, where glucose may be a higher portion (Escuredo et al., 2014) and as a result, these types of honey, normally, have a quick crystallization.

Honey is an important source of calories for the human body because it is easy to digest and the main components (glucose and fructose) are quickly transport to blood and serves the required energy. Interestingly, 100g of honey provides 304 kcal equivalents to 64 kcal in a serving of one tablespoon (21g) (USDA, 2015b), while daily doses approximately 21 g covers on 3% of the daily recommended energy intake.

1.3.1.2. Proteins, amino acids and enzymes in honey

Depending on the species of honeybee the content of proteins are variable. For example, honey from *Apis cerana* contains 0.1 to 3.3% of proteins, whereas honey from *Apis mellifera* contains 0.2 to 1.6% of proteins, respectively (Won et al., 2008). Though proteins in honey are recognized both to vegetable and animal sources but the pollen is the main source of proteins.

The properties of amino acid of the honey depend on the origin of the nectar and honeydew. Amino acid contributes for 1% (w/w) component of honey, while proline is the major one. Usually proline is created from the salivary discharge of honeybees (*Apis mellifera* L.) at the conversion time of nectar into honey and it represents about 50 to 80% of total amino acid contents (Iglesias et al., 2004; Truzzi et al., 2014). For the maturation of the honey proline has been used as an indicator and sometimes for adulteration with sugars. In the pure honey, 180 mg/kg of proline is a minimum accepted value (Manzanares et al.). In addition, other amino acids indentified in honeys are glutamic acid, aspartic acid, glutamine, histidine, glycine, threonine, b-alanine, arginine, a-alanine, aminobutyric acid, proline, tyrosine, valine, methionine, cysteine, isoleucine, leucine, tryptophan, phenylalanine, ornithine, lysine, serine, asparagine and alanine (Hermosín et al., 2003).

Honey also represents a small portion of proteins in form of enzymes. For example, invertase (sucrose, α -and β-glucosidase) hydrolyzes sucrose into fructose. Invertase present in the honey sustains its activity when honey is ripened. Another enzyme is diastase (α -and β-amylases), which hydrolyzes starch chain into dextrin and maltose. This enzyme is used as an indicator of honey quality, more the amount of this enzyme, more the quality of honey. Lastly, glucoseoxidase converts glucose into δ-gluconolactone, which produces gluconic and acid hydrogen peroxide (bactericidal properties) (Bogdanov et al., 2008).

1.3.1.3. Organic acids in honey

Based on the previous investigation, all honeys have a minor acidity because of the presence of about 0.57% organic acids. These organic acids are directly acquired from the nectar or from sugars by enzymes secreted by honeybees while converting the nectar into honey (da Silva et al., 2016).

Organic acids are used as a marker for differentiating the botanical or geographical origin and they are related to the color, flavor and acidity, pH and electrical conductivity. Moreover, the presence of these acids increases the stability of honey against microorganism and partly associated for bactericidal properties (Alvarez-Suarez et al., 2013). From the different regions of the world, various organic acid are identified in honey, while gluconic acid is the main component and other acid are aspartic acid, butyric acid, citric acid, acetic acid, formic acid, fumaric acid, galacturonic acid, glutamic acid, glutaric acid, glyoxylic acid, 2-hydroxybutyric acid, α-hydroxyglutaric acid, isocitric acid, α-ketoglutaric acid, lactic acid, malic acid, malonic acid, methylmalonic acid, 2-oxopentanoic acid, propionic acid, pyruvic acid, quinic acid, shikimic acid, succinic acid, tartaric acid and oxalic acid (da Silva et al., 2016).

1.3.1.4. Vitamins in honey

Honey represents a very small amount of vitamin, within this vitamin B complex are the major include thiamine (B1), riboflavin (B2), nicotinic acid (B3), pantothenic acid (B5), pyridoxine (B6), biotin (B8 or H) and folic acid (B9). Vitamin C is also present in the honey but the determination of this vitamin is unstable due to chemical and enzymatic oxidation and an accelerated rate of alteration (oxygen, light or heat) (Bogdanov et al., 2008). The reduction of vitamin content in honey may be due to commercial filtration for

the elimination of pollen and oxidation by the hydrogen peroxide formed by glucose oxidase (da Silva et al., 2016).

1.3.1.5. Minerals in honey

The mineral content of honey is variable from 0.04% to 0.2% and depends on the light and dark honey types. Botanically honey can be classified by estimating the mineral element which depends on the geographical origin, type of soil in which the plant and nectar were found (da Silva et al., 2016).

Minerals play an important role in human biological system through retaining normal metabolism, protecting excessive production of free radicals, controlling the circulatory system and reproduction and catalyst different biochemical reactions. Thus it is necessary they are supplied by diet. Honey contains several mineral elements of which potassium are the majority, corresponding usually to one third of the total mineral element identified in honey and other mineral also present in small quantity are sodium, iron, copper, silicon, manganese, calcium and magnesium (da Silva et al., 2016).

1.3.1.6. Aroma and volatile in honey

The aroma of honey is generated by complex mixture of various volatile compounds, which may vary on the floral or botanical origin, processing and storage conditions. Unifloral honey has a typical aroma of the plants because of the presence of specific volatile compounds from the nectars (Castro-Vázquez et al., 2007). The flavor of honey is a vital quality for its implication in food industry as well as a selection criterion for the consumer's choice. According to the evidence in the literature, until now about 500 various volatile compounds have been recognized in the different types of honey in the different botanical origins of the world. Within these the most famous are cis-rose, t-8-þmenthan-oxide-1,2-diol and 3,9-epoxy-1-þ-mentadieno, which have been used as a characteristic marker for lemon honey; sulfur compounds, diketones and alkanes are used as a marker eucalyptus honey; hep-tanal and hexanal are used as a marker for lavender honey; methyl anthranilate, lilac aldehyde, hotrienol and 1-p-menthen-al used as a marker for citrus honey etc. (Alvarez-Suarez et al., 2013; da Silva et al., 2016).

1.3.2. Phenolic profile of honey

The phenolic compounds of honey are secondary metabolites of plant, biosynthesized mainly for defense against oxidative damage and stress and finally transmitted through the nectar to the honey. There are two major families of phenolic compounds which are identified in honey: flavonoids and phenolic acid. The phenolic profile of honey mostly depends on the floral origins and sources. This variability corresponds to the basis of the two major research themes belonging to the study of honey phenolic fraction: (i) the evaluation of the overall bioactive properties of honey from different botanical or geographical origins and (ii) the floral and/or the geographical origin of honey on the basis of the presence and the abundance of one or more specific phenolic compounds, therefore proposed as chemical marker(s) of origin (Figure 1.15).

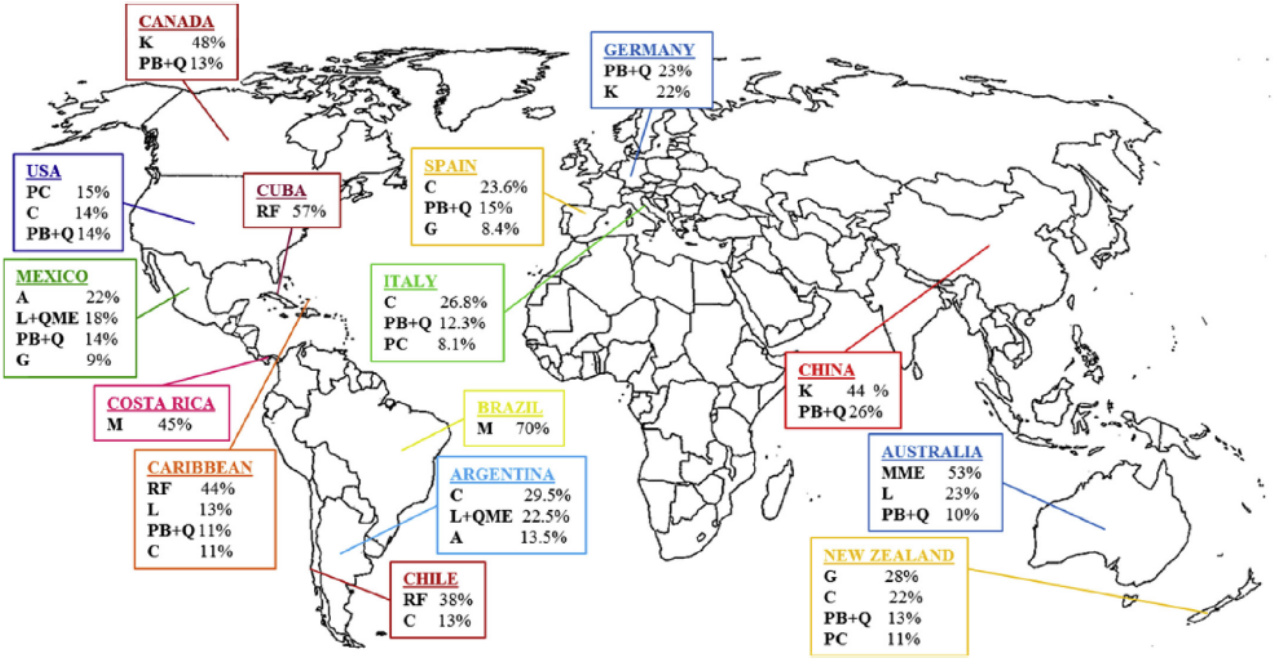

Figure 1.15. Worldwide differences in honey composition. Figure adapted from Badolato et al., (2017). A: Apigenin, C: Chrysin, K: Kaempferol, G: Galangin, L: Luteolin, M: Myricetin, MME: Myricetin 3-methyl ether, PB: Pinobanksin, PC: Pinocembrin, Q: Quercetin, QME: Quercetin 3-methyl ether, RB: Riboflavine.

1.3.2.1. Flavonoids in honey

Flavonoids are the main functional component of honey. They have a C6–C3–C6 nuclear structure, linking two benzene rings joined by a pyran ring. Replacement on the rings results in major classes of flavonoids: flavonols, flavones and flavanones. The concentration of flavonoids in honey is about 20 mg/kg and it differs on the botanical

origin of honey (Alvarez-Suarez et al., 2010b). According to the different studies, the major flavonoids compounds are identified in honey are flavonols: quercetin, myricetin, kaempferol etc., flavones: chrysin, apigenin, luteolin, diosmetin etc., flavanones: hesperetin, pinocembrin, naringenin etc., and flavanols: catechin, epicatechin, epigalloctocatechin, epigalloctocatechin gallate etc. (Figure 1.16).

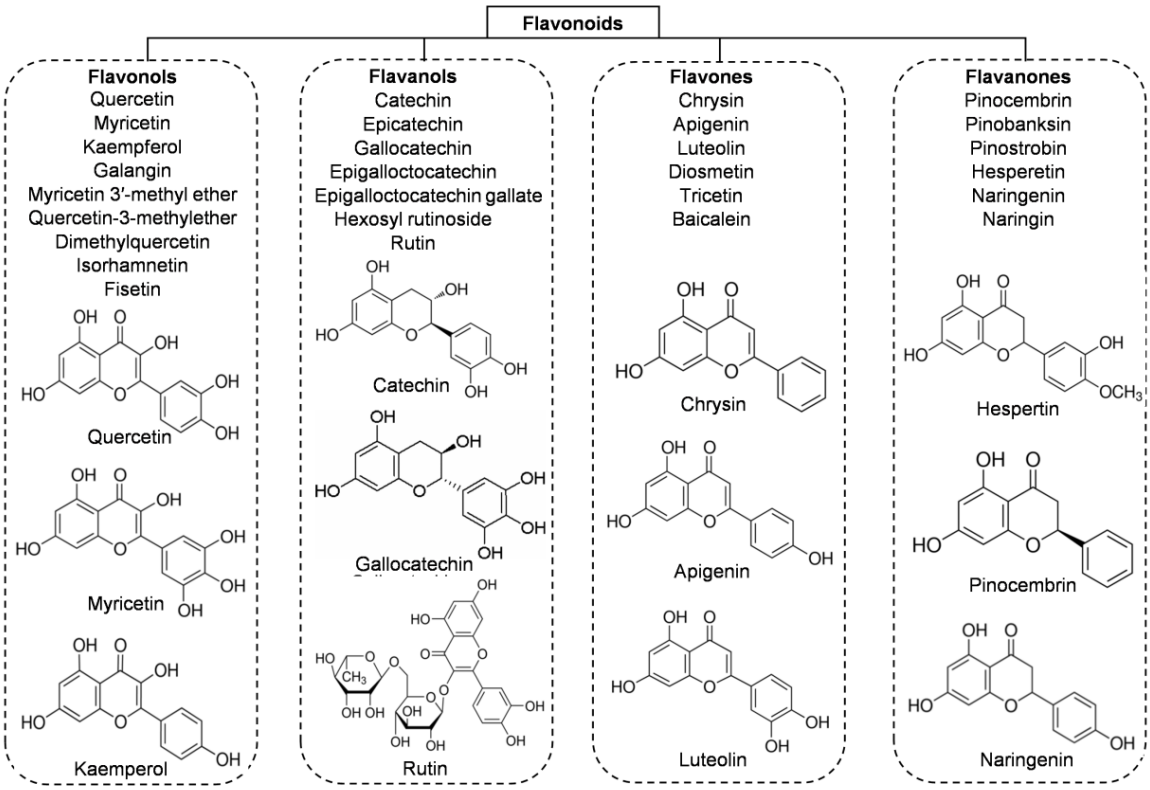

Figure 1.16. Main classes of honey flavonoids with their chemical structure (Ciulu et al., 2016).

The highest content of flavonoids are found in Manuka honey (MH), a new Zealand monofloral honey, Tualang honey, a multifloral honey originated from Malaysian and Buckwheat honey, the monofloral derived from various geographical origins, whereas the lowest content is observed in Gelam honey and acacia honey (Porcza et al., 2016). The variation usually depends on the floral, botanical and geographical origins together with high-performance liquid chromatography (HPLC) method used for the determination of the compounds (Ciulu et al., 2016).

1.3.2.2. Phenolic acids in honey

The phenolic acids of honey can be divided into subgroups depending on their chemical structure: the hydroxybenzoic and hydroxycinnamic acids. Hydroxybenzoic acids share

C1–C6 nuclear structure, derived from benzoic acid but the difference can be observed in hydroxylation and methylation of the aromatic ring (da Silva et al., 2016). The most common hydroxybenzoic acids found in honey are benzoic acid, vanillic acid, syringic acid, salicylic acid, gallic acid and ellagic acid (Figure 1.17).

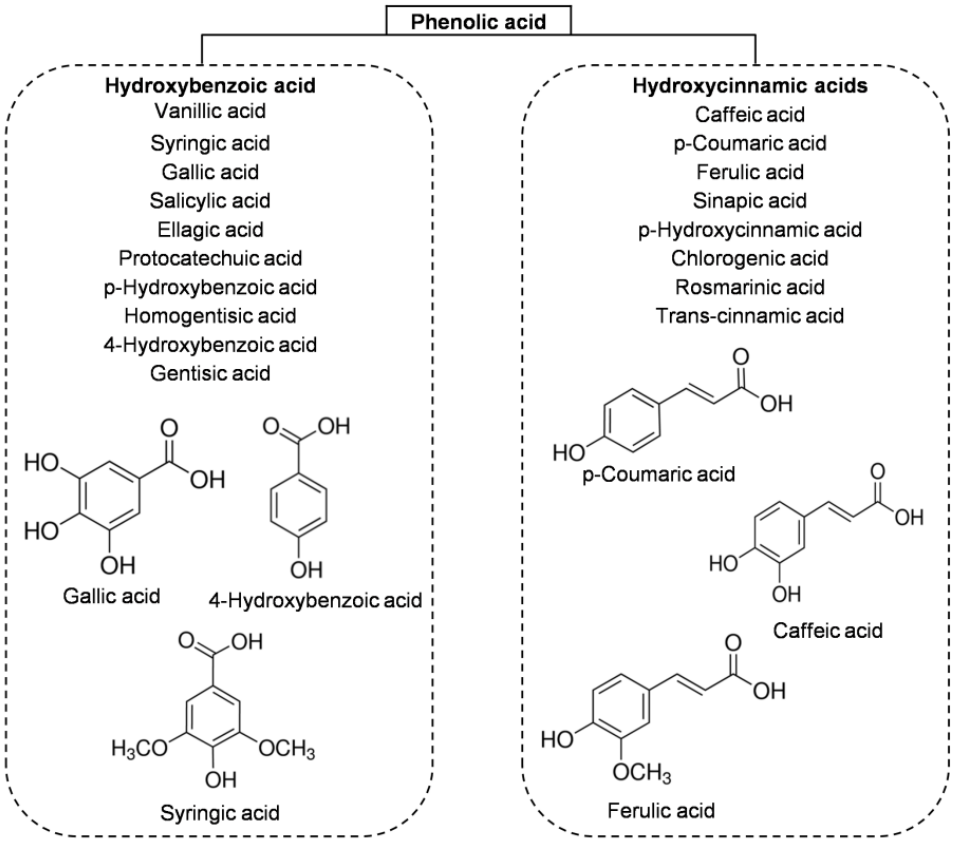

Figure 1.17. Main classes of honey phenolic acids with their chemical structure (Ciulu et al., 2016).

The nuclear structure C3–C6 is usually shared by hydroxycinnamic acids and exhibits differences in the originate ring such as phenylacetic acids and acetophenones. The major identified hydroxycinnamic acids in honeys are caffeic acid, p-coumaric acid, ferulic acid and sinapic acids. Other phenolic acids such as p-hydroxycinnamic acids and chlorogenic acid are also present in honey depending on the botanical origin (Alvarez-Suarez et al., 2013; da Silva et al., 2016).

1.3.2.3. Antioxidant properties of honey

Free radicals from endogenous and exogenous sources are important in the pathogenesis of several diseases. Honey is a good source of natural antioxidants and the antioxidant activity of honey is renowned from ancient times; its capacity depends mainly on the phenolic compounds and also other substrates such as amino acids, proteins, vitamins and carotenoids derivatives present in the honey. Like other phenolic compounds, the antioxidant activity of honey also differs on the botanical and geographical origin and the climate conditions. According to the previous studies, a strong correlation was observed between the total polyphenol and flavonoid contents and the antioxidant capacity of honey (Alvarez-Suarez et al., 2010a; Moniruzzaman et al., 2013).

The antioxidant activity is accredited to bioactive compounds of honey due to their ability to scavenge or reduce the formation of free radicals, along with the improvement of mitochondrial functionality and the inhibition of DNA damage and lipid peroxidation (Alvarez-Suarez et al., 2016). Several methods have already been well known for determining the antioxidant activity of honey *in vitro*, such as the ferric reducing antioxidant power (FRAP) spectrophotometric assay, the 2,2-diPhenyl-1-picrylhydrazyl (DPPH) radical scavenging method and trolox equivalent antioxidant capacity (TEAC) assay (Alvarez-Suarez et al., 2010b). Table 1.2 reports a variety of antioxidant properties of honey in different floral and geographical origin.

Table 1.2. Antioxidant properties of most common honeys according to different methods reported by different studies.*

Floral and geographical origin of honey	Antioxidant properties
Manuka honey from New Zealand	FRAP, (μmol Fe(II)/ 100g honey ± SD): 648.25 ± 0.92 FRAP, (μmol TE/ 100g honey ± SD): 110 ± 3.0 DPPH, (μmol TE/ 100g honey ± SD): 43 ± 2.2
Taulang honey from Malaysia	DPPH, IC_{50} (mg/ml ± SD): 5.80 ± 0.12 FRAP, (μmol Fe(II)/ 100g honey ± SD): 121.89 ± 3.87
Gelam honey from Malaysia	FRAP, (μmol Fe(II)/ 100g honey ± SD): 327.79 ± 1.55 DPPH, IC_{50} (mg/ml ± SD): 6.68 ± 0.28
Strawberry tree honey from Sardinia	DPPH, (mmol TE/ Kg honey ± SD): 4.5 ± 1.1 TEAC, (mmol TE/ Kg honey ± SD): 5.9 ± 1.5 FRAP, (mmol TE/ Kg honey ± SD): 12.0 ± 2.2
Rosemary honey from Portugal	DPPH, IC_{50} (mg/ml ± SD):168.94 ± 19.20
Acacia honey from Italy	FRAP, (μmol Fe(II)/ Kg honey ± SD): 79.5 ± 3.7 DPPH, IC_{50} (mmol TE/ Kg honey ± SD): 45.45 ± 0.04
Thymus honey from Italy	DPPH, IC_{50} (mg/ml ± SD):31.4 ± 1.57 FRAP, (mmol Fe(II)/ Kg honey ± SD): 1.837 ± 0.092
Lime honey from Poland	DPPH, (mmol TE/ Kg honey ± SD): 0.4 ± 0.1 FRAP, (mmol Fe(II)/ Kg honey ± SD): 1.4 ± 0.4
Morning glory honey from Cuba	ORAC, (μmol TE/ g honey ± SD): 9.26 ± 0.46 ABTS, (μmol TE/ g honey ± SD): 2.01 ± 0.21
Linen vine honey from Cuba	ORAC, (μmol TE/ g honey ± SD): 12.89 ± 0.28 ABTS, (μmol TE/ g honey ± SD): 2.94 ± 0.23
Buckwheat honey from Poland	DPPH, (mmol TE/ Kg honey ± SD): 1.2 ± 0.2 FRAP, (mmol Fe(II)/ Kg honey ± SD): 5.7 ± 0.9

* Data obtained from Alvarez-Suarez et al., (2016); Kishore et al., (2011); Moniruzzaman et al., (2013) and Ciulu et al., (2016).

FRAP: ferric reducing antioxidant power; DPPH: 2,2-diphenyl-1-picrylhydrazyl radical; TEAC: Trolox equivalent antioxidant capacity; ORAC: oxygen radical absorbance capacity; AEAC, ascorbic acid equivalent antioxidant content, IC_{50}, 50% inhibitory concentration; TE: Trolox equivalents; SD: standard deviation.

1.4. Bioavailability and metabolites of honey

From a nutritional point of view, bioavailability is the fraction of a nutrient present in a food that is absorbed, retained, and used for physiological function through normal pathways. It is well established from animal and human studies that ingested phenolic compounds (from food sources) survive digestion in the upper digestive tract and reach different parts of the proximal and distal colon in substantial doses (Figure 1.18).

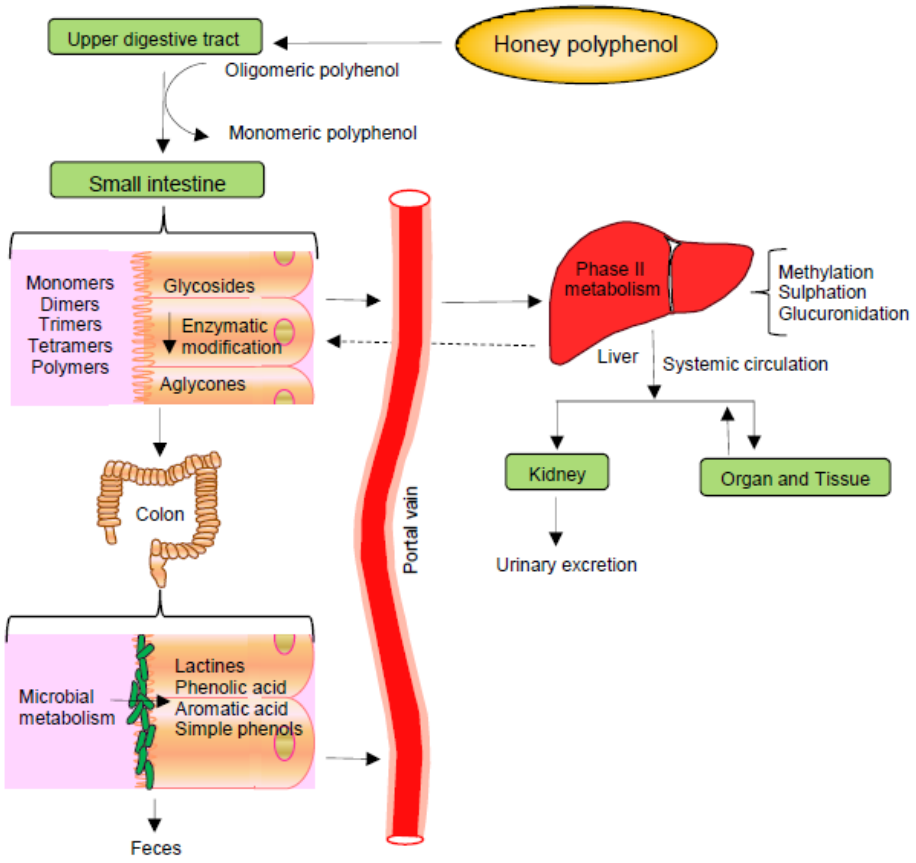

Figure 1.18. Schematic diagram of organs involved in the absorption and metabolism of honey polyphenols. Figure slightly modified form Afrin et al., (2016).

During the absorption process, phenolics are conjugated (usually methylated, sulphated and glucuronidated) in the small intestine and later in the liver, a metabolic detoxification process that facilitates biliary and urinary elimination. Hence, the colonic epithelia can be in contact with both the parent phenolic compounds and their degradation products which are extensively metabolized to simpler phenolics by colonic microbiota and finally phenolic metabolites can be detected in urine, feces, blood and tissue (Figure 1.18) (Manach et al., 2005).

The sequence of absorption and quick elimination of the phenolic compounds makes the final plasma concentration of oligomeric flavanoids to 1 μM/ L whiles the flavanones to 5 μM/ L. In the case of phenolic acids, the bioavailabilities are much lower due to the esterification process (Manach et al., 2004; Manach et al., 2005). Up to date, only one study observed the bioavailability of buckwheat honey polyphenols in healthy human subjects. However, two types of buckwheat honey 1.5 mg/ kg (containing 0.796 ±0.02 and 1.716 ±0.21 mg of phenolic antioxidants per gram) was supplemented in 40 subjects. The total phenolic content along with the antioxidant and reducing capacities of plasma significantly increased 2 h after the honey supplementation and remained high up to 6 h (Schramm et al., 2003). This investigation supports that the phenolic compounds of honey are not only bioavailable but also exhibit attractive antioxidant activity for inducing defensive mechanism against oxidative stress.

Furthermore, evidence from literature support that the bioavailability of flavonoids is complicated due to their chemical structure. Flavonoids (in form of glycoside) encourage the Na^+ dependent transport of ATPase of monosaccharides in the epithelial cells of intestine. After that, they are generally hydrolyzed to aglycones for the absorbed by intestinal absorptive cells enterocytes. Interestingly, honeys flavonoids are present in form aglycones itself because of the presence of glycosidase enzyme in the salivary gland of bee, which may be maked easy to bioavailable of honey flavonoids (Alvarez-Suarez et al., 2013).

1.5. The potential impact of honey on human health

The potential health benefits of honey have attracted increasing interest due to its high content of several nutritive and non-nutritive bioactive compounds, which are implicated in various health-promoting and disease preventive effects. A plethora of studies have examined the benefits of honey and its bioactive compounds on wound management, antimicrobial effects, prevention of inflammation disorders and oxidative stress, reduction heart disease risk and protection against various types of cancer (Alvarez-Suarez et al., 2013; Pasupuleti et al., 2017).

Traditionally, honey is famous not only for its wound healing properties but also for its antimicrobial effects (Pasupuleti et al., 2017). Several evidences support that the sensitivity, specificity and effectiveness of honey are better than the conventional dressing agents and sometimes induce healing even in infected wound that does not cure by

antibiotics or antiseptics. However, the antioxidant and antimicrobial effects of honey prevent diabetic food ulcer, peptic ulcer and gastrointestinal disorder by suppressing microbial infection together with increasing healing process (Pasupuleti et al., 2017). Honey induced antioxidant defense system is previously proven by various experimental models by improving the antioxidant enzymes, decreasing the ROS, lipid per-oxidation and other oxidative stress (Alvarez-Suarez et al., 2016; Miguel et al., 2017). Moreover, honey shows antioxidant activities that have a potential preventive effect on the oxidative stress induced liver and pancreatic damaged. Additionally, significantly reduced blood glucose levels were observed after honey treatments (Pasupuleti et al., 2017).

Chronic inflammation is associated with numerous pathologies, including cardiovascular disease, atherosclerosis, metabolic syndrome, type 2 diabetes, Alzheimer's disease, and cancer. Considerable evidence supports that the ingestion of honey improves the anti-inflammatory effects by suppressing pro-inflammatory molecules, ROS and at the same time increasing immunostimulatory abilities (Miguel et al., 2017). In the case of upper respiratory tract infections, honey is used for the cough treatments because it is superior to other treatments (Shadkam et al., 2010). Honey consumption significantly decreases the risk of metabolic and cardiovascular diseases through improving vasodilatation, balancing vascular homeostasis, reduces the ability of platelets to form clots, and improves lipid profile and endothelial functions (Afroz et al., 2016).

As mentioned above, honey is a rich source of several bioactive compounds including sugars, minerals, vitamins and polyphenols, which are the most diffused and interesting compounds present in this food (Alvarez-Suarez et al., 2013). In the last few years, a large number of studies have observed the potential health benefits not only on raw honey but also on most of the phenolic compounds of honey starting from antioxidant capacity to anti-inflammatory, antibacterial, anti-hypertensive and anti-cancer capabilities (Khalil and Sulaiman, 2010; Pasupuleti et al., 2017; Subramanian et al., 2016).

1.5.1. Honey and cancer

Currently, cancer is a major public health issue in the world, associated with a high mortality rate. Nowadays, this is not a new concept that a healthy lifestyle and balanced diet are closely associated to a good human health and people are becoming more and more alarmed about it. Therefore, in the recent years, there has been much more attention on honey and its chemopreventive effects on various type of cancer. In laboratory studies

using cell cultures and experimental animal models, raw honey or purified bioactive compounds from honey have been implicated in a wide spectrum of anticancer activities from initiation to progression (Badolato et al., 2017; Porcza et al., 2016).

Several honey types have been used for investigated the growth inhibitory effects *in vitro* on different cancer cells. Acacia, Manuka, Tualang, Tyme, Gelam, Nenas, Buckwheat, Spanish and Indian honey induced cytotoxicity in breast cancer and liver cancer by suppressing cell proliferation, arresting cell cycle, modulating oxidative stress, inducing DNA repair, activating apoptosis and anti-inflammation, modulating immune response, activating tumor-suppressor genes and suppressing oncogenes, regulating growth-factor, inhibiting invasion, angiogenesis and metastasis by targeting diverse range of molecular mechanisms. Additionally, in contrast limited but promising studies are available for other forms of cancers including skin, oral, bone, prostate, bladder, endometrial, kidney and cervix (Badolato et al., 2017; Erejuwa et al., 2014; Porcza et al., 2016).

There is an increasing amount of evidence in the literature about the antiproliferative, anticancer and antimetastasis effects of honey in rodent model of cancer. Manuka, Tualang, Gealm, pure unfractionated and Jungle honey suppressed melanoma, breast, liver, lung and bladder cancer progression through improving the survival rate of animal, increasing pro-apoptotic proteins, suppressing inflammation, stimulating the immune system, inhibiting angiogenesis and invasion by modulation of multiple molecular targets (Badolato et al., 2017; Erejuwa et al., 2014; Porcza et al., 2016).

Additionally, a positive correlation has been found between the anticancer activity and the amount of flavonoids (apigenin, chrysin, quercetin, pinocembrin and acacetin) and phenolic acids (*p*-coumaric, caffeic, ellagic, vanillic, protocatechuic and *p*-hydroxybenzoic acids) present in honey (Badolato et al., 2017; Miguel et al., 2017). Regarding colon cancer, several *in vitro* cell studies have exposed consistent anticancer effects of Gelam, Nenas, Manuka and Indian honey, including inhibition of cell proliferation, suppression of inflammation, DNA damage, arresting cell cycle, increasing ROS generation, apoptotic effects, modulating growth factors and suppressing invasion. These effects are mediated by the regulation of cyclins and cyclin-dependent kinases that induce cell cycle arrest (mainly at G_1/S phase), whereas apoptosis is mediated by activation of caspases 3, 9, cleavage of poly (ADP-ribose) polymerase (c-PARP), upregulation of Bax and downregulation of Bcl-2, and activation of MAPK pathway. Furthermore, an anti-inflammatory effect is mediated by suppressing the expression of NFκB and pro-inflammatory cytokines while anti-

invasive effects is associated by decreasing the MMP-2 and MMP-9 activity (Subramanian et al., 2016).

As mention above, though a lot of studies have observed the chemopreventive effects of honey on colon cancer cells, in our present works we try to focus on the preventive effects of MH and Strawberry tree honey (STH) on different points of view focusing from initiation to progression by targeting different signaling pathways and finally observing the synergistic or addictive effects on chemotherapeutic drug. In Figure 1.19 the principal mechanisms of action proposed for MH and STH protection in colon cancer are summarized.

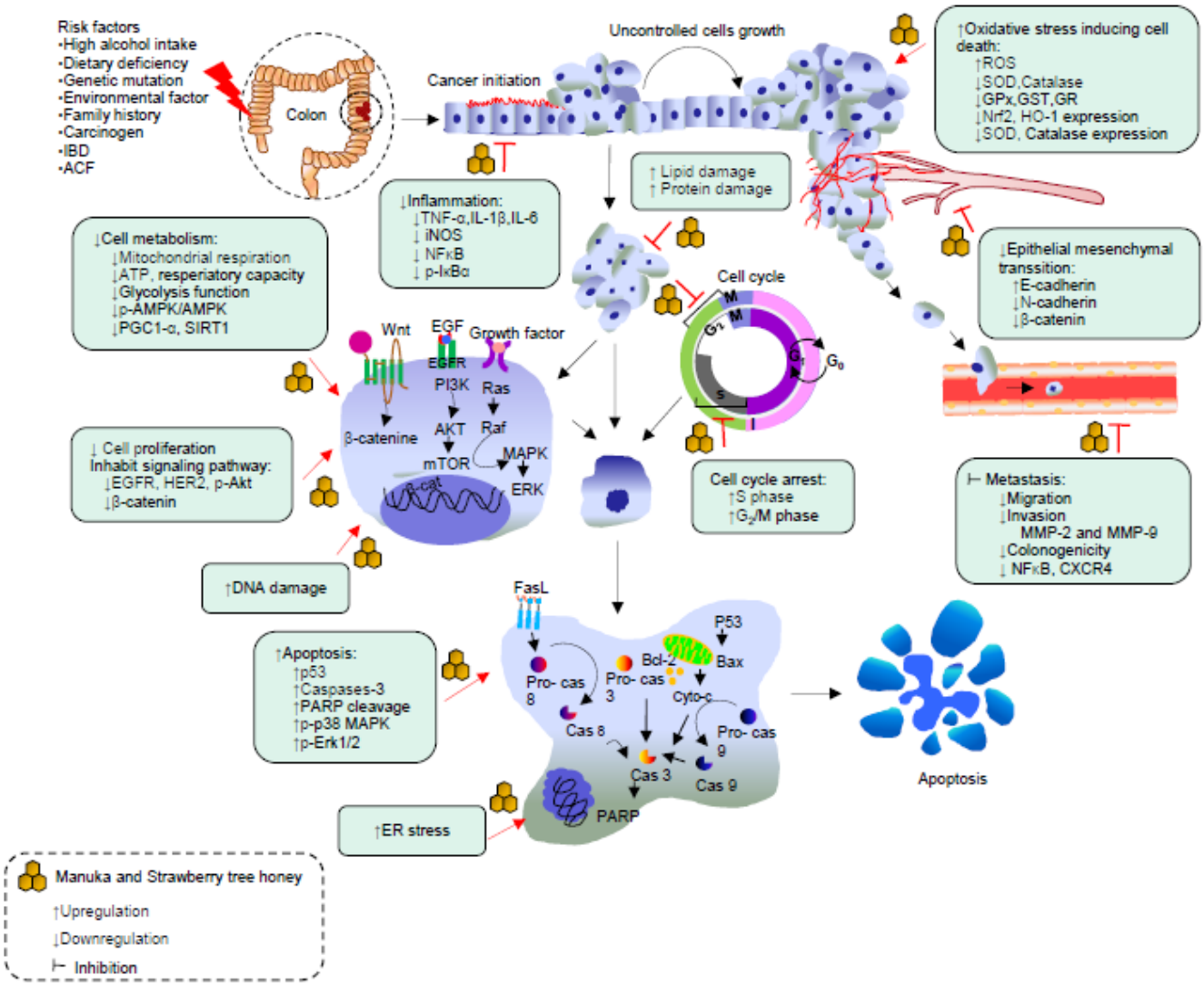

Figure 1.19. Proposed mechanisms for Manuka honey (MH) and Strawberry tree honey (STH) actions in colon cancer cells by targeting on cellular functions and signal transduction pathways associated with anti-inflammatory, antiproliferative, cell cycle regulation, apoptotic, oxidative stress, metabolism alteration, endoplasmic reticulum (ER) stress and anti-metastasis mechanism. Figure slightly modified form Afrin et al., (2016).

OBJECTIVE

The main objective of the present work was **to evaluate the anticancer potential of MH and STH on *in vitro* colon cancer models targeting on different molecular aspects**.

For such purpose two cell models were used: human colon adenocarcinoma cells (HCT-116) and Dukes' type C, grade IV, colon metastasis cells (LoVo), which were treated with MH and STH and the following specific objectives were set:

1. To characterize the phytochemical contents and their antioxidant capacity MH and STH honey.
2. To evaluate the growth inhibitory effects of MH and STH on human colon cancer cells through performing cell viability, cell cycle, apoptosis and intracellular ROS production assay.
3. To evaluate effect of MH and STH on the expression of proteins related to inflammation, apoptosis, ER stress and EGFR signaling in both colon cancer cell lines.
4. To characterize the energy metabolism by observing several parameters of mitochondrial respiration or oxygen consumption rate (OCR) and glycolysis or extracellular acidification rate (ECAR) in both colon cancer cell lines.
5. To determine the anti-metastasis effects of MH and STH human colon cancer cells through migration and colony formation assay, as well as by observing the expression of invasion, EMT and metastasis markers.
6. To evaluated the synergistic or additive effects of MH and STH on one of the most used chemotherapeutic drug in both colon cancer cell lines.

CHAPTER 2. MATERIALS AND METHOD

2. MATERIALS AND METHODS

2.1. Honey samples

MH is a well-known honey worldwide and has been extensively studied. The sample of MH originating from New Zealand was imported to Italy by EfitSrl (Figure 2.1a). STH samples were collected from 5 different areas of Sardinia, Italy, namely Monti, Luras, Sadali, Olbia and Berchidda area (Figure 2.2b). All samples were stored at 4°C before analysis.

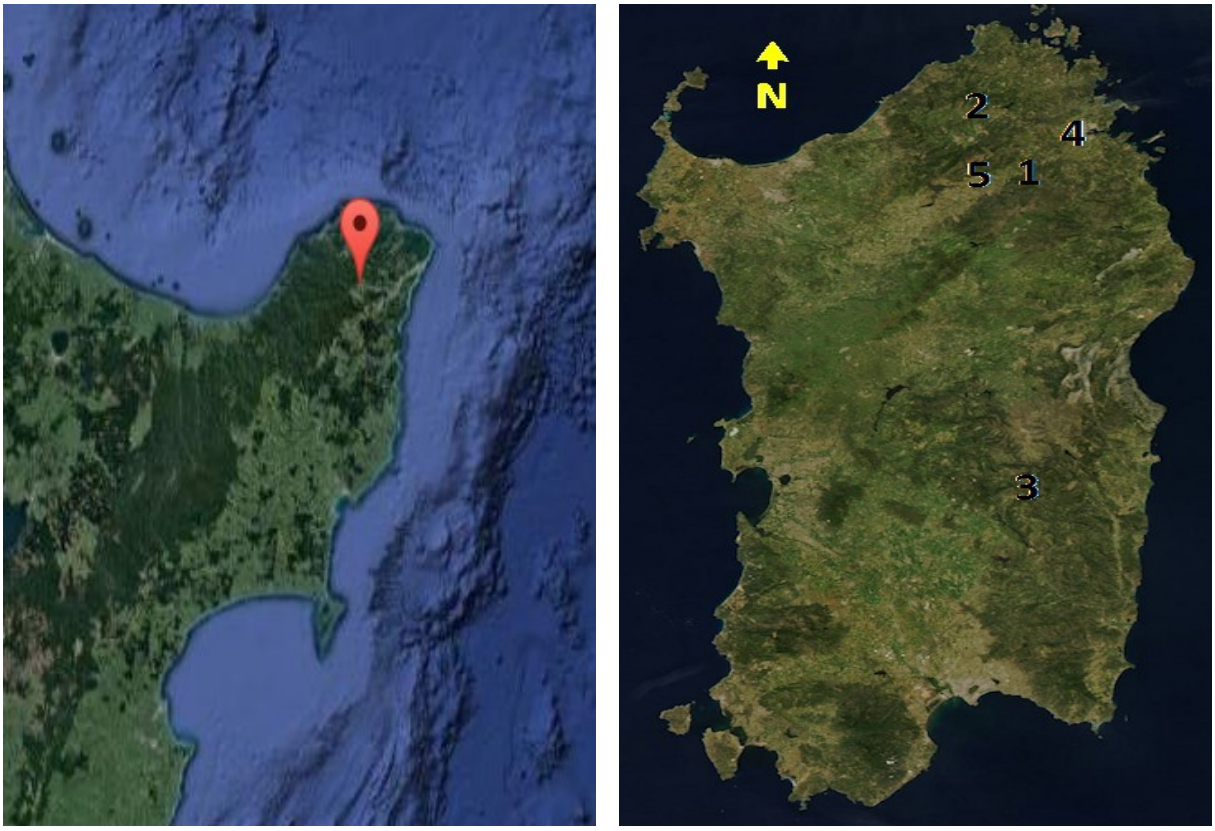

Figure.2.1. Geographical origin of the MH and five STH samples. MH originated from New Zealand (a) and STH originated from Sardinia (b). In brackets, the GPS DD coordinates of each sampling site. 1, Monti (40.80137 N, 9.34511 E); 2, Luras (40.97606 N, 9.16776 E), 3, Sadali (39.81678 N, 9.27006 E); 4, Olbia (40.92334 N, 9.50395 E); 5, Berchidda (40.784760 N, 9.165100 E).

2.2. Reagents and antibodies

All reagents were purchased from Sigma-Aldrich (Milan, Italy), Extrasynthese (Genay, France) and SAFC (St. Louis, MO, USA). The primary antibodies p53, caspase-3, cleaved-PARP (c-PARP), NFκB, phosphorylated (p)-IκBα, IL-1β, IL-6, iNOS, TNF-α, p-p38MAPK, p-Erk1/2, EGFR, HER2, p-Akt, 8-Oxoguanine DNA glycosylase (OGG1),

Nrf2, superoxide dismutase (SOD), catalase, hemeoxygenase 1 (HO-1), ATF6, XBP1, p-AMPK, PGC1α, SIRT1, MMP-2, MMP-9, E-cadherin, N-cadherin, β-catenin, C-X-C chemokine receptor type 4 (CXCR4) and glyceraldehyde-3-phosphate dehydrogenase (GADPH) were purchased from Santa Cruz Biotechnology (Dallas, TX, USA), while goat anti-rabbit IgG peroxidase secondary antibody was purchased from Sigma-Aldrich (Milan, Italy). The Tali® Cell Cycle Kit, Tali™ Apoptosis Assay Kit-Annexin V Alexa Fluor® 488 and Tali™ CellROX® Orange Reagents were purchased from Invitrogen TM, Life Technologies (Milan, Italy). Purified Millipore water was used throughout this works.

2.3. Determination of total polyphenol content and total flavonoid content

Polyphenol and flavonoid contents of honey samples were determined according to procedures previously described by Alvarez-Suarez et al., (2010a) with minor modifications. Total polyphenol content (TPC) was determined based on the Folin–Ciocalteu method. One gram of honey sample was dissolved in 10 mL distilled water and filtered through Minisart filter of 45 μm (PBI International). In 500 μL of filtered sample 2.5 mL of 0.2 N Folin–Ciocalteu reagents were added and kept 5 min at room temperature. Then it was mixed with 0.7 M Na_2CO_3 and incubated in the dark at room temperature for 2 h. The absorbance was measured at 760 nm using a Beckman Du 640 spectrophotometer (Instruments Inc., Fullerton, CA, USA). Gallic acid was used as a standard to calculate the calibration curve (50-300 mg/L). TPC was expressed as g of gallic acid equivalents (GAE) per kg of honey. For determination of total flavonoid content **(**TFC), 250 μL of honey solution (50% w/v in methanol) was mixed with 1.25 mL distilled water and 75 μL of a 5% NaNO2 solution. After 6 min, 150 μL of 10% $AlCl_3.H_2O$ solution was added, and after a wait of another 5 min 500 μL 1 M NaOH was added. Then the mixture was brought to 2.5 mL with the addition of distilled water and the absorbance was measured at 515 nm using a Beckman Du 640 spectrophotometer (Instruments Inc., Fullerton, CA, USA). (+)-Catechin was used as a standard to calculate the calibration curve (5-50 mg/L). TFC was expressed as mg of (+)-catechin equivalents (CAE) per kg of honey.

2.4. Extraction, identification and quantification procedure for phenolic compounds

2.4.1. Solid-phase extraction and HPLC condition

Honey samples were pre-concentrated with Strata X-A cartridges 33u Polymeric Strong Anion sorbent (60 mg, 3 mL size) from Phenomenex (Torrance, CA, USA). The solid-

phase extraction (SPE) method was carried out according to a slight modification of Dimitrova et al., (2007) and Sun et al., (2016). HPLC measurements were made by using a Thermo Scientific System equipped with a Spectra SYSTEM P 4000 pump, a Spectra SYSTEM AS 3000 autosampler and a Finnigan Surveyor PDA Plus Detector. Chromatographic separations were performed with a Luna C18 analytical column (150 x 3 mm ID, 3-µm particle) with a guard column (4 x 3 mm ID) containing the same packing material, both from Phenomenex (Torrance, CA, USA).

2.4.2. Determination of flavonols and phenolic acids

An aliquot of honey extract (20 µL) was injected into the column and eluted at 35°C with a constant flow rate of 0.4 mL/min. The mobile phase was composed of water/formic acid/acetonitrile (87:10:3), v/v/v; Component A) and water/formic acid/acetonitrile (40:10:50, v/v/v; Component B) for flavonols and for phenolic acids the mobile phase was composed of 2% (v/v) acetic acid in water (Component A) and of acetic acid in water and acetonitrile (1:49:50, v/v/v; Component B). The following gradient was used for flavonols: 90% A, changed to 75% A in 10 min, changed to 69% A in 5 min, changed to 60% A in 5 min, changed to 50% A in 10 min, changed to 0% in 10 min, held for 5 min and, finally changed to 90% A in 5 min giving an analysis time of 50 min. Similarly, for phenolic acid the following gradient was used: 90% A for 10 min, changed to 45% A in 50 min, changed to 2% A in 10 min, changed to 90% A in 2 min and, finally held for 10 min giving an analysis time of 82 min. A photodiode-array detector was employed in full-scan mode (range between 200 and 600 nm) for the determination of phenolic acids and flavonols.

2.5. Determination of total protein and free amino acid content

The protein content of honey was determined by Bradford's method (Bradford, 1976). A 100 µL honey solution (50% w/v in methanol) was added to 5 mL of the Coomassie Brilliant Blue reagent mixture. The Coomassie Brilliant Blue formed a blue complex with the protein. After incubation (2 min), the absorbance was determined at 595 nm against the blank (the reactive solution without the sample) using a spectrophotometer (Beckman Du 640, Beckman, Brea, CA, USA). Bovine serum albumin (BSA) was used as a standard for calculating the calibration curve (10-100 µg/0.1 mL) in 0.15 M NaCl. The protein content was expressed as g of BSA per 100 g of honey.

The free amino acid content was measured with the Cd-ninhydrin method as performed by Doi et al., (1981). The reaction solution consisted of 0.8 g of ninhydrin mixed in 80 mL of 99.5% ethanol and 10 mL of acetic acid, followed by adding a solution of 1.24 g of cadmium chloride hemi (pentahydrate) in 1 mL of distilled water. Honey sample (1.25 g) was diluted into 25 mL of distilled water. Next, 1 mL of honey solution was added in 2 mL of the reaction solution and heated for 5 min at 84 °C, and then cooled in ice. The absorbance was determined at 507 nm against the blank (the same mixture without the sample) using a spectrophotometer (Beckman Du 640, Beckman). L-Leucine was employed for the calibration curve (1.2-42 mg/L), and free amino acid content was expressed as mg of L-Leucine equivalents (LE) per 100 g of honey.

2.6. Determination of total antioxidant capacity

For total antioxidant capacity **(**TAC) determination of honey samples, three different methods were used: the FRAP, the TEAC and the DPPH assays.

2.6.1. Ferric reducing antioxidant power assay

The FRAP assay was performed according to a modified method as described by Benzie and Strain, (1996). The principle of this method is based on the reduction of a ferric 2,4,6-tripyridyl-S-triazine complex (Fe^{3+}-TPTZ) to its ferrous colored form (Fe^{2+}-TPTZ) in the presence of antioxidants. One gram of honey sample was dissolved in 10 mL of distilled water and then 200 µL of diluted honey solution was mixed with 1.8 mL FRAP reagent. The fresh FRAP reagent contained 2.5 mL of a 10 mM TPTZ solution in 40 mM HCl, 2.5 mL of 20 mM $FeCl_3$ and 25 mL of 0.3 M acetate buffer, pH 3.6 and kept in the dark at 37°C. The reaction mixture was incubated at 37°C for 10 min and the absorbance was measured at 593 nm using a Beckman Du 640 spectrophotometer (Instruments Inc., Fullerton, CA, USA). Trolox (15-200 mM) and ammonium ferrous sulphate (25-250 mM) was used as the standard to calculate the calibration curves. The results were expressed as mmoles of Trolox equivalents (TE) per 100 g of honey and mmoles of ammonium ferrous sulphate ($Fe^{(II)}$) per 100 g of honey.

2.6.2. Trolox equivalent antioxidant capacity assay

The TEAC assay was performed according to the method previously described by Re et al., (1999). This method is based on the ability of antioxidant compounds to quench the 2,2′-azino-bis (3-ethylbenzothiazoline-6-sulfonic acid) (ABTS) radical cation ($ABTS^{+}$) and reduce the radical to the colorless neutral form. The solution of ABTS radical cation ($ABTS^{+}$) was produced by reacting 7 mM ABTS aqueous stock solution with 2.45 mM K_2SO_4 and maintained in the dark at 25°C for 12 h before use. Immediately before analysis, the working solution was obtained by diluting the stock solution with ethanol. One gram of honey sample was diluted in 1 mL distilled water, and then 10 µL of sample was added in 1 mL of $ABTS^{+}$ working solution. The reaction mixture was incubated at room temperature for 90s and the color inhibition of the $ABTS^{+}$ radical was measured at 734 nm using a Beckman Du 640 spectrophotometer (Instruments Inc., Fullerton, CA, USA). The percentage of radical-scavenging activity (RSA) was calculated according to the following equation: % RSA = (Abs control - Abs sample/Abs control) x 100, where Abs is the absorbance. Trolox was used for the calibration curve (50-500 µM), and the results were expressed as mmol of TE per 100 g of honey.

2.6.3. Diphenyl-1 picrylhydrazyl assays

DPPH radical assay was performed to determine the free radical-scavenging activity of honey based on the modified method described by Ferreira et al., (2009). This method is based on the ability of DPPH to react with the phenolic compounds present in the honey sample. The DPPH radical is a persistent molecule, characterized by its violet color. One gram of honey is dissolved in 1 mL of distilled water then 300 µL of this solution is mixed with 2.7 mL of methanolic solution containing DPPH radicals (6 $X10^{-5}$ mol/L). The inhibition of the DPPH radical was calculated by measuring the absorption at 515 nm using a Beckman Du 640 spectrophotometer (Instruments Inc., Fullerton, CA, USA). The percentage of RSA was calculated according to the following equation: % RSA = (Abs control - Abs sample/Abs control) x 100, where Abs is the absorbance. Trolox was used for the calibration curve (50-500 µM), and the results were expressed as mmol of TE per 100 g of honey.

2.7. Preparation of artificial honey

An artificial honey (AH) was prepared by the slightly modified method described by Alvarez-Suarez et al., (2016). The honey sample containing the main sugars component which presents in natural honey samples: 100g AH was prepared by dissolving 1.5 g of sucrose, 7.5 g of maltose, 40.5 g of fructose and 33.5 g glucose in 17 mL of purified water. This AH was used to determine the viability of cells to evaluate the contribution of honey sugars to the cytotoxic effects on colon cancer cells.

2.8. Cell culture

To carry out the experimental design three cell lines were used: human colon carcinoma (HCT-116), Dukes' type C, grade IV, colon metastasis (LoVo) and normal human dermal fibroblast (HDF). HCT-116, LoVo and HDF cells were purchased from the American Type Culture Collection (ATCC, Manassas, VA, USA) and cultured as recommended by this biological research center. Media and reagents for cell culture were obtained from Carlo Erba Reagents (Milan, Italy). McCoy's 5A media with addition of 10% heat-inactivated fetal bovine serum and 100 IU/mL penicillin and 100 µg /mL streptomycin were used for HCT-116 cell culture and F-12K medium with addition of 10% heat-inactivated fetal bovine serum and 100 IU/mL penicillin and 100 µg /mL streptomycin were used for LoVo cell culture. Finally, DMEM media with addition of 10% heat-inactivated fetal bovine serum and 100 IU/mL penicillin and 100 µg /mL streptomycin was used for HDF cells. The cells were sub-cultured until 80-90% of confluence. All the cell lines were maintained in an incubator at 37°C in a humidified atmosphere (95% air, 5% CO2). For maintenance the cell culture, the medium was replaced every 2 to 3 days and cells were passaged at 80 to 90% confluence by trypsinization. For the subsequent experiment, cells were used between the 6^{th} and 10^{th} passages.

2.9. Determination of cell viability by MTT assay

Cells were seeded at a density of 5×10^3 cells/well into 96-well plates using the specific complete growth medium. To allow cell attachment, they were incubated overnight. After overnight incubation, the HCT-116 cells were treated with 0 to 20 mg/mL of MH and STH for 24, 48 and 72 h. Similarly, LoVo and HDF cells were treated with 0 to 60 mg/mL of MH and STH for 24, 48 and 72 h. AH was used for treated both cell lines at a

concentration 0 to 20 mg/mL for HCT-116 cells and 0 to 60 mg/mL for LoVo cells for the similar time's incubation.

Serially diluted test samples of 5-FU ranging from 0 to 100 µM were used for treated HCT-116 and LoVo cells for 24 and 48 h. Finally, in HCT-116 cells the combination treatment of 5-FU with 5, 10, 20 and 50 µM concentrations was supplemented with dosages of 5, 10 and 15 mg/mL of MH and 3, 6 and 9 mg/mL of STH for 48 h. Similarly, in LoVo cells the combination treatment of 5-FU with 10, 20, 50 and 80 µM concentrations were supplemented with dosages of 20, 30 and 40 mg/mL of MH and 10, 20 and 30 mg/mL of STH for 48 h.

After the treatment time, 30 µL of RPMI medium containing 2 mg/mL of the 3-(4,5-Dimethyl-2-thiazolyl)-2,5-diphenyl-2H-tetrazolium bromide (MTT) were added and cells were incubated for other 2 to 4 h. The generated formazan crystals were dissolved by adding 100 µL of dimethyl sulfoxidein each well and measured by a microplate reader (Thermo Scientific Multiskan EX, Thermo Fisher Scientific, Waltham, MA, USA) at 590 nm. The proportion of viable cells was computed as absorbance of treated cells/ absorbance of control cells x100. The final results were expressed as the concentration that inhibits cell growth by 50% (IC_{50} values) versus control cells (untreated cells).

The effectiveness of 5-FU, in combination with MH and STH to inhibit cell growth of HCT-116 and LoVo, was determined by combination index (CI) (Chou, 2006). CI was calculated according to the equation CI= (Dose of 5-FU)/ (IC_{50} of 5-FU) + (Dose of MH or STH)/ (IC_{50} of MH or STH) for each drug and honey combination tested. Therefore, the fractional inhibitory concentrations were calculated by dividing the concentrations of each 5-FU and MH or STH that in combination inhibited the cell growth by 50% (IC_{50}) by the concentrations required to reach the IC_{50} of each 5-FU and MH or STH separately. In this equation, the sum of 5-FU and MH or STH reveals 50% inhibition of cell survival. CI below 1 indicate synergism, 1 to 1.2 indicate addition effects and above 1.2 indicate antagonism effects.

2.10. Cell cycle analysis by Tali® Image-Based Cytometer

Cell cycle analysis was determined by the Tali® Cell Cycle Kit containing propidium iodide (PI), RNase A, and Triton® X-100 to label cells for cell cycle analysis using the Tali® Image-Based Cytometer (ThermoFisher Scientific, Milan, Italy). Cell were cultured

in 6-well plates, at a density of 4×10^5 cells/ well and incubated with various concentration of MH 0, 5, 10, 15, 20 mg/mL for HCT-116 cells and 0, 20, 30, 40 and 50 mg/mL for LoVo cells for 48 h. Similarly, STH was used at a concentration of 0, 3, 6, 9 and 12 mg/mL for HCT-116 cells and 0, 10, 20, 30, 40 mg/mL for LoVo cells for 48 h. These concentrations were chosen according to the MTT viability assay ensuring 80 to 40% cells were viable at 48 h. The IC_{50} values of 5-FU, MH, STH and combination doses of MH+5-FU and STH+5-FU were also used for treated the cultured cells in 6-well plates for 48 h.

Then, cells were trypsinized and centrifuged for 5 min at 500 x *g* after removing the excess media, resuspending with PBS, centrifuging for 5 min at 500 x *g* and transferring the cells into ice. Briefly, the cells were harvested and fixed with 70% cold ethanol at -20°C overnight. The fixed cells were washed twice with PBS, re-suspended in 100 µL PBS-based PI solution containing 0.1% Triton® X-100, 0.2 mg/ml RNase A (Invitrogen), and 20 µg/ml PI (Invitrogen), and incubated for 30 min at room temperature protected from the light. For each sample, 25 µL of cell suspension was loaded into one Tali™ Cellular Analysis Slide's chamber (Invitrogen) and analyzed in the Tali™ Image-Based Cytometer. The results were expressed as the percentage of cells in each phase and all data were reported as a mean value of three independent analyses ± standard deviation (SD).

2.11. Determination of apoptotic cells by Tali® Image- Based Cytometer

Apoptotic cells were identified by the Tali™ Apoptosis Assay Kit–Annexin V Alexa Fluor® 488 (Invitrogen) according to manufacturer's instructions. Cells were seeded at a density of 1.5×10^5 cells/well into 6 well and treated for 48 h with the MH (0, 5, 10, 15 and 15 mg/mL for HCT-116 cells and 0, 20, 30, 40 and 50 mg/mL for LoVo cells) and STH (0, 3, 6, 9 and 12 mg/mL for HCT-116 cells and 0, 10, 20, 30 and 40 mg/mL for LoVo cells). These concentrations were chosen according to the MTT viability assay ensuring 80 to 40% cells were viable at 48 h. The IC_{50} values of 5-FU, MH, STH and combination doses of MH+5-FU and STH+5-FU were also used for treated the cultured cells in 6-well plates for 48 h.

Cells were harvested 48 h post-treatment and centrifuged for 15 min at 1500 rpm at 4°C. After removing the supernatant and re-suspending the cells with 100 µL of Annexin binding buffer (ABB, Component C), 5 µL of Annexin V Alexa Fluor® 488 (Component A) was added to each 100 µL of re-suspended cells. The mixture of cell and Annexin V

Alexa Fluor® 488 was incubated at room temperature into the dark for 20 minutes and then again centrifuged. After removing the excess mixture and re-suspending with 100 µL of AB, samples were incubated at room temperature into the dark for 1 to 5 minutes after adding 1 µL of Tali™ PI (component B). For each sample, 25 µL of cell suspension was loaded into one Tali™ Cellular Analysis Slide's chamber and analyzed in the Tali™ Image-Based Cytometer. The instrument works at different excitation/emission wavelengths: 530/580 nm and 458/495 nm for the PI and Annexin V, respectively. The Tali™ Image-Based Cytometer was evaluated the live, apoptotic and dead cells. The annexin V-negative/PI negative cells were identified as viable cells by the cytometer software whereas the annexin-V positive/PI negative cells were recognized as apoptotic cells. Similarly, the annexin V positive/PI positive cells were identified as dead cells. All data were reported as a mean value of three independent analyses ± SD.

2.12. Determination of intracellular ROS levels by Tali® Image-Based Cytometer

Intracellular ROS accumulation was determined by the CellROX® Oxidative Stress kit following the manufacturer's instructions. Cells were seeded at a density of 1.5×10^5 cells/well into 6 well plates and incubated for 48 h with the MH (0, 5, 10, 15 and 15 mg/mL for HCT-116 cells and 0, 20, 30, 40 and 50 mg/mL for LoVo cells) and STH (0, 3, 6, 9 and 12 mg/mL for HCT-116 cells and 0, 10, 20, 30 and 40 mg/mL for LoVo cells). These concentrations were chosen according to the MTT viability assay ensuring 80 to 40% cells were viable at 48 h. The IC_{50} values of 5-FU, MH, STH and combination doses of MH+5-FU and STH+5-FU were also used for treated the cultured cells in 6-well plates for 48 h.

Cells were harvested 48 h post-treatment and centrifuged for 10 min at 1500 rpm. Next, CellROX® Orange reagent (2 µL/ mL) was added and cells were incubated at 37°C for 30 min. Again, cells were centrifuged for 10 min at 1500 rpm to take out excess dye and medium and then resuspended with 100 µL PBS. For each sample, 25 µL of cell suspension was loaded into one Tali™ Cellular Analysis Slide's chamber and analyzed in the Tali™ Image-Based Cytometer. In this assay, "RFP fluorescence" (530 nm EX/580 nm EM) represented the fluorescence signal from CellROX® Orange Reagent. Untreated cells, which were also labeled with CellROX® Orange Reagent, were used to determine baseline levels of oxidative activity. Cells are fluorescent in an oxidation state and non-fluorescent

in a reduced state. The results were expressed as the fold change and all data were reported as a mean value of three independent analyses ± SD.

2.13. Cellular lysates preparation

Cells were seeded in T75 flasks at a density of 4 x 10^4 cells/cm^2 and treated for the indicated times with the MH (0, 5, 10, 15 and 15 mg/mL for HCT-116 cells and 0, 20, 30, 40 and 50 mg/mL for LoVo cells) and STH (0, 3, 6, 9 and 12 mg/mL for HCT-116 cells and 0, 10, 20, 30 and 40 mg/mL for LoVo cells). These concentrations were chosen according to the MTT viability assay ensuring 80 to 40% cells were viable at 48 h. The IC_{50} values of 5-FU, MH, STH and combination doses of MH+5-FU and STH+5-FU were also used for treated the cultured cells in 6-well plates for 48 h. After the treatment time, the medium was removed and cells were washing two times with PBS.

The cellular lysates were prepared by using the RIPA buffer (Sigma-Aldrich, Milan, Italy) for the oxidative marker (lipid and protein) and antioxidant enzyme activity determination. One mL RIPA buffer (Sigma-Aldrich, Milan, Italy) was added into each flask after the desire treatments and the cells were incubated at 4°C for 5 to 8 minutes. After the incubation time cells were scraped and collected in a micro-centrifuge tube and stored at -80°C until analysis. Before analysis, the cells lysates were thawed at 4°C and centrifuged at 8000 x *g* for 10 minutes at 4°C for the precipitation of cells debris.

2.14. Determination of oxidative stress markers

2.14.1. Determination of lipid peroxidation by TBARS assay

Lipid peroxidation was quantified by the thiobarbituric acid-reactive substances (TBARS) assay according to a modified method described by Ohkawa et al., (1979). Briefly, 300 µL of cellular lysate was mixed with thiobarbituric acid reagent (TBA, 0.37% in 0.2 M HCl) and 15 % trichloroacetic acid (TCA) and heated at 95 °C for 20 min. Then, the mixture was cooled, centrifuged at 1200 *x g* for 15 min at 4°C and the absorbance of supernatant was measured at 532 nm in a Beckman DU-640 spectrophotometer. The amount of the formed MDA was calculated considering the MDA extinction coefficient as 1.56 x 10^5 M^{-1} cm^{-1}. The MDA values were calculated using 1,1,3,3-tetraethoxypropane as standard and expressed as nmoles of MDA per mg of proteins. All data were reported as a mean value of three independent analyses ± SD.

2.14.2. Determination of protein carbonyl content

Protein carbonyl content was determined by the dinitrophenylhydrazine (DNPH) method as previously described by Levine, (1990) with minor modifications. This method is based on the reaction between DNPH and protein carbonyl, appearance a schiff base to produce the corresponding hydrazone that can be detected spectrophotometrically. Briefly, 25 µL of cellular lysate was taken in two micro-centrifuge tubes with 25 µL of TCA (20%), then centrifugation at 2800 x *g* for 10 min at 4°C. One micro-centrifuge tube represented the sample and another one the control. Then added 750 µL of DNPH (10 mM) in the treatment tubes and 250 µL of HCl (2.5 M) into the control tubes and incubated 1 h in the dark at room temperature with stirring at every 15 min interval. After the incubation, 750 µL of TCA (10%) was added into both the solutions (treatment and control) and again incubated at room temperature for another 15 min. The mixture was centrifuge for 10 min at 3400 x *g* at 4°C and the sample precipitation were washed two times with 500 µL of an ethanol-ethylacetate (1:1) solution to remove excess DNPH and the final precipitations were dissolved in 625 µL of guanidine hydrochloride (6 M). Lastly, for removing the left over debris, the samples were centrifuged for 10 min at 3400 x *g* at 4°C and the absorbance of supernatant was measured at 370 nm in a microplate reader (Thermo Scientific Microplate Reader, Multiskan® EX, USA), against the control. The protein carbonyl content was expressed as nmole per mg protein. All data were reported as a mean value of three independent analyses ± SD.

2.15. Determination of antioxidant enzyme activity

2.15.1. Determination of glutathione peroxidase

The activity of glutathione peroxidase (GPx) was measured by the modification method was previously described by Sies et al., (1979). The assay is based on the ability of GPx to remove H_2O_2 by coupling its reduction to H_2O with oxidation of reduced glutathione. Briefly, 50 µL of cellular lysate or 50 µL of PBS-EDTA buffer (for the blank) was mixed with 795 µL of PBS-EDTA buffer (50 mM to 0.40 mM, pH 7.4), 25 µL of glutathione (40 mM), 25 µL of glutathione reductase (5 UI/mL), 50 µL of sodium azide (1 mM) and 50 µL NADPH (2 mM). Finally, the reaction was started by adding 5 µL of H_2O_2 (0.25 mM) and the GPx activity was determined by the disappearance of NADPH in the samples. The intensity was measured at 340 nm against blank at 10 s intervals for 3 min, in a Beckman DU-640 spectrophotometer. The results were expressed as nmole of NADPH oxidizes per

min per mg of protein. All data were reported as a mean value of three independent analyses ± SD.

2.15.2. Determination of glutathione transferase

The activity of glutathione transferase (GST) was measured by the modification method was previously described by Habig et al., (1974). This method is based on the capacity of GST to conjugate 1-chloro-2,4-dinitro benzene (CDNB) with reduced glutathione and producing a dinitrophenyl thioether which can be easily measured. Briefly, 300 µL of cellular lysate or 300 µL of PBS (for the blank) was mixed with 1.475 mL of PBS (100 mM, pH 6.8), 200 µL of reduced glutathione (1 mM) and 25 µL of CDNB (1 mM). The development of CDNB- glutathione conjugate was measured immediately and after 1 min against blank at 340 nm in a Beckman DU-640 spectrophotometer. The results were expressed as the amount of enzyme producing 1 mmol of CDNB- glutathione conjugate per min per mg protein. All data were reported as a mean value of three independent analyses ± SD.

2.15.3. Determination of glutathione reductase

The activity of glutathione reductase (GR) was measured by the modification method was previously described by Carlberg and Mannervik, (1985). This assay is based on the capacity of GR to reduce oxidized glutathione reverse to reduced glutathione. Briefly, 50 µL of cellular lysate or 50 µL of PBS (for the blank) was mixed with 800 µL of PBS (100 mM, pH 7.6), 50 µL of EDTA (0.5 mM), 50 µL of NADPH (2 mM) and 50 µL of glutathione disulphide (20 mM). The activity of GR was determined following the NADPH oxidation in the samples. The intensity was measured at 340 nm against blank at 10 s intervals for 3 min, in a Beckman DU-640 spectrophotometer and the results were expressed as nmole of NADPH oxidized per min per mg protein. All data were reported as a mean value of three independent analyses ± SD.

2.15.4. Determination of superoxide dismutase

The activity of SOD was measured by the method described by Kakkar et al., (1984) with slight modification. In this method, the SOD activity was determined by using a superoxide radical generator (chemical, photochemical or enzymatic) and a detector (blue tetrazolium, NBT). The NBT is reduced to formazan, a blue chromogen in the presence of superoxide.

The intensity of blue chromagen can be measured by 540 to 560 nm in a Beckman DU-640 spectrophotometer. Briefly, 100 µL of cellular lysate or 100 µL PBS (for the blank) was mixed with 600 µL of sodium pyrophosphate buffer (0.025 M, pH 8.3), 50 µL of phenazine methosulphate (186 µM), 150 µL of NBT (300 µM) and 500 µL de-ionized water. Finally, the reaction was started by adding 100 µL of NADH and the mixture was incubated at 30°C for 90 seconds. The reaction was blocked by the addition of 500 µL of glacial acetic acid and the mixture was shaken by adding 2 mL of n-butanol. Then the tube allowed standing for 10 min at room temperature and centrifuge at 1500 rpm for 1 min. The intensity of the chromogen in the butanol layer was measured at 540 nm in a microplate reader (Thermo Scientific Microplate Reader, Multiskan® EX, USA) coupled to an Ascent software (Thermo LabSystems Oy, Version 2.6). To realize a standard curve, a serial standard dilution of SOD (ranging from 25 to 500 IU/mL) was treated and read together with the samples. All data were reported as a mean value of three independent analyses ± SD.

2.15.5. Determination of catalase

The activity of catalase was measured by the modification method was previously described by Aebi, (1984). This assay is based on the decomposition of hydrogen peroxide by action of the enzyme. Briefly, 10 µL of cellular lysate or 10 µL of PBS (for the blank) was mixed with 990 µL of sodium phosphate buffer (50 mM; pH 7.0) and 600 µL of H_2O_2 (30%). The absorbance was decreased due to H_2O_2 degradations and it was measured at 240 nm against blank for 10 to 70 seconds of reaction, in a Beckman DU-640 spectrophotometer. One unit of catalase was defined as the amount of enzyme that decomposed 1 µmol of H_2O_2 per min per mg protein. All data were reported as a mean value of three independent analyses ± SD.

2.16. Bioenergetic assay

2.16.1. Determination of the mitochondrial functionality

The OCR, an indicator of mitochondrial respiration, was assessed by using mitochondrial stress kit by an Agilent Seahorse XF24 Analyzer (Seahorse Bioscience, North Billerica, MA, USA) according to the manufacturer's protocol. HCT-116 and LoVo cells were seeded in XF24 cell culture plate at a density of 3.0 $X10^4$ cells/ well and allowed to adhere for 20 to 24 h. After that, the cells were treated with MH (0, 5, 10, 15 and 15 mg/mL for

HCT-116 cells and 0, 20, 30, 40 and 50 mg/mL for LoVo cells) and STH (0, 3, 6, 9 and 12 mg/mL for HCT-116 cells and 0, 10, 20, 30 and 40 mg/mL for LoVo cells). These concentrations were chosen according to the MTT viability assay ensuring 80 to 40% cells were viable at 48 h. The IC_{50} values of 5-FU, MH, STH and combination doses of MH+5-FU and STH+5-FU were also used for treating the cultured cells in XF24 plates for 48 h.

At the end of the incubation time, the medium was replaced with 500 µL/ well of XF assay media (supplemented with 25 mM glucose, 2 mM glutamine, 1mM sodium pyruvate, without serum) and plates were pre-incubated in the absence of CO2 in the XF Prep Station at 37°C. In the intervention time, several inhibitors were loaded into the injection ports of the calibration plate: 55 µL oligomycin (an inhibitor of complex V, inhibits ATP synthesis by blocking the proton channel of the F0 portion ATP synthase), 61 µL of 2,4-dinitrophenol (2,4-DNP) (allowing protons to leak across the inner mitochondrial membrane and thus bypass ATP synthase) and 68 µL of rotenone/antimycin (an inhibitor of complex I and III respectively, shut down mitochondrial respiration and enable both the mitochondrial and non-mitochondrial fractions contributing to respiration), to reach working concentrations of 3 µg/mL, 300 µM and 1µM/10µM, respectively. Calibration plate was placed into the XF24 Extracellular Flux Analyzer, and at the end of the calibration plate was replaced by the plate containing the cells. A minimum of five wells per treatment were utilized in any given experiment.

Agilent Seahorse XF24 Analyzer allows for the sensitive measurement of multiple parameters of mitochondrial respiration, such as basal OCR, ATP-linked respiration, proton leak, spare respiratory capacity (SRC) and maximal respiration rate (MRC) from intact cultured cells after sequential addition of inhibitors. Following equation was used for determination of specific parameter,

ATP-linked respiration = Basal $_{\text{OCR value}}$ - Oligomycin $_{\text{OCR value}}$

Proton leak = Oligomycin $_{\text{OCR value}}$ - Rotanone / Antimycin $_{\text{OCR value}}$

SRC = 2,4-DNP$_{\text{OCR value}}$ - Basal $_{\text{OCR value}}$

MRC = 2,4-DNP$_{\text{OCR value}}$ - Rotanone / Antimycin $_{\text{OCR value}}$

OCR was reported in picomoles per minute (pmole/min) per 3.0 x 10^4 cells and all data were reported as a mean value of three independent analyses ± SD.

2.16.2. Determination of the glycolysis function

The ECAR, an indicator of glycolysis, was performed by glycolytic stress test an Agilent Seahorse XF24 Analyzer (Seahorse Bioscience, North Billerica, MA, USA) according to the manufacturer's protocol. HCT-116 and LoVo cells were seeded in XF24 cell culture plate at a density of 3.0 $X10^4$ cells/ well and allowed to adhere for 20 to 24 h. After that, the cells were treated with MH (0, 5, 10, 15 and 15 mg/mL for HCT-116 cells and 0, 20, 30, 40 and 50 mg/mL for LoVo cells) and STH (0, 3, 6, 9 and 12 mg/mL for HCT-116 cells and 0, 10, 20, 30 and 40 mg/mL for LoVo cells). These concentrations were chosen according to the MTT viability assay ensuring 80 to 40% cells were viable at 48 h. The IC_{50} values of 5-FU, MH, STH and combination doses of MH+5-FU and STH+5-FU were also used for treating the cultured cells in XF24 plates for 48 h.

At the end of the incubation time, the medium was replaced with 500 µL/ well of XF assay media without glucose and serum and plates were pre-incubated in the absence of CO_2 in the XF Prep Station at 37°C. In the intervention time, several inhibitors were loaded into the injection ports of the calibration plate: 55 µL of rotenone (1 µM, an inhibitor of complex I), 61 µL of glucose (30 mM, supply energy) and 68 µL of 2-Deoxy-D-glucose (2-DG), (100 mM, inhibits glycolysis by binding glucose hexokinase). Calibration plate was placed into the XF24 Extracellular Flux Analyzer, and at the end of the calibration was replaced by the plate containing the cells.

Agilent Seahorse XF24 Analyzer allows for the sensitive measurement of multiple parameters of glycolysis function, such as basal ECAR, glycolysis, glycolytic capacity and glycolytic reserve from intact cultured cells after sequential addition of inhibitors. A minimum of five wells per treatment was utilized in any given experiment. Following equation was used for determination of specific parameter,

Glycolysis = Glucose $_{\text{ECAR value}}$ - Basal $_{\text{ECAR value}}$

Glycolytic capacity = Glucose $_{\text{ECAR value}}$ – 2-DG $_{\text{ECAR value}}$

Glycolytic reserve = the amount of glycolytic capacity - the amount of glycolysis

ECAR was reported in pmole/min per 3.0 x 10^4 cells and all data were reported as a mean value of three independent analyses ± SD.

2.17. Wounding assay

Wounding assay was performed as previously described method by Liang et al., (2007). Briefly, a linear wound was created in HCT-116 and LoVo confluent cellular population

by scratching the base of the plate with a sterile pipette (200 µL) tip. After the scratch, cells were washed two times with PBS and incubated with specific media of each cells containing 2% serum. The wounds were then photographed at zero time and incubated for 48 h after the treatment. The media contained different treatments, such as MH (0, 5, 10, 15 and 15 mg/mL for HCT-116 cells and 0, 20, 30, 40 and 50 mg/mL for LoVo cells) and STH (0, 3, 6, 9 and 12 mg/mL for HCT-116 cells and 0, 10, 20, 30 and 40 mg/mL for LoVo cells). These concentrations were chosen according to the MTT viability assay ensuring 80 to 40% cells were viable at 48 h. The IC_{50} values of 5-FU, MH, STH and combination doses of MH+5-FU and STH+5-FU were also used for treating the cultured cells in 6 well plates for 48 h. After the incubation time, cells were fixed with methanol and stained with 0.2% methylene blue stain. The photographs were taken by light microscope and the wound area was calculated by Image J software for calculating of the percentage of wound closure after the treatments.

2.18. Colony formation assay

The colony formation assay was performed on the slightly modified method described by Waghela et al., (2015). HCT-116 and LoVo cells were seeded at a density of 5×10^5 cells/well into 6 well and allowed to adhere for 20 to 24 h. After that, the cells were treated with MH (0, 5, 10, 15 and 15 mg/mL for HCT-116 cells and 0, 20, 30, 40 and 50 mg/mL for LoVo cells) and STH (0, 3, 6, 9 and 12 mg/mL for HCT-116 cells and 0, 10, 20, 30 and 40 mg/mL for LoVo cells). These concentrations were chosen according to the MTT viability assay ensuring 80 to 40% cells were viable at 48 h. The IC_{50} values of 5-FU, MH, STH and combination doses of MH+5-FU and STH+5-FU were also used for treated the cultured cells in 6-well plates for 48 h. After the treatment time, cells were trypsinized and 1000 cells were seeded in a 6 well plate. Cells were allowed to grow for 10 to 12 days until small colonies were visible. The colonies were fixed with methanol and stained with 0.2% methylene blue stain.

The plating efficiency (PE) was considered by the ability of a single cell to survive and to grow in a form of colony. The PE was defined by the following formula: Percentage PE = (Number of colonies formed/Number of cells seeded) x100.

2.19. Protein extraction and western blotting

Cells were seeded in T75 flasks at a density of 4 x 10^4 cells/cm^2 and treated for the indicated times with the MH (0, 5, 10, 15 and 15 mg/mL for HCT-116 cells and 0, 20, 30, 40 and 50 mg/mL for LoVo cells) and STH (0, 3, 6, 9 and 12 mg/mL for HCT-116 cells and 0, 10, 20, 30 and 40 mg/mL for LoVo cells). These concentrations were chosen according to the MTT viability assay ensuring 80 to 40% cells were viable at 48 h. The IC_{50} values of 5-FU, MH, STH and combination doses of MH+5-FU and STH+5-FU were also used for treated the cultured cells in 6-well plates for 48 h. After the treatment time, the medium was removed and cells were washing two times with PBS.

Protein lysates were prepared from cell pellets by using lysis buffer (120 mmol/L NaCl, 40 mmol/L Tris (pH 8), 0.1% NP40) with protease inhibitor cocktails (Sigma) and centrifuged at 13000 x *g* for 15 min. Proteins from cell supernatants were alienated on 8 or 10% polyacrylamide gel and then transferred into a nitrocellulose membrane, using the trans-blot SD semidry electrophoretic transfer cell (Bio-Rad, Hercules, CA, USA). The membranes were blocked with 5% non-fat-milk with Tris HCl buffered saline with Tween 20 (TBST) for 1 h at room temperature. P53, caspase-3, c-PARP, NFκB, p-IκBα, IL-1β, IL-6, iNOS, TNF-α, p-p38MAPK, p-Erk1/2, EGFR, HER2, p-Akt, OGG1, Nrf2, SOD, Catalase, HO-1, ATF6, XBP1, AMPK, p-AMPK, PGC1α, SIRT1, MMP-2, MMP-9, E-cadherin, N-cadherin, β-catenin, CXCR4 and GADPH primary antibodies (1:500 dilutions) were used after overnight incubation at 4°C. Membranes were washed 3 times by TBST and incubated with their specific alkaline phosphatase conjugated secondary antibodies (1:80,000) for another 1h. Immunolabeled proteins were identified by using a chemiluminescence method (C-DiGit Blot Scanner, LICOR, Bad Homburg, Germany) and bands were quantified by image studio digits software 3.1 (C-DiGit Blot Scanner, LICOR, Bad Homburg, Germany).

2.20. Statistical analysis

The results are expressed as the mean values with SD of three experiments and the statistical analysis was performed using STATISTICA software (Statsoft Inc., Tulsa, OK, USA). The significant differences represented by letters were obtained by a one-way analysis of variance (ANOVA) followed by Tukey's honestly significant difference (HSD) post hoc test ($p < 0.05$). Correlations were determined on a honey mean basis, according to Pearson's correlation coefficient (r). Differences at $P < 0.05$ were considered to be statistically significant.

CHAPTER 3. RESULTS AND DISCUSSION

RESULTS: PART I

3.1. Nutritional characterization of MH and STH

Several unifloral MH and STH were analyzed for their phenolic, flavonoid, amino acid and protein contents, as well as their radical scavenging activities.

3.1.1. Phytochemical content of MH and STH

To evaluate the phytochemical composition of MH and STH, TPC and TFC were determined. As shown in Table 3.1, significant differences ($p<0.05$) among the different groups were observed for TPC (Berchidda > MH > Monti > Luras > Sadali > Olbia) and TFC (Berchidda > Monti > MH > Luras > Olbia > Sadali). STH from Berchidda area showed the highest content of TPC (1.00 ± 0.02 g GAE/Kg) followed by the area of Monti (0.86 ± 0.01 g GAE/Kg), Luras (0.77 ± 0.02 g GAE/Kg), and Sadali (0.76 ± 0.02 g GAE/Kg), while the lowest value corresponded to Olbia (0.69 ± 0.01 g GAE/Kg). Compared to MH (0.89 ± 0.00 g GAE/Kg), STH from Berchidda area showed the highest value, Monti area showed a similar value and the STHs from Luras, Sadali and Olbia areas had lower values.

Table 3.1. Total polyphenol and flavonoid content of Manuka honey (MH) and Strawberry tree honey (STH).

Type of Honey	**Total Polyphenols** (g GAE/Kg)	**Total Flavonoids** (mg CAE/kg)
Manuka Honey	0.89 ± 0.00^{ab}	71.90 ± 0.03^{bc}
Strawberry tree honey		
Monti	0.86 ± 0.01^{b}	92.68 ± 14.17^{ab}
Luras	0.77 ± 0.02^{bc}	69.96 ± 3.62^{bc}
Sadali	0.76 ± 0.02^{bc}	65.74 ± 2.50^{c}
Olbia	0.69 ± 0.01^{c}	66.18 ± 0.61^{c}
Berchidda	1.00 ± 0.02^{a}	108.20 ± 2.69^{a}

GAE, Gallic acid equivalent; CAE, (+)-Catechin equivalents. Data are presented as mean ± standard deviation (SD) of three independent experiments. Columns associated with the same set of data with different symbolic letters are significantly different ($p < 0.05$).

In the case of TFC, STH from Berchidda (108.20 ± 2.69 mg CAE/kg) and Monti (92.86 ± 14.17 mg CAE/kg) areas showed the highest values compared to the STHs from the area of Luras (69.96 ± 3.62 mg CAE/kg), Sadali (65.74 ± 2.50 mg CAE/kg) and Olbia (66.18 ± 0.61 mg CAE/kg) (Table 3.1).

The phenolic compounds identified in MH and STH by HPLC diode array detector (DAD) analysis are reported in Table 3.2 and Table 3.3. Two different families have been determined: flavonols including rutin, myricetin, fisetin, quercetin, luteolin, apigenin, kaempferol and isorhamnetin and phenolic acids including gallic acid, protocatechuic acid, 4-hydroxybenzoic acid, vanillic acid, caffeic acid, syringic acid, *p*-coumaric acid, *trans*-ferulic acid, ellagic acid and *trans*-cinnamic acid. All concentrations were calculated using the calibration curves of each analyte.

With respect to flavonols, quercetin represents the 46.62% for MH and kaempferol represents the 41.12% for STH of the total flavonols identified. On the other hand, gallic acid is the main phenolic acid for both kinds' honeys representing the 48.98% for MH and 54.44% for STH of the total phenolic acids.

Table 3.2. CAS number, retention time (RT, min), maximum absorption wavelengths (λ, nm) and concentration (mg/100 g of honey) for the considered phenolic compounds determined in MH.

Phenolic compounds	CAS number	RT (min)	λ (nm)	Concentration (mg/100 g of honey)
Flavonols				
Rutin	153-18-4	13.34	352	nd
Myricetin	529-44-2	17.07	368	nd
Fisetin	528-48-3	19.73	361	nd
Quercetin	117-39-5	24.65	371	3.73±1.83
Luteolin	491-70-3	25.69	347	2.62±0.60
Apigenin	520-36-5	31.91	337	0.06±0.01
Kaempferol	520-18-3	31.93	365	1.17±0.50
Isorhamnetin	480-19-3	34.83	370	0.42±0.20
Total flavonols content				8.00
Phenolic acids				
Gallic acid	149-91-7	3.11	270	11.55±1.80
Protocatechuic acid	99-50-3	5.65	259	nd
4-Hydroxybenzoic acid	99-96-7	10.52	254	0.58±0.01
Vanillic acid	121-34-6	15.65	260	nd
Caffeic acid	331-39-5	16.54	322	0.53±0.02
Syringic acid	530-57-4	19.87	274	10.28±1.61
p-coumaric acid	501-98-4	27.46	308	0.12±0.03
trans-ferulic acid	537-98-4	33.19	322	0.19±0.01
Ellagic acid	476-66-4	38.08	251	nd
trans-cinnamic acid	140-10-3	55.88	273	0.33±0.07
Total phenolic acid content				23.58

nd: not detected. Data are means (n=2).

Table 3.3. CAS number, RT (min), maximum absorption wavelengths (λ, nm) and concentration (mg/100 g of honey) for the considered phenolic compounds determined in STH.

Phenolic compounds	CAS number	RT (min)	λ (nm)	Concentration (mg/100 g of honey)
Flavonols				
Rutin	153-18-4	13.34	352	nd
Myricetin	529-44-2	17.07	368	0.61±0.04
Fisetin	528-48-3	19.73	361	nd
Quercetin	117-39-5	24.65	371	0.90±0.02
Luteolin	491-70-3	25.69	347	0.79±0.10
Apigenin	520-36-5	31.91	337	0.19±0.06
Kaempferol	520-18-3	31.93	365	1.90±0.05
Isorhamnetin	480-19-3	34.83	370	0.23±0.07
Total flavonols content				4.62
Phenolic acids				
Gallic acid	149-91-7	3.11	270	3.92±0.16
Protocatechuic acid	99-50-3	5.65	259	nd
4-Hydroxybenzoic acid	99-96-7	10.52	254	1.29±0.02
Vanillic acid	121-34-6	15.65	260	nd
Caffeic acid	331-39-5	16.54	322	1.22±0.06
Syringic acid	530-57-4	19.87	274	nd
p-coumaric acid	501-98-4	27.46	308	0.10±0.03
trans-ferulic acid	537-98-4	33.19	322	0.53±0.00
Ellagic acid	476-66-4	38.08	251	nd
trans-cinnamic acid	140-10-3	55.88	273	0.14±0.01
Total phenolic acid content				7.20

nd: not detected. Data are means (n=2).

3.1.2. Total protein and free amino acid content of MH and STH

Honey protein content depends on the type of plant species: since it is variable, the protein content of honey can be characterized by the presence of enzymes introduced by the bees themselves, and others derived from the nectar (Alvarez-Suarez et al., 2010b). The amino acid of honey could play an important role in its antioxidant activity (Meda et al., 2005). Total protein and free amino acid content were determined by colorimetric methods, and results are shown in Table 3.4. Total protein content decreased in this order: Berchidda > MH > Monti, Olbia > Luras, Sadali and free amino acid content decreased in this order: Berchidda > Monti > MH > Olbia > Luras > Sadali. STH from Berchidda area presented the highest concentration of total protein (0.07 ± 0.00 g BSA/100g) and free amino acid content (51.67 ± 9.64 mg LE/100g) than other areas (0.03 to 0.04 g BSA/100g and 10.28 to 14.56 mg LE/100g); also higher than MH contents (0.05 ± 0.00 g BSA/100g and 14.34 ± 0.13 mg LE/100g, respectively) (Table 3.4). Regarding the values obtained for the other STHs, only the STH from Monti area presented similar values of free amino acids compared to MH; all the others presented lower contents (Table 3.4).

Table 3.4. Total protein and free amino acid content of MH and STH.

Type of Honey	**Total protein** (g BSA/100 g)	**Total free amino acids** (mg LE/100 g)
Manuka Honey	0.05 ± 0.00^{ab}	14.34 ± 0.13^{b}
Strawberry tree honey		
Monti	0.04 ± 0.00^{bc}	14.56 ± 0.93^{b}
Luras	0.03 ± 0.00^{c}	12.86 ± 0.05^{b}
Sadali	0.03 ± 0.00^{c}	10.28 ± 0.86^{b}
Olbia	0.04 ± 0.01^{bc}	13.18 ± 1.35^{b}
Berchidda	0.07 ± 0.00^{a}	51.67 ± 9.64^{a}

BSA, Bovine serum albumin; LE, Leucineequivalents.Data are presented as mean ± SD of three independent experiments. Columns associated with the same set of data with different symbolic letters are significantly different ($p < 0.05$).

3.1.3. Total antioxidant capacity of MH and STH

The TAC of MH and STH was quantified by FRAP, TEAC and DPPH assays (Table 3.5). The FRAP, TEAC and DPPH content were found in this order: Berchidda > Monti > Luras > Sadali > Olbia > MH; Berchidda > MH > Luras, Sadali, Olbia > Monti and Berchidda >

Monti, Luras, Sadali, Olbia > MH, respectively. TAC of MH was 0.29 ± 0.00 mmol Fe(II)/100 g and 0.14 ± 0.00 mmol TE/100 g (FRAP), 0.22 ± 0.00 mmol TE/100 g (TEAC), and 0.06 ± 0.00 mmol TE/100 g (DPPH) and STH from Berchidda area was 0.92 ± 0.02 mmol Fe(II)/100 g and 0.54 ± 0.00 mmol TE/100 g (FRAP), 0.39 ± 0.01 mmol TE/100 g (TEAC), and 0.20 ± 0.01mmol TE/100 g (DPPH) (Table 3.5).

Table 3.5. Total antioxidant capacity of MH and STH.

Type of Honey	**FRAP values**		**TEAC values**	**DPPH values**
	mmol TE/100 g	mmol Fe(II)/100 g	mmol TE/100 g	mmol TE/100 g
Manuka Honey	0.14 ± 0.00^{f}	0.29 ± 0.00^{f}	0.22 ± 0.00^{b}	0.06 ± 0.00^{c}
Strawberry tree honey				
Monti	0.39 ± 0.00^{b}	0.81 ± 0.00^{b}	0.10 ± 0.00^{c}	0.09 ± 0.00^{b}
Luras	0.30 ± 0.00^{c}	0.68 ± 0.00^{c}	0.11 ± 0.00^{c}	0.09 ± 0.00^{b}
Sadali	0.24 ± 0.00^{d}	0.63 ± 0.00^{d}	0.11 ± 0.00^{c}	0.09 ± 0.00^{b}
Olbia	0.21 ± 0.00^{e}	0.51 ± 0.00^{e}	0.11 ± 0.00^{c}	0.09 ± 0.00^{b}
Berchidda	0.54 ± 0.00^{a}	0.92 ± 0.02^{a}	0.39 ± 0.01^{a}	0.20 ± 0.01^{a}

FRAP, ferric reducing antioxidant power assay; TEAC, Trolox equivalent antioxidant capacity assay; DPPH, Diphenyl-1-picrylhydrazyl assay; TE, Trolox equivalents; Fe(II), Ferrous ammonium sulphate. Data are presented as mean ± SD of three independent experiments. Columns associated with the same set of data with different symbolic letters are significantly different ($p < 0.05$).

3.1.4. Correlations between biochemical parameters and antioxidant potentials of MH and STH

A significant correlation ($p < 0.05$) was found between biochemical and antioxidant parameters of the honeys (Table 3.6). There was a high correlation between the TPC and TFC ($r = 0.856$, $p \leq 0.03$). Also a strong correlation was observed between FRAP and DPPH ($r = 0.808$, $p \leq 0.002$), as well as TEAC and DPPH ($r = 0.704$, $p \leq 0.01$). Simultaneously, a significant correlation was found between TPC and TEAC ($r = 0.870$, $p \leq 0.002$), while low correlation coefficients were obtained between TPC and FRAP ($r = 0.663$, $p \leq 0.05$) and DPPH ($r = 0.678$, $p \leq 0.05$). In addition, a high correlation was found among TFC and FRAP ($r = 0.878$, $p \leq 0.002$) and DPPH ($r = 0.796$, $p \leq 0.009$), while low correlations were obtained between TFC and TEAC ($r = 0.678$, $p \leq 0.04$) (Table 3.6).

Moreover, scanty amounts of protein and amino acid are present in honey and they are significantly correlated between the TPC ($r = 0.863$, $p \leq 0.002$ for protein and $r = 0.728$, $p \leq 0.05$ for amino acid) and TFC ($r = 0.817$, $p \leq 0.05$ for protein and $r = 0.740$, $p \leq 0.05$) (Table 3.6). Protein and amino acid contribute to the antioxidant potential of honey and these bioactive compounds strongly correlated with TEAC ($r = 0.923$, $p \leq 0.002$ for protein and $r = 0.899$, $p \leq 0.01$ for amino acid), DPPH ($r = 0.772$, $p \leq 0.01$ for protein and $r = 0.922$, $p \leq 0.003$ for amino acid), FRAP ($r = 0.660$, $p \leq 0.05$ for protein and $r = 0.694$, $p \leq 0.05$ for amino acid) and also with each other ($r = 0.947$, $p \leq 0.004$) (Table 3.6).

Table 3.6. Correlation matrix (Pearson's correlation coefficients) showing the interrelation between quantitative determinations in the MH and STH.[a]

Variable	TPC	TFC	FRAP	TEAC	DPPH	Protein
TFC	0.856*					
FRAP	0.663*	0.878**				
TEAC	0.870**	0.678*	0.586^{ns}			
DPPH	0.678*	0.796**	0.807**	0.704**		
Protein	0.863**	0.817*	0.660*	0.923**	0.772**	
Free AA	0.728*	0.740*	0.694*	0.899*	0.922**	0.947**

TPC, Total phenolic content; TFC, Total flavonoid content; FRAP, ferric reducing antioxidant power assay; TEAC, Trolox equivalent antioxidant capacity assay; DPPH, Diphenyl-1-picrylhydrazyl assay; Free AA, Free amino acid.[a] 95% confidence interval, * Significant at $p \leq 0.05$, ** Significant at $p \leq 0.01$.

DISCUSSION: PART I

The aim of my first part of PhD project was to evaluate nutritional characterization of MH and STH in order to investigate the phytochemical composition and antioxidant properties. MH and STH were chosen as the natural food as well as for their higher content of phenolic compounds (Alvarez-Suarez et al., 2016; Chan et al., 2013; Marshall et al., 2014) and antioxidant capacity (Afrin et al., 2017; Alvarez-Suarez et al., 2016; Cherchi et al., 1994; Tuberoso et al., 2013).

MH has been extensively studied for antibacterial and antioxidant activity, as well as for wound healing mechanisms due to a large quantity of physicochemical properties and attractive therapeutic molecules (Alvarez-Suarez et al., 2014; Alvarez-Suarez et al., 2016; Bischofberger et al., 2016; Bogdanov et al., 2008; Carter et al., 2016). MH contains numerous phenolic compounds, including flavonoids (pinobanksin, pinocembrin, chrysin, luteolin, quercetin, 8-methoxy kaempferol, isorhamnetin, kaempferol and galangin) (Chan et al., 2013), phenolic acids (phenylacetic acid, phenyllacticacid, 4-hydroxybenzoic acid, kojicacid, 2-methoxybenzoic acid, syringic acid, and 4-methoxyphenyllactic acid) and other compounds (methylsyringate, leptosin, glyoxal, 3-deoxyglucosulose and methylglyoxal) (Alvarez-Suarez et al., 2014). Several studies have reported that methylglyoxal induces non-peroxide antibacterial activity even at very low concentrations (Carter et al., 2016; Mavric et al., 2008).

However, despite its high reputation, there are insufficient data on its phytochemical composition or biological properties. Only few studies have investigated the organic acid profile of STH, and its melissopalynological and physicochemical properties (Ciulu et al., 2016; Rosa et al., 2011; Spano et al., 2009a; Spano et al., 2009b; Ulloa et al., 2015). STH expresses exceptional antioxidant properties due to its high amounts of phenolic compounds, mainly flavonoids and phenolic acids (Cherchi et al., 1994; Tuberoso et al., 2013). Homogentisic acid (2,5-dihydroxyphenylacetic acid) is the main phenolic marker of the STH (Cabras et al., 1999; Scanu et al., 2005) and particularly known for its attractive antioxidant, antiradical and protective effects, such as defensive actions against thermal cholesterol degradation (Rosa et al., 2011; Spano et al., 2006).

The TPC content obtained in the present work (Table 3.1) were very close to those obtained by Alzahrani et al. for MH (899.09 ± 11.75 mg GAE/kg) (Alzahrani et al., 2012) and by Rosa et al. for STH (972 mg GAE/kg) (Rosa et al., 2011). TPC of STH from Brechidda area was also higher compared to other previously reported Cuban honey such

as amber honey (595.8 ± 6.8 mg GAE/kg) (Alvarez-Suarez et al., 2010a), Malaysian honey such as Tualang honey (251.7 ± 7.9 mg/kg) (Mohamed et al., 2010), Portuguese honey (406.2 ± 17.2 mg GAE/kg) (Ferreira et al., 2009) and Algerian honey (498.16 ± 1.32 mg GAE/kg) (Khalil et al., 2012). Furthermore, honey exerts anti-proliferative effects that is associated with high phenolic content (Jaganathan and Mandal, 2009a).

The TFC reported by Alvarez-Suarez et al. (Alvarez-Suarez et al., 2016) (77 ± 0.021 mg/kg) was also similar to the values obtained by our study for MH (Alvarez-Suarez et al., 2016). However, TFC of STHs were also higher than the Linen vine honey (25.2 ± 0.3 mg CE/kg) (Alvarez-Suarez et al., 2010a), Algerian honey (71.78 ± 0.84 mg CE/kg) (Khalil et al., 2012), Gelam honey (46.11 ± 0.71 mg QE / 100 g) and Tualang honey (50.45 ± 1.83 mg QE/ 100 g) (Kishore et al., 2011), and lower than the values reported for Portuguese honey (587.42 ± 0.46 mg/kg) (Ferreira et al., 2009) and Sourwood honey (156.82 mg/kg) (Moniruzzaman et al., 2013).

The concentrations of the 18 phenolic compounds quantified in MH and STH are listed in Table 3.2 and Table 3.3. For MH, it was found that gallic acid (36.57%) and syringic acid (32.55%) were the main components (11.55 and 10.28 mg/100 g honey, respectively). The other phenolic acids were presented in low proportions ranging from 1.84% to 1.68% for 4-hydroxybenzoic acid and caffeic acid (0.58 and 0.53 mg/100 g honey), respectively. In a recent study, Ahmed et al. analyzed the phenolic composition of 17 multifloral and cactus honey samples (Ahmed et al., 2016). 4-Hydroxybenzoic acid was the main phenolic compound identified in all the studied honeys, followed by gallic acid with similar concentrations to those found in the present study. As flavonols, the highest concentrations of quercetin, luteolin and kaempferol were found in this family (3.73, 2.62 and 1.17 mg/ 100 g of honey). They represented 11.81%, 8.30% and 3.70% of the total phenolic content, respectively. All these three compounds have also been identified in MH by Marshall et al. (Marshall et al., 2014) and by Suarez et al. (Alvarez-Suarez et al., 2016). Finally, it is remarkable that kaempferol, quercetin and myricetin possess antimicrobial properties, a well-known characteristic of MH (Atrott and Henle, 2009; Weston et al., 1999).

In the case of STH, it was found that gallic acid (33.16%) and kaempferol (16.07%) were the main components (3.92 and 1.90 mg/100 g honey, respectively). Other flavonols (quercetin and luteolin; 0.90 and 0.79 mg/100 g honey, respectively) and phenolic acids (4-hydroxybenzoic acid and caffeic acid; 1.29 and 1.22 mg/100g honey, respectively) were also presented in low concentrations. Two previous studies addressed the characterization

of the phenolic composition in STH. Petettro et al. studied the phenolic composition on ten monofloral honeys by HPLC-DAD analysis (Petretto et al., 2015). As in the present study, kaempferol and luteolin were the main flavonols identified in STH, showing a concentration of 1.06 and 0.96 mg/100 g of honey, respectively. In another study, Tuberoso et al. determined two phenolic compounds in STH (homogentisic acid and gallic acid) (Tuberoso et al., 2013). With respect to homogentisic acid, STH is characterized by high concentrations of such compound. In fact, sometimes it could be considered as a marker of STH (Cabras et al., 1999; Deiana et al., 2015), showing an average amount of 414.1±69.8 mg/kg (Tuberoso et al., 2009).

STH from Brechidda area presented the higher concentration of total protein and free amino acid content than other areas, even also higher than MH contents (Table 3.4). These results are in correspondence with the values obtained by Spano et al. who reported that free amino acid of STH was ranged between 7.3 to 53.8 mg/100g (Spano et al., 2009b). Moreover, the values of free amino acid and total protein obtained from MH were lower than the values reported by Moniruzzaman et al. (Moniruzzaman et al., 2013). Regarding the values obtained for the others STHs, only the STH from Monti area presented similar values of free amino acids respect to MH; all the others presented lower content (Table 3.4). Moreover, the protein content of STH from Brechidda area was lower than the values reported for Algerian honey (4,097.00 ± 3.54 mg/kg) (Khalil et al., 2012), Sourwood honey (5.59 ± 0.01 g/kg) (Moniruzzaman et al., 2013), Bangladeshi honeys (8.6 ± 0.0 mg/g) (Islam et al., 2012) but higher than Linen vine honey (92.3 ± 12.3 mg LE/100 g) and Christmas vine honey (12.0±14.3 mg LE/100 g) (Alvarez-Suarez et al., 2010a). The protein content in honeys can be attributed to the presence of enzymes introduced by the bees themselves, and others derived from the nectar (Alvarez-Suarez et al., 2010b) and it also contributes to the antioxidant capacity (Alvarez-Suarez et al., 2010a).

TAC of MH and STH were significantly different ($p < 0.05$) among each other (Table 3.5). TAC of MH (286.93 ± 2.83 µmol Fe(II) /100 g and 142.34 ± 1.41 µmol TE/100 g (FRAP), 220.92 ± 2.53 µmol TE/100 g (TEAC), and 63.82 ± 0.99 µmol TE/100 g (DPPH)) was slightly lower than the value reported by other studies (Henderson et al., 2015; Moniruzzaman et al., 2013). On the other hand, the values obtained from Brechidda area were significantly higher ($p < 0.05$) than those obtained for other areas samples (Monti, Luras, Sadali and Olbia) but they were lower than previously reported values (1200 ± 2.2 µmol Fe(II) /100 g for FRAP, 590 ± 1.5 µmol TE/100 g for TEAC and 450 ± 1.1 µmol

TE/100 g for DPPH) by Tuberoso et al. (Tuberoso et al., 2013). There were significant differences ($p < 0.05$) between FRAP values of the MH and STHs (Table 3.5), suggesting that they may have diverse antioxidant potentials. Similarly, STH from Brechidda area had the highest TEAC and DPPH values among all the investigated honey, which specifies its significant reducing power and antioxidant activity. It is noted that MH presented higher TEAC values and lower DPPH values than other STHs of Sardinia (Table 3.5). Overall, the TAC of STH from Brechidda area was higher than that previously reported Cuban honey (Alvarez-Suarez et al., 2010a), Portuguese honey (Ferreira et al., 2009), Malaysian honey (Kishore et al., 2011; Moniruzzaman et al., 2013), and Algerian honey (Khalil et al., 2012).

The correlation between the biochemical and antioxidant parameters of the MH and STH are shown in Table 3.6. In our works, there was a high correlation among the TPC, TFC and TAC (Table 3.6). Likewise, a similar correlation was found between TPC and TFC values ($r = 0.831$, $p \leq 0.05$) in Cuban honey (Alvarez-Suarez et al., 2010a). In Algerian honey, Khalil et al. also found a correlation between the TPC and TFC ($r = 0.776$, $p \leq 0.01$) (Khalil et al., 2012). In a previous study on Cuban honey, a significant correlation was found between TPC and TAC ($r = 0.89$, $p \leq 0.006$ by FRAP and $r = 0.96$, $p \leq 0.001$ by TEAC) and also between TFC and TAC ($r = 0.89$, $p \leq 0.05$ by FRAP and $r = 0.8315$, $p \leq 0.05$ by TEAC) (Alvarez-Suarez et al., 2010a). Similarly, a positive correlation was observed on Malaysian honey between TPC and TAC ($r = 0.761$, $p \leq 0.01$ by FRAP, $r = 0.837$, $p \leq 0.05$ by TEAC and $r = 0.789$, $p \leq 0.05$ by DPPH), and also TFC and TAC ($r = 0.782$, $p \leq 0.05$ by FRAP, $r = 0.735$, $p \leq 0.05$ by TEAC and $r = 0.607$, $p \leq 0.05$ by DPPH) (Moniruzzaman et al., 2013). According to the correlation values, the results confirmed that polyphenols and flavonoids significantly contribute to the TAC of honeys.

Moreover, though very little amounts of protein and amino acid are present in honey and they are significantly correlated between the TPC and TFC (Table 3.6). A similar correlation was predicted in Algerian honey samples (Khalil et al., 2012). Protein and amino acid contribute to the antioxidant potential of honey and these bioactive compounds strongly correlated with TEAC, DPPH, FRAP and also with each other (Table 3.6). Our results are compatible with previously observed values of Malaysian (Moniruzzaman et al., 2013), Algerian (Khalil et al., 2012), Bangladeshi (Islam et al., 2012), and Indian honeys (Saxena et al., 2010).

RESULTS: PART II

3.2. Chemopreventive effect of MH and STH on human colon cancer HCT-116 and LoVo cells

3.2.1. Effect of MH and STH on HCT-116 and LoVo cells proliferation

The MTT assay was performed to investigate the anti-proliferative effects of MH and STH on HCT-116 and LoVo cells. Cells were treated with different concentrations of MH and STH ranging from 0 to 20 mg/mL for 24, 48 and 72 h for HCT-116 cells and from 0 to 60 mg/mL for LoVo cells. As shown in Figure 3.1 and Figure 3.2, percentage of viable cells was reduced in the treated HCT-116 and LoVo cells compared to control (no treatment) in a dose and time-dependent manner. The range of concentrations used to treat the LoVo cells was higher than the range used for HCT-116 because of its metastatic nature. In LoVo cells, at lower concentration there was no significant cytotoxic effect. In HCT-116 and LoVo cells, the IC_{50} (concentrations necessary for 50% inhibition of cell growth) of MH were 21.98 mg/mL and 62.85 mg/mL at 24 h, 15.10 mg/mL and 40.97 mg/mL at 48 h, and 13.35 mg/mL and 22.73 mg/mL at 72 h, respectively (Figure 3.1).

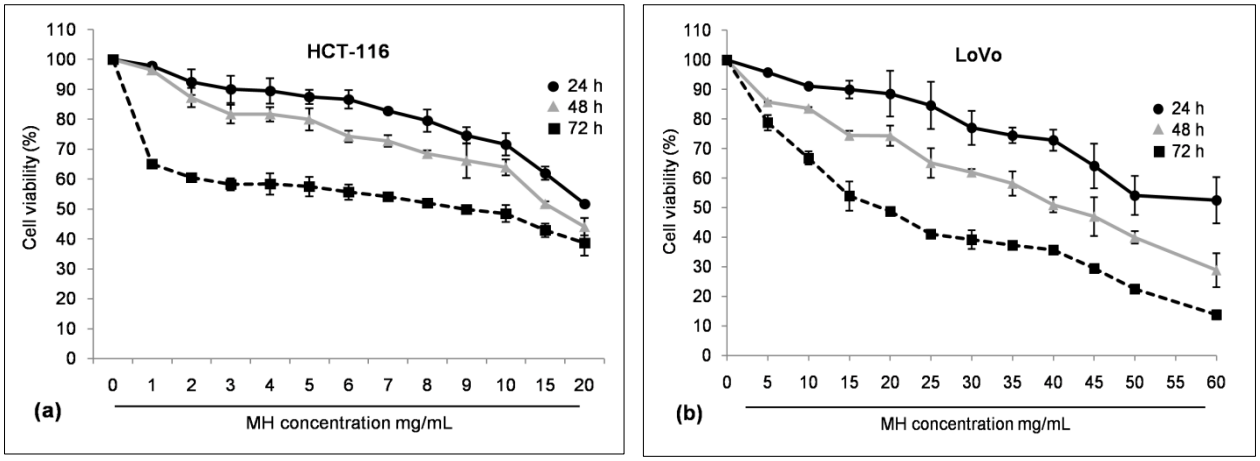

Figure 3.1. Inhibition of cell proliferation by MH in HCT-116 (a) and LoVo (b) cell lines. After 24 h of cell seeding (5×10^3 cells/well), HCT-116 and LoVo cells were treated with different concentrations of MH for 24, 48 and 72 h. Cell viability was measured by using MTT assay and results were expressed as a % of viable cells compared to control cells. All data are expressed as the mean ± SD of three experiments.

In the case of STH, the IC_{50} concentration of HCT-116 and LoVo cells were 14.65 mg/mL and 56.33 mg/mL at 24 h, 10.29 mg/mL and 35.12 mg/mL at 48 h and 9.17 mg/mL and 26.88 mg/mL at 72 h, respectively (Figure 3.2).

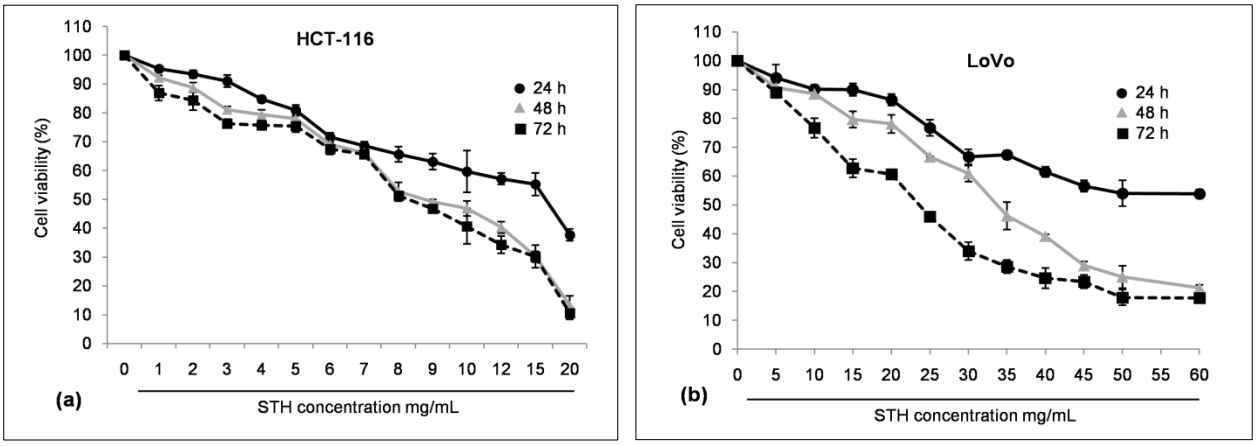

Figure 3.2. Inhibition of cell proliferation by STH in HCT-116 (a) and LoVo (b) cell lines. After 24 h of cell seeding (5×10^3 cells/well), HCT-116 and LoVo cells were treated with different concentrations of STH for 24, 48 and 72 h. Cell viability was measured by using MTT assay and results were expressed as a % of viable cells compared to control cells. All data are expressed as the mean ± SD of three experiments.

As shown in Figures 3.1 and Figures 3.2, MH and STH decreased cell viability in a dose and time dependent manner. In both cell lines, the treatment with STH caused a greater decrease in cellular viability at lower concentrations than MH.

Similar concentrations of MH and STH treatment were used for 24, 48 and 72 h for the cytotoxic effects on non-cancer HDF cells (Figure 3.3). In the case of non-cancer HDF cells, both honeys exhibited no toxic effects compared to control until 48 h in the concentrations from 0 to 40 mg/mL (Figure 3.3).

After 72 h, the cell viability was affected at the concentrations of 20 mg/mL for STH and 50 mg/mL for MH by inducing less toxic effects (Figure 3.3). In all cases, non-cancer HDF cells were significantly ($p < 0.05$) less sensitive to toxicity for both honeys compared to colon cancer HCT-116 and LoVo cells.

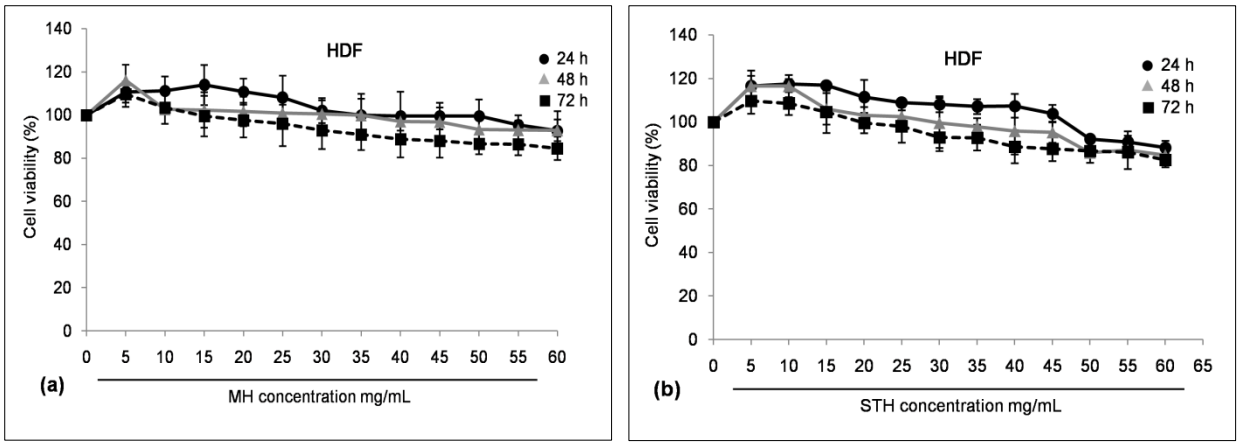

Figure 3.3. Inhibition of cell proliferation by MH (a) and STH (b) in HDF cell lines. After 24 h of cell seeding (5×10^3 cells/well), HDF cells were treated with different concentrations of MH and STH for 24, 48 and 72 h. Cell viability was measured by using MTT assay and results were expressed as a % of viable cells compared to control cells. All data are expressed as the mean ± SD of three experiments.

Honey represents a good source of sugar. To confirm the cytotoxic effect of both honeys, we performed the cytotoxic effect of AH on both cell lines at similar concentrations and time duration and we found that it was not associated with its sugar content (Figure 3.4). AH showed no cytotoxic effects on HCT-116 and LoVo cells until 48 h. At 72 h, it induced less toxic effect at higher concentrations (Figure 3.4). It is suggested that the toxic effect of both honey is not associated with its sugar content.

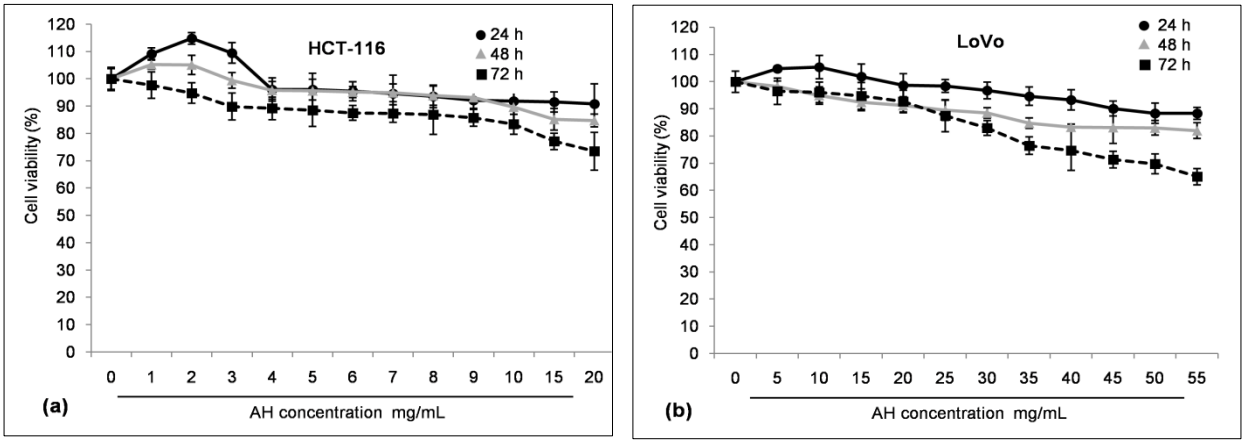

Figure 3.4. Inhibition of cell proliferation by artificial honey (AH) in HCT-116 (a) and LoVo (b) cell lines. After 24 h of cell seeding (5×10^3 cells/well), HCT-116 and LoVo cells were treated with different concentrations of AH for 24, 48 and 72 h. Cell viability was measured by using MTT assay and results were expressed as a % of viable cells compared to control cells. All data are expressed as the mean ± SD of three experiments.

According to these results, the MH concentrations were 5, 10, 15 and 20 mg/mL for HCT-116 and 20, 30, 40 and 50 mg/mL for Lovo cells and STH concentrations were 3, 6, 9 and 12 mg/mL for HCT-116 and 10, 20, 30 and 40 mg/mL for Lovo cells that were selected for further experiments. In all cases 48 h were used for treatment duration. The selected concentrations correspond to those concentrations at which approximately 80% to 40% cells were viable.

3.2.2. Effect of MH and STH on cell cycle arrest on HCT-116 and LoVo cells

Cell proliferation is correlated with the regulation of cell cycle progression. We therefore determined the effects of MH and STH on cell cycle arrest on HCT-116 and LoVo cells. Cell cycle distribution was evaluated using Tali™ Image-based Cytometer with PI staining to determine which phases of the cells cycle were arrested in cells treated with MH and STH. As shown in Figure 3.5, there was an accumulation of cells in Sub-G_1 phase compared to control, indicating the percentage of apoptosis in HCT-116 and LoVo cells treated with MH after 48 h incubation.

MH treatment increased the accumulation of cells at Sub-G_1 phase of about 6% at high concentration (20 mg/mL) in HCT-116 cells, at the same time in LoVo cells it was 20% at high concentration (50 mg/mL) (Figure 3.5). In HCT-116 cells, the percentage of cells in the S phase was significantly ($p < 0.05$) increased from 30 to 43% after MH treatment compared to control (23 to 26%) while the percentage of cells was significantly ($p < 0.05$) decreased in the G_0/G_1 and G_2/M phase (Figure 3.5).

At the same time, in LoVo cells, the percentage of cells in the G_2/M phase was significantly ($p < 0.05$) increased from 29 to 40% after MH treatment compared to control (20 to 24%) while the percentage of cells in the G_0/G_1 and S phase were significantly ($p < 0.05$) decreased (Figure 3.5).

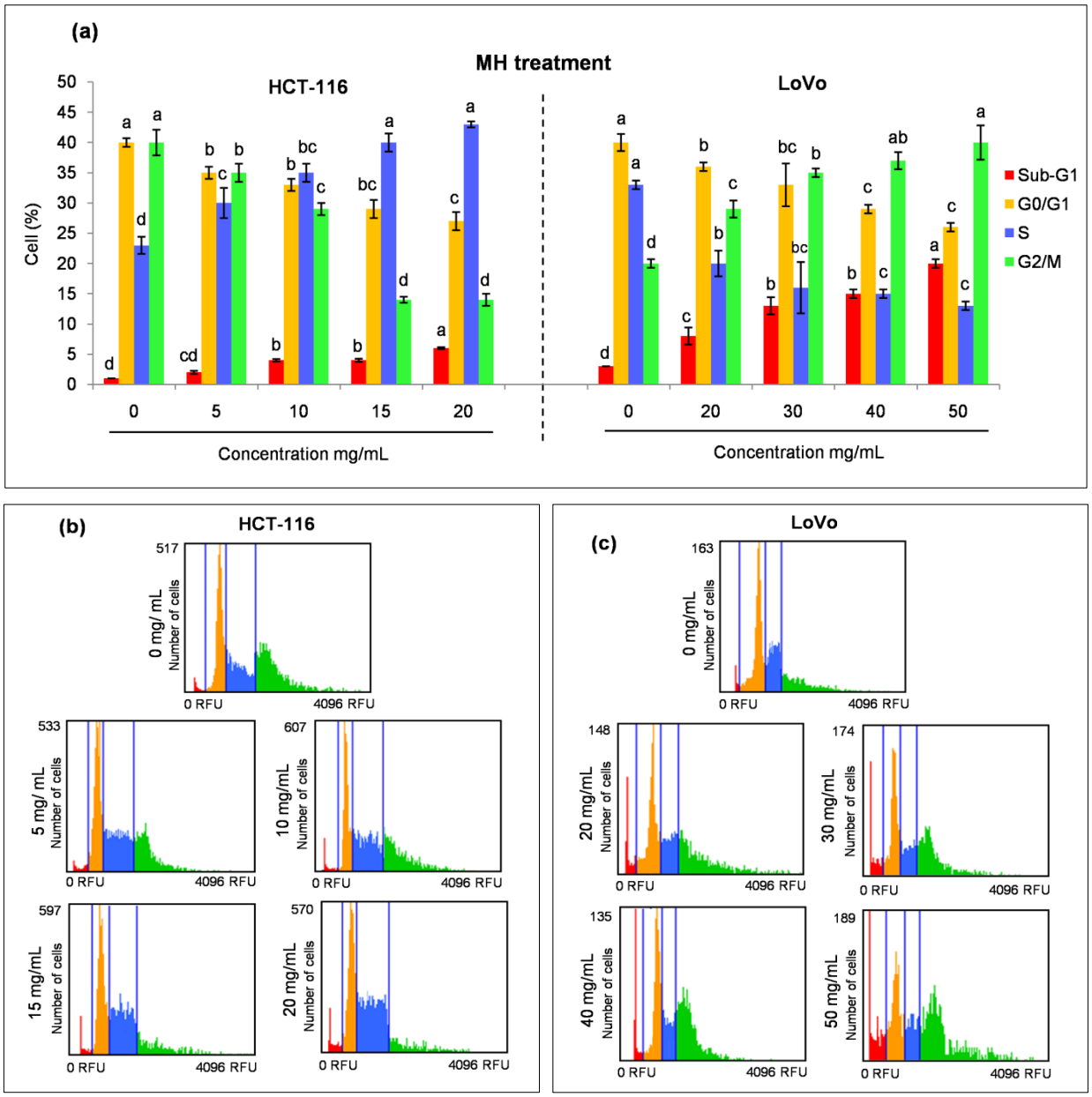

Figure 3.5. Cell cycle alteration induces by MH in HCT-116 and LoVo cells (a). After 24 h seeding, HCT-116 and LoVo cells were exposed with different concentrations of MH for 48 h. The concentration of 0 mg/mL corresponds to control (untreated cells). Propidium Iodide (PI) was used for staining the cells and DNA content of cells was analyzed for determination the effect of MH on HCT-116 and LoVo cell cycle distribution. The percentages of cells in each phase Sub-G_1 (apoptotic cells), G_0/G_1, S and G_2/M were calculate by the Tali® Cell Cycle Assay kit and Tali™ Image-based Cytometer. Representative fluorescence image of HCT-116 cells (b) and LoVo cells (c) cycle shows the effect of MH with or without treatment: red colour corresponds to Sub-G_1 phase, yellow colour corresponds to G_0/G_1 phase, blue colour corresponds to S phase and green yellow colour corresponds to G_2/M phase. All data shown were the mean ± SD of three independent experiments. Different superscripts letter for each column indicated significant differences ($p < 0.05$).

In Figure 3.6, there was an accumulation of cells in Sub-G_1 phase compared to control, indicating the percentage of apoptosis in HCT-116 and LoVo cells treated with STH after 48 h incubation. STH treatment increased the accumulation of cells at Sub-G_1 phase was of 10% for HCT-116 at 12 mg/mL and 14% for LoVo at 40 mg/mL (Figure 3.6). In HCT-116 cells, the percentage of cells in the S phase was significantly ($p < 0.05$) increased from 29 to 42% after STH treatment (Figure 3.6) compared to control (23 to 26%) while the percentage of cells were significantly ($p < 0.05$) decreased in the G_0/G_1 and G_2/M phase at dose dependently.

Moreover, in LoVo cells, the percentage of cells was significantly ($p < 0.05$) increased from 28 to 38% in the G_2/M phase after STH treatment compared to control (20 to 24%) while the percentage of cells in the G_0/G_1 and S phase were significantly ($p < 0.05$) decreased (Figure 3.6).

According to these results, we evaluated that the both honey varieties arrest the cell cycle at S phase in HCT-116 cells and G_2/M phase in LoVo cells.

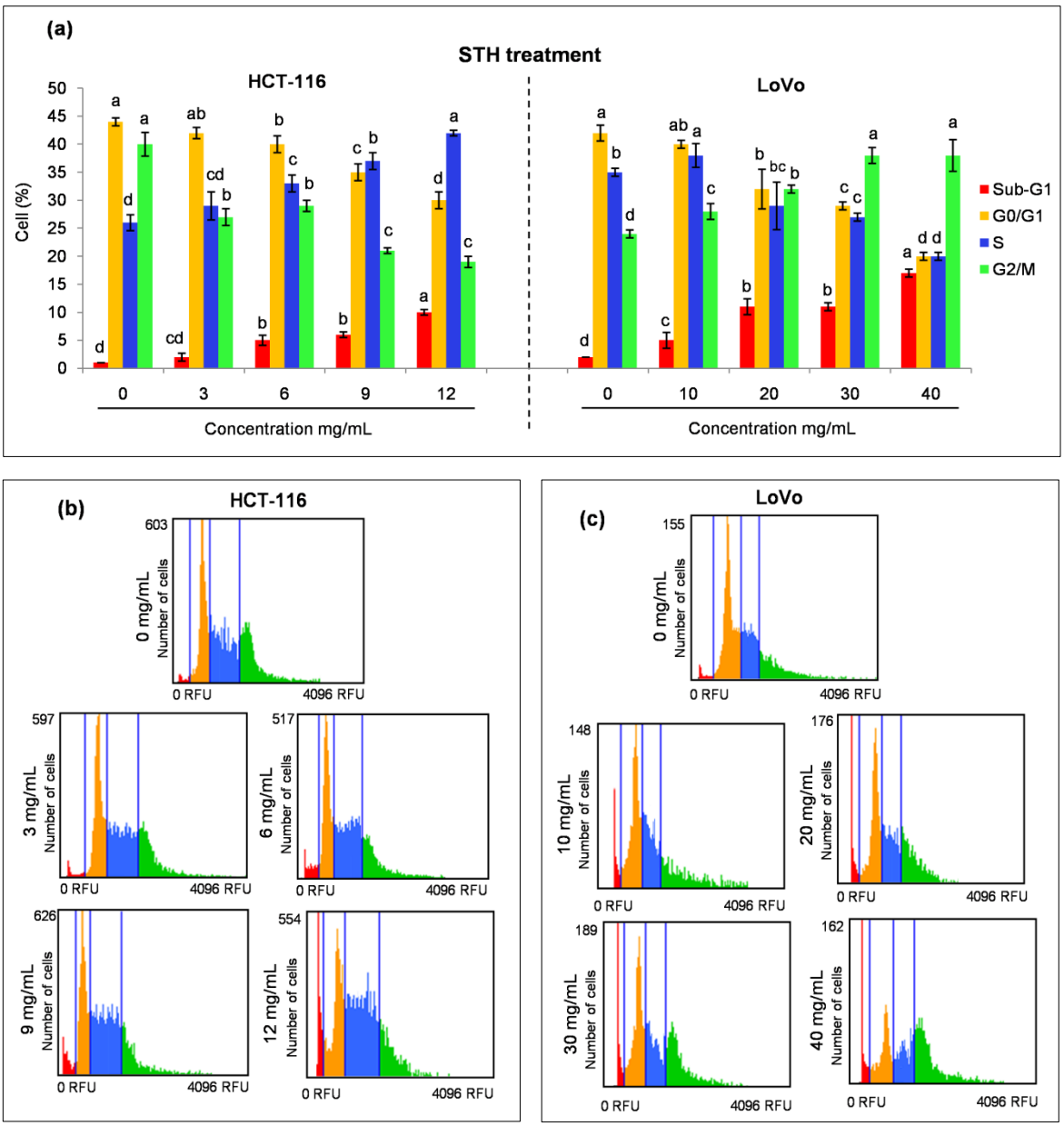

Figure 3.6. Cell cycle alteration induces by STH in HCT-116 and LoVo cells (a). After 24 h seeding, HCT-116 and LoVo cells were exposed with different concentrations of STH for 48 h. The concentration of 0 mg/mL corresponds to control (untreated cells). PI was used for staining the cells and DNA content of cells was analyzed for determination the effect of STH on HCT-116 and LoVo cell cycle distribution. The percentages of cells in each phase Sub-G_1 (apoptotic cells), G_0/G_1, S and G_2/M were calculate by the Tali® Cell Cycle Assay kit and Tali™ Image-based Cytometer. Representative fluorescence image of HCT-116 cells (b) and LoVo cells (c) cycle shows the effect of STH with or without treatment: red colour corresponds to Sub-G_1 phase, yellow colour corresponds to G_0/G_1 phase, blue colour corresponds to S phase and green yellow colour corresponds to G_2/M phase. All data shown were the mean ± SD of three independent experiments. Different superscripts letter for each column indicated significant differences ($p < 0.05$).

3.2.3. Effect of MH and STH on apoptosis on HCT 116 and LoVo cells

We evaluated the Tali^{TM} apoptosis assay kit with the Tali™ Image-based Cytometer for analyzing the number of live, apoptosis and dead cells to confirm whether MH and STH induced cytotoxic effect is associated with apoptosis. In order to determine the apoptotic effect, HCT-116 and LoVo cells were treated for 48 h with or without various concentrations of MH (5 to 20 mg/mL for HCT-116 cells and 20 to 50 mg/mL for LoVo cells) and STH (3 to 12 mg/mL for HCT-116 cells and 10 to 40 mg/mL for LoVo cells).

After MH treatment, the number of apoptotic cells was significantly ($p < 0.05$) increased from 1.75 to 3.38 fold in HCT-116 cells and 2.17 to 4.95 fold in LoVo cells, respectively compared to control (Figure 3.7). The highest number of apoptotic cells was observed at 15 mg/mL dose for HCT-116 cells and 40 and 50 mg/mL dose for LoVo cells (Figure 3.7); however the induction of apoptosis was more robust in LoVo cells than in HCT-116 cells treated with MH.

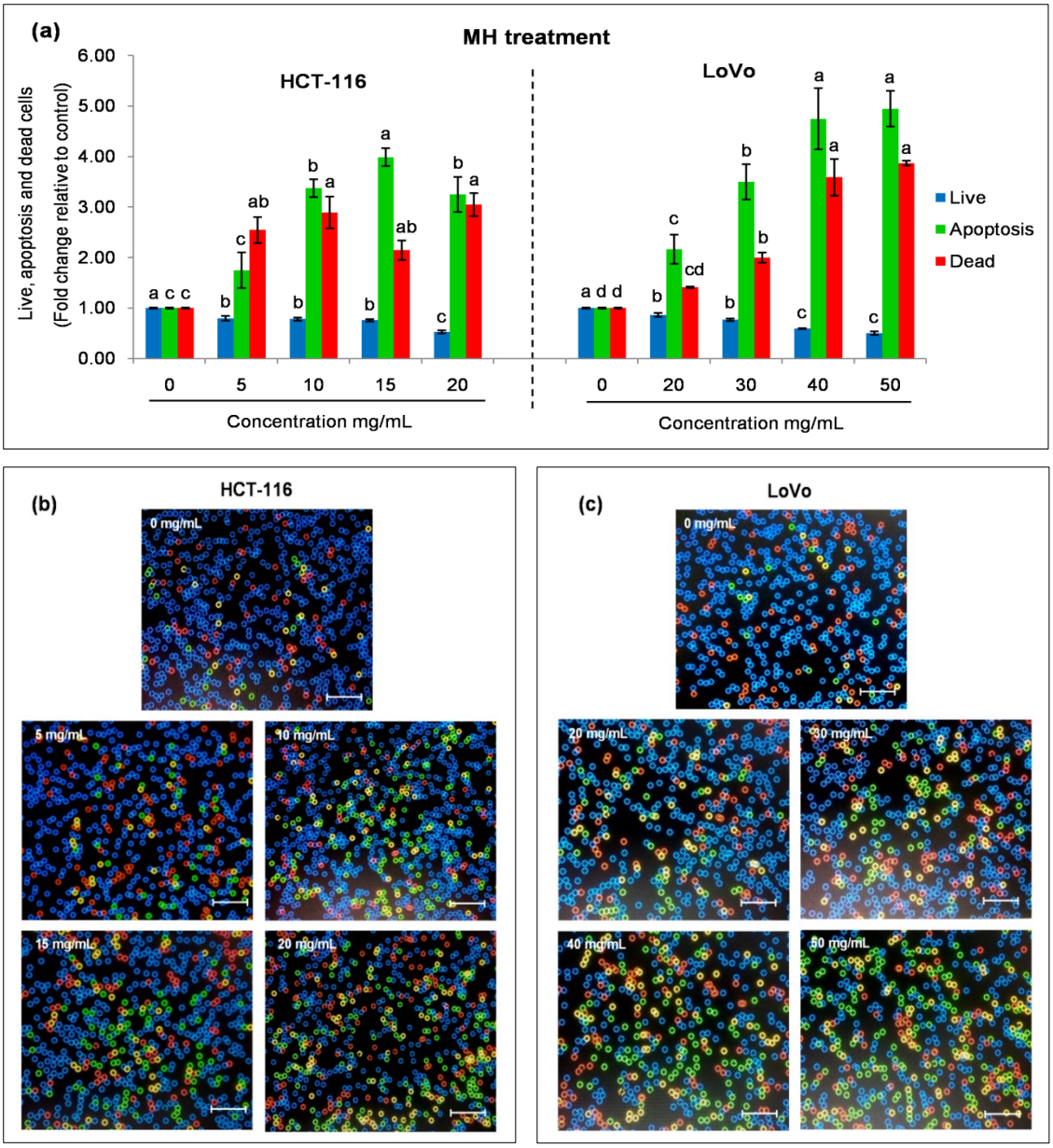

Figure 3.7. Apoptosis induction by MH in HCT-116 and LoVo cells (a). After 24 hincubation, HCT-116 and LoVo cells were treated with different concentrations of MH for 48 h. The concentration of 0 mg/mL corresponds to control (untreated cells). Annexin V Alexa Fluor® 488 and PI staining was used for determination of apoptotic effect of MH on HCT-116 and LoVo cells. Viable, death and apoptotic cells were calculated by using the Tali™ apoptosis kit and the Tali™ Image-based Cytometer. Representative fluorescence image of HCT-116 cells (b) and LoVo cells (c) shows the effect of MH with or without treatment: blue colour corresponds to live cells, green colour corresponds to apoptotic cells and red and yellow colour corresponds to dead cells.Scale bar = 50 µm. All data shown were the mean ± SD of three independent experiments. Different superscripts letter for each column indicated significant differences ($p < 0.05$).

In the case of STH, the number of apoptotic cells was increased in a dose-dependent manner from 1.83 to 3.11 fold for HCT and 1.75 to 4.12 fold for LoVo cells (Figure 3.8). The most effective concentration of STH that increased the apoptotic cell number was 12 mg/mL for HCT-116 and 40 mg/mL for LoVo cells (Figure 3.8). Both treatments decreased the number of live and dead cells at different concentration in each cell lines.

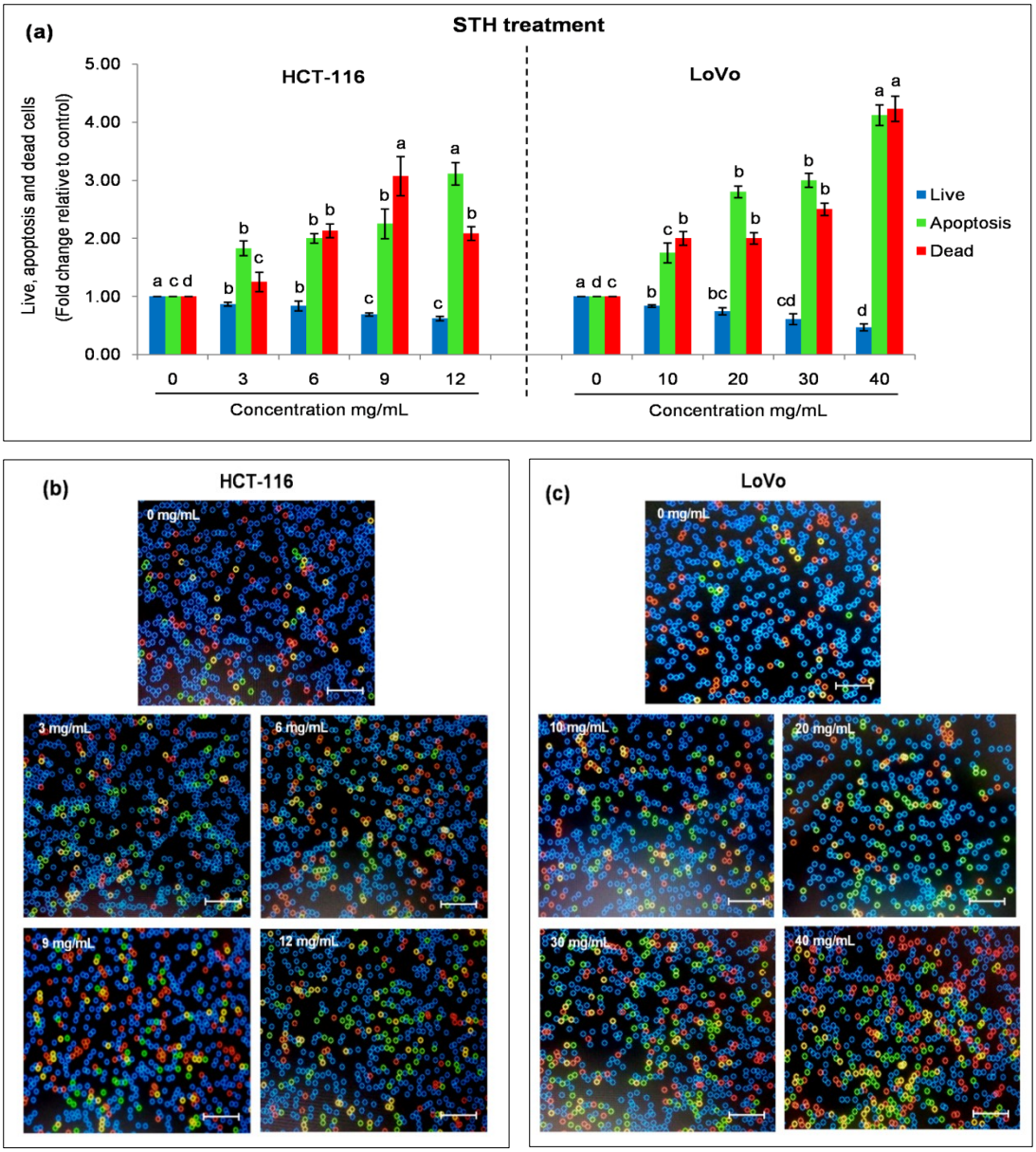

Figure 3.8. Apoptosis induction by STH in HCT-116 and LoVo cells (a). After 24 h incubation, HCT-116 and LoVo cells were treated with different concentrations of STH for 48 h. The concentration of 0 mg/mL corresponds to control (untreated cells). Annexin V Alexa Fluor® 488 and PI staining was used for determination of apoptotic effect of STH on HCT-116 and LoVo cells. Viable, death and apoptotic cells were calculated by using the Tali™ apoptosis kit and the Tali™ Image-based Cytometer. Representative fluorescence image of HCT-116 cells (b) and LoVo cells (c) shows the effect of STH with or without treatment: blue colour corresponds to live cells, green colour corresponds to apoptotic cells and red and yellow colour corresponds to dead cells. Scale bar = 50 µm. All data shown were the mean ± SD of three independent experiments. Different superscripts letter for each column indicated significant differences ($p < 0.05$).

On the other hand, the molecular mechanism by which MH and STH induced apoptosis was investigated by western blot analysis. Exposure of HCT-116 and LoVo cells to MH and STH caused significantly ($p < 0.05$) increased the protein expression of p53, caspase-3 and c-PARP levels in a dose dependent way (Figure 3.9 and Figure 3.10). In HCT-116 cells, the expression was increased from 1.11 to 1.58 fold, 1.22 to 1.75 fold and 1.21 to 1.86 fold after MH treatment (Figure 3.9) and 1.17 to 2.35 fold, 1.41 to 2.16 fold and 1.38 to 2.33 fold after STH treatment (Figure 3.10).

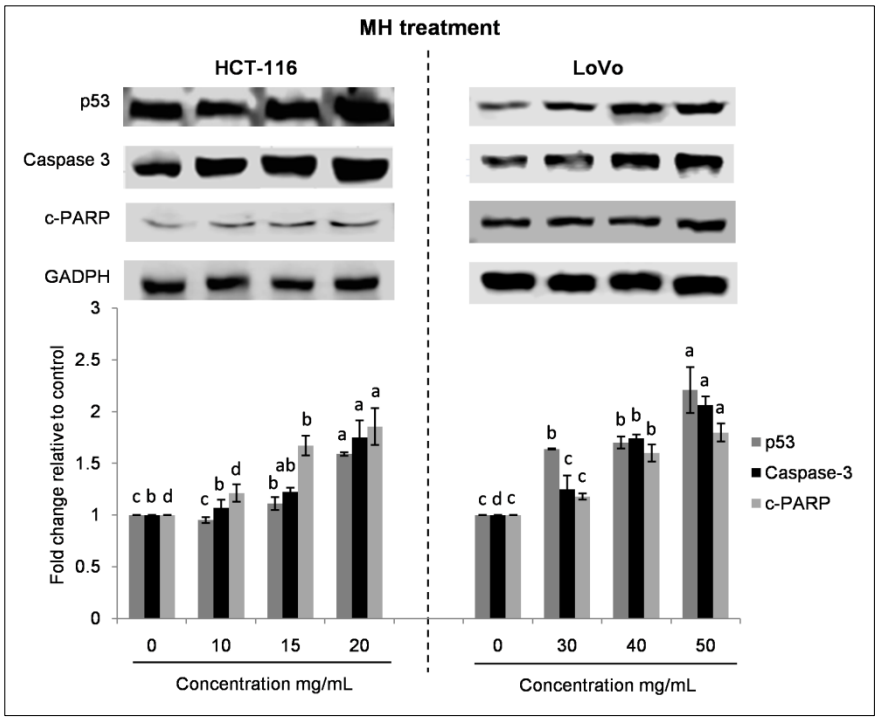

Figure 3.9. MH treatment increases apoptotic protein expression in HCT-116 and LoVo cells. After 24 h incubation, HCT-116 and LoVo cells were treated with different concentrations of MH for 48 h. The concentration of 0 mg/mL corresponds to control (untreated cells). The expression of apoptotic markers p53, caspase-3 and cleaved PARP (c-PARP) were determined by western blotting analysis. GADPH was used as a loading control. All data shown were the mean ± SD of three independent experiments. Different superscripts letter for each column indicated significant differences ($p < 0.05$).

Similarly, in LoVo cells, the protein expression was increased from 1.63 to 2.21 fold, 1.25 to 2.06 fold and 1.18 to 1.80 fold after MH treatment (Figure 3.9) and 1.32 to 2.27 fold, 1.69 to 3.09 fold and 1.65 to 2.70 fold, respectively after STH treatment (Figure 3.10). Taken together, the data show that treatment with MH and STH could induce apoptosis in a dose dependent manner in HCT-116 and LoVo cell lines.

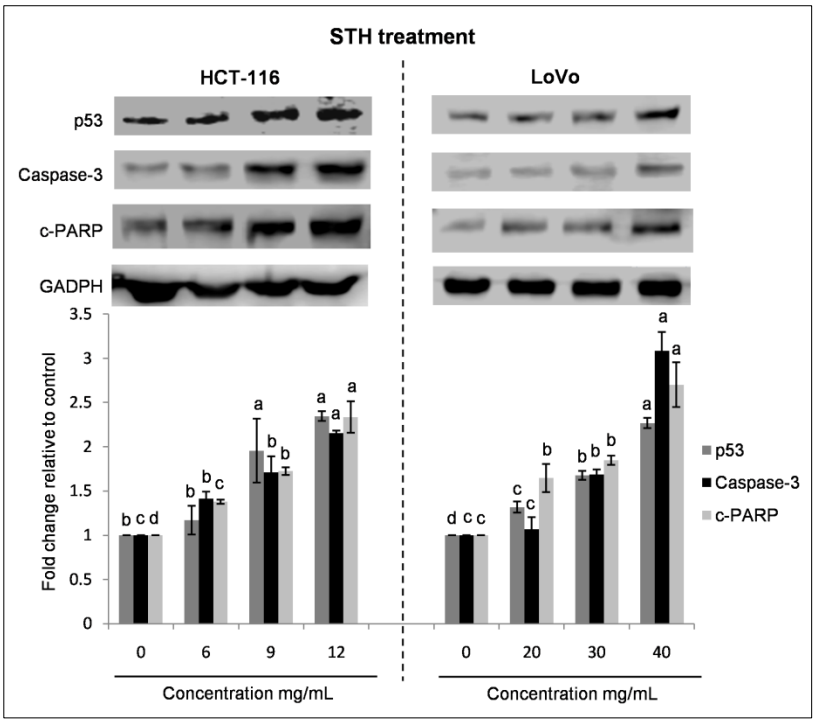

Figure 3.10. STH treatment increases apoptotic protein expression in HCT-116 and LoVo cells. After 24 h incubation, HCT-116 and LoVo cells were treated with different concentrations of STH for 48 h. The concentration of 0 mg/mL corresponds to control (untreated cells). The expression of apoptotic markers p53, caspase-3 and c-PARP were determined by western blotting analysis. GADPH was used as a loading control. All data shown were the mean ± SD of three independent experiments. Different superscripts letter for each column indicated significant differences ($p < 0.05$).

3.2.4. Anti-inflammatory effect of MH and STH on HCT-116 cells

In colorectal and colitis-associated tumors, NFκB activation has been observed, leading to the increase of a number of pro-inflammatory cytokines and mediators, such as TNF-α, IL1β, IL-6, iNOS, COX-2 and PGE2 which play an important role in the progression of CRC development (Klampfer, 2011; Ohta et al., 2006). Anti-inflammatory activity of MH and STH was characterized by measuring the protein expression of NFκB, p-IκBα, IL1β, IL-6, iNOS and TNF-α biomarkers in HCT-116 cells. The expression of NFκB, p-IκBα, IL1β, IL-6, iNOS and TNF-α was significantly suppressed by up to 0.51 fold, 0.31 fold, 0.43 fold, 0.44 fold, 0.31 fold and 0.69 fold in response to MH treatment (Figure 3.11a). In the case of STH, the expression was suppressed up to 0.66 fold, 0.57 fold, 0.55 fold, 0.61 fold, 0.35 fold and 0.32 fold after STH treatment, respectively (Figure 3.11b).

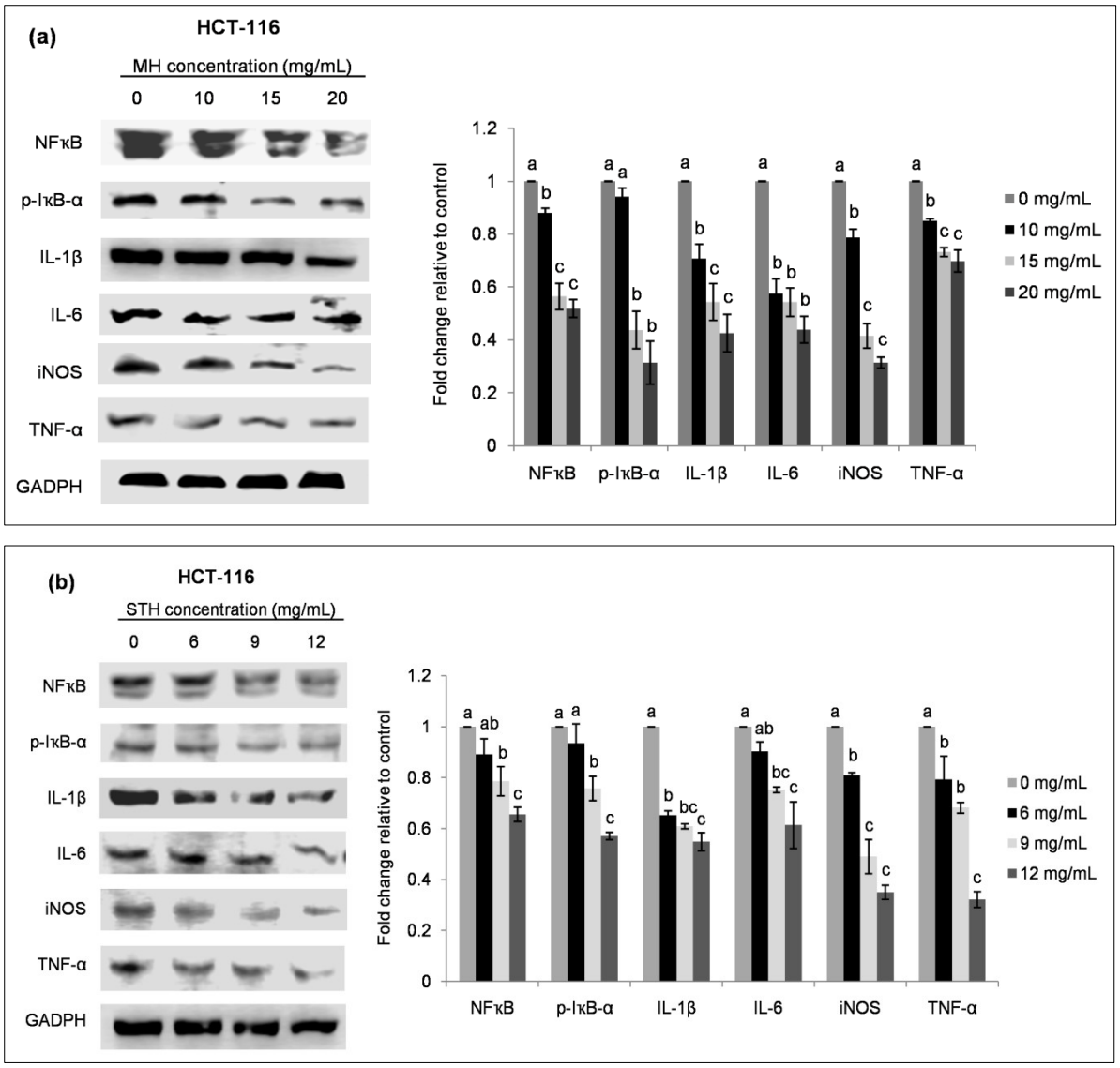

Figure 3.11. Anti-inflammatory effects of MH (a) and STH (b) in HCT cells. After 24 h incubation, HCT-116 cells were treated with different concentrations of MH and STH for 48 h. The concentration of 0 mg/mL corresponds to control (untreated cells). The expression of inflammatory markers NFκB, p-IκBα, IL1β, IL-6, iNOS and TNF-α were determined by western blotting analysis. GADPH was used as a loading control. All data shown were the mean ± SD of three independent experiments. Different superscripts letter for each column indicated significant differences ($p < 0.05$).

3.2.5. Effect of MH and STH on MAPK and EGFR signaling pathways on HCT-116 and LoVo cells

MAPKs, consisting of JNK, Erk1/2 and p38 MAPK, are known to communicate, enlarge and integrate signals from a wide variety of stimuli in controlling cellular proliferation, development, differentiation, inflammatory responses and apoptosis in CRC (Dhillon et al., 2007). Therefore, the western blot analysis was performed to investigate whether these

signaling pathways were functionally involved in the apoptosis effect of MH and STH in HCT-116 and LoVo cells.

As shown in Figure 3.12, MH increased the phosphorylation of p38MAPK and Erk1/2 protein from 1.82 to 2.63 fold and 1.49 to 2.60 fold for HCT-116 cells at dose 10 to 20 mg/mL and 1.50 to 2.48 fold and 2.11 to 3.29 fold for LoVo cells at dose 30 to 40 mg/mL, respectively.

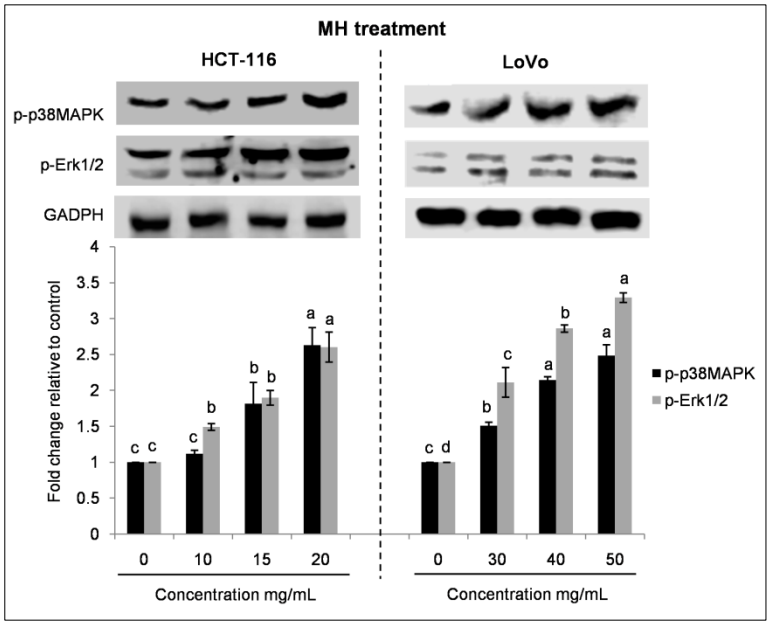

Figure 3.12. MH treatment induces apoptosis via MAPK signaling in HCT-116 and LoVo cells. After 24 h incubation, HCT-116 and LoVo cells were treated with different concentrations of MH for 48 h. The concentration of 0 mg/mL corresponds to control (untreated cells). The expression of p-p38MAPK, and p-Erk1/2 were determined by western blotting analysis. GADPH was used as a loading control. All data shown were the mean ± SD of three independent experiments. Different superscripts letter for each column indicated significant differences ($p < 0.05$).

Moreover, the expression levels of p38MAPK and Erk1/2 proteins were also significantly elevated after STH treatment (9 to12 mg/mL and 20 to 40 mg/mL) in both cell lines from 1.65 fold to 2.25 fold and 1.78 fold to 2.94 fold for HCT-116 cells and 1.20 fold to 1.85 fold and 1.26 fold to 2.09 fold for Lovo cells (Figure 3.13).

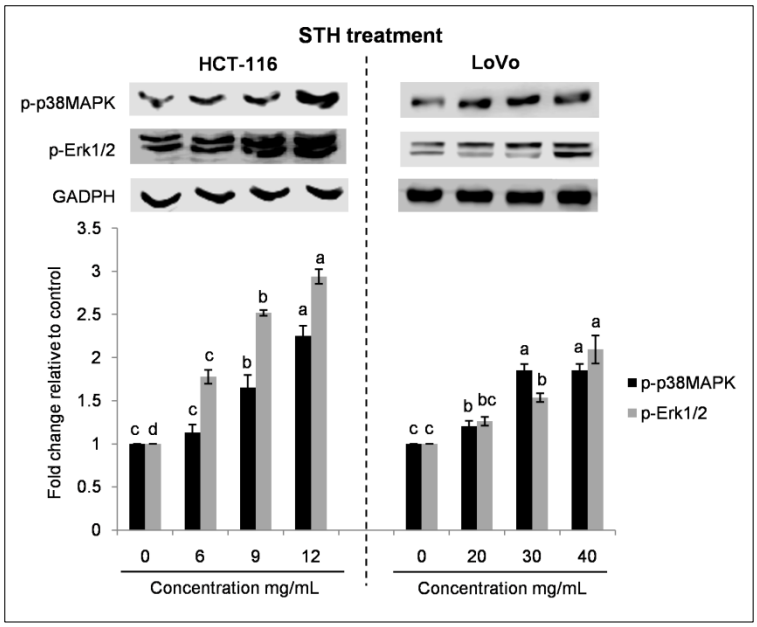

Figure 3.13. STH treatment induces apoptosis via MAPK signaling in HCT-116 and LoVo cells. After 24 h incubation, HCT-116 and LoVo cells were treated with different concentrations of STH for 48 h. The concentration of 0 mg/mL corresponds to control (untreated cells). The expression of p-p38MAPK, and p-Erk1/2 were determined by western blotting analysis. GADPH was used as a loading control. All data shown were the mean ± SD of three independent experiments. Different superscripts letter for each column indicated significant differences ($p < 0.05$).

Activation of EGFR usually has pore prognosis and contributes to the chemoresistances in multiple types of cancer (Cunningham et al., 2004). We further examined the effects of MH and STH on membrane protein EGFR and HER2 and their downstream signaling protein p-Akt on HCT-116 and LoVo cells.

As shown in Figure 3.14 and Figure 3.15, treatment with both honeys dose-dependently suppressed the expression levels of EGFR up to 0.52 fold for HCT-116 cells and up to 0.40 fold for LoVo cells. Similarly, the expression of HER2 was also suppressed up to 0.51 fold and 0.56 fold in HCT-116 cells and up to 0.38 fold and 0.56 fold for LoVo cells, respectively (Figure 3.14).

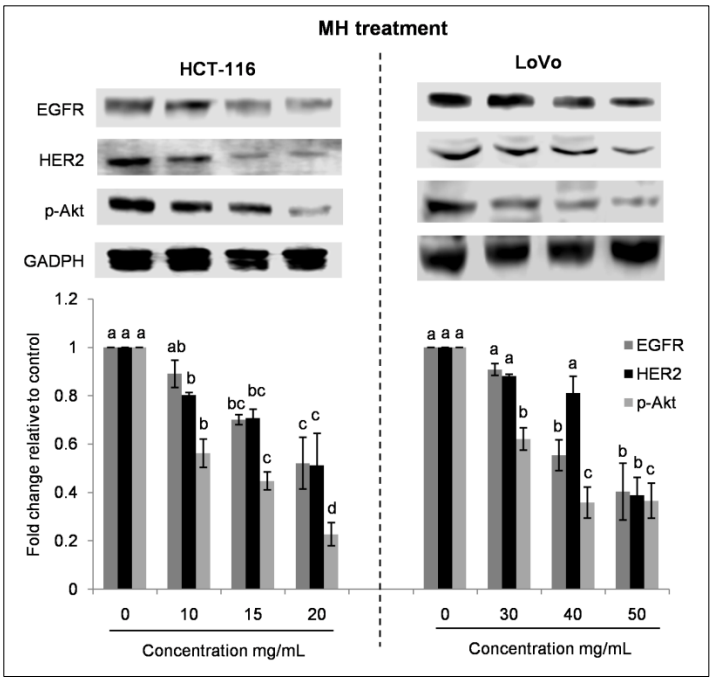

Figure 3.14. The effect of MH treatment on EGFR signaling in HCT-116 and LoVo cells. After 24 h incubation, HCT-116 and LoVo cells were treated with different concentrations of MH for 48 h. The concentration of 0 mg/mL corresponds to control (untreated cells). The expression of EGFR, HER2 and p-Akt were determined by western blotting analysis. GADPH was used as a loading control. All data shown were the mean ± SD of three independent experiments. Different superscripts letter for each column indicated significant differences ($p < 0.05$).

Additionally, MH treatment at high concentration significantly suppressed the expression of p-Akt up to 0.22 fold for HCT-116 and up to 0.37 fold LoVo cells (Figure 3.14). In the case of STH treated cells, the expression was suppressed up to 0.42 fold for both cell lines in a dose-dependent manner (Figure 3.15).

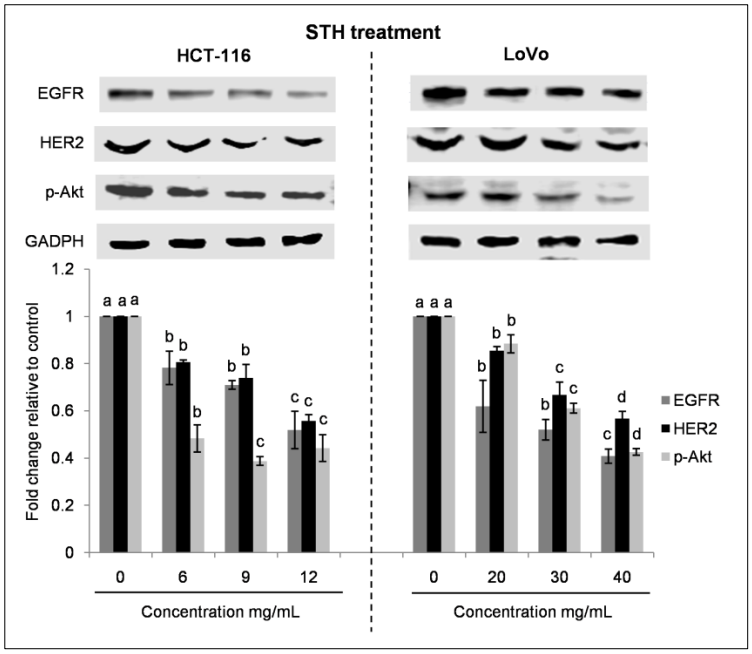

Figure 3.15. The effect of STH treatment on EGFR signaling in HCT-116 and LoVo cells. After 24 h incubation, HCT-116 and LoVo cells were treated with different concentrations of STH for 48 h. The concentration of 0 mg/mL corresponds to control (untreated cells). The expression of EGFR, HER2 and p-Akt were determined by western blotting analysis. GADPH was used as a loading control. All data shown were the mean ± SD of three independent experiments. Different superscripts letter for each column indicated significant differences ($p < 0.05$).

3.2.6. Effect of MH and STH on oxidative stress induction on HCT-116 and LoVo cells

In oxidative stress, there is an imbalance among production of ROS or other oxidants and their abolition by defensive mechanisms of antioxidants enzymes. Disorder in this redox equilibrium can lead to damage the main components of the cell (lipids, proteins and DNA), enhancing the possibility of various chronic diseases, including cancer (Nogueira and Hay, 2013). However, recent research methods have demonstrated that natural compounds have the properties to prompt ROS generation, which promotes oxidative stress inducing cancer cells death (Bhardwaj et al., 2016; Gunasekaran et al., 2015; Liao et al., 2015; Santandreu et al., 2011; Sivagami et al., 2012) and it is one of the important therapeutic regimes between conventional therapeutic management.

3.2.6.1. Effect of MH and STH induces intracellular ROS production on HCT-116 and LoVo cells

Since earlier studies have indicated that ROS are moderators of intracellular signaling cascades and can activate a sequence of pathways for programmed cell death. In the present work, we investigated the intracellular ROS production in HCT-116 and LoVo cells. In order to determine the intracellular ROS levels, HCT-116 and LoVo cells were treated for 48 h with or without various concentrations of MH (5 to 20 mg/mL for HCT-116 cells and 20 to 50 mg/mL for LoVo cells) and STH (3 to 12 mg/mL for HCT-116 cells and 10 to 40 mg/mL for LoVo cells). The results were analyzed by using the CellROX® Orange assay kit by Tali™ Image-based Cytometer.

We found that both honey treatments significantly ($p < 0.05$) increased intercellular ROS accumulation in HCT-116 and LoVo cells in a dose dependent manner (Figure 3.16 and Figure 3.17). MH treatment induced more amount of ROS production in LoVo cells 34% at the concentration of 40 mg/mL while in HCT-116 cells it induced 22% ROS at the concentration of 20 mg/mL (Figure 3.16a).

Fluorescence intensity showed a significant and dose-dependently increase in intracellular ROS levels in HCT-116 and LoVo cells after being treated with MH (Figure 3.16b and Figure 3.16c) for 48 h.

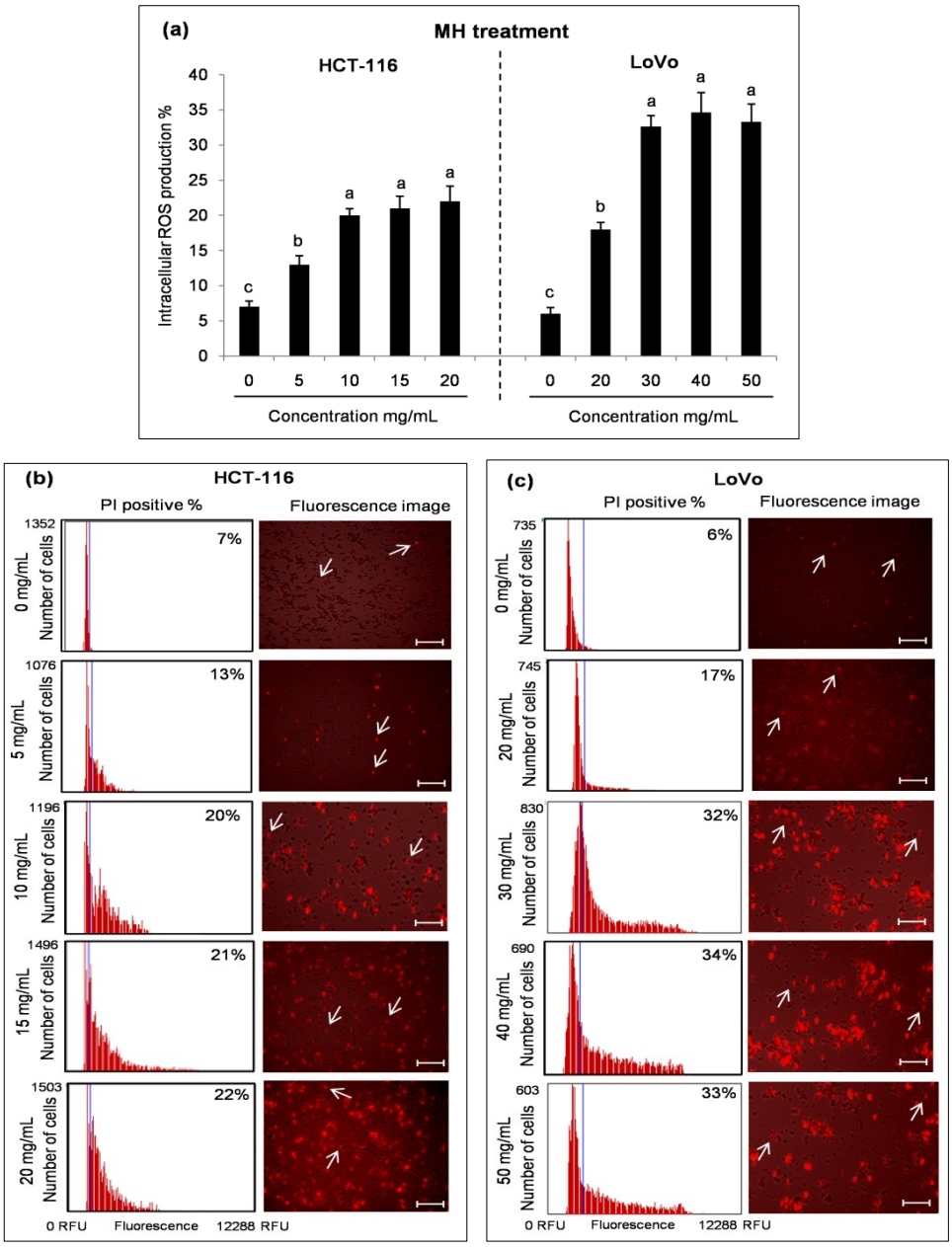

Figure 3.16. MH induces ROS generation in HCT-116 and LoVo cells (a). After 24 h incubation, HCT-116 and LoVo cells were treated with different concentrations of MH for 48 h. The concentration of 0 mg/mL corresponds to control (untreated cells). Intracellular ROS levels were calculated by using CellROX® Orange assay kit and the Tali™ Image-based Cytometer. The blue line of the thumbnail histogram indicated the set threshold. Representative fluorescence image of HCT-116 (b) and LoVo (c) cells shows the effect of MH treatment at 48 h: non-fluorescent while in a reduced state and bright red fluorescence upon oxidation by ROS. Scale bar = 50 µm, arrows indicate single cell (cell size =10 µm). All data shown were the mean ± SD of three independent experiments. Different superscripts letter for each column indicated significant differences ($p < 0.05$).

Similar trend also observed after STH treatment. In LoVo cells, it induced 38% of ROS production at the concentration of 20 and 30 mg/mL while in HCT-116 cells it induced 20.5% ROS production at the concentration of 6 and 9 mg/mL (Figure 3.17a).

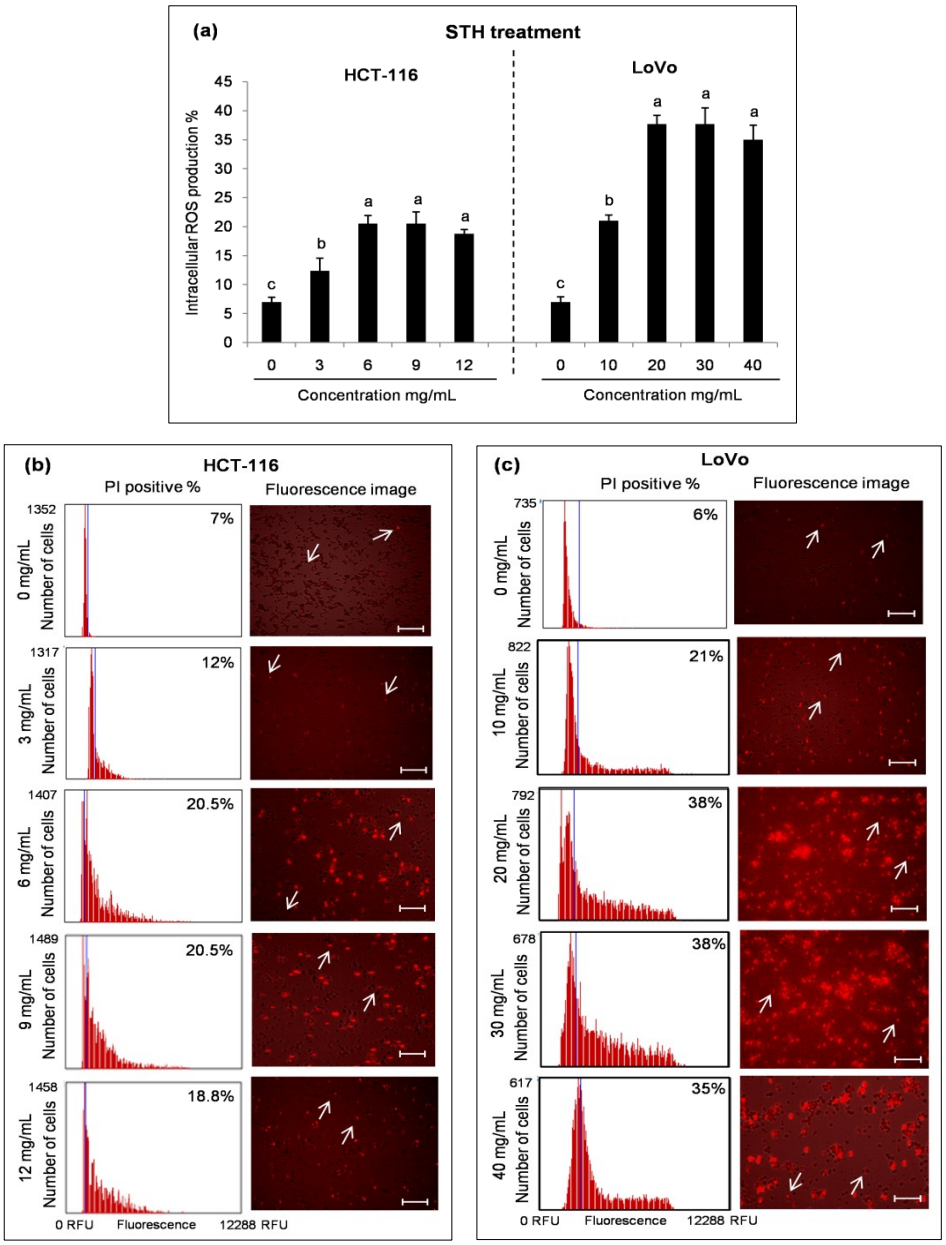

Figure 3.17. STH induces ROS generation in HCT-116 and LoVo cells (a). After 24 h incubation, HCT-116 and LoVo cells were treated with different concentrations of STH for 48 h. The concentration of 0 mg/mL corresponds to control (untreated cells). Intracellular ROS levels were calculated by using CellROX® Orange assay kit and the Tali™ Image-based Cytometer. The blue line of the thumbnail histogram indicated the set threshold. Representative fluorescence image of HCT-116 (b) and LoVo (c) cells shows the effect of STH treatment at 48 h: non-fluorescent while in a reduced state and bright red fluorescence upon oxidation by ROS. Scale bar = 50 µm, arrows indicate single cell (cell size =10 µm). All data shown were the mean ± SD of three independent experiments. Different superscripts letter for each column indicated significant differences ($p < 0.05$).

In HCT-116 cells both honey induced similar amount of ROS production but STH needs less concentration compared to MH. Similarly in LoVo cells, STH induced more amount of ROS production at less concentration than MH. Fluorescence intensity showed a significant and dose-dependently increase in intracellular ROS levels in HCT-116 and LoVo cells after being treated with STH (Figure 3.17b and Figure 3.17c) for 48 h.

3.2.6.2. Effect of MH and STH on the biomarkers of oxidative stress and the antioxidant system on HCT-116 and LoVo cells

Next, we measured the biomarkers of oxidative damaged of lipid (TBARS level), protein (carbonyl content) and DNA (OGG1 expression) after MH and STH treatment. Our results showed that TBARS levels and protein carbonyl content were significantly ($P < 0.05$) increased 137 to 245% and 130 to 263% in HCT-116 cells and 138 to 192% and 127 to 279% in LoVo cells after MH treatment compared to control (Figure 3.18a).

In the case of STH, TBARS level and protein carbonyl content were 165 to 222% and 174 to 233% in HCT-116 cells and 102 to 166% and 149 to 242% in LoVo cells respectively after STH treatment compared to control (Figure 3.18b). MH induced most effective results for increasing the levels of TBARs and protein carbonyl content in both cell lines compared to STH.

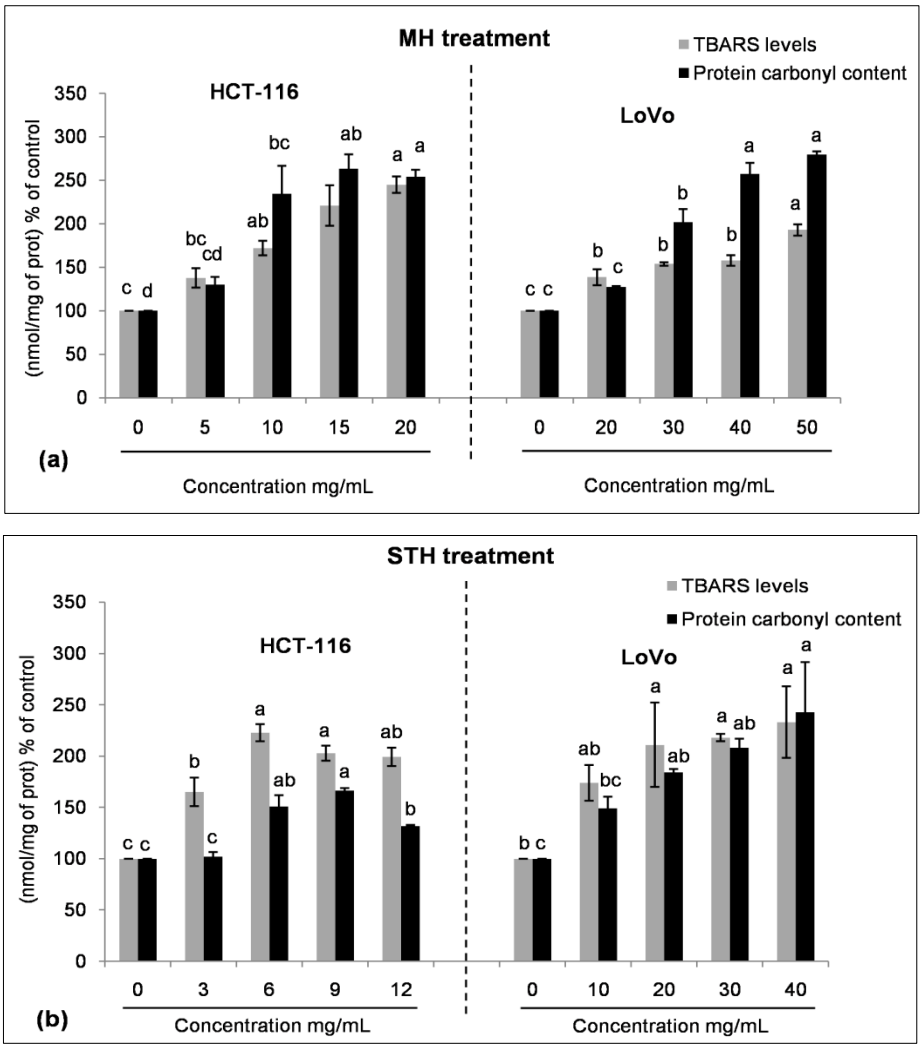

Figure 3.18. MH (a) and STH (b) induce oxidative stress in HCT-116 and LoVo cells. Lipid and protein oxidative damage was evaluated from the TBARS levels and protein carbonyl content. After 24 h incubation, HCT-116 and LoVo cells were treated with different concentrations of MH and STH for 48 h. The concentration of 0 mg/mL corresponds to control (untreated cells).The results were measured as unit per mg protein and expressed as the percent of the control. All data shown were the mean ± SD of three independent experiments. Different superscripts letter for each column indicated significant differences ($p < 0.05$).

Western blot analysis revealed that MH treatment increased the protein expression of OGG1 from 1.3 to 2.5 fold in HCT-116 cells and from 1.1 to 1.8 fold in LoVo cells compared to control, indicating DNA damage (Figure 3.19a). The protein expression OGG1 was also increased from 1.2 to1.9 fold in HCT-116 cells and from 1.26 to 2.35 fold in LoVo cells compared to control after STH treatment (Figure 3.19b). In HCT-116 cells, MH treatment induced most effective results while in LoVo cells STH induced most effective results.

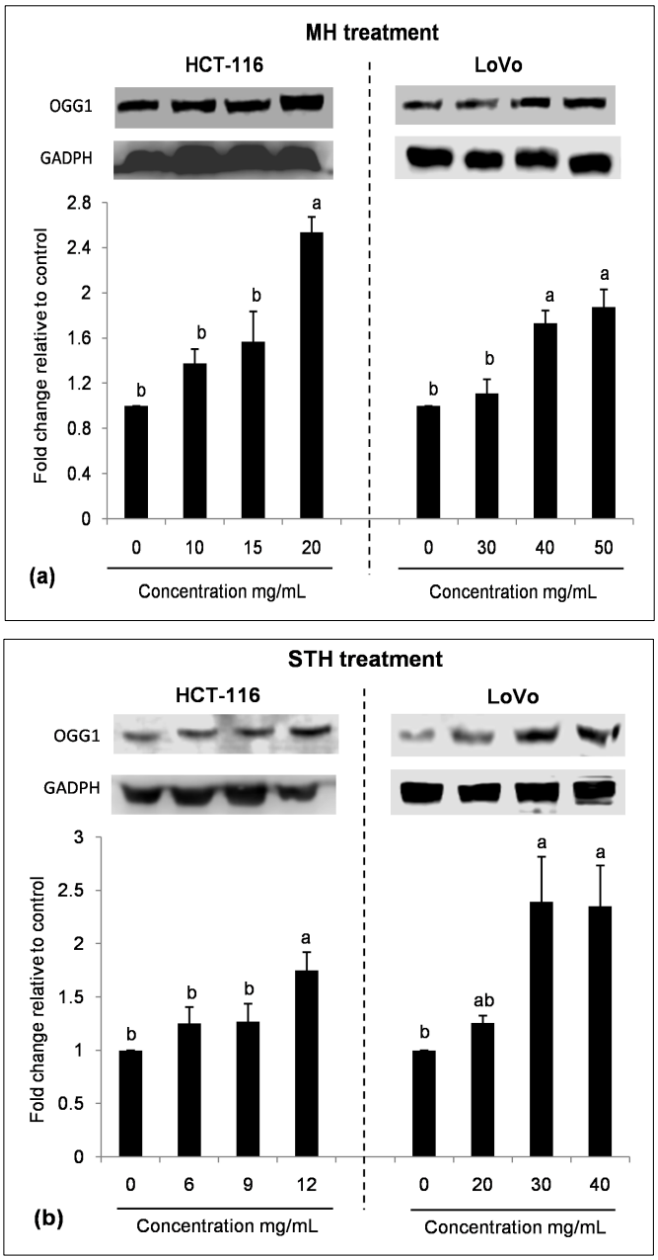

Figure 3.19. MH (a) and STH (b) induce DNA damage in HCT-116 and LoVo cells. After 24 h incubation, HCT-116 and LoVo cells were treated with different concentrations of MH and STH for 48 h. The concentration of 0 mg/mL corresponds to control (untreated cells).The expression of OGG1 was determined by western blotting analysis. GADPH was used as a loading control. All data shown were the mean ± SD of three independent experiments. Different superscripts letter for each column indicated significant differences ($p < 0.05$).

Furthermore, the activity and the expression of the antioxidant enzymes were examined by both honeys in HCT-116 and LoVo cells. Our data showed that the activity of GPx, GST and GR was decreased from 89 to 43%, 74 to 46% and 72 to 39% for HCT-116 cells and 78 to 35%, 88 to 60% and 85 to 48% for LoVo cells, respectively, compared to control (100%) after MH treatment (Figure 3.20a). Similar trends were also found for STH treatment: the activity of GPx, GST and GR was decreased up to 93 to 49%, 75 to 51% and 92 to 47%, in HCT-116 cells and 84 to 30%, 91 to 48% and 90 to 45% in LoVo cells, respectively, compared to control (100%) (Figure 3.20b).

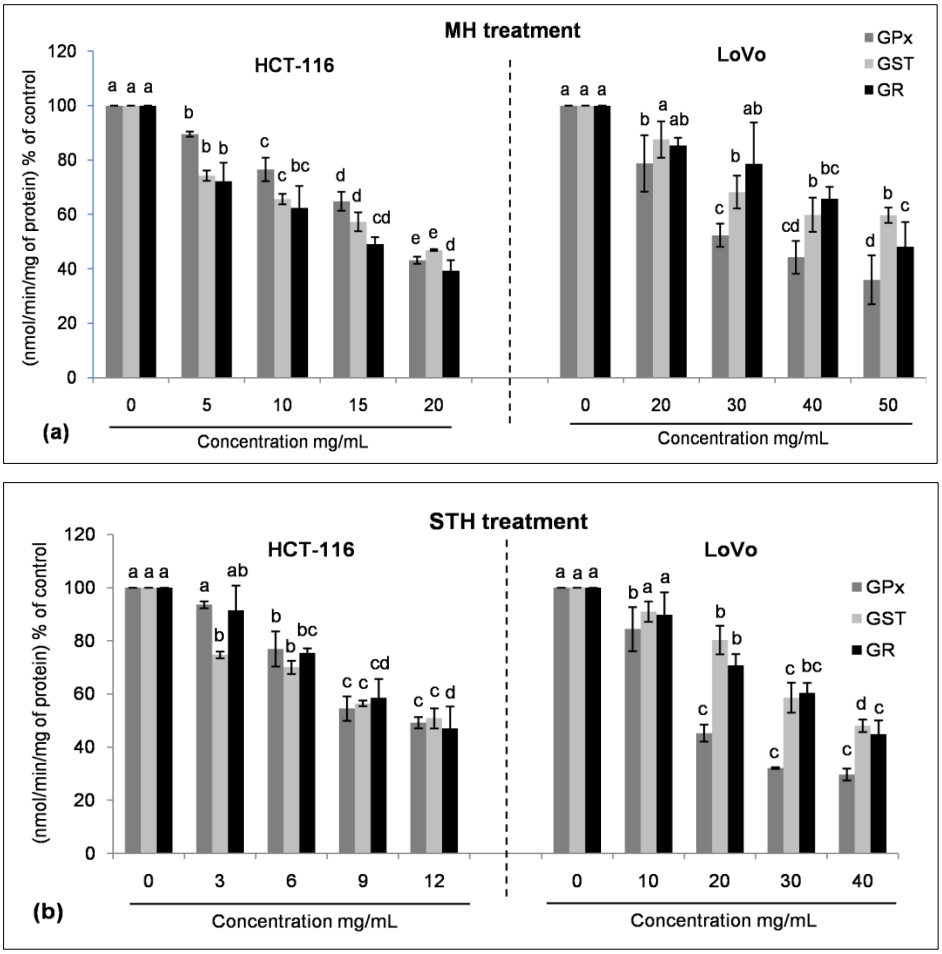

Figure 3.20. MH (a) and STH (a) treatment suppresses the antioxidant enzyme GPx, GST and GR activity in HCT-116 and LoVo cells. After 24 h incubation, HCT-116 and LoVo cells were treated with different concentrations of MH and STH for 48 h. The concentration of 0 mg/mL corresponds to control (untreated cells). GPx, GST and GR activity was expressed as unit per mg protein and results were expressed as the percent of the control. All data shown were the mean ± SD of three independent experiments. Different superscripts letter for each column indicated significant differences ($p < 0.05$).

Moreover, the activity of SOD and catalase also decreased after MH and STH treatment in both CRC cell lines (Figure 3.21). In HCT-116 cells, MH treatment decreased SOD and catalase activity were from 74 to 55% and 82 to 47% and in LoVo cells from 87 to 66% and from 91 to 53 % respectively, compared to control (100%) (Figure 3.21a). Similarly, STH also reduced SOD and catalase activity were from 91 to 58% and from 66 to 28% in HCT-116 cells and from 84 to 36% and from 87 to 33% in LoVo cells, respectively, compared to control (100%) (Figure 3.21b).

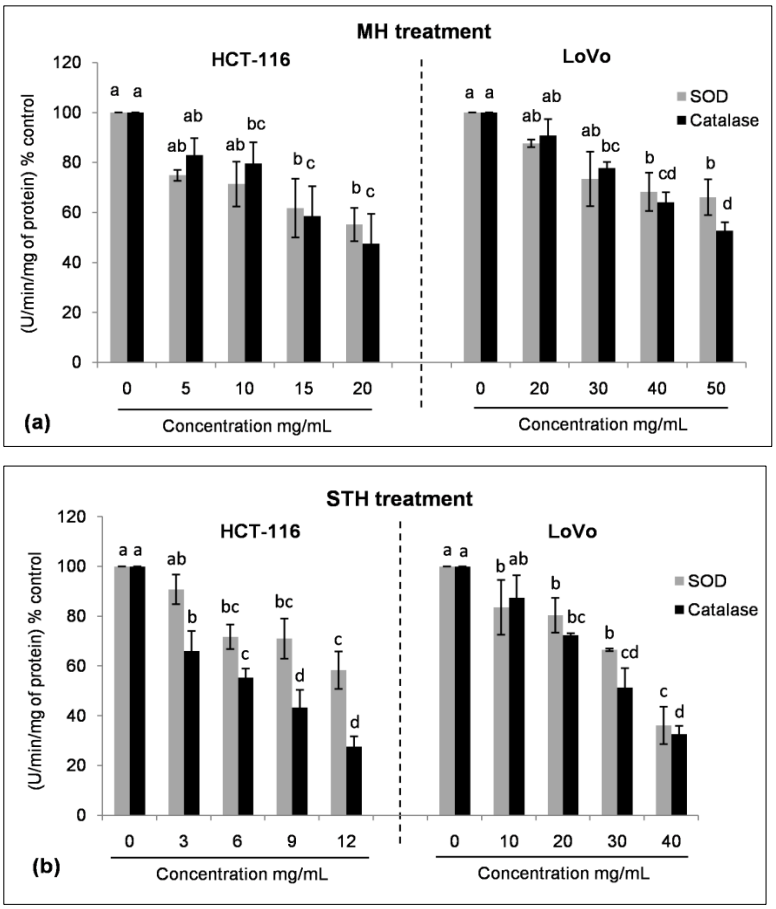

Figure 3.21. MH (a) and STH (a) treatment suppresses the antioxidant enzyme SOD and catalase activity in HCT-116 and LoVo cells. After 24 h incubation, HCT-116 and LoVo cells were treated with different concentrations of MH and STH for 48 h. The concentration of 0 mg/mL corresponds to control (untreated cells). SOD and catalase activity was expressed as unit per mg protein and results were expressed as the percent of the control. All data shown were the mean ± SD of three independent experiments. Different superscripts letter for each column indicated significant differences ($p < 0.05$).

Furthermore, the protein expression of the transcription factor Nrf2 and other antioxidant enzyme SOD, catalase and HO-1 was found to be lowered by 0.85 to 0.55 fold, 0.81 to 0.58 fold, 0.86 to 0.46 fold and 0.91 to 0.29 fold in HCT-116 cells and 0.58 to 0.32 fold, 0.86 to 0.62 fold, 0.87 to 0.57 fold and 0.78 to 0.63 fold in LoVo cells compared to control after MH treatment at different concentrations (Figure 3.22).

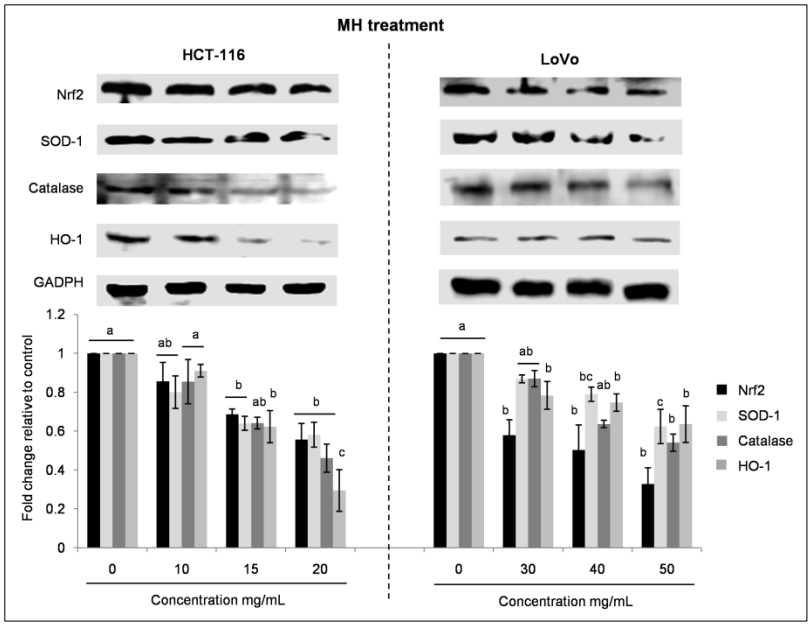

Figure 3.22. MH treatment suppresses the expression of antioxidant enzyme in HCT-116 and LoVo cells. After 24 h incubation, HCT-116 and LoVo cells were treated with different concentrations of MH for 48 h. The concentration of 0 mg/mL corresponds to control (untreated cells). Nrf2, SOD-1, catalase and HO-1 protein expressions were analyzed by western blotting. GADPH was utilized as a loading control. All data shown were the mean ± SD of three independent experiments. Different superscripts letter for each column indicated significant differences ($p < 0.05$).

Similarly, the expression of Nrf2, SOD, catalase and HO-1 was also suppressed from 0.83 to 0.50 fold, 0.71 to 0.48 fold, 0.76 to 0.29 fold and 0.74 to 0.50 fold in HCT-116 cells and 0.85 to 0.55 fold, 0.67 to 0.38 fold, 0.93 to 0.31 fold and 0.73 to 0.52 fold in loVo cells, respectively at different concentration of STH treatment (Figure 3.23).

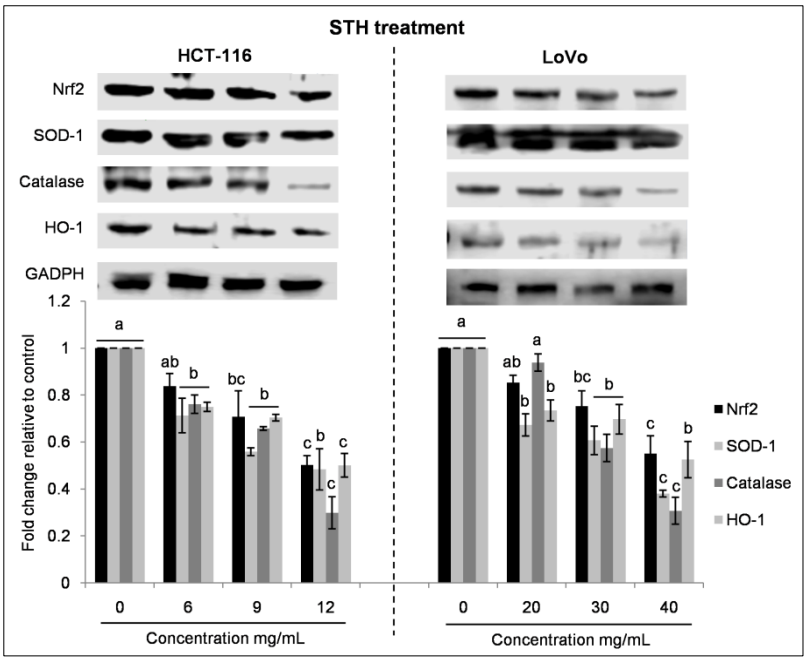

Figure 3.23. STH treatment suppresses the expression of antioxidant enzyme in HCT-116 and LoVo cells. After 24 h incubation, HCT-116 and LoVo cells were treated with different concentrations of STH for 48 h. The concentration of 0 mg/mL corresponds to control (untreated cells). Nrf2, SOD-1, catalase and HO-1 protein expressions were analyzed by western blotting. GADPH was utilized as a loading control. All data shown were the mean ± SD of three independent experiments. Different superscripts letter for each column indicated significant differences ($p < 0.05$).

3.2.7. Effect of MH and STH on ER stress induction on HCT-116 and LoVo cells

Previous studies reported that various natural compounds are involved in activation of ER stress, which is a common phenomenon in stress-induced apoptosis (Khan et al., 2016; Zhang et al., 2013b). The protein level of ER stress-associated molecules, ATF6 and XBP1, was investigated by western blotting. As shown in Figure 3.24, the lower concentration of MH did not cause an upregulation of ATF6 and XBP1 expressions in both cell lines, but after treatment with higher concentrations the expression of these two proteins was upregulated 1.77 to 2.15 fold and 1.16 to 1.75 fold in HCT-116 cells and 1.42 to 2.56 fold and 1.91 to 2.62 fold in Lovo cells compared to control, respectively.

In the case of STH, all the concentration increased the expression of both ER stress genes from 1.29 to 2.27 fold and 1.27 to 2.12 fold for HCT-116 cells and 1.48 to 2.44 fold and 1.10 to 2.58 fold for LoVo cells compared to control (Figure 3.25).

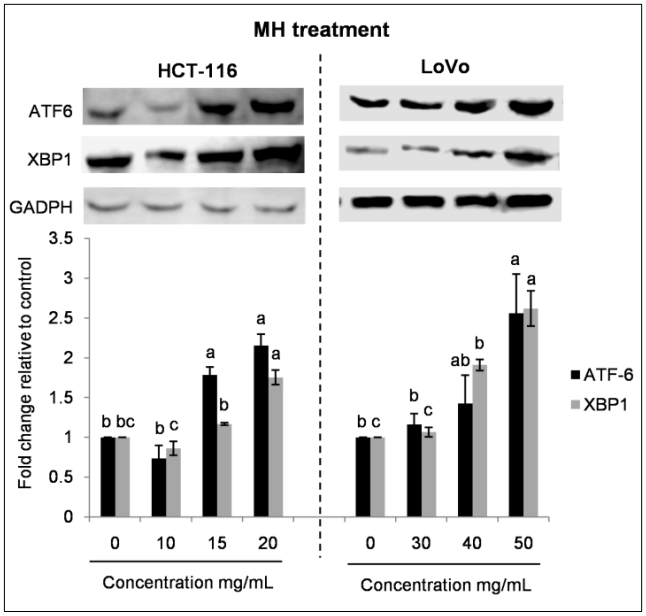

Figure 3.24. MH induces ER stress in HCT-116 and LoVo cells. After 24 h incubation, HCT-116 and LoVo cells were treated with different concentrations of MH for 48 h. The concentration of 0 mg/mL corresponds to control (untreated cells). ATF6 and XBP1 protein expressions were analyzed by western blotting. GADPH was utilized as a loading control. All data shown were the mean ± SD of three independent experiments. Different superscripts letter for each column indicated significant differences ($p < 0.05$).

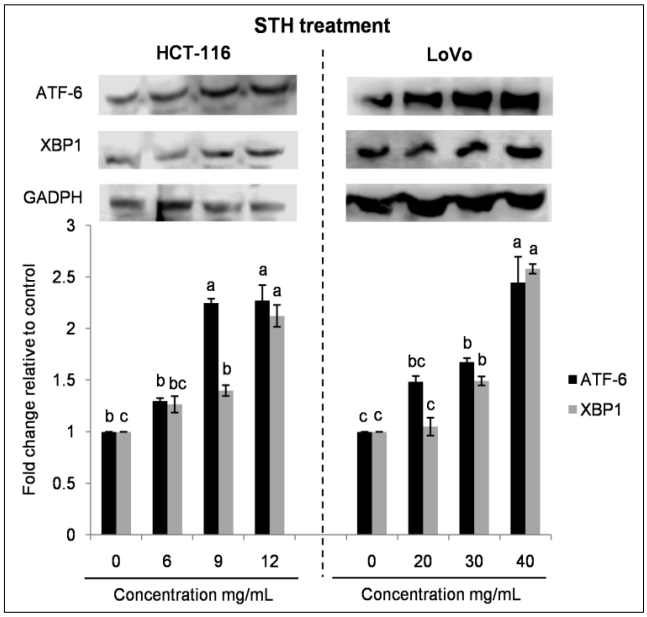

Figure 3.25. STH induces ER stress in HCT-116 and LoVo cells. After 24 h incubation, HCT-116 and LoVo cells were treated with different concentrations of STH for 48 h. The concentration of 0 mg/mL corresponds to control (untreated cells). ATF6 and XBP1 protein expression were analyzed by western blotting. GADPH was utilized as a loading control. All data shown were the mean ± SD of three independent experiments. Different superscripts letter for each column indicated significant differences ($p < 0.05$).

3.2.8. Effect of MH and STH on HCT-116 and LoVo cells metabolism

Cancer cells have the ability to reprogramming the metabolic profile by the metabolic shift from mitochondrial oxidative phosphorylation (OXPHOS) to aerobic glycolysis in order to maintain the requested energy level for continuous growth, rapid proliferation, and other typical characteristics.

3.2.8.1. Effect of MH and STH on mitochondrial resperiation on HCT-116 and LoVo cells

We investigated the effect of MH and STH treatment on the OCR in cultured HCT-116 and LoVo cells. By using the XF cell Mito stress test profile basal respiration, ATP production and proton leak, as well as SRC and MRC were calculated (Figure 3.26a and Figure 3.27a) by using specific inhibitors. Depending to the origin of the cell type, we observed different effect in each cells.

The results showed that MH treatment significantly ($p < 0.05$) reduced the basal OCR dose dependently up to 119.00 ±10.82 pmol/min per 3 $\times 10^4$ cells for HCT-116 cells and 33.17 ± 3.45 pmol/min per 3 $\times 10^4$ cells for LoVo cells compared to control cells (Figure 3.26b). Furthermore, MH treatment also suppressed the activity of the ATP-linked respiration, the proton leak, the SRC and the MRC up to 91.29 ± 10.08, 16.63 ± 4.38, 22.39 ± 0.25 and 117.27 ± 0.50 pmol/min per 3 $\times 10^4$ cells, compared to the control in HCT-116 cells (Figure 3.26b and Figure 3.26c). Similarly, in LoVo cells the activity was suppressed up to 21.56 ± 1.18, 8.60 ± 1.84, 24.62 ± 0.138 and 46.18 ± 0.81 pmol/ min per 3 $\times 10^4$ cells, compared to the control in LoVo cells (Figure 3.26b and Figure 3.26c).

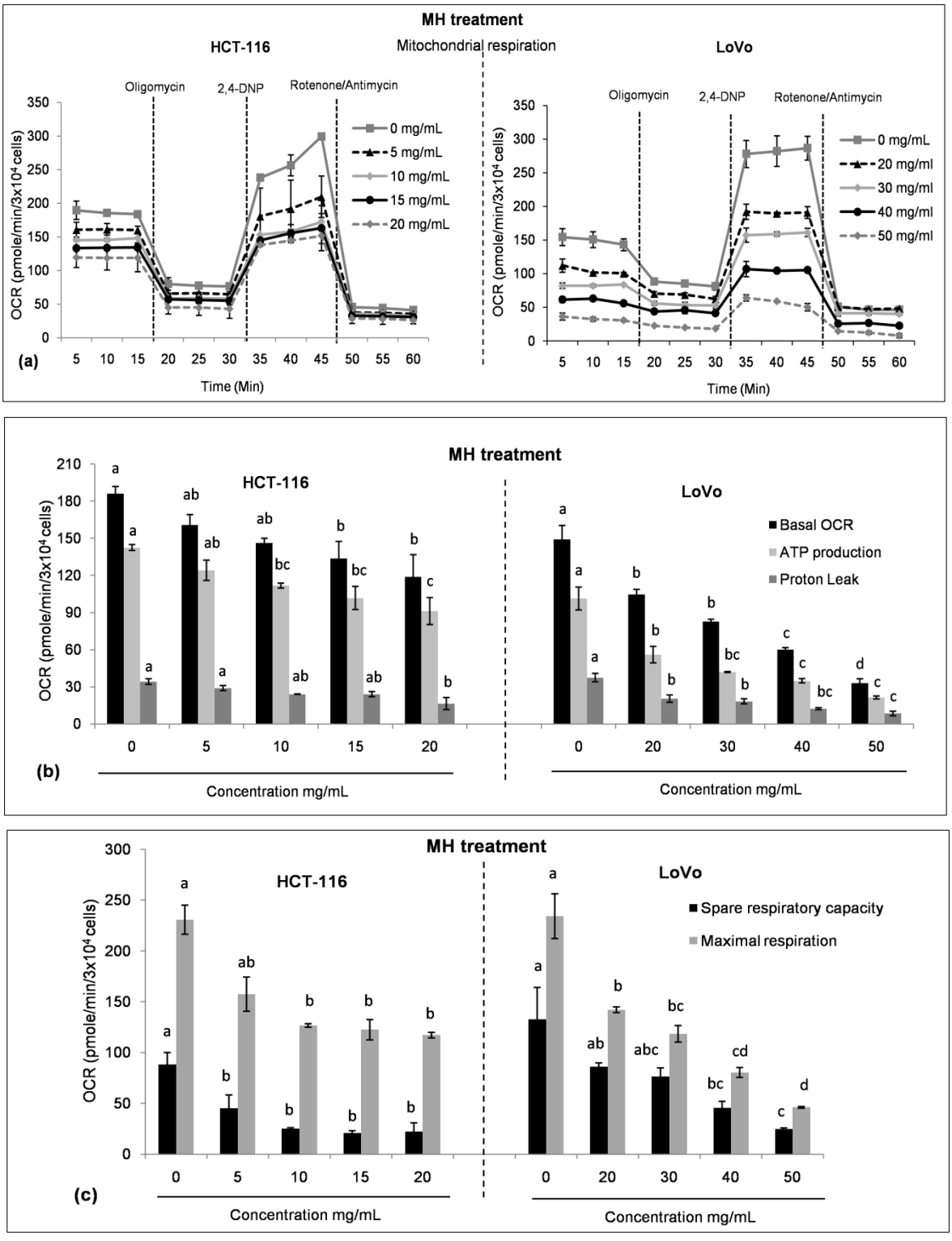

Figure 3.26. Regulation of mitochondrial respiration by MH in HCT-116 and LoVo cells. After 24 h incubation, HCT-116 and LoVo cells were treated with different concentrations of MH for 48 h. The concentration of 0 mg/mL corresponds to control (untreated cells). OCR was determined by using the Seahorse XF-24 Extracellular Flux Analyzer after the following sequential injections: oligomycin (3µg/ml), 2,4-DNP (300 µM), and rotenone/antimycin (1µM/10µM). From the XF cell Mito stress test profile (a), basal respiration, ATP production and proton leak (b) as well as spare capacity and maximal respiration (c) were calculated. All data shown were the mean ± SD of three

independent experiments. Different superscripts letter for each column indicated significant differences ($p < 0.05$).

In the case of STH treatment, basal OCR were significantly ($p < 0.05$) reduced up to 64.69 ± 9.07 pmol/min per 3 $\times 10^4$ cells compared to the control in HCT-116 cells and 31.84 ± 5.32 pmol/min per 3 $\times 10^4$ cells compared to the control in LoVo cells (Figure 3.27b). The activity of the ATP-linked respiration, the proton leak, the SRC and the MRC was also suppressed dose dependently in HCT-116 cells up to 44.14 ± 10.05, 12.11 ± 0.69, 13.60 ± 6.95 and 53.74 ± 2.10 pmol/ min per 3 $\times 10^4$ cells, compared to the control (Figure 3.27b and Figure 3.27c). Furthermore, in LoVo cells the activity suppressed up to 16.60 ± 8.19, 6.18 ± 1.58, 10.26 ± 2.00 and 26.87 ± 10.20 pmol/ min per 3 $\times 10^4$ cells, compared to the control (Figure 3.27b and Figure 3.27c). The most effective results were observed after STH treatment in both colon cancer cell lines compared to MH.

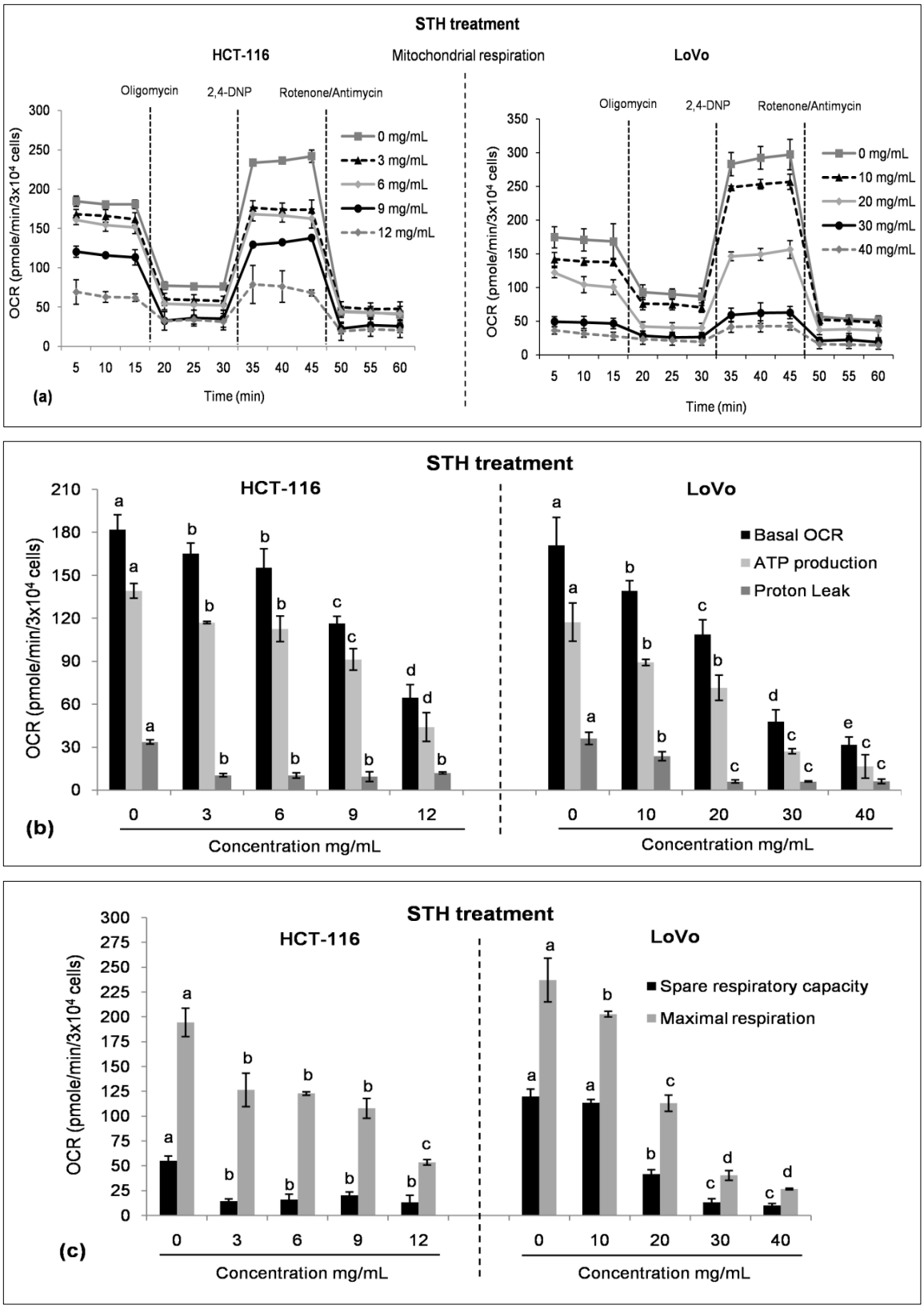

Figure 3.27. Regulation of mitochondrial respiration by STH in HCT-116 and LoVo cells. After 24 h incubation, HCT-116 and LoVo cells were treated with different concentrations of STH for 48 h. The concentration of 0 mg/mL corresponds to control (untreated cells). OCR was determined by using the Seahorse XF-24 Extracellular Flux Analyzer after the following sequential injections: oligomycin (3μg/ml), 2,4-DNP (300 μM), and rotenone/antimycin (1μM/10μM). From the XF cell Mito stress test profile (a) basal respiration, ATP production and proton leak (b) as well as spare capacity and maximal respiration (c) were calculated. All data shown were the mean ± SD of three

independent experiments. Different superscripts letter for each column indicated significant differences ($p < 0.05$).

3.2.8.2. Effect of MH and STH on glycolysis on HCT-116 and LoVo cells

Regarding the ECAR, we observed that MH treatment reduced the basal values by 23.52 ± 0.87 to 10.51 ± 0.90 mpH/ min per 3×10^4 for HCT-116 cells and 13.38 ± 0.87 to 8.18 ± 0.58 mpH/ min per 3×10^4 for LoVo cells compared to control (Figure 3.28a). Furthermore, in both cell lines MH treatment markedly reduced the glycolysis (up to 14.82 ± 0.55 and 8.01 ± 0.71 mpH/ min per 3 x 10^4 cells), glycolytic capacity (up to 7.52 ±1.10 and 13.36 ± 0.19 mpH/ min per 3 $X10^4$ cells) and gylcolytic reserve (up to 5.89 ± 2.20 and 5.35 ± 0.47 mpH/ min per 3×10^4 cells) compared to control in a dose-dependent manner (Figure 3.28b).

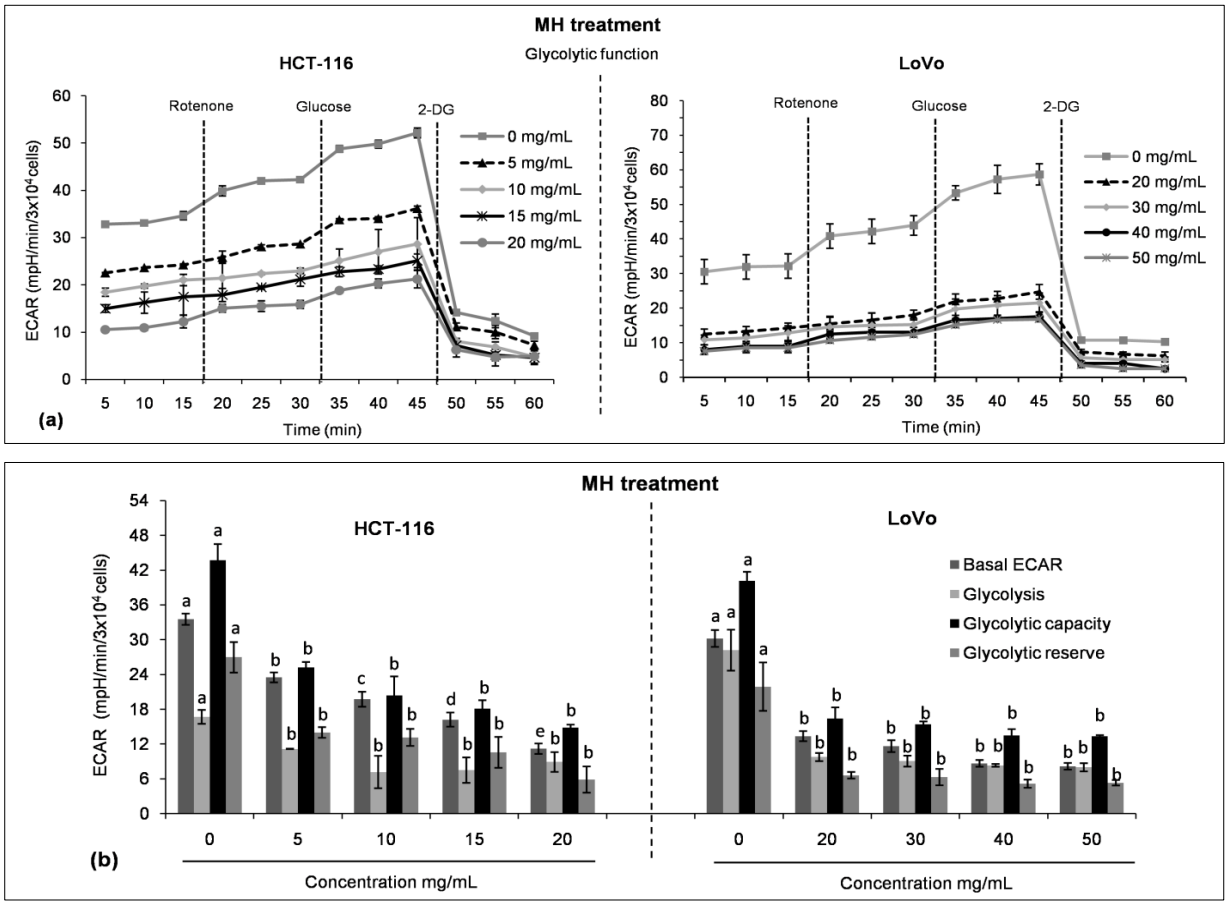

Figure 3.28. Regulation of glycolysis by MH in HCT-116 and LoVo cells. After 24 h incubation, HCT-116 and LoVo cells were treated with different concentrations of MH for 48 h. The concentration of 0 mg/mL corresponds to control (untreated cells). ECAR was determined by using the Seahorse XF-24 Extracellular Flux Analyzer after the following sequential injections: rotenone (1 µM), glucose (30 mM), and 2-DG (100 mM). From the XF glycolysis stress test profile (a) basal ECAR, glycolysis, glycolytic capacity and glycolytic reserves (b) were calculated. All data shown were the mean ± SD of three independent experiments. Different superscripts letter for each column indicated significant differences ($p < 0.05$).

At the same time, as shown in (Figure 3.29), STH treatment decreased the basal ECAR values (up to 5.25 ± 1.04 and 10.61 ± 1.05 mpH/ min per 3 x 10^4 cells),glycolysis (up to 6.09 ± 2.14 and 6.12 ± 1.41mpH/ min per 3 x 10^4 cells), glycolytic capacity (up to 8.47 ± 2.29 and 14.05 ± 2.83 mpH/ min per 3 X10^4 cells) and gylcolytic reserve (up to 2.39 ± 0.90 and 7.48 ± 1.41mpH/ min per 3×10^4 cells) compared to control in HCT-116 and LoVo cells in a dose-dependent manner.

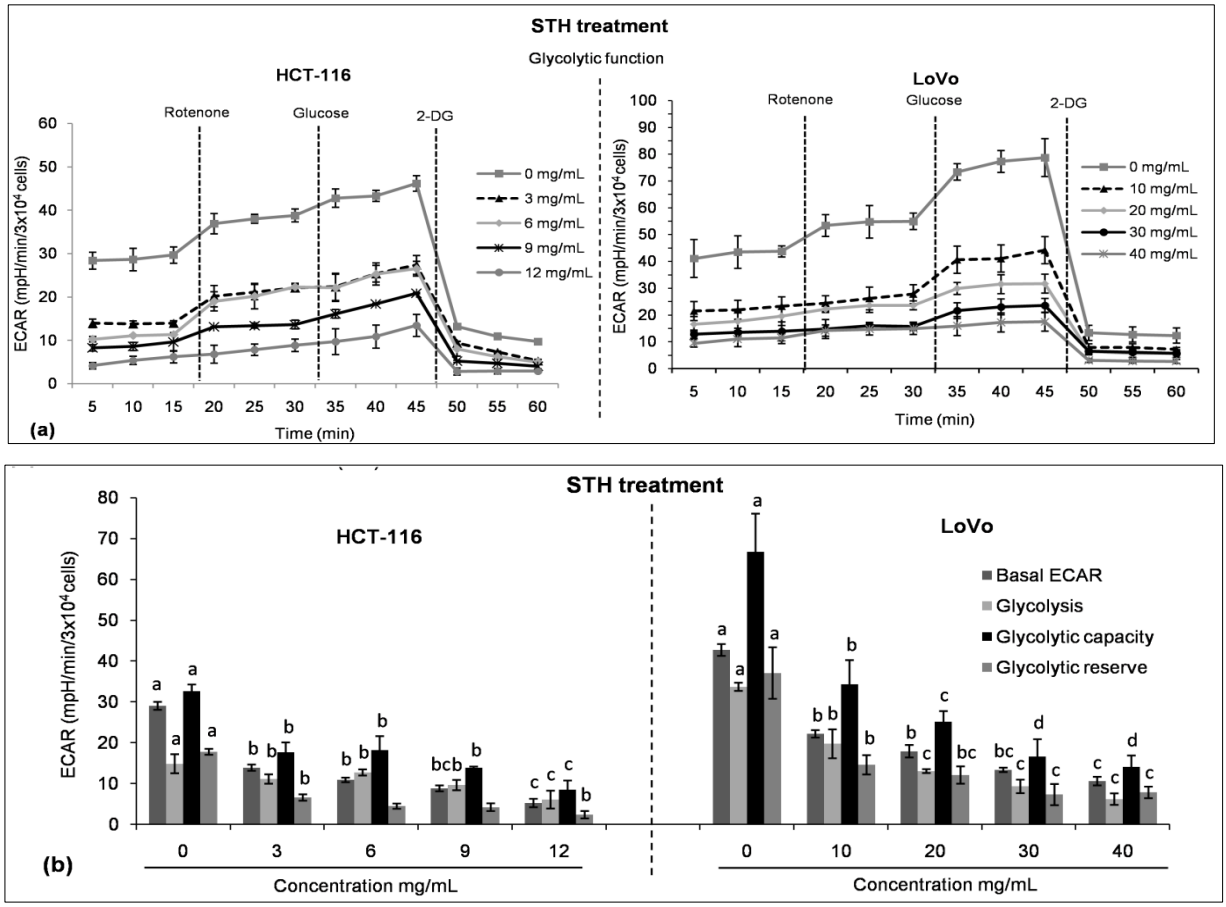

Figure 3.29. Regulation of glycolysis by STH in HCT-116 and LoVo cells. After 24 h incubation, HCT-116 and LoVo cells were treated with different concentrations of STH for 48 h. The concentration of 0 mg/mL corresponds to control (untreated cells). ECAR was determined by using the Seahorse XF-24 Extracellular Flux Analyzer after the following sequential injections: rotenone (1 µM), glucose (30 mM), and 2-DG (100 mM). From the XF glycolysis stress test profile (a) basal ECAR, glycolysis, glycolytic capacity and glycolytic reserves (b) were calculated. All data shown were the mean ± SD of three independent experiments. Different superscripts letter for each column indicated significant differences ($p < 0.05$).

3.2.8.3. Effect of MH and STH on AMPK signaling pathway on HCT-116 and LoVo cells

AMPK signaling pathway is known to be involved in promoting tumor cell survival by increasing mitochondrial biogenesis and inducing metabolic adaptation during glucose limiting condition (Chaube et al., 2015). In the present work, western blot analysis were performed in order to investigate the expression of the proteins related to the AMPK signaling cascade, including its downstream targets PGC1α and SIRT1 in HCT-116 and LoVo cells after treatment with different concentrations of MH and STH. As shown in Figure 3.30, the expressions of p-AMPK/AMPK, PGC1α and SIRT1 were significantly decreased ($P < 0.05$) after MH treatment from 0.56 to 0.22 fold, 0.67 to 0.35 fold and 0.43 to 0.23 fold in HCT-116 cells and 0.69 to 0.57 fold, 0.55 to 0.40 fold and 0.81 to 0.49 fold in LoVo cells compared to control, respectively.

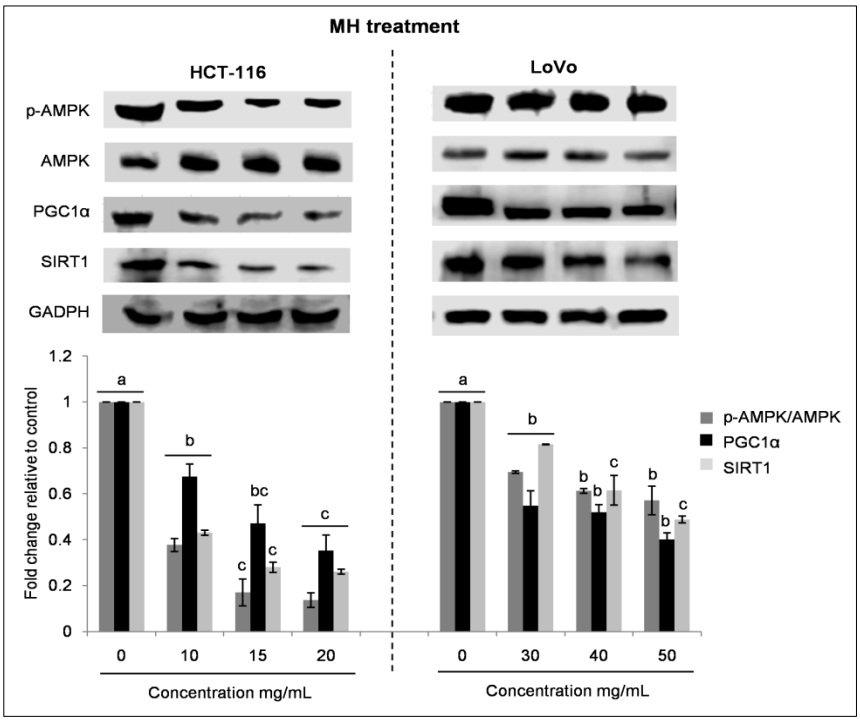

Figure 3.30. MH suppresses the cellular biogenesis by targeting AMPK pathway in HCT-116 and LoVo cells. After 24 h incubation, HCT-116 and LoVo cells were treated with different concentrations of MH for 48 h. The concentration of 0 mg/mL corresponds to control (untreated cells). The protein expressions of p-AMPK, AMPK, PGC1α and SIRT1 were determined by western blotting analysis. GADPH was used as a loading control. All data shown were the mean ± SD of three independent experiments. Different superscripts letter for each column indicated significant differences ($p < 0.05$).

Furthermore, STH treatment suppressed the expression of p-AMPK/AMPK, PGC1α and SIRT1 from 0.57 to 0.27 fold, 0.94 to 0.45 fold and 0.63 to 0.32 fold for HCT-116 cells and 0.71 to 0.38 fold, 0.62 to 0.48 fold and 0.90 to 0.37 fold for LoVo cells at different concentration (Figure 3.31). Together these results suggested that MH and STH treatment decreased AMPK activation leading to a diminution of PGC1α and SIRT1 expressions, which constrained HCT-116 and LoVo cells survival by inhibiting stress adaptation.

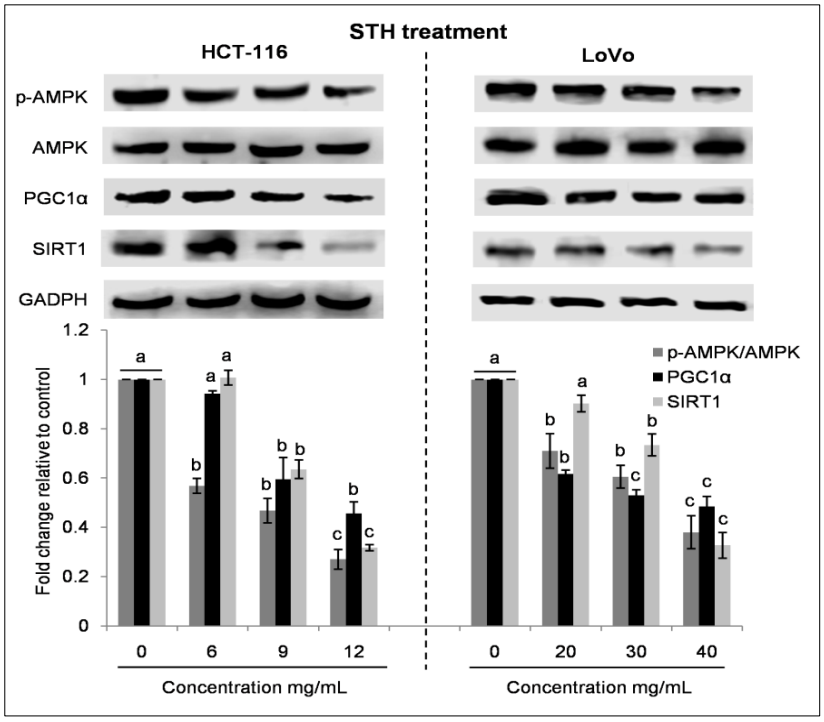

Figure 3.31. STH suppresses the cellular biogenesis by targeting AMPK pathway in HCT-116 and LoVo cells. After 24 h incubation, HCT-116 and LoVo cells were treated with different concentrations of STH for 48 h. The concentration of 0 mg/mL corresponds to control (untreated cells). The protein expressions of p-AMPK, AMPK, PGC1α and SIRT1 were determined by western blotting analysis. GADPH was used as a loading control. All data shown were the mean ± SD of three independent experiments. Different superscripts letter for each column indicated significant differences ($p < 0.05$).

3.2.9. Effect of MH and STH on metastasis activity on HCT-116 and Lovo cells

3.2.9.1. Effect of MH and STH on migration and invasion ability of HCT-116 and Lovo cells

In this part, we evaluated the inhibitory effects of MH and STH on migration and invasion in colon cancer HCT-116 and LoVo cell lines. As shown in Figure 3.32, after 48 h of culture, both cells not subjected to treatments were able to migrate and partially fill the wound empty area while exposure to MH and STH. MH treatment reduced the migration

ability of HCT-116 cells from 37% to 88% compared to control (10%) and in LoVo cells from 30% to 79% compared to control (15%) in a dose dependent manner.

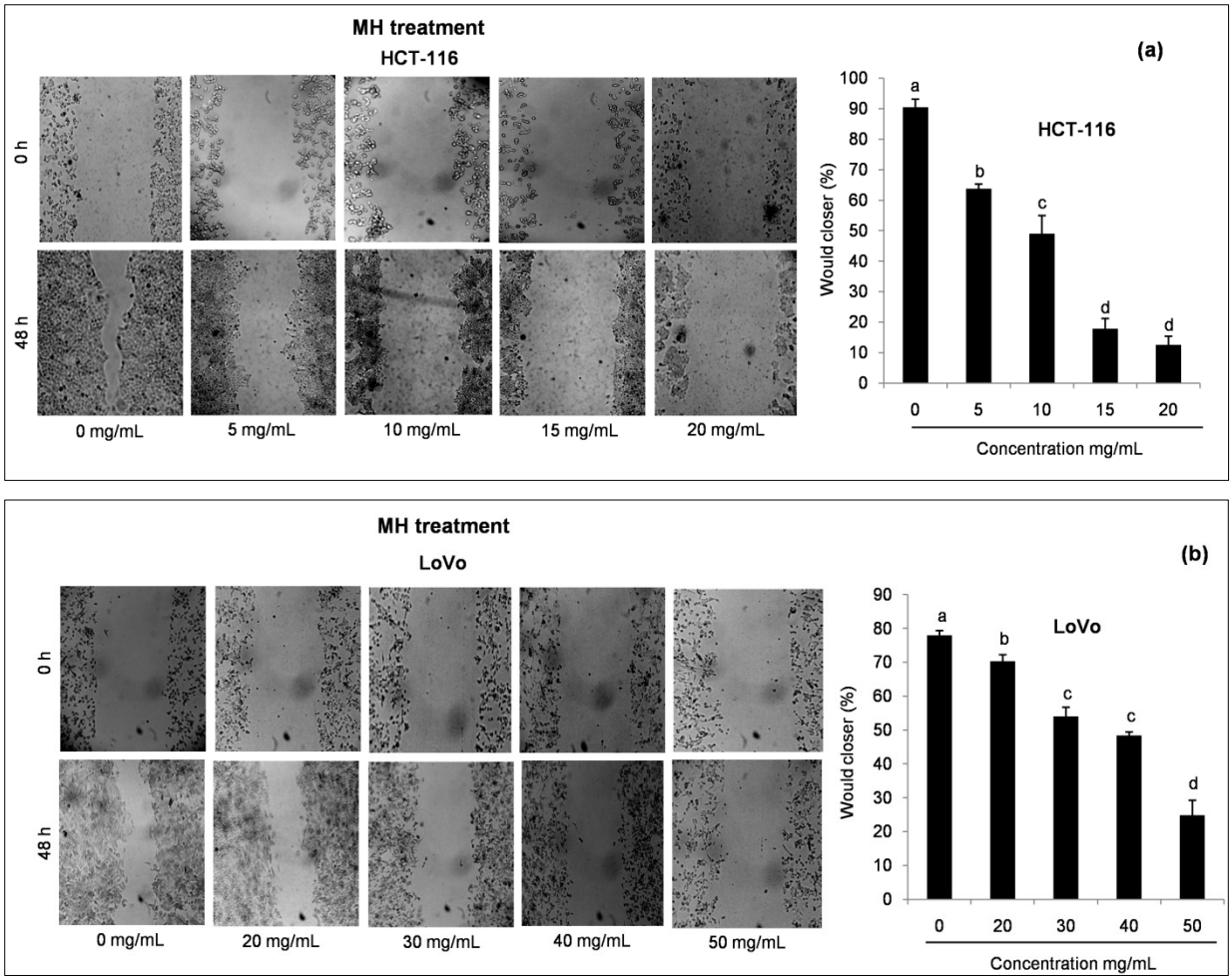

Figure 3.32. MH reduces migration ability of HCT-116 (a) and LoVo (b) cells by wound healing assay. After 24 h incubation, HCT-116 and LoVo cells were treated with different concentrations of MH for 48 h. The wound closure percentages were analyzed by Image J software. All data shown were the mean ± SD of three independent experiments. Different superscripts letter for each column indicated significant differences ($p < 0.05$).

In addition, STH treatmet on HCT-116 and LoVo cells exerted migration inhibitory effects from 31% to 65% compared to control (9%) and 35% to 64% compared to control (20%), respectively (Figure 3.33).

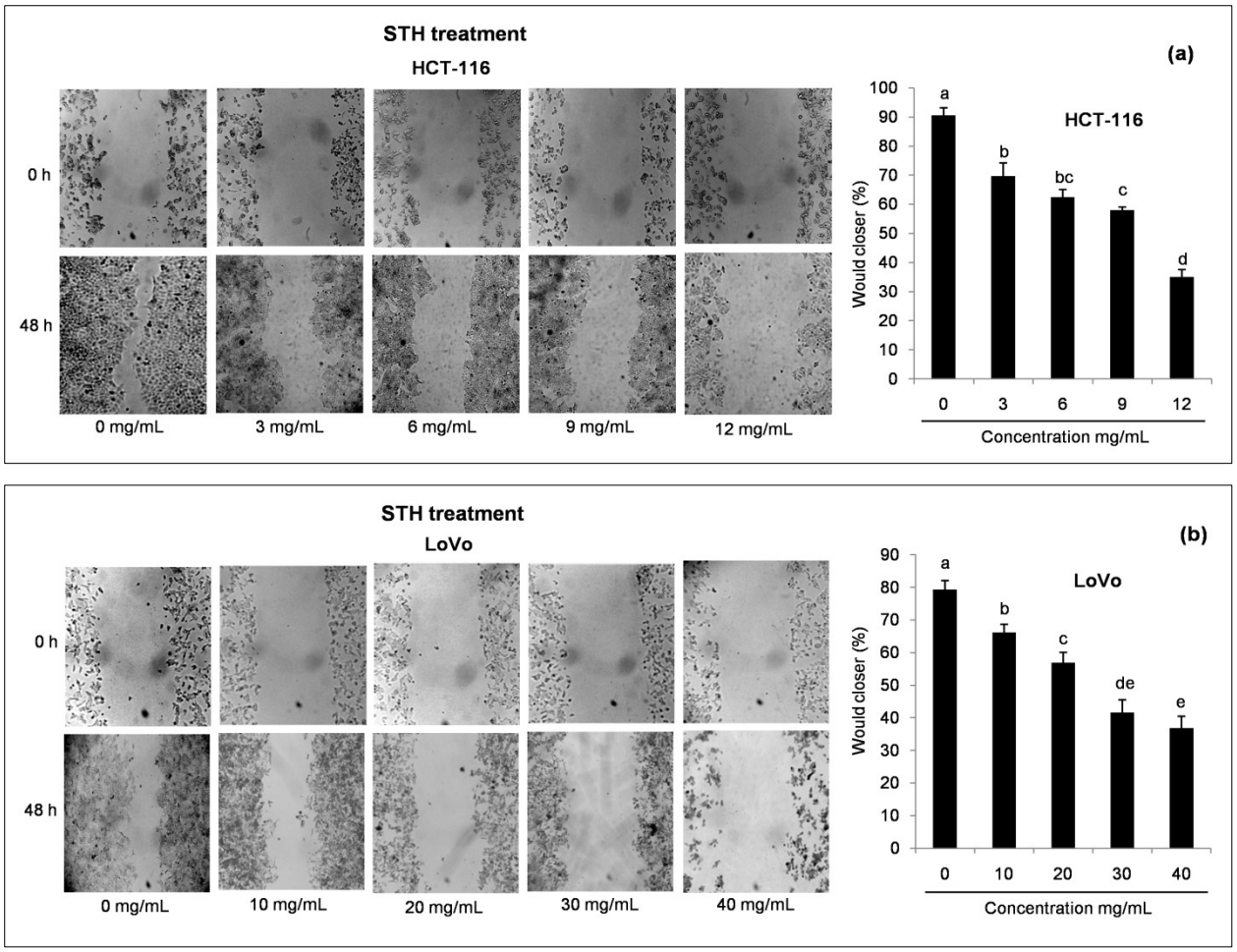

Figure 3.33. STH reduces migration ability of HCT-116 (a) and LoVo (b) cells by wound healing assay. After 24 h incubation, HCT-116 and LoVo cells were treated with different concentrations of STH for 48 h. The wound closure percentages were analyzed by Image J software. All data shown were the mean ± SD of three independent experiments. Different superscripts letter for each column indicated significant differences ($p < 0.05$).

MH and STH inhibited the invasion of HCT-116 and LoVo cells in comparision with the control in a dose dependent manner (Figure 3.34 and Figure 3.35). We observed the MMP-2 and MMP-9 protein expression by western blot. In HCT-116 cells, MH suppressed the expression of both invasion proteins up to 0.50 fold at the concentration 15 and 20 mg/mL and in LoVo cells its suppressed up to 0.39 fold and 0.28 fold at the concentration of 50 mg/mL (Figure 3.34).

At the same time, STH treatment decresed the expression of MMP-2 and MMP-9 up to 0.55 fold and 0.43 fold at the concentration 12 mg/mL in HCT-116 cells and up to 0.48 fold and 0.59 fold at the concentration 40 mg/mL in LoVo cells (Figure 3.35).

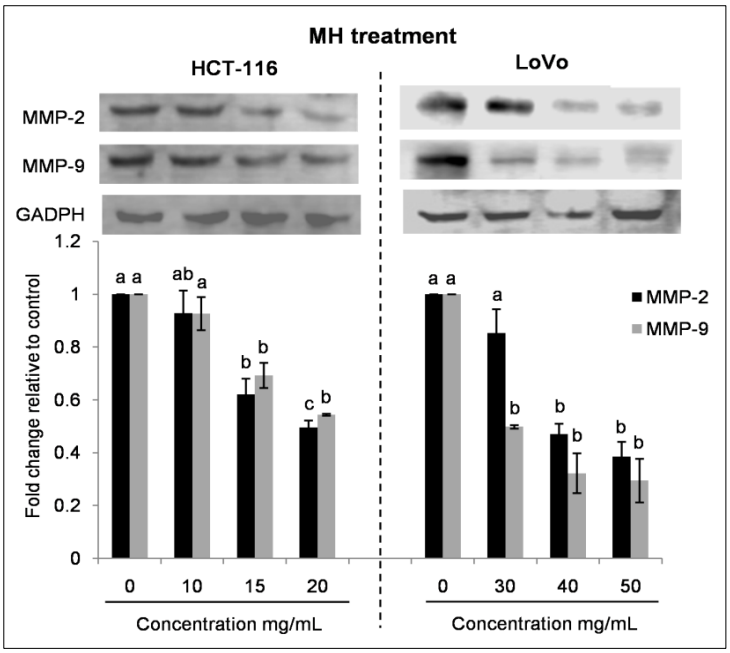

Figure 3.34. MH reduces invasion ability of HCT-116 and LoVo cells by suppressing MMP-2 andMMP-9 expression. After 24 h incubation, HCT-116 and LoVo cells were treated with different concentrations of MH for 48 h. The concentration of 0 mg/mL corresponds to control (untreated cells).The protein expressions of MMP-2 and MMP-9 were determined by western blotting analysis. GADPH was used as a loading control. All data shown were the mean ± SD of three independent experiments. Different superscripts letter for each column indicated significant differences ($p < 0.05$).

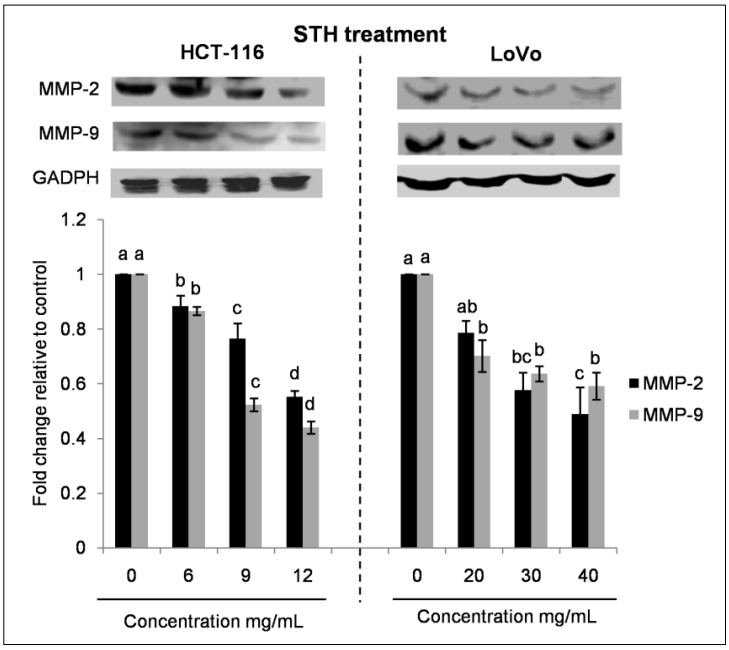

Figure 3.35. STH reduces invasion ability of HCT-116 and LoVo cells by suppressing MMP-2 and MMP-9 expression. After 24 h incubation, HCT-116 and LoVo cells were treated with different concentrations of STH for 48 h. The concentration of 0 mg/mL corresponds to control (untreated cells). The protein expressions of MMP-2 and MMP-9 were determined by western blotting analysis. GADPH was used as a loading control. All data shown were the mean ± SD of three independent experiments. Different superscripts letter for each column indicated significant differences ($p < 0.05$).

3.2.9.2. Effect of MH and STH on the colony formation ability of HCT-116 and LoVo cells

To observe whether chronic exposure to MH and STH could affect the proliferative ability of HCT-116 and LoVo cells, the cells were seeded at a low density (1000 cells/well) and allowed to form colonies for 12 days in complete growth media supplemented with different treatments. This in *in vitro* cell survival assay is based on the ability of a single cell to grow into a colony. As shown in Figure 3.36, chronic exposure to MH decreased colonies formation from 20% to 79% in HCT-116 cells and 15% to 80% in LoVo cells compared with control (100%) in a dose dependent manner.

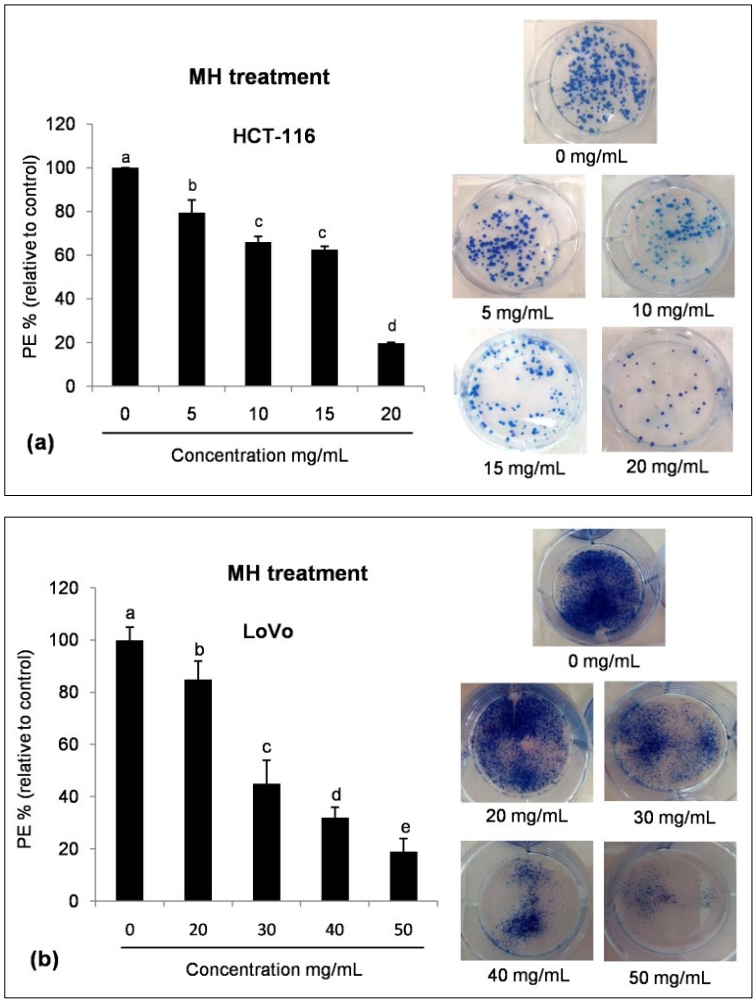

Figure 3.36. Effect of MH on HCT-116 (a) and LoVo (b) cells colony formation. Representative images of the colony wells. Cells were seeded at low density in McCoy's 5A and F-12K media supplement with different concentrations of MH for 12 days. The concentration of 0 mg/mL corresponds to control (untreated cells). The colonies were subsequently fixed with 70% ethanol and stained with methylene blue for analysis of colony formation. Quantitative image analysis of colonies in cultured HCT-116 and LoVo cells. All data shown were the mean ± SD of three independent experiments. Different superscripts letter for each column indicated significant differences ($p < 0.05$).

In Figure 3.37, chronic exposure to STH decreased colonies formation from 15% to 85% in HCT-116 cells and 17% to 77% in LoVo cells compared with control (100%) in a dose dependent manner.

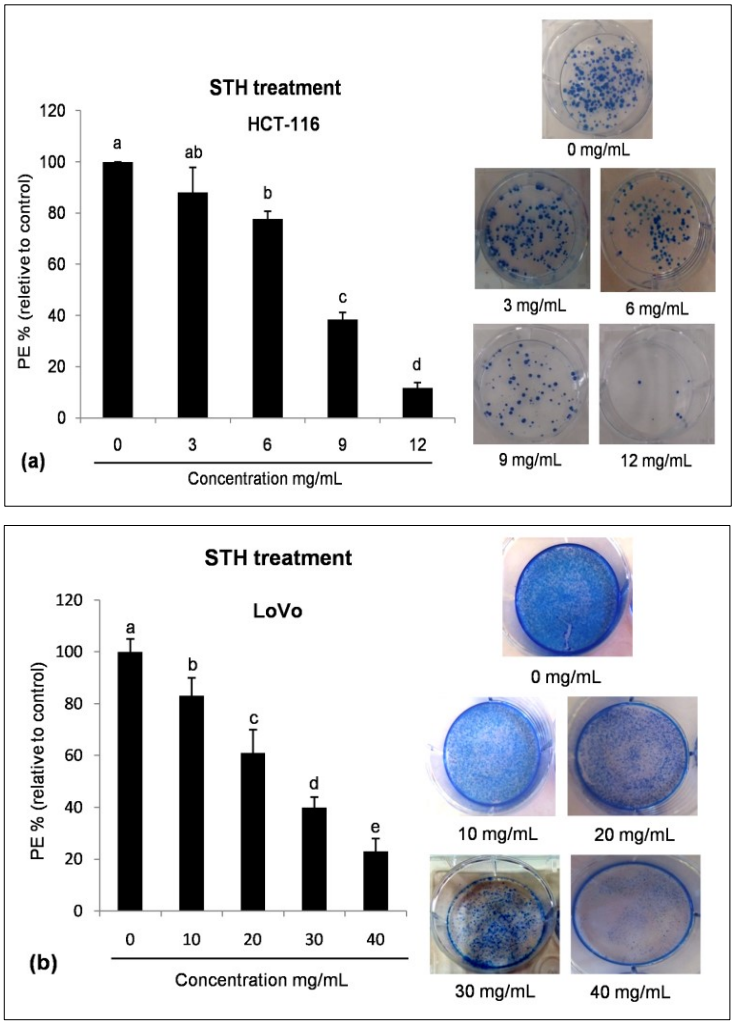

Figure 3.37. Effect of STH on HCT-116 (a) and LoVo (b) cells colony formation. Representative images of the colony wells. Cells were seeded at low density in McCoy's 5A and F-12K media supplement with different concentrations of STH for 12 days. The concentration of 0 mg/mL corresponds to control (untreated cells). The colonies were subsequently fixed with 70% ethanol and stained with methylene blue for analysis of colony formation. Quantitative image analysis of colonies in cultured HCT-116 and LoVo cells. All data shown were the mean ± SD of three independent experiments. Different superscripts letter for each column indicated significant differences ($p < 0.05$).

3.2.9.3. Effect of MH and STH on the expressions of EMT-related genes in HCT-116 and LoVo cells

The process of EMT is an essential event for cancer cell since migration and invasion are required for the progression of metastasis cancer. In this step, we examined the effect of MH and STH on the expression of EMT related markers of E-cadherin, N-cadherin and β-catenin in colon cancer HCT-116 and LoVo cell lines. As shown in Figure 3.38, the expression of E-cadherin was increased up to 2.36 fold and 2.75 fold for both cells, whereas the expression of N-cadherin and β-catenin was decreased up to 0.50 fold and 0.44 fold for HCT-116 cells and 0.46 fold and 0.37 fold for LoVo cells, respectively compared to control by MH.

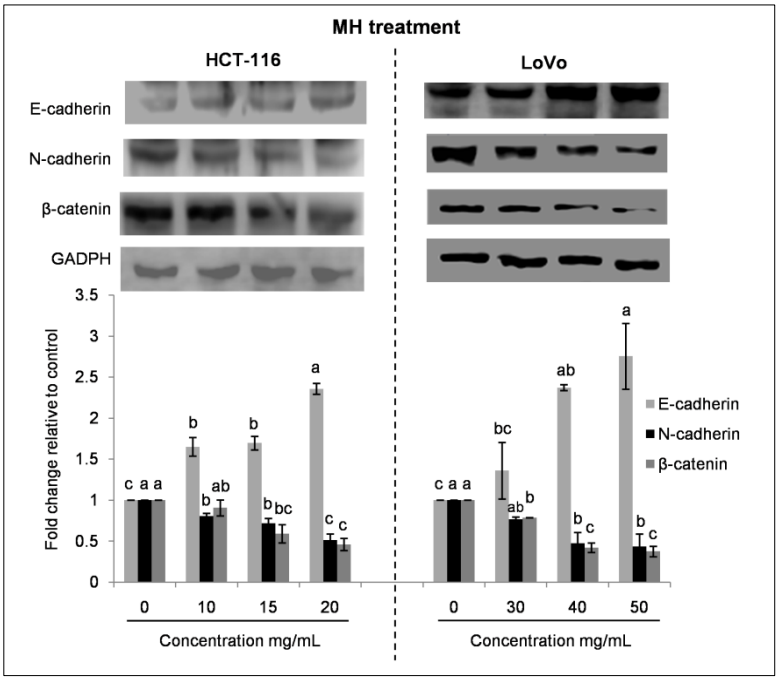

Figure 3.38. MH regulates the expression of EMT related gene in HCT-116 and LoVo cells. After 24 h incubation, HCT-116 and LoVo cells were treated with different concentrations of MH for 48 h. The concentration of 0 mg/mL corresponds to control (untreated cells). The protein expressions of E-cadherin, N-cadherin and β-catenin were determined by western blotting analysis. GADPH was used as a loading control. All data shown were the mean ± SD of three independent experiments. Different superscripts letter for each column indicated significant differences ($p < 0.05$).

In the case of STH, the expression of E-cadherin was upregulated up to 2.35 fold for HCT-116 and 2.75 fold for LoVo cells at the dose 12 mg/mL and 40 mg/mL. At the same time, the expression of N-cadherin and β-catenin was downregulated, with an almost similar trend for both cell lines up to 0.25 fold and 0.40 fold at the dose 12 mg/mL and 40 mg/mL, respectively (Figure 3.39).

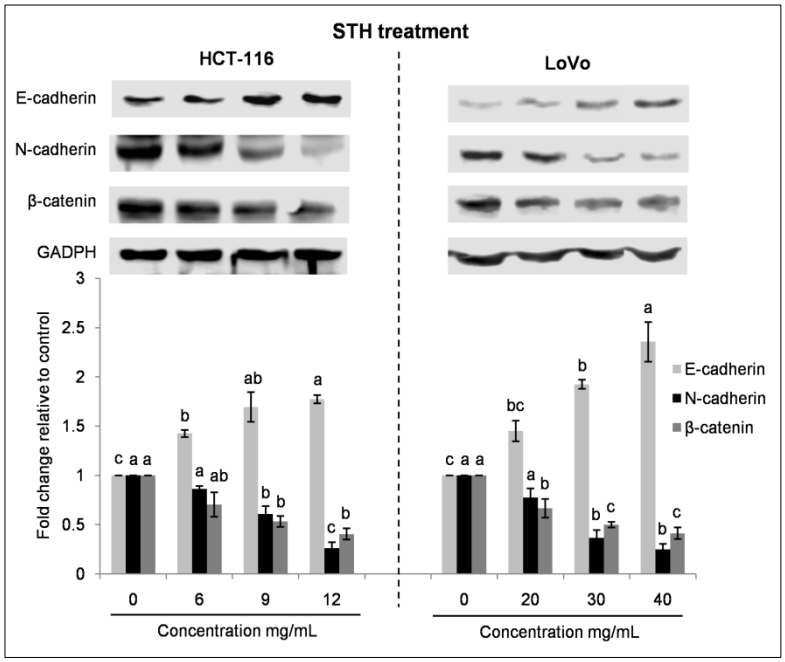

Figure 3.39. STH regulates the expression of EMT related gene in HCT-116 and LoVo cells. After 24 h incubation, HCT-116 and LoVo cells were treated with different concentrations of STH for 48 h. The concentration of 0 mg/mL corresponds to control (untreated cells). The protein expressions of E-cadherin, N-cadherin and β-catenin were determined by western blotting analysis. GADPH was used as a loading control. All data shown were the mean ± SD of three independent experiments. Different superscripts letter for each column indicated significant differences ($p < 0.05$).

3.2.9.4. Effect of MH and STH on the metastasis promoting factor expression CXCR4 and NFκB in Lovo cells

To examine, whether MH and STH has the ability to suppress the metastatic activity, we observed the expression of tumor metastasis promoting factor CXCR4 and NFκB on metastasis colon cancer LoVo cells. The expression of both proteins was significantly suppressed from 0.51 to 0.33 fold and 0.77 to 0.40 fold by MH (30-50 mg/mL) treatment (Figure 3.40a) and from 0.56 to 0.34 fold and 0.78 to 0.51 fold by STH (20-40 mg/mL) treatment, respectively (Figure 3.40b).

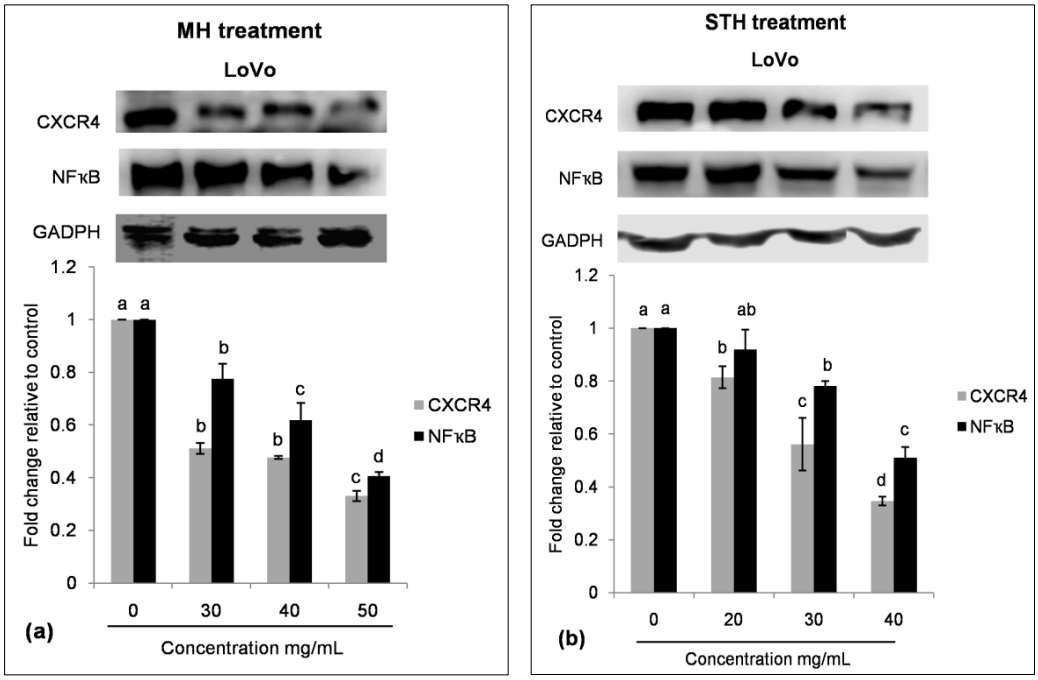

Figure 3.40. MH (a) and STH (b) regulate the expression of tumor metastasis promoting factor CXCR4 and NFκB on metastasis colon cancer LoVo cells. After 24 h incubation, HCT-116 and LoVo cells were treated with different concentrations of MH and STH for 48 h. The concentration of 0 mg/mL corresponds to control (untreated cells). The protein expressions of CXCR4 and NFκB were determined by western blotting analysis. GADPH was used as a loading control. All data shown were the mean ± SD of three independent experiments. Different superscripts letter for each column indicated significant differences ($p < 0.05$).

DISCUSSION: PART II

The second aim of my PhD project was to evaluate the chemopreventive effects of MH and STH on human colon adenocarcinoma (HCT-116) and Dukes' type C, grade IV, colon metastasis (LoVo) cell lines focusing on different molecular targets. To the best of our knowledge, this is the first report to demonstrate the chemopreventive effects of MH and STH against HCT-116 and LoVo cells.

The five-year survival rate of colon cancer is still low (12%) due to its resistance to chemotherapy drug (Siegel et al., 2017b). However, no proper treatment options are available for this type of cancer. Therefore, there is an urgent need to establish novel preventive and therapeutic approaches for this disease.

Natural compounds have the potential anti-cancer activity for the treatment of CRC by stimulating a cytotoxic effect on tumor cells and, at the same time, they exert fewer or non-toxic activities on healthy or normal colonic epithelial cells (Afrin et al., 2016; Bhardwaj et al., 2016; Phang et al., 2016). Honey is a good source of natural therapeutic molecules with antibacterial, wound healing, anti-oxidant, anti-hypertensive, anti-inflammatory, anti-proliferative and anti-cancer properties (Ahmed et al., 2016; Alvarez-Suarez et al., 2014; Alvarez-Suarez et al., 2013; Alvarez-Suarez et al., 2016; Alvarez-Suarez et al., 2010b; Erejuwa et al., 2014; Jaganathan and Mandal, 2009a). MH is well known for its anti-microbial and wound healing capacities (Alvarez-Suarez et al., 2014; Alvarez-Suarez et al., 2016), but its chemopreventive property is still elusive in spite of its phenolic compounds, most of which induce potential antitumor effects (Jaganathan and Mandal, 2009a) and, to date, there are only data reported by our groups on the biological effects of STH on colon cancer cells (Afrin et al., 2017).

The main feature of cancer cells is aberrant proliferation and it is a leading focus for conventional chemotherapeutics and novel therapies. To evaluate the anti-proliferative effect of honey on colon cancer cell line, it was necessary to use different concentrations, most likely due to variations in honey content, particularly in polyphenols and antioxidant activities (Erejuwa et al., 2014; Jaganathan et al., 2015; Jaganathan and Mandal, 2009a). Our present results documented the capability of MH and STH in the suppression of the human colon cancer HCT-116 and LoVo cell proliferation at different concentrations and times (Figure 3.1 and Figure 3.2). According to different investigations, phenolic compounds such as quercetin, luteolin, kaempferol, gallic acid and caffeic acid, which are also present in the MH (Table 3.2), play an essential function in the suppression of cancer

cell proliferation (González-Vallinas et al., 2013a; Lee et al., 2011). The IC_{50} values of MH on colon cancer HCT-116 cells were 22.03 mg/mL, 15.10 mg/ mL and 13.35 mg/mL after 24, 48 or 72 h and on LoVo cells were 63.85 mg/mL, 40.97 mg/mL and 22.73 mg/mL after 24, 48 or 72 h of revelation to MH treatment, respectively (Figure 3.1). By using the same honey, Fernandez-Cabezudo et al. reported the IC_{50} value of 20 and 10 mg/mL in the colon cancer CT-29 cells at 24 and 72 h (Fernandez-Cabezudo et al., 2013). These results are quite similar to ours.

STH represented phenolic compounds were kaempferol, quercetin, luteolin, gallic acid, 4-hydroxybenzoic acid etc. (Table 3.3), which are already known for their anti-proliferative effects on different cancer cells (Guo et al., 2017; Lee et al., 2014; Liu et al., 2017; Pandurangan et al., 2015). Furthermore, the IC_{50} values of STH on colon cancer HCT-116 cells were 14.65 mg/mL, 10.29 mg/ mL and 9.17 mg/mL after 24, 48 or 72 h and on LoVo cells were 56.33 mg/mL, 35.12 mg/mL and 26.88 mg/mL after 24, 48 or 72 h, respectively (Figure 3.2). In both cell lines, the treatment with STH caused a greater decrease in cellular viability at lower concentrations than MH. Based on the viability data on the other types of honeys, Gelam honey IC_{50} values were 39 and 88 mg/ mL (Wee et al., 2015; Wen et al., 2012) and Nenas honey IC_{50} values were 85.5 mg/mL (Wen et al., 2012) on human colon cancer HT-29 and HCT-116 cells at 24 h. In other cancer cells, pure unfractionated honey IC_{50} values were 20 to 40 mg/mL (Ghashm et al., 2010; Swellam et al., 2003; Wee et al., 2015; Wen et al., 2012) and Tualang honey IC_{50} values were 35 and 40 mg/mL (Ghashm et al., 2010). These variations are mainly due to honey composition, specifically in different types of flavonoids and phenolic acids, which are known as chemopreventive agents (Ahmed and Othman, 2013; Erejuwa et al., 2014; Jaganathan and Mandal, 2009b).

Plant-derived natural compounds are important sources of chemopreventive agents because they induce less toxicity in non cancer cells (Bhardwaj et al., 2016; Phang et al., 2016). In our present works, we also observed that MH and STH induced less toxicity of non-cancer cells (Figure 3.3). According to other studies, Tualang honey induced the cytotoxic effects on breast cancer cell while it did not exert cytotoxic effects on the normal breast cell line (Fauzi et al., 2011). Additionally, Gelam honey induced cytotoxic effect on liver cancer cells and at higher concentration it induced toxicity of the non-cancer cells (Jubri et al., 2012).

The chemopreventive effect may be related to the phenolic composition of honey or the metabolism of sugars. So it is an important issue, when honey is tested *in vitro*

chemoprevention studies, is the effects of sugars on cancer cell proliferation. Glucose is an important nutrient for cancer cell growth and honey presents a high amount of sugars. It is important to find out the effects of sugar on cancer cell proliferation. In our present work, we observed the anti-proliferative effects of AH on HCT-116 and LoVo cells (Figure 3.4). At higher concentration of sugars, it did not induce any toxic effect on both cancer cells (Figure 3.4). Wang et al. investigated the anti-mutagenic effects of different types of honey and their individual sugar components (Wang et al., 2002). The anti-mutagenic effects were observed on the monosaccharide sugars, as well as honeys against food mutagen Trpp-1 (3-amino-1,4-dimethyl-5H-pyrido[4,3-b]indole) (Wang et al., 2002). Another study investigated the effects of honey and sugar mixture on the proliferation of different type cancer cells, highlighting that only in some cancer cells the difference between the effect of honey and the sugars (Porcza et al., 2016). So, the effects of honey can be different on the type of honey and at the same time the cell lines investigated.

Dysregulation of cell cycle is one of the features of carcinogenesis which contributes to the abounded proliferation in human cancer. The cell cycle can be divided into four different phases—G_1, S, G_2 and M. At the S phase, DNA synthesis takes place, at the M phase the cell divides into two identical daughter cells and both these phases are separated by gap phase G_1 and G_2 (Williams and Stoeber, 2012). At the G_1 phase, the cells are response to extracellular signals to progress towards mitosis or withdrawal from the cell cycle into a resting or inactive stage known as G_0 phase (Sherr, 1994) while cells undergoing apoptosis were known as an accumulated cell population in the Sub-G_1 region (Okuma et al., 2000). Several studies reported that honey or its various phenolic and flavonoids compounds have the ability to arrest the cell cycle at different phases (Jaganathan and Mandal, 2009b; Mu et al., 2007; Priyadarsini et al., 2010; Song et al., 2014; Zhang et al., 2008). Jaganathan el al. reported that the different Indian commercial honey increased the accumulation of cells at Sub-G_1 phase and arrest the cell cycle at G_0/G_1 phase in colon cancer HCT-15 and HT-29 cells (Jaganathan and Mandal, 2009b; Jaganathan and Mandal, 2010). Similarly, pure unfractionated honey and Acacia honey arrest the cell cycle at G_0/G_1 phase in bladder and human melanoma cell lines (Pichichero et al., 2010; Swellam et al., 2003). Other phenolic compounds like chrysin, quercetin, kaempferol and *p*-coumaric acid (present in large amount in honey) have the ability to arrest the cell cycle at different phases such as G_0/G_1, G_1 and G_2/M accumulating the cells at Sub-G_1 phase in different cancer cell lines (Jaganathan et al., 2013; Mu et al., 2007; Priyadarsini et al., 2010; Song et al., 2014; Zhang

et al., 2008). In our present work, similar effect was observed by both honey treatment, with an arrest in the progression of cell cycle at S phase for HCT-116 cells and in G_2/M phase for LoVo cells (Figure 3.5 and Figure 3.6). The cells in Sub-G_1 phase were also observed in both cell lines after MH and STH treatment but it was more prominent in LoVo cells (Figure 3.5 and Figure 3.6).

Apoptosis process play a critical role in cancer pathogenesis: indeed, a failure to undergo apoptosis results in the development and progression of cancer. Several molecules and processes modulate the apoptosis process, largely through caspases, which breakdown specific proteins in the cytoplasm and nucleus triggering cell death (Elmore, 2007). Pure unfractionated honey or its bioactive compounds have been studied in various cancer cell lines for their ability to induce apoptosis by modulating several mechanism of action. For example, in colon cancer HCT-15 and HT-29 cells, treated with Indian commercial honey, apoptosis was activated through increasing p53, c-PARP, Bax, caspase-3 and decreasing Bcl-2 expression, increasing thus the percentage of apoptotic cells (Jaganathan and Mandal, 2009b; Jaganathan and Mandal, 2010). Another *in vitro* study of breast and cervical cancer cell lines showed that the Tualang honey induced apoptosis through activating caspase-3/7 and caspase-9 (Fauzi et al., 2011). MH is able to induce apoptotic cell death in colon cancer (CT29), breast cancer (MCF-7) and melanoma (B16.F1) cells by activating PARP, caspase-3 and decreasing Bcl-2 expression (Fernandez-Cabezudo et al., 2013). Furthermore, common flavonoids of honey, such as chrysin, quercetin, ellagic acid and kaempferol, induce apoptotic cell death in colon cancer cells by activation of caspase cascade and Akt inactivation, increasing proapoptotic protein expression (p53, Bax, Bad, Bak and DR5) and decreasing antiapoptotic proteins Bcl-2 (Kasala et al., 2015; Kee et al., 2016; Lee et al., 2014; Umesalma et al., 2015). Like previous results, we also found similar results in the present work. Flow cytometry analysis confirmed the apoptotic cell death induced by MH and STH (Figure 3.7 and Figure 3.8). MH treatment induced more apoptotic cells compared to STH in both cells. We also observed that the molecular mechanism was associated by an increase in the expression of p53, caspase-3 and c-PARP after both honey treatment; again MH induced a more remarkable activation compared to STH (Figure 3.9 and Figure 3.10).

Chronic inflammations are connected with increased risk of cancer, being associated with all stage of tumorgenesis, from initiation to progression (Mantovani, 2009). In our present work we observed the anti-inflammatory effects of MH and STH on HCT-116 cells. NFκB

pathways are important for the inflammatory response and have the ability to resist apoptosis of cancer cells, as well as play an important role in regulating cancer angiogenesis and invasiveness (Fan et al., 2013b). Activation of these pathways also associated with increased levels of several inflammatory proteins (COX-2, CRP and LOX-2) and cytokines (IL-1β, IL-6 and TNF-α), which are already known to play an important role in the inflammatory related etiology in cancer (Goldberg and L Schwertfeger, 2010). The anti-inflammatory effects of honey can be ascribed to its phenolic compounds and flavonoids (Khan et al., 2011). For example, the flavanone chrysin is effective in reducing the early hepatocarcinogenesis in Wistar rats by decreasing the mRNA levels of NFκB (Khan et al., 2011). In prostate cancer cells, Acacia honey decreases the activation of TNF-α and IL-1β levels compared to control (Aliyu et al., 2012). The extract of Gelam honey and quercetin induces anti-inflammatory effects in hamster pancreatic cell line by suppressing NFκB pathways and reducing the expression of pro-inflammatory cytokines (IL-1β, IL-6 and TNF-α) (Batumalaie et al., 2013; Safi et al., 2016). In another study by using the same honey the expression of IL-6, TNF-α, iNOS and COX-2 was inhibited, and the NFκB translocation to the nucleus was markedly suppressed as well as the IκB-α degradation in rat paw tissue (Hussein et al., 2012; Hussein et al., 2013). Similarly, in the present work we found that MH and STH suppressed the key inflammatory pathways NFκB and p-IκBα, and other inflammatory markers (IL1β, IL-6, iNOS and TNF-α) in HCT-116 cells (Figure 3.11), which play an important function in the pathogenesis of development of colon cancer from ulcerative colitis or inflammatory colitis.

As already explained in the introduction, the impact of MAPK pathway in colon cancer is very considerable. Until now there is no information about the effect of honey on MAPK pathway but several investigations have reported that natural compounds have the ability to activate MAPK pathways which can regulate a wide number of stimuli and markers of apoptosis in CRC (Kee et al., 2016; Phang et al., 2016; Ryu and Chung, 2015). For example, quercetin (common flavonoids of MH) increases MAPK activation through the activation of p-Erk, p-JNK and p-38MAPK in colon cancer CT26 cells, leading to apoptosis (Kee et al., 2016). Furthermore, flavokawain C increases the expression of p-Erk1/2 and p-p38MAPK in colon cancer HCT-116 for inducing cell death by apoptosis (Phang et al., 2016). Similarly, another compound gingerol induces mitochondrial apoptosis through activating MAPK pathways by increasing p-JNK, p-p38MAPK and p-Erk1/2 in HCT-116 colon cancer cells (Ryu and Chung, 2015). Therefore, in this work we

investigated the involvement of p-p38MAPK and p-Erk1/2 pathways in the apoptotic properties of MH and STH. The results suggested that both honey increased the expression of p-p38MAPK and p-Erk1/2 in HCT-116 and LoVo cells (Figure 3.12 and Figure 3.13). In particular, in HCT-116 cells, MH treatment increased more p-38MAPK expression while STH exerted more p-Erk1/2 expression. In LoVo cell, MH induced more activation of p-p38MAPK and p-Erk1/2 compared to STH.

The EGFR and in a smaller extent the HER2 are key surface receptors which can activate or over express a number of oncogenic pathways which play an important function in colon cancer proliferation, survival, angiogenesis, invasion and metastasis (Custodio and Feliu, 2013; Mendelsohn and Baselga, 2000). Even if the EGFR pathway is an attractive therapeutic target for anticancer therapy, there is still little information on the effect of honey on growth factor signaling; a lot number of study have addressed the effect on EGFR signaling by other phenolic compounds (Johnson and Mukhtar, 2007). After curcumin treatment, a reduction has been observed in EGFR expression by decreasing the transcription factor Egr-1 in colon cancer Caco-2 and HT-29 cells (Johnson and Mukhtar, 2007). At the same time, green tree polyphenols suppressed EGFR induced Akt activation in cervical cancer cells (Sah et al., 2004). In endometrial cancer cells, quercetin treatment significantly decreased EGF gene and related-protein expression (Kaneuchi et al., 2003). Furthermore, caffeic acid phenethyl ester, a compound derived from honey bee propolis, suppresses total and phosphorylation of EGFR in breast cancer cells (Wu et al., 2011). Tahir et al. reported that the Gelam honey alone or combined with ginger suppresses the expression of PI3K/Akt pathways in colon cancer cells HT-29 (Tahir et al., 2015). Similarly, flavokawain C arrests cell cycle and induces apoptosis in HCT-116 cell by suppressing Akt and increasing p-Erk/12 expression (Phang et al., 2016). In this work, we evaluate the effect of MH and STH on the protein expression of EGFR and HER2 and the activation status of the downstream signaling protein, Akt, in HCT-116 and LoVo cells. We found that both honey suppressed the expression of EGFR, HER2 and p-Akt (Figure 3.14 and Figure 3.15). EGFR was suppressed in a more remarkable manner in LoVo cells while p-Akt was highly suppressed in HCT-116 cells after MH; STH induced similar effect in both cell lines (Figure 3.14 and Figure 3.15).

In cancer cells, there is an unbalanced ROS level due to the defective cell metabolism and proliferative capacity, acting as a pro-tumorigenic factor (Nogueira and Hay, 2013). Moreover, it has been well documented that natural compounds exhibit anti-tumor

potential by inducing high ROS content in cancer cells which renders them more vulnerable to oxidative stress-induced cell death by activating apoptosis or autophagy (Bhardwaj et al., 2016; Enayat et al., 2016; Gunasekaran et al., 2015; Santandreu et al., 2011). In colon cancer cells HCT-15 and HT-29, pure unfractionated honey increases ROS generation for apoptosis activation (Jaganathan and Mandal, 2010). Furthermore, other phenolic compounds of honey, such as p-coumaric acid and chrysin, increase ROS generation for inducing apoptotic cell death by activating MAPK pathway in colon cancer (Jaganathan et al., 2013) and prostate cancer cells (Ryu et al., 2017). We speculated that MH and STH induce toxic effects by generating ROS, resulting in oxidative stress and in a consequent activation of apoptosis in HCT-116 and LoVo cells (Figure 3.16 and Figure 3.17). Our results showed that both honeys increased in a dose dependent manner intracellular ROS levels in LoVo cells and STH induced more effect compared to MH.

The antioxidant system maintains the cellular redox status by scavenging ROS and reducing oxidized glutathione or NADPH/NADP+ ratio (Nogueira and Hay, 2013). According to previous studies, natural compounds can behave as pro-oxidants and have a noticeable oxidative impact on cellular redox status, important for (i) induction of cancer cell death by increasing damage of biological macromolecules such as lipid, protein and DNA (Bhardwaj et al., 2016; Gunasekaran et al., 2015; Ryu et al., 2017; Santandreu et al., 2011; Sivagami et al., 2012), (ii) reduction of Nrf2 gene activation and (iii) disruption of other antioxidant defenses mechanism (Bhardwaj et al., 2016; Gunasekaran et al., 2015; Liao et al., 2015; Santandreu et al., 2011; Sivagami et al., 2012). A similar effect was observed in our work by MH and STH treatment in HCT-116 and LoVo cells. We observed that honey treatment increased the TBARs and protein carbonyl levels, important markers of oxidative stress, in each colon cancer cell (Figure 3.18). Similarly, the expression of OGG1 also increased after honey treatments (Figure 3.19). Additionally, the activity and the expression of antioxidant enzyme were examined in both cell lines: MH and STH treatment provoked the suppression of the activity of antioxidant enzymes, such as GPX, GST, GR, SOD and catalase (Figure 3.20 and Figure 3.21) and the expression of Nrf2 and its downstream targets, SOD, catalase and HO-1 (Figure 3.22 and Figure 3.23); these effects facilitated HCT-116 and LoVo cell cytotoxicity in response to oxidative stress. Interestingly, in a previous study from our groups, we observed that MH has the ability to protect non-cancer cells from oxidative stress by decreasing ROS generation, improving lipid and protein damage and increasing antioxidant enzyme activity (SOD and

catalase) and expressions (Nrf2, SOD and catalase) (Alvarez-Suarez et al., 2016). These findings recommended that the antiproliferative effect of honey is associated with its oxidative stress induced damage and turn down of antioxidant protection mechanism which further stimulate ROS production in human colon cancer HCT-116 and LoVo cells.

ER stress induced cancer cell death has raised growing attention because it seems to increase the treatment efficacy of chemotherapeutic mediators by eradicating the damaged cells via activation of both intrinsic or extrinsic apoptosis pathways (Sano and Reed, 2013) and induction of oxidative stress by increasing ROS accumulation through deregulated or breakage of the disulfide bond formation (Cao and Kaufman, 2014). Furthermore, the ER stress sensor ATF6 (type II transmembrane protein) and its downstream signaling molecule XBP1 (transcriptional activator of UPR genes) play an important role in response to ER stress (Cao and Kaufman, 2014). In the present study, we revealed that MH and STH treatment increased the expression levels of ATF6 and XBP1 (Figure 3.24 and Figure 3.25), indicating that both honeys have the ability to activate ER stress inducing HCT-116 and LoVo cell death. In HCT-116 cells both honey induced similar ER stress but in LoVo cells MH induced more ER stress compared to STH. Earlier studies indicated that the ER stress-induced cancer cell death, by activating ATF6 and XBP1 expression in colon cancer HCT-116 and HT-29 cells, has been assessed by other natural compounds (Khan et al., 2016; Zhang et al., 2013b).

Metabolic changes are one of the hallmarks in the development of tumors. Depending on the energetic metabolism, the chemopreventive and therapeutic strategies are different in different tumors. OXPHOS and glycolysis are closely coupled to assist in retaining the energetic balance in metabolic alteration in cancer cells (Wu et al., 2007). In this report, we first used a novel extracellular flux analyzer to evaluate several parameters of mitochondrial respiration (OCR) and glycolysis (ECAR), to investigate the bioenergetic characterization of human colon cancer HCT-116 and LoVo cells after MH and STH treatment. Our results showed that both honey reduced mitochondrial respiration. In HCT-116 and LoVo cells, oligomycin disrupts OXPHOS by blocking complex V indicating suppressed mitochondrial respiration rate while 2,4-DNP transports proton across the inner mitochondrial membrane instead of proton channel for bypass ATP synthesis and increase respiration. In this experiment, MH and STH treatment at different concentrations suppressed basal levels of mitochondrial respiration, proton leak, SRC and MRC, and this was mainly due to the decreased ATP-linked respiration in the mitochondria (Figure 3.26

and Figure 3.27). Furthermore, HCT-116 and LoVo cells had the ability to increase glycolysis when mitochondrial function is blocked by rotenone. Additionally, MH and STH treatment at different concentrations were capable of decreasing the ECAR, indicating that MH and STH have an inhibitory effect on glycolysis, glycolytic capacity and reserve (Figure 3.28 and Figure 3.29). The observed mitochondrial respiration and glycolysis function was different in each colon cancer HCT-116 and LoVo cells: the effects were more pronounced in LoVo cells compared to HCT-116 cells. These results are closely similar to those obtained in colon cancer cells by carnosine (naturally occurring dipeptide) treatments by Shen et al. (Shen et al., 2014), and in human uterine leiomyoma cells by an anthocyanin rich strawberry extract treatment by Islam et al. (Islam et al., 2017). Moreover, suppressed glycolysis was observed also in hepatocellular carcinoma by chrysin treatments (Xu et al., 2017). Thus all data suggested that MH and STH may represent a regulator of energy metabolism both in the aerobic and anaerobic pathways in HCT-116 and LoVo cells.

AMPK is a master regulator of metabolic and energy homeostasis in tumor cells in energy stress environments by promoting both glycolytic and mitochondrial metabolism (Chaube et al., 2015). The activated AMPK acts as a tumor suppressor (Hardie, 2011; Mihaylova and Shaw, 2011). However, recent evidence showed that AMPK activation is necessary to regulate oxidative stress and enhance cancer cell proliferation in metabolic stress microenvironment (Chaube et al., 2015; Jeon, 2016; Li et al., 2015). Thus, suppression of AMPK might also be a therapeutic approach for cancer treatment. In this report, we showed that MH and STH treatment decreased the p-AMPK/AMPK expression in HCT-116 and LoVo cells (Figure 3.30 and Figure 3.31). More suppression was observed in HCT-116 cells after MH treatment and opposite results was observed in LoVo cells. Kim et al. explained that quercetin (an important flavanoid present in MH) suppresses AMPK activation both in *in vitro* and *in vivo* colon cancer model in hypoxic condition (Kim et al., 2012).

Activation of AMPK increases the expression of downstream targets PGC-1α and its associated genes for cancer cells survive under energetic stress conditions (Chaube et al., 2015). PGC-1α is a major transcription co-activator and it encourages oxidative, mitochondrial and fatty acid metabolism to enhance cancer cell proliferation (Jones et al., 2012) and metastasis (LeBleu et al., 2014). Our data suggested that MH and STH treatment suppressed the PGC-1α expression in HCT-116 and LoVo cells (Figure 3.30 and Figure

3.31). Together with PGC-1α, SIRT1 is another downstream target of AMPK, depending on the nature and phase of the tumor; it acts as a tumor suppressor and an oncoprotein (Chalkiadaki and Guarente, 2015). In CRC patients, elevated levels of SIRT1 expression promote carcinogenesis and are associated with a poor prognosis (Chen et al., 2014). In the present study, we found that MH and STH treatment suppressed the expression of SIRT1 in HCT-116 and LoVo cells at different concentrations (Figure 3.30 and Figure 3.31). In HCT-116 cells, MH treatment was most effective for suppression of both the protein expression while in LoVo cells STH treatment was most effective. The downregulation of PGC-1α and SIRT1 expression by MH and STH suggests that the preventive effects of MH and STH are mediated, at least in part, by regulation of the AMPK pathway.

Migration and invasion are essential steps in the progression of metastasis cancer. Since ancient times, honey has been used as antimicrobial and wound healing agents (Vandamme et al., 2013). Kee et al. evaluated that quercetin exerts anti-metastasis activity by suppressing the migration of colon cancer CT-26 cell in a dose dependent way (Kee et al., 2016). Similarly, caffeic acid, another important phenolic compound of honey, induces anti-metastasis activity through suppression of migration of colon cancer (A549), oral carcinoma (SCC-9) and breast cancer cells (MDA-MB-231) by decreasing motility and the activity of the voltage-gated sodium channels (Bouzaiene et al., 2015; Dziedzic et al., 2014; Fraser et al., 2016). In our present work, we observed that MH and STH treatment decreased cell migration in colon cancer HCT-116 and LoVo cells (Figure 3.32 and Figure 3.33). The most effective results were observed after MH treatment in both cell lines compared to STH treatment. Interestingly, in a recent study, it was found that MH promotes a wound healing mechanism in human dermal fibroblast due to improvement of the antioxidant response by modulating the AMPK/Nrf2 signaling pathway and increases the activity of antioxidant enzymes (Alvarez-Suarez et al., 2016). The wound closure properties of honey depend on the condition of diseases.

The MMPs are the important ECM-degrading enzymes that play vital roles in the migration and invasion of carcinoma (Nabeshima et al., 2002). The effect of honey on MMP activity or expression in cancer was observed in only one study. This work showed that the activity of MMP-2 and MMP-9 was decreased in glioblastoma cells by using Polish honey (Moskwa et al., 2014). Numerous investigations observed the anti-metastatic effects of phenolic and flavonoids compounds present in honey, suppressing both migration and invasion. For example, Chrysin treatment decreased the ECM degradation

and EMT in glioblastoma, gastric cancer and breast cancer cells through downregulating the expression of MMP-2, MMP-9 and MMP-10 (Santos et al., 2015; Xia et al., 2015; Yang et al., 2014). Similarly, gallic acid treatment suppressed the MMP-2 and MMP-9 expression in gastric cancer, breast cancer and osteosarcoma cells (Chen et al., 2016; Ho et al., 2010; Liao et al., 2012). In our experiment, we observed that both honey significantly suppressed the expression of MMP-2 and MMP-9 dose dependently in HCT-116 and LoVo cells (Figure 3.34 and Figure 3.35). The most effective results were found in metastatic colon cancer LoVo cells after MH treatment while STH induced more effects in adenocarcinoma HCT-116 cells.

Several natural compounds were used for inducing colony formation assay on cancer cells. In this context, chronic exposure of pterostilbene reduces colony formation up to 40% and 85% in colon cancer cells (HCT-116 and HT-29) (Nutakul et al., 2011) while carnosine decreases colony formation up to 39.9% in gastric cancer cells (SGC-7901) (Shen et al., 2014); similarly, curcumin and its conjugated reduce colony formation up to 55% and 80% in colon cancer cells (HCT-116) (Waghela et al., 2015). In our work, we observed that both honeys reduced colony formation in HCT-116 and LoVo cells (Figure 3.36 and Figure 3.37): in particular, STH (up to 85%) (Figure 3.37) treatment decreased more percentage of colony formation compared to MH (up to 80%) (Figure 3.36).

The EMT process plays a leading role in the progression of cancer metastasis, by increasing migration and invasion through connecting more stromal-cellular adhesion or cell-matrix adhesion (Gupta and Massagué, 2006). The most common EMT markers, such as E-cadherin, N-cadherin and β-catenin, contribute a significant function for increasing cell to cell adhesion (Thiery and Sleeman, 2006). Based all this observation, in this work we evaluated the expression of E-cadherin, N-cadherin and β-catenin after MH and STH treatments in HCT-116 and LoVo cells. Both honey treatment suppressed the EMT process through increasing the expression of E-cadherin and decreasing the expression of N-cadherin and β-catenin (Figure 3.38 and Figure 3.39). Similar effect was observed in HCT-116 cells after MH and STH treatment but in LoVo cells the most effective results were obtained after STH treatment. There is an increasing amount of evidence on the anti-metastasis effects of isolated phenolic compounds of honey, paying particular attention to the modulation of the expression of EMT related gene in several cancer model in *in vitro*. For example, Kee et al. reported the anti-metastatic effects of quercetin in CRC CT-26 cell by modulating the expression of EMT related genes (N-cadherin, β-catenin and snail) (Kee

et al., 2016). Naringenin, a similar compound like chrysin, is able to decrease metastasis activity of prostate cancer PC-3 cells by suppressing the EMT markers, such as vimentin, N-cadherin, MMP-2 and MMP-9 in both mRNA and protein levels (Lou et al., 2012). All these observations are closely related to our results.

Finally, we also observed the effect of MH and STH on the tumor metastasis promoting factor CXCR4 and NFκB on metastasis colon cancer cell line (LoVo). According to previous reports, several evidences have shown that CXCR4 and NFκB play a vital role in invasion, metastasis and chemoresistance in several types of cancer, including colon cancer (Aggarwal, 2004; Fukuyama et al., 2007; Murakami et al., 2013). Shakibaei et al. reported that curcumin treatment downregulates the expression of CXCR4 and NFκB protein in metastatic and chemoresistance colon cancer cells (Shakibaei et al., 2015). Similarly, in our findings, we observed that the expression of both proteins was significantly suppressed after MH and STH treatment (Figure 3.40) and the most effective results were obtained after MH treatment compared to STH.

RESULTS: PART III

3.3. MH and STH potentiates anticancer effects of 5-FU chemotherapy on human colon cancer HCT-116 and LoVo cells

3.3.1. Effect of 5-FU in a combination of MH and STH on HCT-116 and LoVo cells proliferation

The antiproliferative effect of 5-FU (1-100 µM) on human colon cancer HCT-116 and LoVo cells was determined by the MTT assay after 24 and 48 h incubation. As shown in Figure 3.40, all treatments of 5-FU inhibited the proliferation of the colon cancer cell lines tested in a dose- and time-dependent manner. At the time points tested, the IC_{50} values differed depending on the colon cancer cell lines. In HCT-116 cells it was 75 µM at 24 h and 20 µM at 48 h (Figure 3.40a) and in LoVo cells it was 100 µM at 24 h and 50 µM at 48 h, respectively (Figure 3.40b).

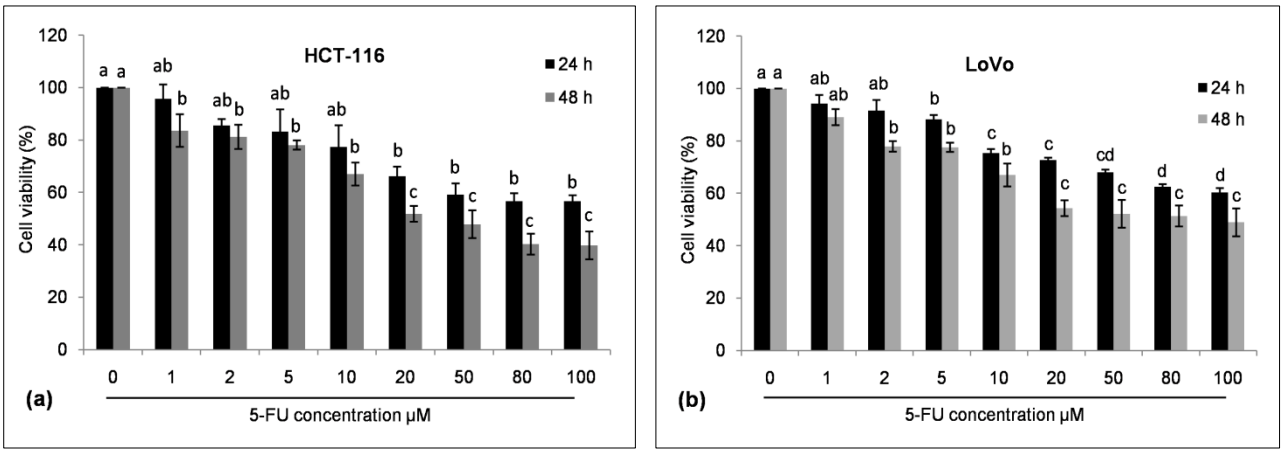

Figure 3.40. Inhibition of cell proliferation by 5-FU in HCT-116 (a) and LoVo (b) cell lines. After 24 h of cell seeding (5×10^3 cells/well), HCT-116 and LoVo cells were treated with different concentrations of 5-FU for 24 and 48 h. Cell viability was measured by using MTT assay and results were expressed as a % of viable cells compared to control cells. All data are expressed as the mean ± SD of three experiments.

Next, we observed the antiproliferative effects of 5-FU in a combination of MH and STH by MTT assay after 48 h incubation. The co-treatment with MH+5-FU and STH+5-FU by using 5, 10, 20 and 50 µM of 5-FU was combined with 5, 10 and 15 mg/mL of MH and 3, 6 and 9 mg/mL STH for HCT-116 cells. In the case of LoVo cells, 10, 20, 50 and 80 µM of 5-FU was combined with 20, 30 and 40 mg/mL of MH and 10, 20 and 30 mg/mL of STH. Previously, we have examined that the IC_{50} values after the treatment of MH were 15.10 mg/mL for HCT-116 cells and 40.97 mg/mL for Lovo cells (Figure 3.1) after 48 h

incubation. Similarly, the IC_{50} values after the treatment of STH were 10.29 mg/mL for HCT-116 cells and 35.12 mg/mL for Lovo cells (Figure 3.2) at 48 h, respectively. Here we observed that the IC_{50} of 5-FU was 20 µM for HCT-116 cells and 50 µM for LOVo cells after 48 h. Interestingly, the combination treatments significantly ($p < 0.05$) decreased the concentration of 5-FU in the presence of MH and STH for obtaining the IC_{50} values compared to single doses of 5-FU (Figure 3.41 and Figure 3.42).

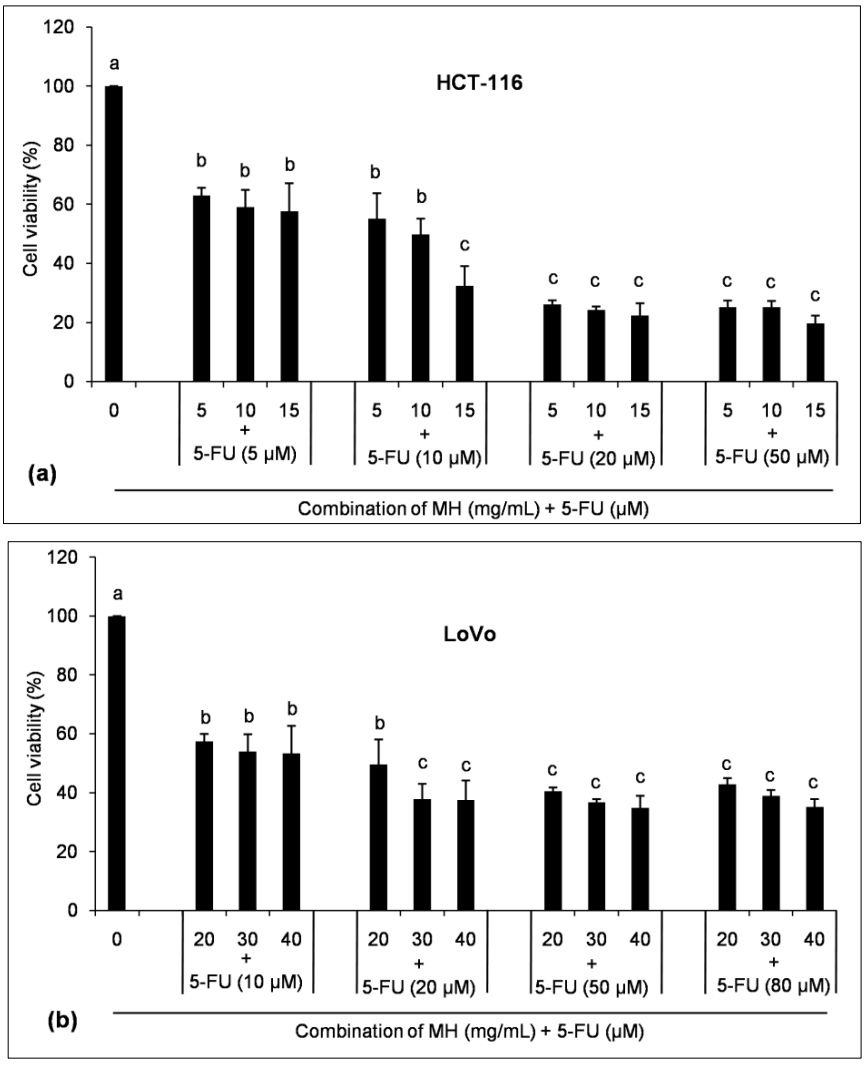

Figure 3.41. Inhibition of cell proliferation by 5-FU in the presence of MH of HCT-116 (a) and LoVo (b) cell lines. After 24 h of cell seeding (5×10^3 cells/well), HCT-116 and LoVo cells were treated with different concentrations of MH and 5-FU for 48 h. Cell viability was measured by using MTT assay and results were expressed as a % of viable cells compared to control cells. All data are expressed as the mean ± SD of three experiments.

In the presence of MH (10 mg/mL) and STH (5 mg/mL), the IC_{50} values of 5-FU were 10 µM at 48 h in HCT-116 cells (Figure 3.41). At the same time, in LoVo cells the IC_{50} values of 5-FU were 20 µM in the presence of MH (20 mg/mL) and STH (10 mg/mL) at 48 h, respectively (Figure 3.42).

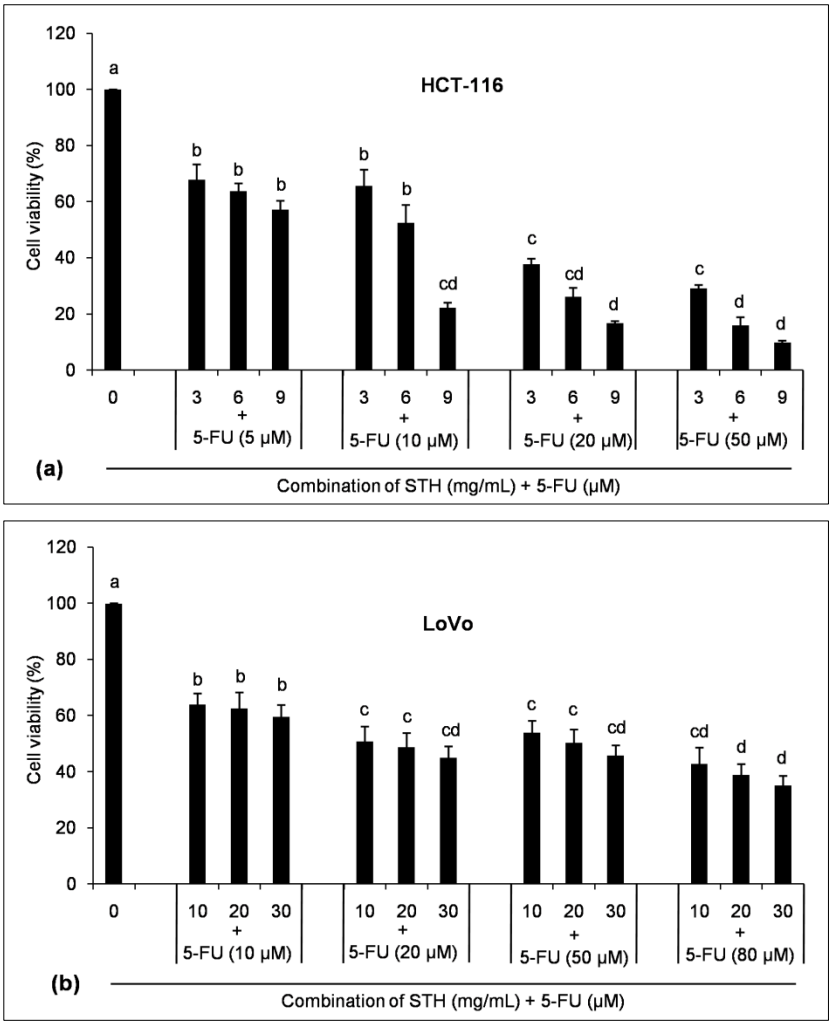

Figure 3.42. Inhibition of cell proliferation by 5-FU in the presence of STH of HCT-116 (a) and LoVo (b) cell lines. After 24 h of cell seeding (5×10^3 cells/well), HCT-116 and LoVo cells were treated with different concentrations of STH and 5-FU for 48 h. Cell viability was measured by using MTT assay and results were expressed as a % of viable cells compared to control cells. All data are expressed as the mean ± SD of three experiments.

According to these results, in HCT-116 cells the IC_{50} values of 5-FU were 20 µM and the IC_{50} values of MH+5-FU were 10 mg/mL (MH) +10 µM (5-FU) and STH+5-FU were 5 mg/mL (STH) +10 µM (5-FU). In LoVo cells the IC_{50} values of 5-FU were 50 µM and the IC_{50} values of MH+5-FU were 20 mg/mL (MH) + 20 µM (5-FU) and STH+5-FU was 10 mg/mL (STH) +20 µM(5-FU). All the IC_{50} were selected for further experiments.

3.2.2. Effect of 5-FU in a combination of MH and STH on cell cycle arrest on HCT-116 and LoVo cells

Cell cycle was evaluated by 5-FU alone or in a combination with MH and STH at doses corresponding to their IC_{50} values after 48 h in HCT-116 and LoVo cells. As shown in Figure 3.43, accumulation of HCT-116 cells in S phase significantly ($p < 0.05$*)* increased at 53% after 5-FU treatment, at 40% after MH treatment and at 36% after STH treatment compared to control 23% (without any treatment). While, the combination treatment of MH+5-FU and STH+5-FU induced 50% and 45% accumulation of HCT-116 cells at S phase, respectively. In the case of MH the effect was almost similar but when combining with STH the effect was slightly less.

Furthermore, the accumulation of cells in Sub-G_1 phase was similar after 5-FU treatment (12%) or combined treatments with MH+5-FU (12%) and STH+5-FU (11%) (Figure 3.43) while MH and STH alone induced 5% and 7% respectively, which indicated the apoptotic effects. The percentage of HCT-116 cells in the G_0/G_1 and G_2/M phase significantly ($p < 0.05$) decreased by 19% and 23% after 5-FU treatment, 27% and 17% after MH treatment and 32% and 20% after STH treatment compared to control 40% (without any treatment). Moreover, the combined treatment decreased the cells at G_0/G_1 and G_2/M phase by 21% and 6% after MH+5-FU treatment, and by 8% and 16% after STH+5-FU treatment, respectively (Figure 3.43), which indicated that the combination treatment was most effective compared to 5-FU for decreasing a number of cells at G_0/G_1 and G_2/M phase.

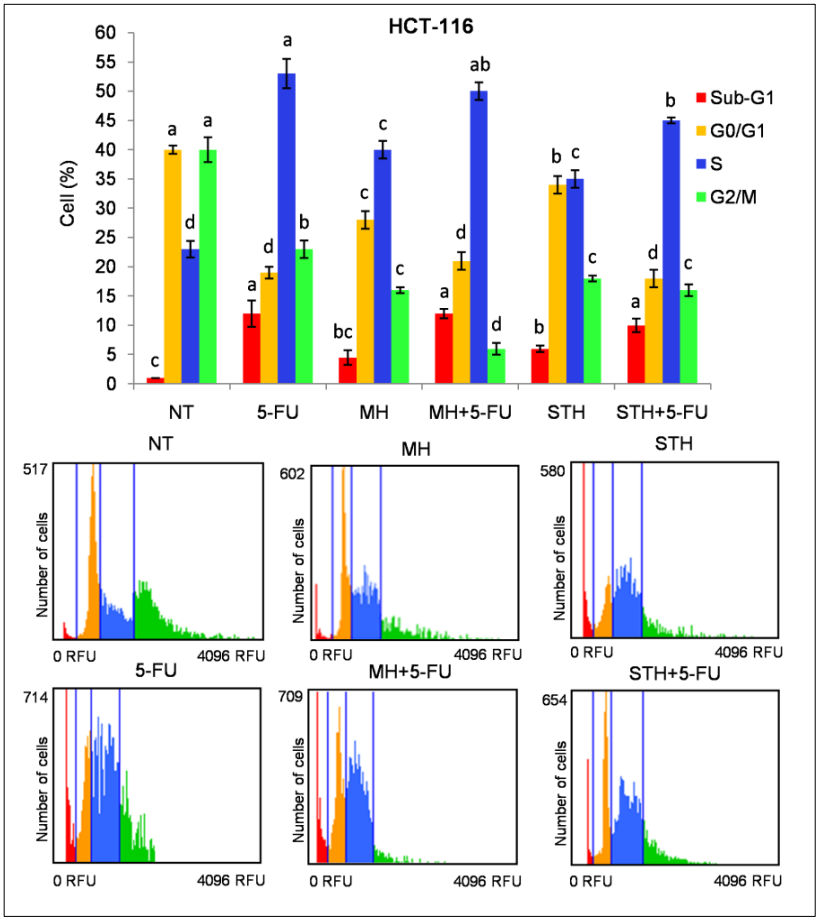

Figure 3.43. Cell cycle alteration induces by 5-FU and/or MH and STH in HCT-116 cells. After 24 hseeding, HCT-116 cells were exposed to IC_{50} doses of 5-FU, MH, STH, MH+5-FU, and STH+5-FU for 48 h. The NT corresponds to not treatment. PI was used for staining the cells and DNA content of cells was analyzed for determiningthe effect of all treatments on HCT-116 cell cycle distribution. The percentages of cells in each phase Sub-G_1, G_0/G_1, S and G_2/M were calculated by the Tali® Cell Cycle Assay kit and Tali™ Image-based Cytometer. Representative fluorescence image of HCT-116 cells cycle shows the effect of the treatments: red colour corresponds to Sub-G_1 phase, yellow colour corresponds to G_0/G_1 phase, blue colour corresponds to S phase and green yellow colour corresponds to G_2/M phase. All data shown were the mean ± SD of three independent experiments. Different superscripts letter for each column indicated significant differences ($p < 0.05$).

In LoVo cells (Figure 3.44), 5-FU treatments accumulated 43% of cells at the G_2/M phase at IC_{50} doses compared with control 20% (without any treatment). On the other hand, MH induced 37% and STH induced 35% accumulation of cells at G_2/M phase, while both combinations induced 40% accumulation of LoVo cells in G_2/M phase which was almost similar effects like 5-FU (Figure 3.44). In Sub-G_1 phase, the accumulation of cells after 5-FU treatment was 22%, after MH treatment was 15% and after STH treatment was 11.5%, while the combination treatments accumulating the cells 17% (MH+5-FU) and 13% (STH+5-FU). Furthermore, the percentage of cells at G_0/G_1 and S phase significantly ($p < 0.05$) decreased by 31% and 15% after 5-FU treatment, 27% and 14% after MH treatment

and 25.5% and 27% after STH treatment compared with control (without any treatment). The combined treatment decreased the cells at G_0/G_1 and S phase by 26% and 14% after MH+5-FU treatment, and 25% and 21% after STH+5-FU treatment, respectively (Figure 3.44), which was more effective compared to 5-FU alone. The results suggested that the combination treatments were most effective in HCT-116 cells compared to LoVo cells for arresting the cell cycle and in the presence of MH; 5-FU induced more effect.

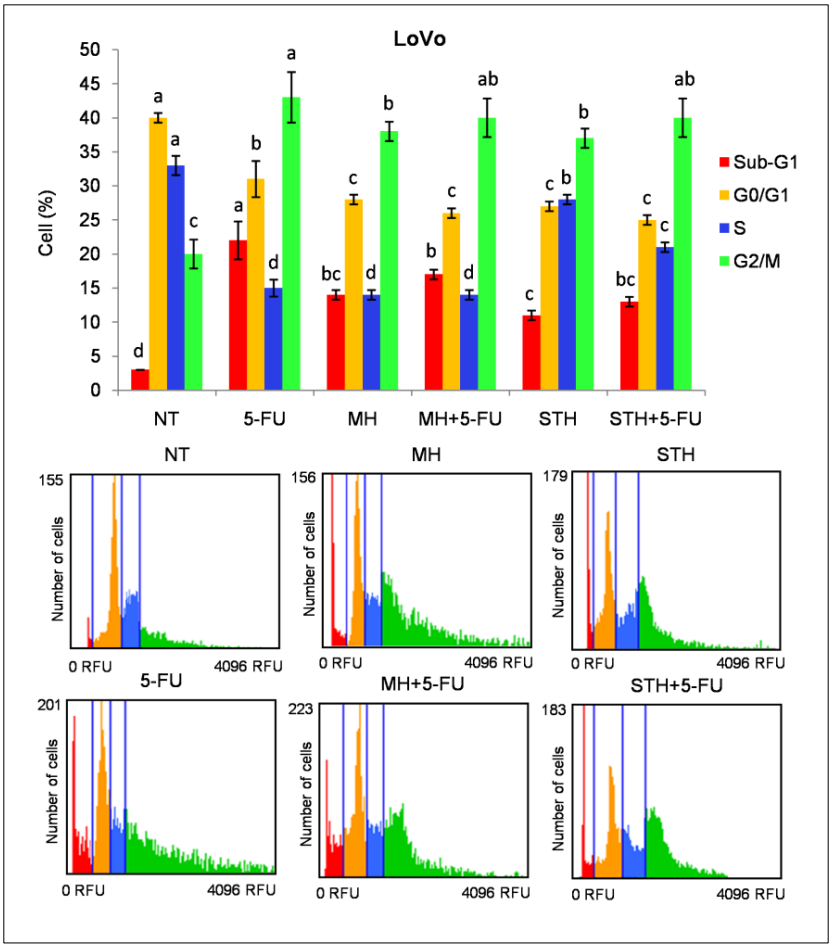

Figure 3.44. Cell cycle alteration induces by 5-FU and/or MH and STH in LoVo cells. After 24 h seeding, LoVo cells were exposed toIC_{50} doses of 5-FU, MH, STH, MH+5-FU and STH+5-FU for 48 h. The NT corresponds to not treatment. PI was used for staining the cells and DNA content of cells was analyzed for determiningthe effect of all treatments on HCT-116 cell cycle distribution. The percentages of cells in each phase Sub-G_1, G_0/G_1, S and G_2/M were calculated by the Tali® Cell Cycle Assay kit and Tali™ Image-based Cytometer. Representative fluorescence image of HCT-116 cells cycle shows the effect of the treatments: red colour corresponds to Sub-G_1 phase, yellow colour corresponds to G_0/G_1 phase, blue colour corresponds to S phase and green yellow colour corresponds to G_2/M phase. All data shown were the mean ± SD of three independent experiments. Different superscripts letter for each column indicated significant differences ($p < 0.05$).

3.3.3. Effect of 5-FU in a combination of MH and STH on apoptosis induction on HCT 116 and LoVo cells

We next evaluated whether 5-FU alone or in the presence of MH and STH induced apoptosis in HCT-116 and LoVo cell lines at doses corresponding to their IC_{50} values after 48 h. In both cell lines, as shown in Figure 3.45 and Figure 3.46, the number of apoptosis cells significantly increased ($p < 0.05$) after 5-FU (5.52 fold and 5.02 fold), MH (3.38 fold and 3.07 fold) and STH (2.17 fold and 3.15 fold) treatments when compared to control (without treatments). In HCT-116 cells, combined treatment exerted slightly less effect (4.17 fold for MH+5-FUand 3.07 fold for STH+5-FU) when compared to 5-FU alone (Figure 3.45).

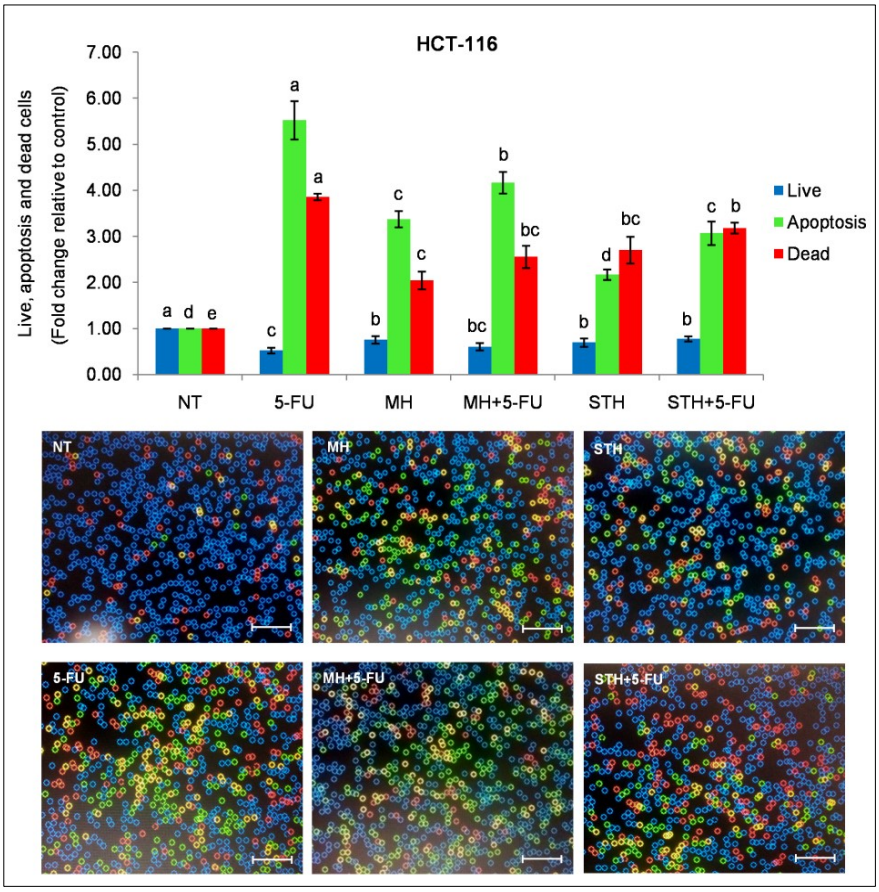

Figure 3.45. Apoptosis induction by 5-FU and/or MH and STH in HCT-116 cells. After 24 h seeding, HCT-116 cells were exposed toIC_{50} doses of 5-FU, MH, STH, MH+5-FU, and STH+5-FU for 48 h. The NT corresponds to not treatment. Annexin V Alexa Fluor® 488 and PI staining was used for determination of the apoptotic effect of all the treatments on HCT-116 cells. Viable, death and apoptotic cells were calculated by using the Tali™ apoptosis kit and the Tali™ Image-based Cytometer. Representative fluorescence image of HCT-116 cells shows the effect of the treatments: blue colour corresponds to live cells, green colour corresponds to apoptotic cells and red and yellow colour corresponds to dead cells. Scale bar = 50 µm. All data shown were the mean ± SD of three independent experiments. Different superscripts letter for each column indicated significant differences ($p < 0.05$).

At the same time, in LoVo cells after combination treatment the apoptotic effect was 3.98 fold for MH+5-FU and 4.17 fold for STH+5-FU (Figure 3.46). The number of live and dead cells was decreased in each treatment and the similar trend also observed when combined treatment was used in both cell lines (Figure 3.45 and Figure 3.46).

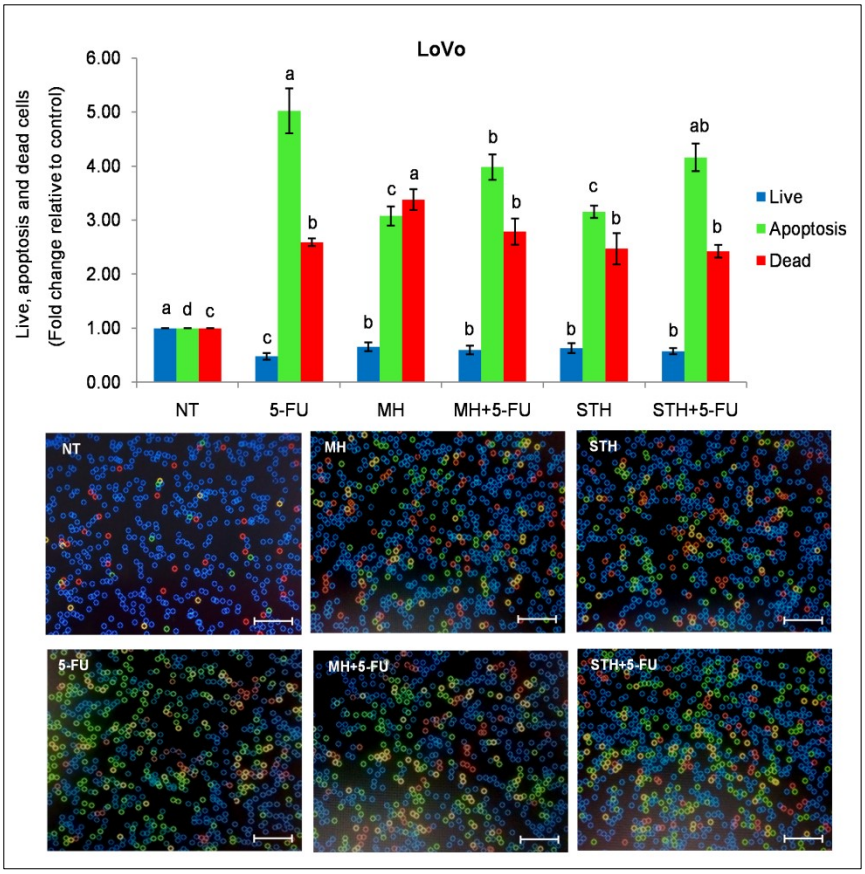

Figure 3.46. Apoptosis induction by 5-FU and/or MH and STH in LoVo cells. After 24 h seeding, LoVo cells were exposed to IC_{50} doses of 5-FU, MH, STH, MH+5-FU and STH+5-FU for 48 h. The NT corresponds to not treatment. Annexin V Alexa Fluor® 488 and PI staining was used for determination of the apoptotic effect of all the treatments on LoVo cells. Viable, death and apoptotic cells were calculated by using the Tali™ apoptosis kit and the Tali™ Image-based Cytometer. Representative fluorescence image of LoVo cells shows the effect of the treatments: blue colour corresponds to live cells, green colour corresponds to apoptotic cells and red and yellow colour corresponds to dead cells. Scale bar = 50 µm. All data shown were the mean ± SD of three independent experiments. Different superscripts letter for each column indicated significant differences ($p < 0.05$).

To add further insight into the molecular mechanisms involved in the 5-FU induced apoptosis either alone or with MH and STH co-treatment, the protein expression of p53, caspase-3 and c-PARP was observed after 48 h treatments at IC_{50} doses in each cells of CRC. In HCT-116 cells, 5-FU significantly ($p < 0.05$) increased the expression of p53, caspase-3 and c-PARP up to 3.75 fold, 2.5 fold and 2.55 fold, MH treatment increased the expression up to 1.55 fold, 1.48 fold and 1.70 fold, and STH treatment increased the

expression up to 2.39 fold and 1.98 fold and 2.19 fold respectively, compared to control (Figure 3.47a). For the combination treatment with MH and STH, the expression was 3.8 fold and 2.39 fold for p53, 2.3 fold and 2.23 fold for caspase-3 and 2.27 fold and 2.40 fold for c-PARP, respectively (Figure 3.47a).

On the other hand, the expression of all these three proteins significantly ($p < 0.05$) increased up to 5.17 fold, 1.97 fold and 2.63 fold after 5-FU treatment, up to 1.72 fold, 1.58 fold and 1.78 fold after MH treatment and up to 1.82 fold, 1.42 fold and 1.80 fold after STH treatment compared to control in LoVo cells (Figure 3.47b). When it combined with MH and STH, the expression was slightly less compared with 5-FU alone (Figure 3.47b). Overall these results suggest that when the 5-FU was combined with MH and STH it induced similar or slightly less effects at the half concentration of 5-FU alone.

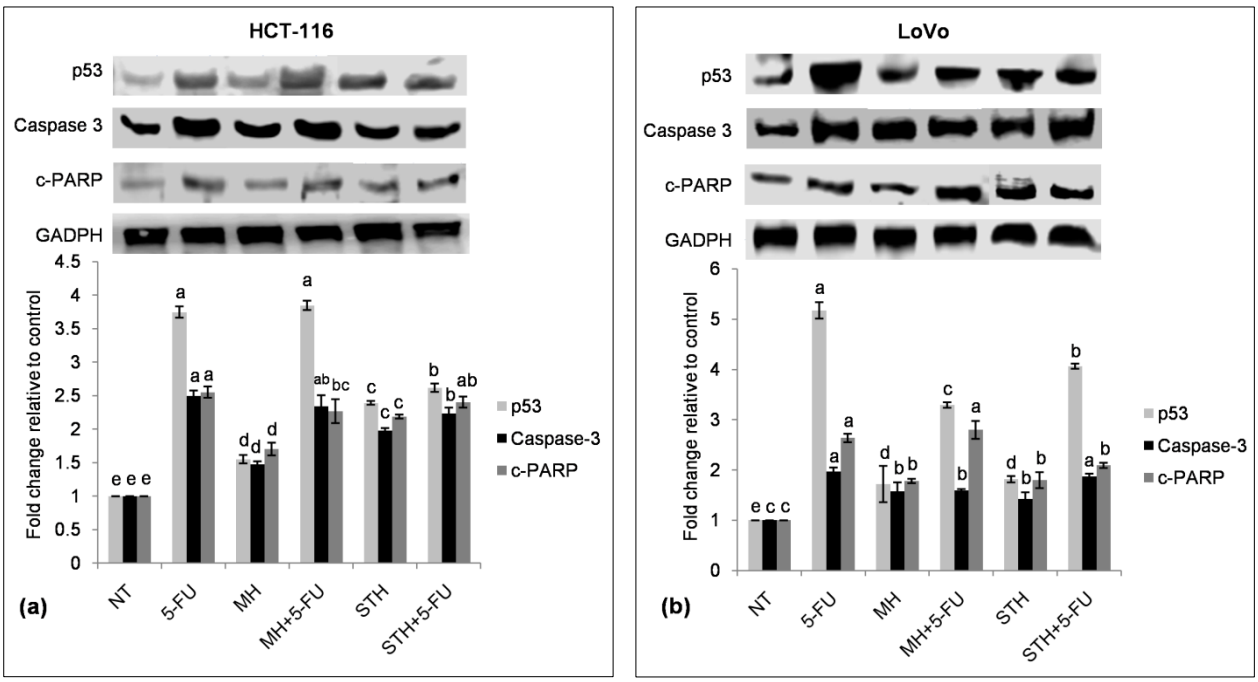

Figure 3.47. The treatment with 5-FU and/or MH and STH increases apoptotic protein expression in HCT-116 (a) and LoVo (b) cells. After 24 h incubation, HCT-116 and LoVo cells were exposed to IC_{50} doses of 5-FU, MH, STH, MH+5-FU and STH+5-FU for 48 h. The NT corresponds to not treatment. The expression of apoptotic marker p53, caspase-3 and c-PARP were determined by western blotting analysis. GADPH was used as a loading control. All data shown were the mean ± SD of three independent experiments. Different superscripts letter for each column indicated significant differences ($p < 0.05$).

3.3.4. Anti-inflammatory effect of 5-FU in a combination of MH and STH on HCT-116 cells

Anti-inflammatory activity was characterized by measuring the protein expression of NFκB, p-IκBα, IL1β, IL-6, iNOS and TNF-α inflammatory biomarkers in HCT-116 cells by treated with 5-FU alone or in the presence of MH and STH after 48 h. The expression of NFκB, IL-6, iNOS and TNF-α was decreased up to 0.48 fold, 0.49 fold, 0.48 fold and 0.39 fold after 5-FU treatment, 0.65 fold, 0.53 fold, 0.52 fold and 0.70 fold after MH treatment and 0.69 fold, 0.50 fold, 0.54 fold and 0.58 fold after STH treatment (Figure 3.48). Interestingly, the expression of the same proteins decreased up to 0.22 fold, 0.26 fold, 0.23 fold and 0.27 fold in the presence of MH+5-FU and 0.26 fold, 0.34 fold, 0.44 fold and 0.24 fold in the presence of STH+5-FU at less concentration of 5-FU (Figure 3.48). The expression of other proteins (p-IκBα and IL1β) also decreased after 5-FU, MH and STH treatment but the combined treatment induced less effect compared to 5-FU alone, even also MH and STH (Figure 3.48).

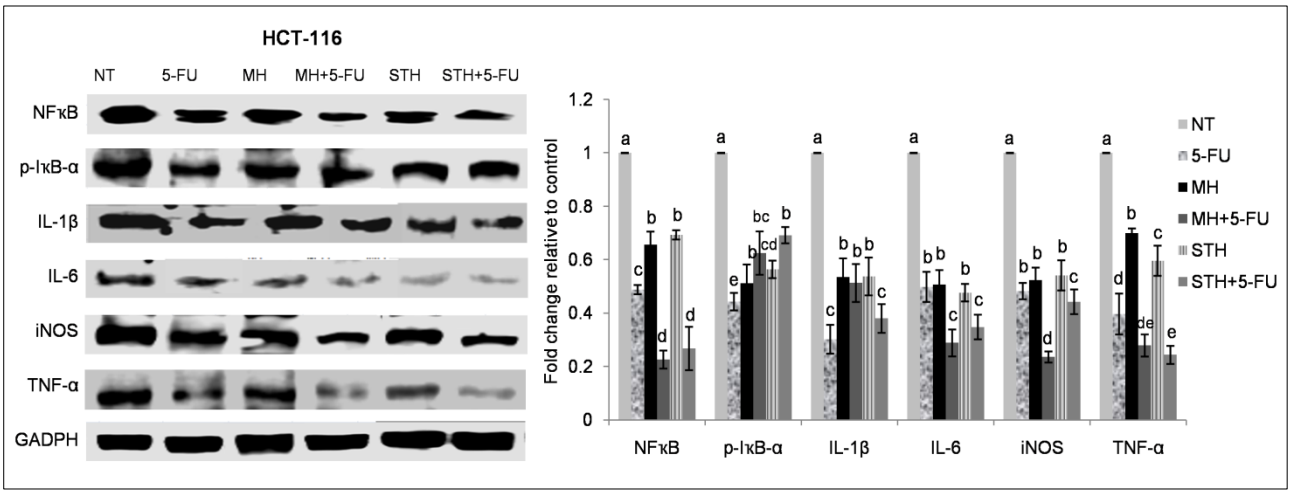

Figure 3.48. Anti-inflammatory effects of 5-FU and/or MH and STH in HCT-116 cells. After 24 h incubation, HCT-116 cells were exposed toIC_{50} doses of 5-FU, MH, STH, MH+5-FU and STH+5-FU for 48 h. The NT corresponds to not treatment. The expression of inflammatory marker NF-κB, p-IκBα, IL1β, IL-6, iNOS and TNF-α were determined by western blotting analysis. GADPH was used as a loading control. All data shown were the mean ± SD of three independent experiments. Different superscripts letter for each column indicated significant differences ($p < 0.05$).

3.3.5. Effect of 5-FU in a combination of MH and STH on MAPK and EGFR signaling pathways in HCT-116 and LoVo cells

It has previously been reported that chemotherapy induced apoptosis in colon cancer cells by activating MAPK pathway (Bragado et al., 2007). As shown in Figure 3.49, 5-FU treatment increased the activation status of major MAPK signaling compounds (p-p38MAPK and p-Erk1/2). In HCT-116 cells, the expression of p-p38MAPK and p-Erk1/2 was increased 1.93 fold and 1.87 fold after 5-FU treatment, 1.72 fold and 1.82 fold after MH treatment and 1.59 fold and 2.41 fold after STH treatment respectively. Regarding the combination treatment with MH+5-FU, the expression of p-p38MAPK and p-Erk1/2 was increased 1.82 fold and 2.09 fold, while p-p38MAPK expression was slightly lower and p-Erk1/2 was slightly upper compared to 5-FU alone (Figure 3.49a). Moreover, combination treatment with STH+5-FU the expression of p-p38MAPK was 1.89 fold which was slightly less and the expression of p-Erk1/2 was 2.49 fold which was significantly ($p < 0.05$) high compared to 5-FU (Figure 3.49a).

In LoVo cells, the expression of p-p38MAPK and p-Erk1/2 was significantly ($p < 0.05$) increased 3.75 fold and 2.82 fold after 5-FU treatment, 2.09 fold and 1.84 fold after MH treatment and 3.76 fold and 2.90 fold after STH treatment (Figure 3.49b). The MH+5-FU induced slightly less expression of the p-p38MAPK (2.98 fold) and p-Erk1/2 (2.51 fold) and the STH+5-FU induced similar expression of p-p38MAPK (3.76 fold) and significantly increased expression p-Erk1/2 (2.90 fold) compared to single agent 5-FU (Figure 3.49b).

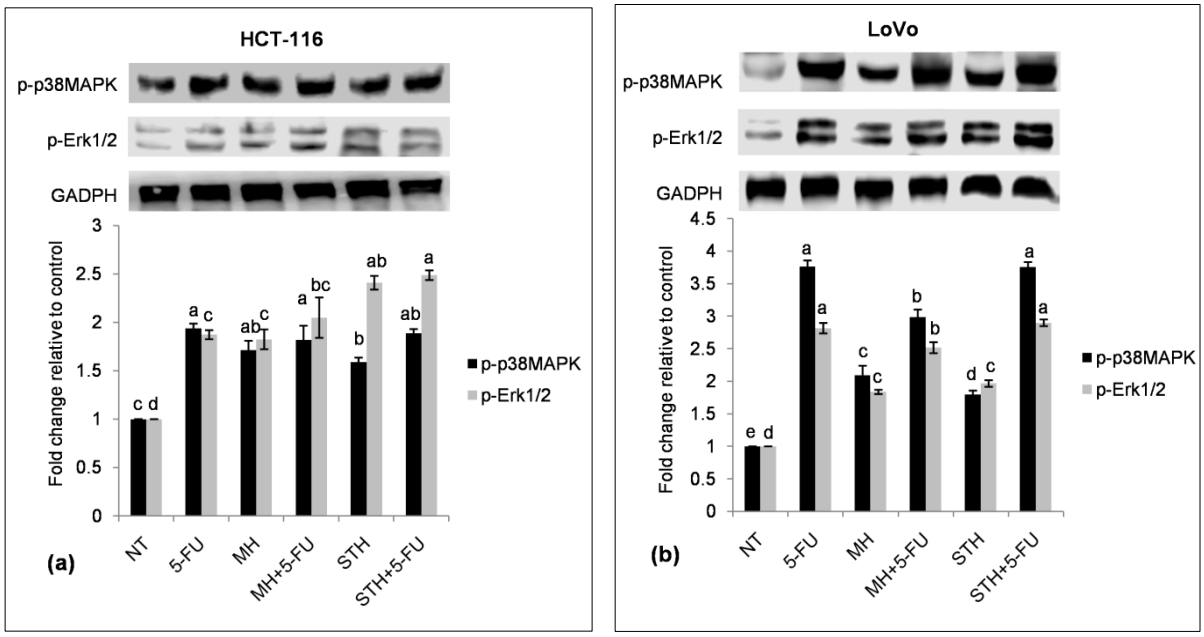

Figure 3.49. Effect of 5-FU and/or MH and STH on MAPK signaling in HCT-116 (a) and LoVo (b) cells. After 24 h incubation, HCT-116 and LoVo cells were exposed to IC_{50} doses of 5-FU, MH, STH, MH+5-FU and STH+5-FU for 48 h. The NT corresponds to not treatment. The expression of p-p38MAPK and p-Erk1/2 were determined by western blotting analysis. GADPH was used as a loading control. All data shown were the mean ± SD of three independent experiments. Different superscripts letter for each column indicated significant differences ($p < 0.05$).

We further evaluated the effect of 5-FU alone or combined with MH and STH on the cell surviving signaling EGFR in HCT-116 and LoVo cells. The expression of EGFR decreased up to 0.58 fold after 5-FU treatment, 0.56 fold after MH treatment and 0.61 fold after STH treatment, while the combination treatment MH+5-FU and STH+5-FU decreased up to 0.35 fold and 0.49 fold in HCT-116 cells (Figure 3.50a). In LoVo cells, the EGFR suppressed 0.49 fold after 5-FU treatment, 0.55 fold after MH treatment and 0.59 fold after STH treatment, while the combination treatments suppressed up to 0.41 fold and 0.36 fold (Figure 3.50b).

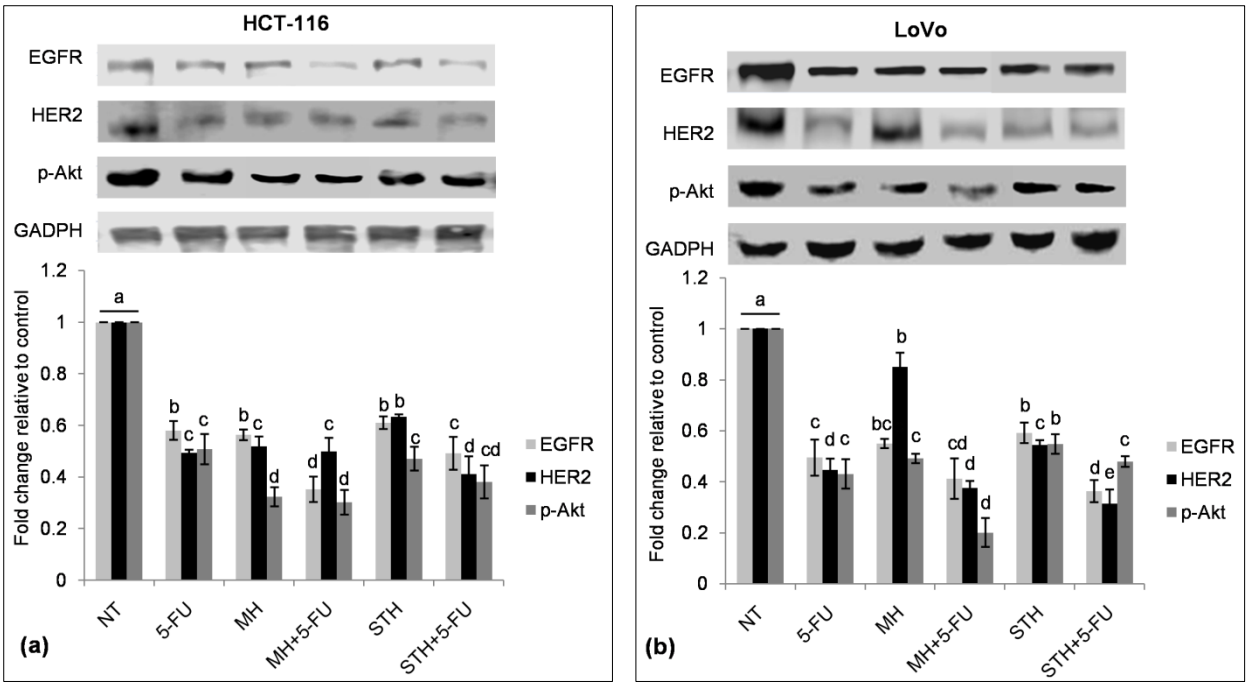

Figure 3.50. Effect of 5-FU and/or MH and STH on EGFR signaling in HCT-116 (a) and LoVo (b) cells. After 24 h incubation, HCT-116 and LoVo cells were exposed to IC_{50} doses of 5-FU, MH, STH, MH+5-FU and STH+5-FU for 48 h. The NT corresponds to not treatment. The expression of EGFR, HER2 and p-Akt were determined by western blotting analysis. GADPH was used as a loading control. All data shown were the mean ± SD of three independent experiments. Different superscripts letter for each column indicated significant differences ($p < 0.05$).

The expression of HER2 decreased up to 0.45 fold after 5-FU treatment in both cell lines. In HCT-116 cells it decreased 0.52 fold after MH treatment and 0.63 fold after STH treatment and in LoVo cells it decreased 0.83 fold after MH treatment and 0.55 fold after STH treatment. In the presence of MH, similar trend was observed like 5-FU while the presence of STH suppressed it more compared to 5-FU alone in HCT-116 cells (Figure 3.50a) but in LoVo cells it decreased up to 0.33 fold in both combination (Figure 3.50b).

In HCT-116 cells, the expression of p-Akt decreased 0.51 fold after 5-FU treatment, 0.32 fold after MH treatment and 0.47 fold after STH treatment, while the single doses of MH and STH were most effective compared to 5-FU (Figure 3.50a). Similarly, in LoVo cells the expression of p-Akt decreased 0.43 fold after 5-FU treatment, 0.49 fold after MH treatment and 0.54 fold after STH treatment, respectively (Figure 3.50b). The expression of p-Akt significantly decreased 0.30 fold for MH+5-FU and 0.38 fold for STH+5-FU in HCT-116 cells (Figure 3.50a), while in LoVo cells the expression decreased 0.20 fold after MH+5-FU treatment and 0.45 fold after STH+5-FU treatment (Figure 3.50b).

3.3.6. Effect of 5-FU in a combination of MH and STH on oxidative stress induction on HCT-116 and LoVo cells

3.3.6.1. Effect of 5-FU in a combination of MH and STH on intracellular ROS production on HCT-116 and LoVo cells

The intracellular ROS levels were determined by the treatment of 5-FU and in the presence of MH and STH in HCT-116 and in LoVo cells following 48 h treatments. In HCT-116 cells, ROS production increased 25.33% after 5-FU treatment, 21.5% after MH treatment and 21% after STH treatment, while in the presence of MH and STH the ROS production increased 28% and 32% after 5-FU treatment compared to control (7%) (Figure 3.51).

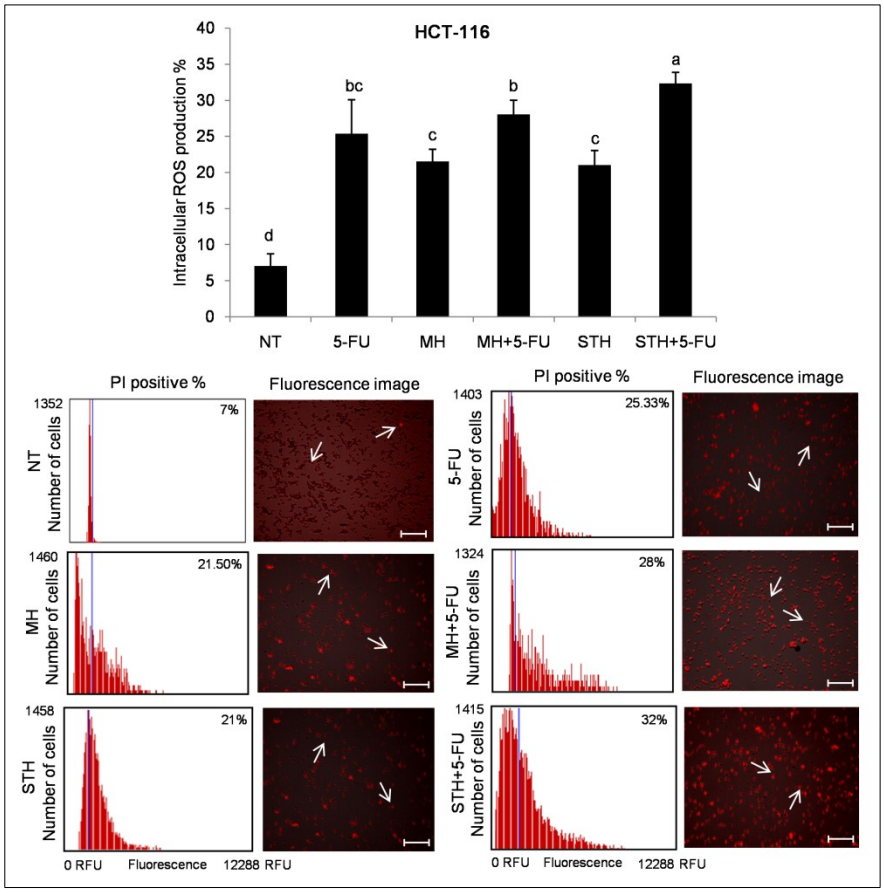

Figure 3.51. Effect of 5-FU and/or MH and STH on intracellular ROS production in HCT-116 cells. After 24 h incubation, HCT-116 cells were exposed to IC_{50} doses of 5-FU, MH, STH, MH+5-FU and STH+5-FU for 48 h. The NT corresponds to not treatment. Intracellular ROS levels were calculated by using CellROX® Orange assay kit and the Tali™ Image-based Cytometer. The blue line of the thumbnail histogram indicated the set threshold. Representative fluorescence image of HCT-116 cells shows the effect of the treatments at 48 h: non-fluorescent while in a reduced state and bright red fluorescence upon oxidation by ROS. Scale bar = 50 µm, arrows indicate single cell (cell size =10 µm). All data shown were the mean ± SD of three independent experiments. Different superscripts letter for each column indicated significant differences ($p < 0.05$).

Similarly, in LoVo cells, treatment with 5-FU increased ROS production by 36%, MH treatment induced ROS production by 34% and STH treatment induced ROS production by 32.68%, respectively compared to control (6%) (Figure 3.52). Furthermore, the combination treatment of MH+5-FU increased 40% ROS production and STH+5-FU increased 44.6% ROS production (Figure 3.52).

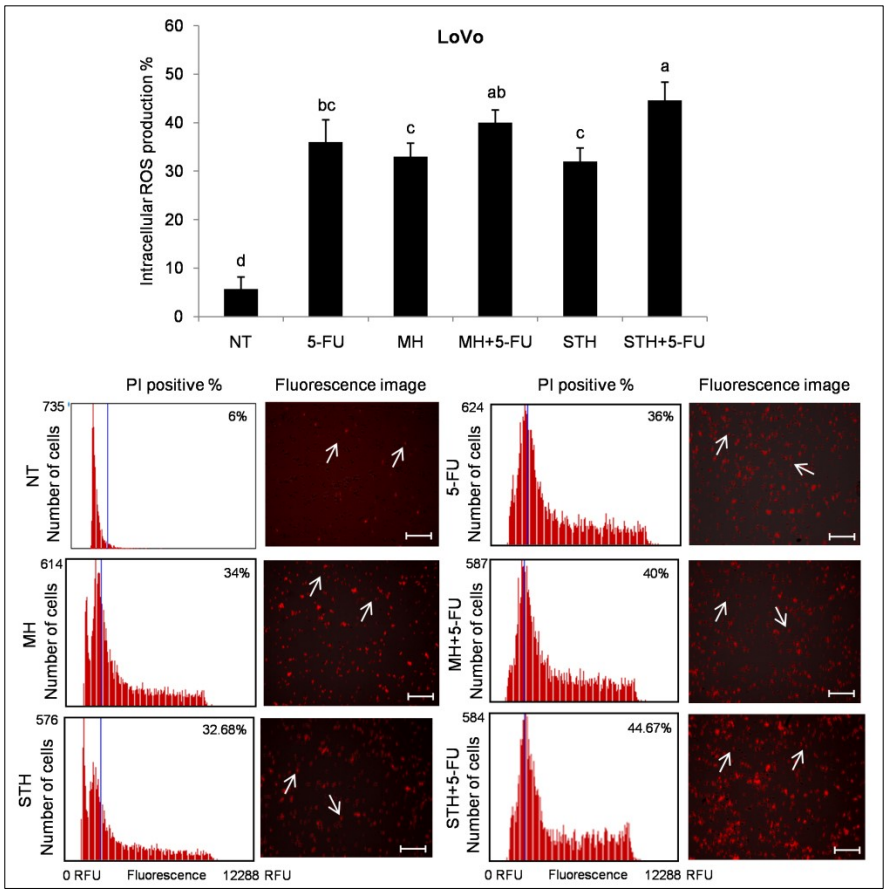

Figure 3.52. Effect of 5-FU and/or MH and STHon intracellular ROS productionin LoVo cells. After 24 h incubation, LoVo cells were exposed toIC50 doses of 5-FU, MH, STH, MH+5-FU and STH+5-FU for 48 h. The NT corresponds to not treatment. Intracellular ROS levels were calculated by using CellROX® Orange assay kit and the Tali™ Image-based Cytometer. The blue line of the thumbnail histogram indicated the set threshold. Representative fluorescence image of LoVo cells shows the effect of the treatments at 48 h: non-fluorescent while in a reduced state and bright red fluorescence upon oxidation by ROS. Scale bar = 50 µm, arrows indicate single cell (cell size =10 µm). All data shown were the mean ± SD of three independent experiments. Different superscripts letter for each column indicated significant differences ($p < 0.05$).

Taken together, it was suggested that the MH and STH enhanced the ROS production of 5-FU in HCT-116 and in LoVo cells compared to 5-FU single doses. Moreover, in LoVo cells the treatments induced more ROS compared to HCT-116 cells, while STH+5-FU combination was most effective.

3.3.6.2. Effect of 5-FU in a combination of MH and STH on the biomarkers of oxidative stress and the antioxidant enzyme on HCT-116 and LoVo cells

The biomarkes of lipid (TBARS level) and protein (carbonyl content) levels were determined after the treatment of 5-FU and in the presence of MH and STH after successive treatment in both colon cancer cells. In HCT-116 and LoVo cells, the levels of TBARS significantly ($p < 0.05$) increased 232% and 220% after 5-FU treatment, 216% and 162% after MH treatment and 199% and 205% after STH treatment (Figure 3.53).

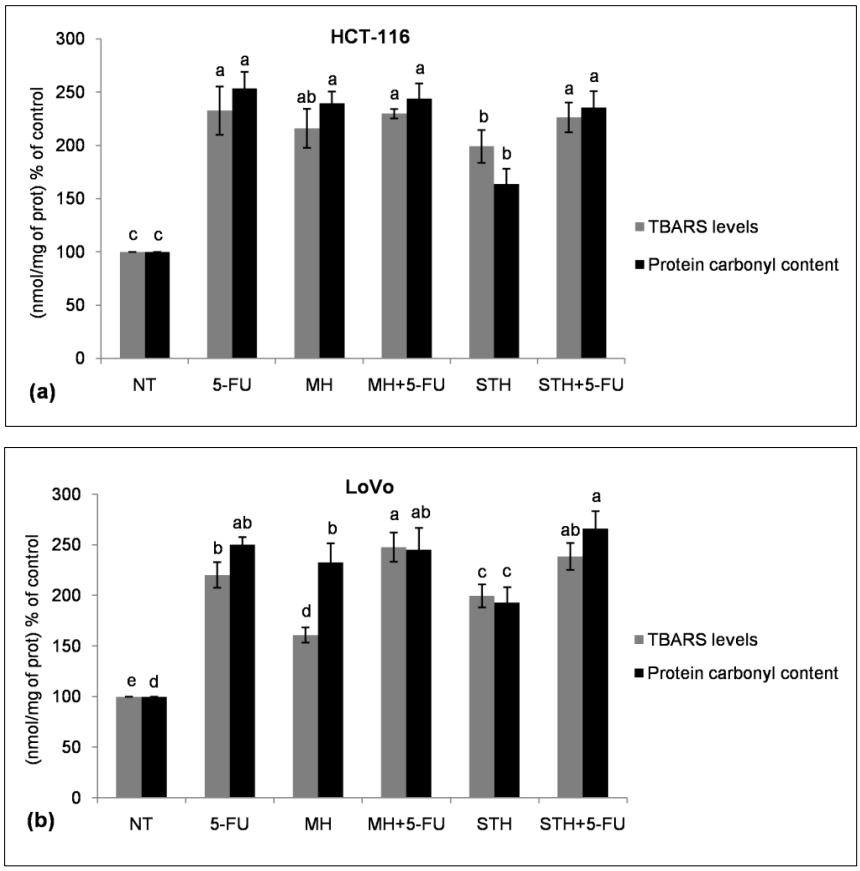

Figure 3.53. Effect of 5-FU and/or MH and STH on the biomarker of oxidative stress in HCT-116 (a) and LoVo (b) cells. Lipid and protein oxidative damage was evaluated from the TBARS levels and protein carbonyl content. After 24 h incubation, HCT-116 and LoVo cells were exposed to IC_{50} doses of 5-FU, MH, STH, MH+5-FU and STH+5-FU for 48 h. The NT corresponds to not treatment. The results weremeasured as unit per mg protein and expressed as the percent of the control. All data shown were the mean ± SD of three independent experiments. Different superscripts letter for each column indicated significant differences ($p < 0.05$).

The combination treatment of MH+5-FU increased the TBARS levels 230% for HCT-116 and 248% for Lovo cells and the combination treatment of STH+5-FU increased the TBARS levels 227% for HCT-116 and 239% for LoVo cells (Figure 3.53).

Similarly, the level of protein carbonyl content was also increased after 5-FU (253% and 249%), MH (239% and 232%) and STH (163% and 193%) treatment in both cell lines (Figure 3.53). Furthermore, the combination treatment of MH+5-FU increased the levels of protein carbonyl content 243% in HCT-116 cells (Figure 3.53a) and 245% in lovo cells (Figure 3.53b), respectively compared to control. Similarly, the combination treatment of STH+5-FU increased the levels of protein carbonyl content 235% in HCT-116 cells (Figure 3.53a) and 265% in LoVo cells (Figure 3.53b) compared to control. The combination treatment was most effective in LoVo cells compared to HCT-116 and STH potentiated more the effect of 5-FU in both cell line compared to 5-FU alone.

The DNA damage was also highlithed by increasing the expression of OGG1 protein 2.23 fold and 2.85 fold after 5-FU treatment in HCT-116 and in LoVo cells (Figure 3.54). Additionally, the treatment with MH increased 1.67 fold and 1.84 fold and the treatment with STH increased 1.58 fold and 2.30 fold in both cell lines (Figure 3.54). The combination of MH+5-FUinduced the expression of OGG1 1.97 fold in HCT-116 cells and 1.87 fold in LoVo cells, while the combination of STH+5-FU induced similar effect like 5-FU in both cell lines (Figure 3.54).

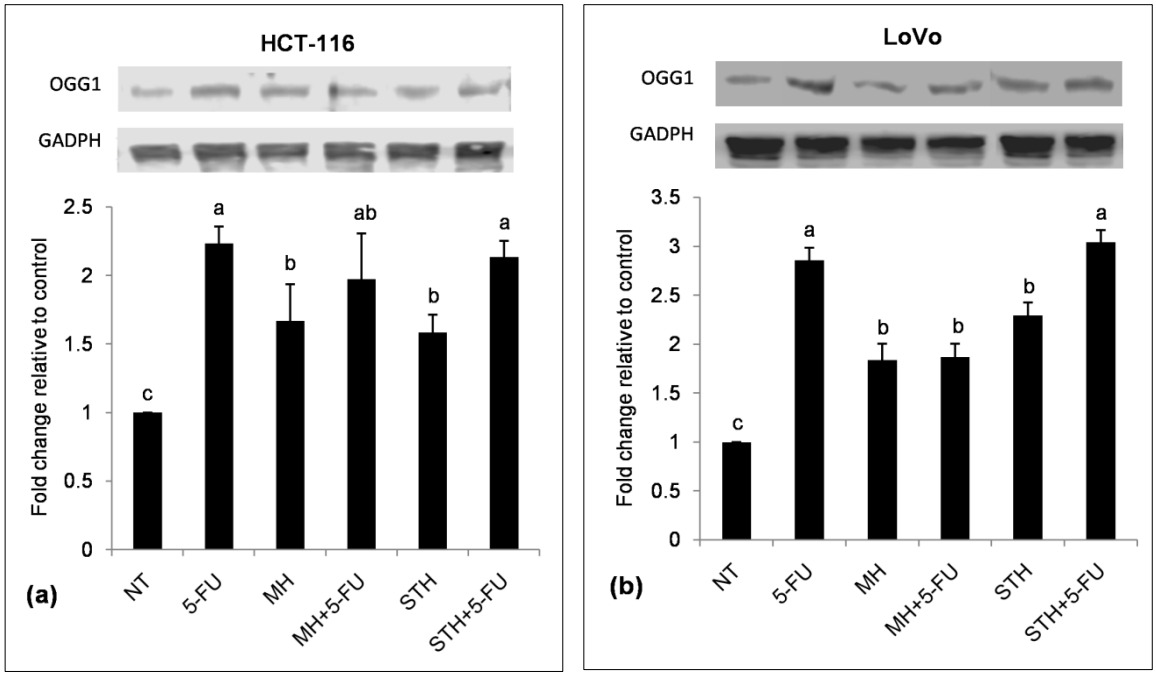

Figure 3.54. Effect of 5-FU and/or MH and STH onthe DNA damage in HCT-116 (a) and LoVo (b) cells. After 24 h incubation, HCT-116 and LoVo cells were exposed to IC_{50} doses of 5-FU, MH, STH, MH+5-FU and STH+5-FU for 48 h. The NT corresponds to not treatment. The expression of OGG1 was determined by western blotting analysis. GADPH was used as a loading control. All data shown were the mean ± SD of three independent experiments. Different superscripts letter for each column indicated significant differences ($p < 0.05$).

In the next step, we evaluated the effect of 5-FU and MH+5-FU or STH+5-FU treatments on the activity and the expression of the antioxidant enzymes in HCT-116 and Lovo cells. In HCT-116 cells, the activity of GPx, GST and GR was decreased to 65%, 69% and 59% compared to control (100%) after 5-FU treatment. After MH and STH treatments, all the activities decreased more compared to 5-FU alone, while the combination treatments were most effective, such as MH+5-FU decreased the activity of GPx 44%, GST 46% and GR 33%. Similarly, STH+5-FU decreased the activity of GPx 35%, GST 42% and GR 55% compared to control (Figure 3.55a).

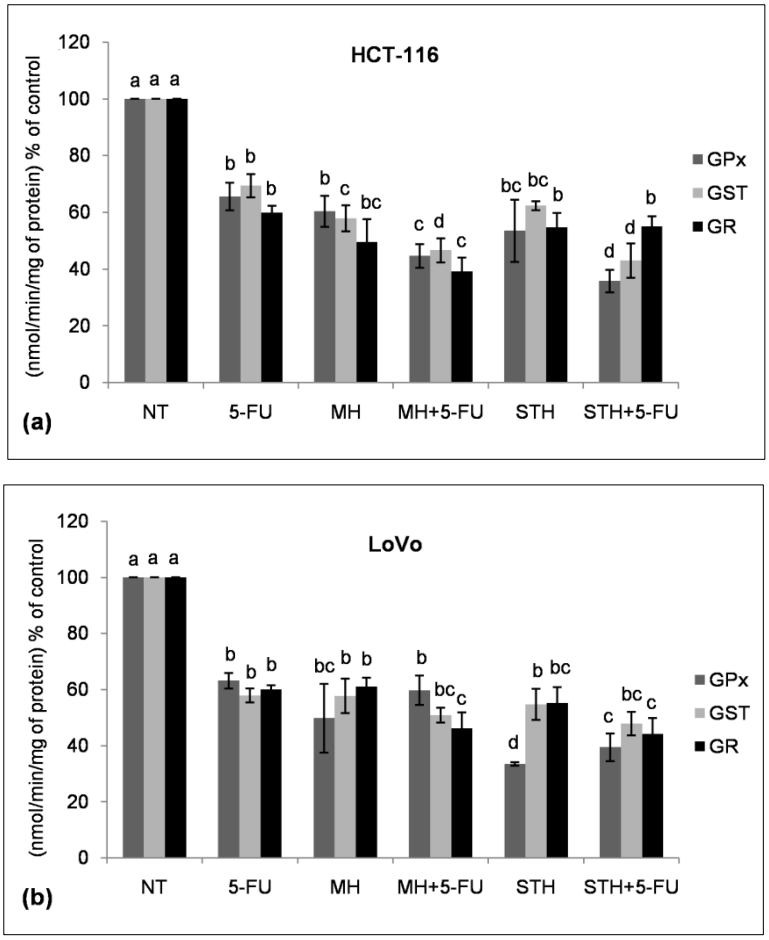

Figure 3.55. Effect of 5-FU and/or MH and STH on the antioxidant enzyme GPx, GST and GR activity in HCT-116 (a) and LoVo (b) cells. After 24 h incubation, HCT-116 and LoVo cells were exposed to IC_{50} doses of 5-FU, MH, STH, MH+5-FU and STH+5-FU for 48 h. The NT corresponds to not treatment. GPx, GST and GR activity was expressed as unit per mg protein and results were expressed as the percent of the control. All data shown were the mean ± SD of three independent experiments. Different superscripts letter for each column indicated significant differences ($p < 0.05$).

In Lovo cells, the activity of GPx, GST and GR decreased to 63%, 57% and 60% after 5-FU, while the combination of MH+5-FU reduced the activity to 59%, 50% and 46% and STH+5-FU reduced to 39%, 47% and 44%, respectively (Figure 3.55b). Taken together it was suggested that the combination treatment of MH+5-FU was most effective in HCT-116 cells, while in LoVo cells STH+5-FU was most effective.

The activity of SOD and catalase was reduced to 77% and 88% in HCT-116 cells and 71% and 69% in LoVo cells after 5-FU treatment compared to control (100%) (Figure 3.56). After the treatment with MH, the activity was 65% and 56% in HCT-116 cells and 63%

and 68% in LoVo cells (Figure 3.56a). Similarly, STH reduced the SOD and catalase activity 72% and 42% in HCT-116 cells and 67% and 62% in LoVo cells (Figure 3.56b).

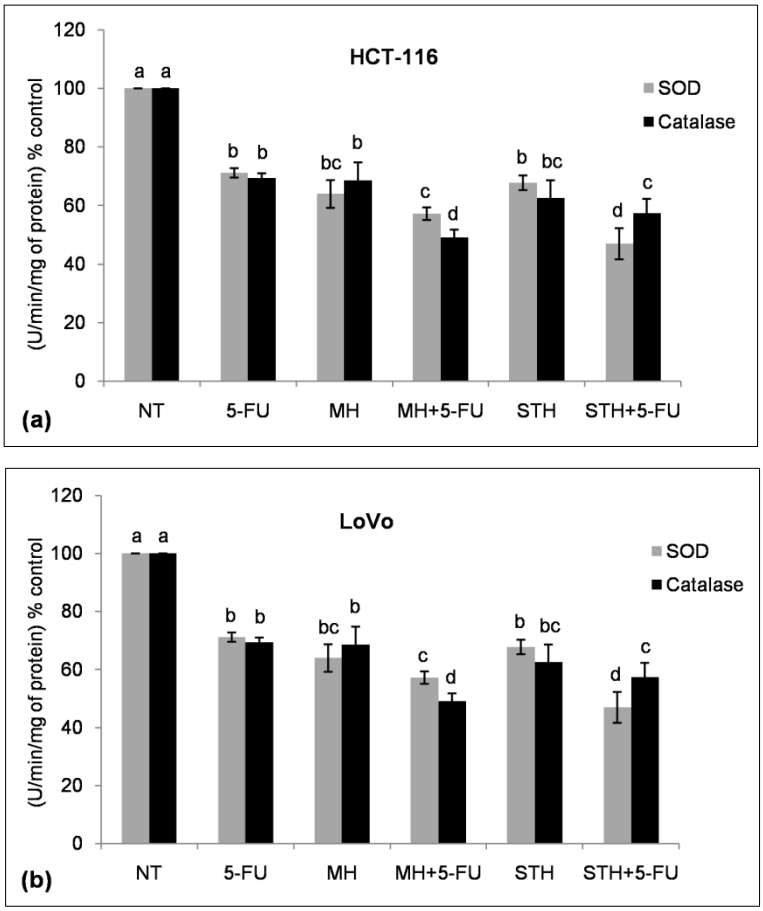

3.56. Effect of 5-FU and/or MH and STH on the antioxidant enzyme SOD and catalase activity in HCT-116 (a) and LoVo (b) cells. After 24 h incubation, HCT-116 and LoVo cells were exposed to IC_{50} doses of 5-FU, MH, STH, MH+5-FU and STH+5-FU for 48 h. The NT corresponds to not treatment. SOD and catalase activity was expressed as unit per mg protein and results were expressed as the percent of the control. All data shown were the mean ± SD of three independent experiments. Different superscripts letter for each column indicated significant differences ($p < 0.05$).

In the presence of MH the SOD activity decreased up to 60% and 57% and catalase activity decreased up to 42% and 49% after 5-FU treatment in both cell lines (Figure 3.56). Furthermore, in the presence of STH the activity of both enzyme decreased up to 61% and 51% in HCT-116 cells and 46% and 57% in LoVo cells (Figure 3.56).

Similar trend was also observed in the expression of the transcription factor Nrf2 and other antioxidant enzyme SOD, catalase and HO-1 (Figure 3.57 and Figure 3.58). In HCT-116 cells, the expression of Nfr2, SOD, catalase and HO-1 was decreased up to 0.76 fold, 0.78 fold, 0.87 fold and 0.90 fold after 5-FU treatment, 0.55 fold, 0.54 fold, 0.73 fold and 0.64

fold after MH treatment and 0.53 fold, 0.54 fold, 0.37 fold and 0.70 fold after STH treatment, respectively compared to control (Figure 3.57). The MH+5-FU treatment decreased the expression up to 0.59 fold, 0.58 fold, 0.56 fold and 0.60 fold and STH+5-FU treatment decreased the expression up to 0.63 fold, 0.48 fold, 0.33 fold and 0.52 fold, respectively (Figure 3.57).

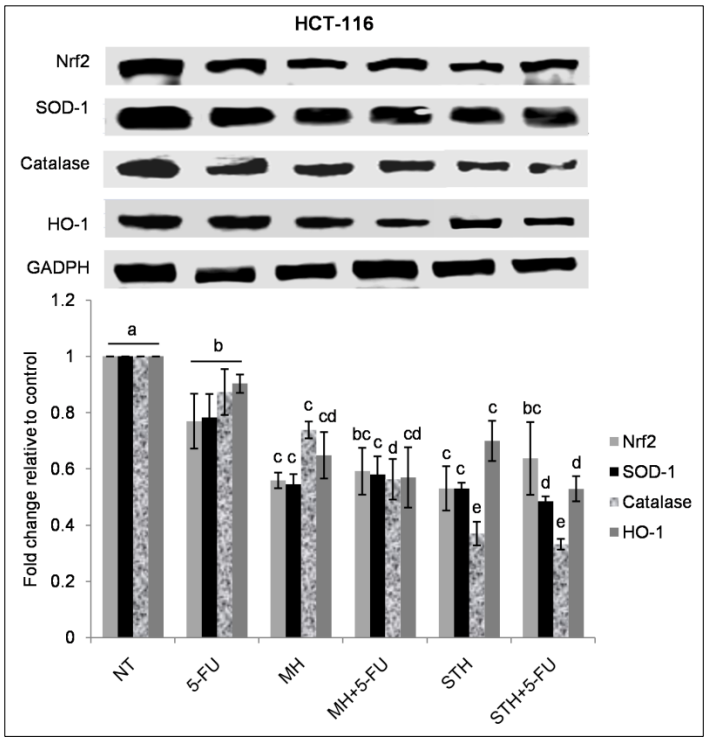

Figure 3.57. Effect of 5-FU and/or MH and STH on the expression of antioxidant enzymes in HCT-116 cells. After 24 h incubation, HCT-116 cells were exposed to IC_{50} doses of 5-FU, MH, STH, MH+5-FU and STH+5-FU for 48 h. The NT corresponds to not treatment. Nrf2, SOD-1, catalase and HO-1 protein expressions were analyzed by western blotting. GADPH was utilized as a loading control. All data shown were the mean ± SD of three independent experiments. Different superscripts letter for each column indicated significant differences ($p < 0.05$).

In the case of LoVo cells, the expression of Nfr2, SOD, catalase and HO-1 was decreased up to 0.89 fold, 0.80 fold, 0.83 fold and 0.91 fold after 5-FU treatment, 0.56 fold, 0.71 fold, 0.52 fold and 0.77 fold after MH treatment and 0.47 fold, 0.61 fold, 0.63 fold and 0.76 fold after STH treatment, correspondingly (Figure 3.58). The combination treatment was more profound in LoVo cells compared to HCT-116 cells (Figure 3.58). The combination of MH+5-FU significantly ($p < 0.05$) decreased the expression of Nfr2, SOD, catalase and HO-1 up to 0.33 fold, 0.30 fold, 0.52 fold and 0.62 fold, and STH+5-FU decreased the expression up to 0.39 fold, 0.34 fold, 0.61 fold and 0.47 fold (Figure 3.58).

Taken together, it was suggested that the MH and STH enhanced the pro-oxidative effects of 5-FU at less concentration for inducing the cell death by oxidative stress.

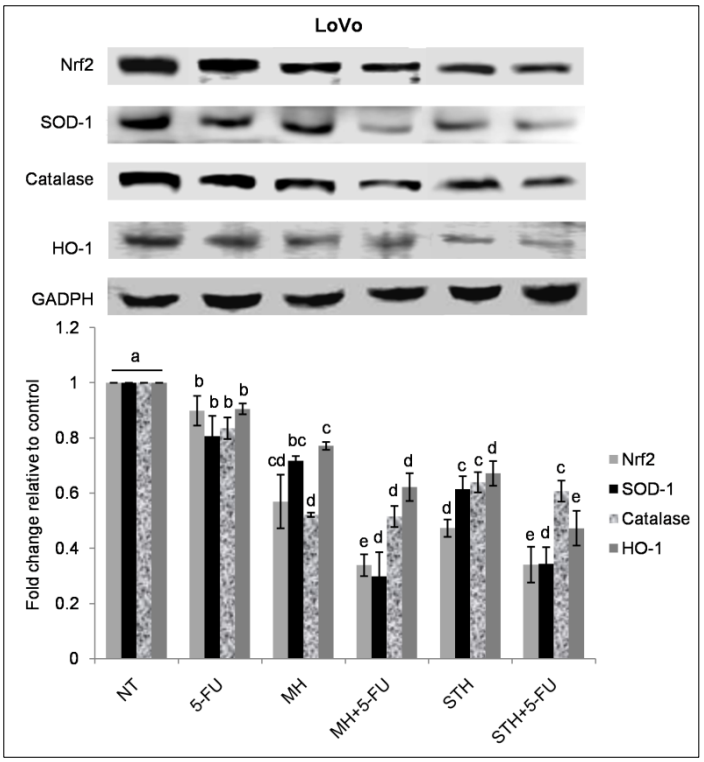

Figure 3.58. Effect of 5-FU and/or MH and STH on the expression of antioxidant enzymes in LoVo cells. After 24 h incubation, LoVo cells were exposed to IC_{50} doses of 5-FU, MH, STH, MH+5-FU and STH+5-FU for 48 h. The NT corresponds to not treatment. Nrf2, SOD-1, catalase and HO-1 protein expressions were analyzed by western blotting. GADPH was utilized as a loading control. All data shown were the mean ± SD of three independent experiments. Different superscripts letter for each column indicated significant differences ($p < 0.05$).

3.3.7. Effect of 5-FU in a combination of MH and STH on the ER stress induction on HCT-116 and LoVo cells

In this step, we evaluated the effect of 5-FU alone or in the presence of MH and STH on the expression of ER stress-associated molecules, ATF6 and XBP1. As shown in Figure 3.59a, the combination of MH+5-FU increased 2.27 fold the expression of ATF6, while the 5-FU and STH+5-FU induced 1.8 fold in HCT-116 cells. The expression of XBP1 was increased up to 2.21 fold after 5-FU and STH+5-FU treatment, but MH+5-FU increased up to 2.03 fold (Figure 3.59a). Additionally, both ER markers were increased after MH (1.69 fold and 1.32 fold) and STH (1.79 fold and 1.50 fold) treatments but it was less effective compared to other treatments.

In LoVo cells, 5-FU treatment increased the expression of ATF6 and XBP1 proteins up to 2.03 fold and 2.69 fold, MH up to 1.53 fold and 1.72 fold, and STH up to 1.72 fold (Figure 3.59b). The treatment of MH+5-FU increased both proteins 1.83 fold and 2.21 fold and STH+5-FU increased 1.9 fold and 1.88 fold (Figure 3.59b). Both combination treatments were most effective in HCT-116 cells compared to LoVo cells for induction of ER stress.

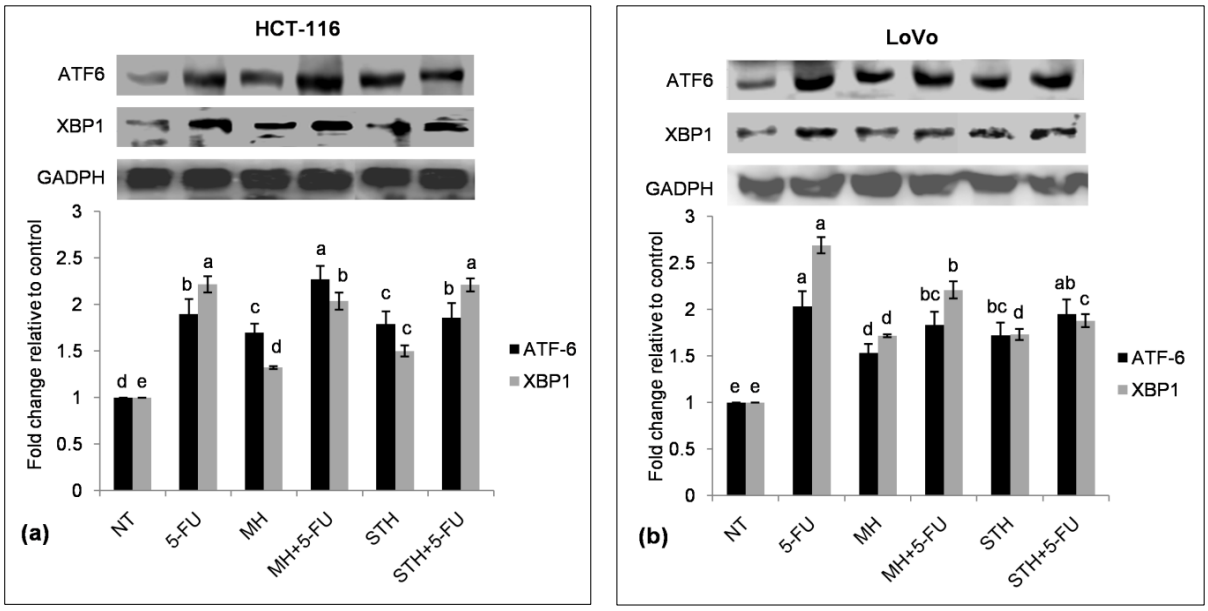

Figure 3.59. Effect of 5-FU and/or MH and STH on the ER stress in HCT-116 (a) and LoVo (b) cells. After 24 h incubation, HCT-116 and LoVo cells were exposed toIC_{50} doses of 5-FU, MH, STH, MH+5-FU and STH+5-FU for 48 h. The NT corresponds to not treatment. ATF6 and XBP1 protein expression were analyzed by western blotting. GADPH was utilized as a loading control. All data shown were the mean ± SD of three independent experiments. Different superscripts letter for each column indicated significant differences ($p < 0.05$).

3.3.8. Effect of 5-FU in a combination of MH and STH on HCT-116 and LoVo cells metabolism

3.3.8.1. Effect of 5-FU in a combination of MH and STH on mitochondrial respiration on HCT-116 and LoVo cells

Our next effort was to investigate the effect of 5-FU alone and in combination with MH or STH on mitochondrial respiration on each CRC cell lines. As shown in Figure 3.60, 5-FU treatment significantly ($p < 0.05$) reduced the basal OCR, the ATP-linked respiration, the proton leak, the SRC and the MRC, up to 85.33 ± 2.82, 61.00 ± 6.30, 7.33 ± 1.60, 12.33 ± 3.29 and 73.50 ± 3.06 pmol/min per 3 $\times 10^4$ cells, respectively compared to the control, in HCT-116 cells. The above parameters also decreased after the treatment with MH (138.00 ± 7.82, 104.80 ± 5.10, 24.05 ± 1.83, 17.68 ± 4.80 and 122.57 ± 9.98 pmol/min per 3 $\times 10^4$ cells) and STH (116.33 ± 4.02, 89.50 ± 9.90, 10.30 ± 2.27, 17.23 ± 2.29 and 106.87 ± 7.66 pmol/min per 3 $\times 10^4$ cells) (Figure 3.60).

In addition, the MH+5-FU significantly decreased the basal OCR (96.83 ± 3.23), the ATP-linked respiration (74.50 ± 1.71), the proton leak (14.33 ± 0.94), the SRC (16.71 ± 0.71) and the MRC (90.00 ± 1.41) but induced slightly less effects compared to 5-FU alone (Figure 3.60). On the other hand, the STH+5-FU was more effective compared to 5-FU: basal OCR was 69.50 ± 5.89, the ATP-linked respiration was 48.17 ± 2.06, the proton leak was 4.83 ± 0.25, the SRC was 15.00 ± 1.89 and the MRC was 63.00 ± 1.18, respectively (Figure 3.60).

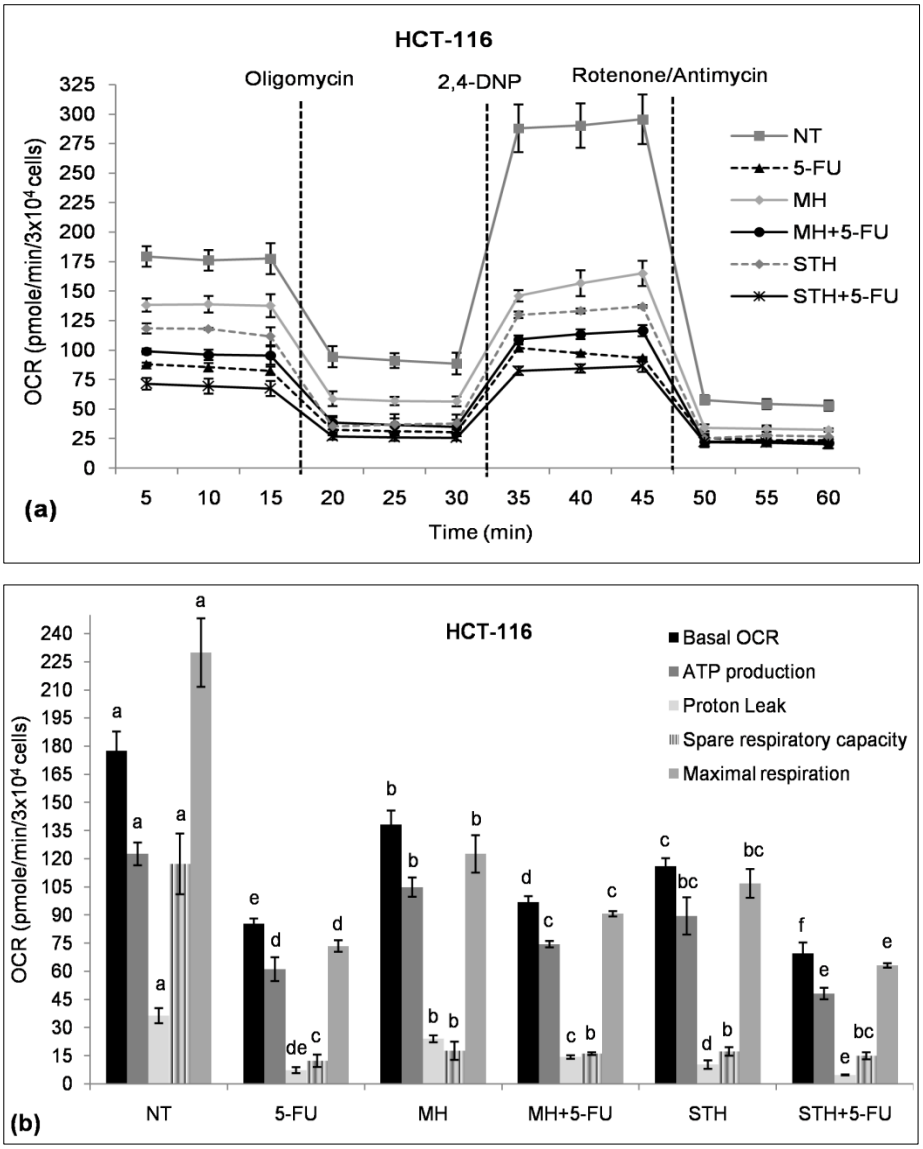

Figure 3.60. Regulation of mitochondrial respiration by 5-FU and/or MH and STH in HCT-116 cells. After 24 h incubation, HCT-116 cells were exposed to IC_{50} doses of 5-FU, MH, STH, MH+5-FU and STH+5-FU for 48 h. The NT corresponds to not treatment. OCR was determined by using the Seahorse XF-24 Extracellular Flux Analyzer after the following sequential injections: oligomycin (3 μg/ml), 2,4-DNP (300 μM), and rotenone/antimycin (1μM/10μM). From the XF cell Mito stress test profile (a), basal respiration, ATP production, proton leak, spare respiratory capacity and maximal respiration (b) were calculated. All data shown were the mean ± SD of three independent experiments. Different superscripts letter for each column indicated significant differences ($p < 0.05$).

Furthermore, in LoVo cells both combinations were more effective compared to 5-FU alone on the mitochondrial respiration. The basal OCR, the ATP-linked respiration, the proton leak, the SRC and the MRC were decreased 37.15 ± 0.97, 25.60 ± 4.29, 15.43 ± 3.85, 27.22 ± 4.09 and 46.90 ± 4.37 pmol/min per 3 $\times 10^4$ cells after 5-FU treatment, 60.23 ± 1.55, 35.04 ± 1.72, 48.46 ± 2.05, 45.50 ± 6.61 and 84.00 ± 4.89 pmol/min per 3 $\times 10^4$ cells after MH treatment and 42.41 ± 1.82, 24.90 ± 1.52, 5.65 ± 1.08, 15.23 ± 1.02 and 41.93 ± 2.55 pmol/min per 3 $\times 10^4$ cells after STH treatment, respectively compared to

control (Figure 3.61). The combination of MH+5-FU and STH+5-FU decreased all these parameters up to 33.03 ± 1.43 and 22.48 ± 1.73, 16.48 ± 0.48 and 8.31 ± 1.57, 4.39 ± 1.86 and 4.64.03 ± 0.91, 21.68 ± 3.23 and 10.13 ± 0.49, and 40.45 ± 2.75 and 32.32 ± 2.06 pmol/min per 3 $\times 10^4$ cells (Figure 3.61).

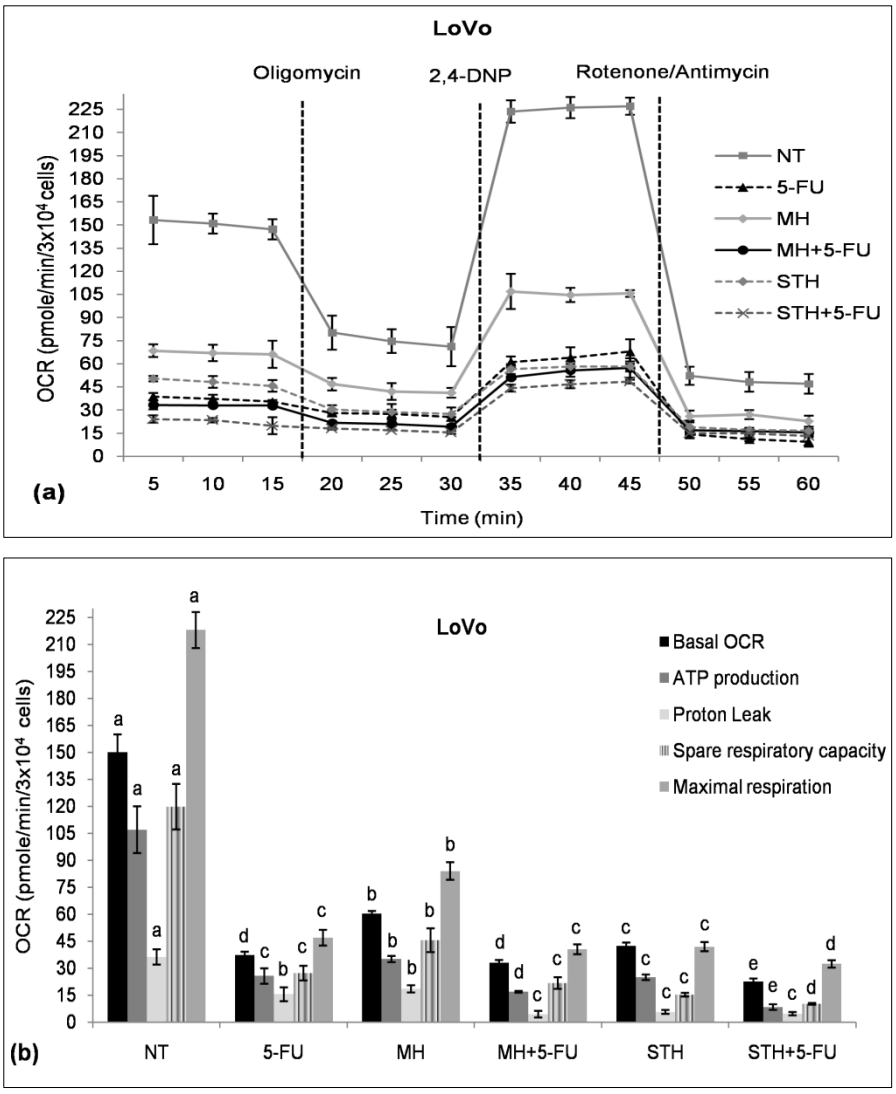

Figure 3.61. Regulation of mitochondrial respiration by 5-FU and/or MH and STH in LoVo cells. After 24 h incubation, LoVo cells were exposed to IC_{50} doses of 5-FU, MH, STH, MH+5-FU and STH+5-FU for 48 h. The NT corresponds to not treatment. OCR was determined by using the Seahorse XF-24 Extracellular Flux Analyzer after the following sequential injections: oligomycin (3 μg/ml), 2,4-DNP (300 μM), and rotenone/antimycin (1μM/10μM). From the XF cell Mito stress test profile (a), basal respiration, ATP production, proton leak, spare respiratory capacity and maximal respiration (b) were calculated. All data shown were the mean ± SD of three independent experiments. Different superscripts letter for each column indicated significant differences ($p < 0.05$).

Taken together, it was suggested that the combination treatment was more effective in LoVo cells compared to HCT-116 cells and STH+5-FU was most effective.

3.3.8.2. Effect of 5-FU in a combination of MH and STH on glycolysis on HCT-116 and LoVo cells

Regarding the ECAR, we observed that 5-FU reduced the basal values 10.00 ± 0.72, while MH and STH reduced it 20.40 ± 0.49 and 12.46 ± 0.95 mpH/ min respectively per 3×10^4 in HCT-116 cells compared to control (Figure 3.62). After the treatment of MH+5-FU and STH+5-FU, the basal values were 15.37 ± 1.93 and 10.96 ± 1.77 mpH/ min per 3×10^4 (Figure 3.62).

Furthermore, the activity of glycolysis, glycolytic capacity and glycolytic reserve were decreased to 6.00 ± 1.00, 13.07 ± 0.87 and 8.00 ± 1.00 mpH/ min per 3×10^4 after 5-FU treatment, 8.35 ± 0.16, 22.06 ± 1.07 and 15.32 ± 0.67 mpH/ min per 3×10^4 after MH treatment and 7.48 ± 0.26, 17.09 ± 1.00 and 9.56 ± 0.05 mpH/ min per 3×10^4 after STH treatment, respectively (Figure 3.62).

In the presence of MH and STH, 5-FU reduced the activity of glycolysis up to 10.04 ± 1.50 and 9.81 ± 0.23, glycolytic capacity up to 19.67 ± 1.00 and 15.05 ± 2.60, and glycolytic reserve up to 9.62 ± 0.76 and 5.40 ± 0.36 mpH/ min per 3×10^4, respectively compared to control (Figure 3.62).

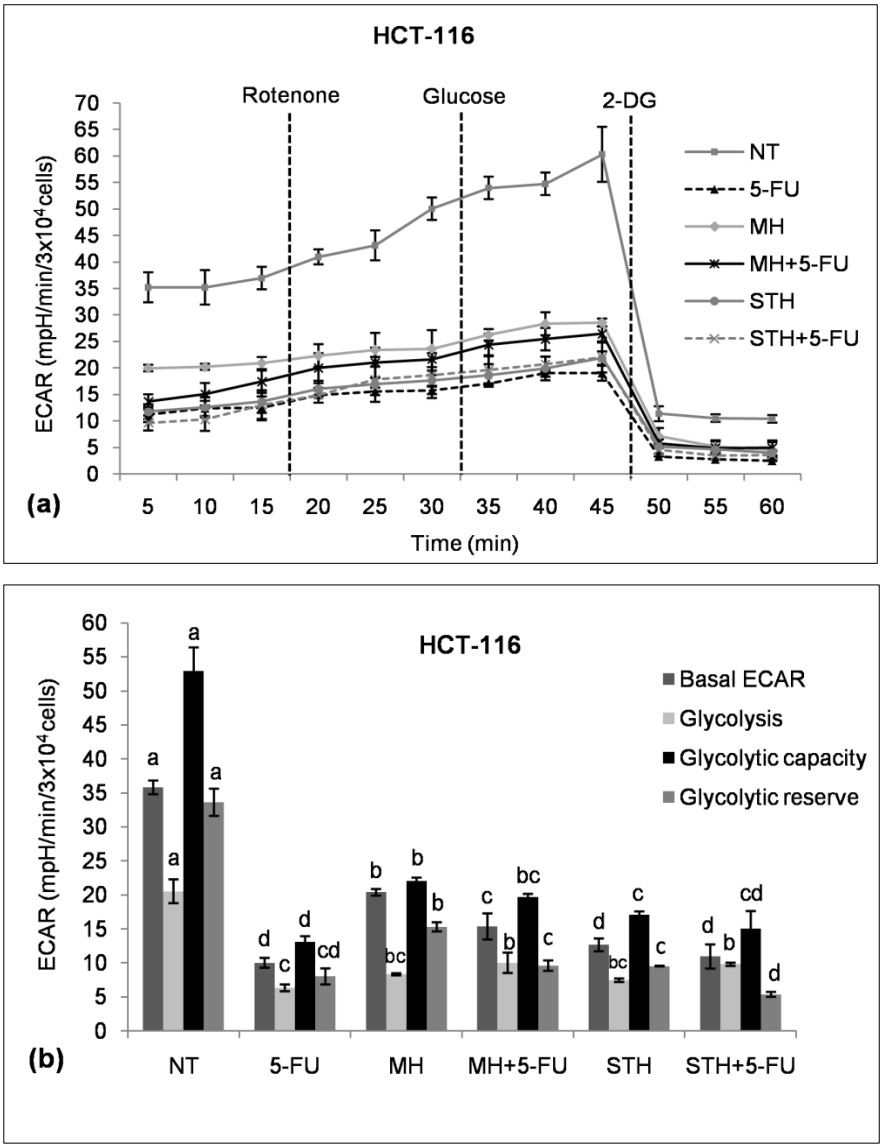

Figure 3.62. Regulation of glycolytic function by 5-FU and/or MH and STH in HCT-116 cells. After 24 h incubation, HCT-116 cells were exposed to IC_{50} doses of 5-FU, MH, STH, MH+5-FU and STH+5-FU for 48 h. The NT corresponds to not treatment. ECAR was determined by using the Seahorse XF-24 Extracellular Flux Analyzer after the following sequential injections: rotenone (1 μM), glucose (30 mM), and 2-DG (100 mM). From the XF glycolysis stress test profile (a) basal ECAR, glycolysis, glycolytic capacity and glycolytic reserves (b) were calculated. All data shown were the mean ± SD of three independent experiments. Different superscripts letter for each column indicated significant differences ($p < 0.05$).

In LoVo cells, the combination of MH+5-FU and STH+5-FU exerted similarly or more efficient effects compared to 5-FU alone (Figure 3.63). The basal ECAR was 8.53 ± 0.32 mpH/ min per 3×10^4 after 5-FU, while after the treatment with MH and STH it was 10.86 ± 0.77and 14.21 ± 0.82 mpH/ min per 3×10^4, respectively compared to control (Figure 3.63). The effect of combination treatment was 7.02 ± 0.67 mpH/ min per 3×10^4 after MH+5-FU and 5.03 ± 0.49 mpH/ min per 3×10^4 after STH+5-FU treatment (Figure 3.63).

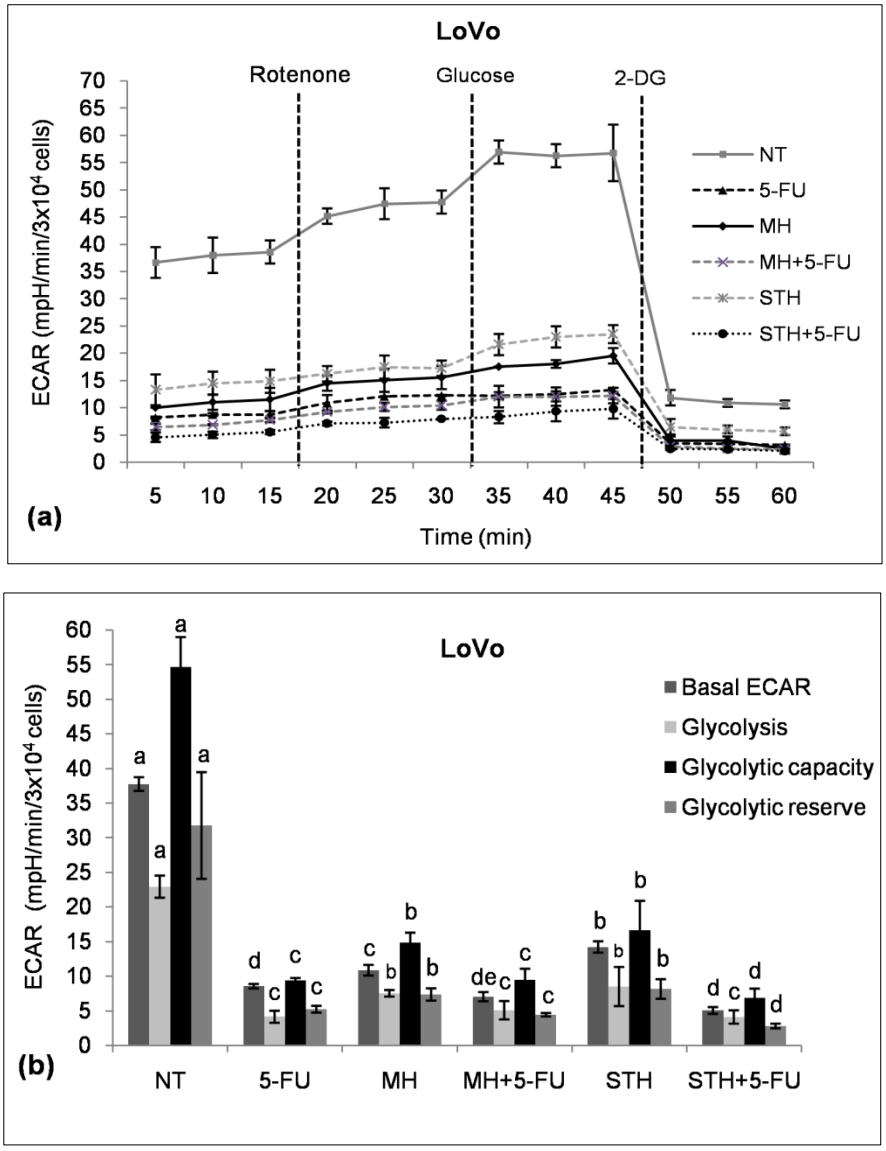

Figure 3.63. Regulation of glycolysis by 5-FU and/or MH and STH in LoVo cells. After 24 h incubation, LoVo cells were exposed to IC_{50} doses of 5-FU, MH, STH, MH+5-FU and STH+5-FU for 48 h. The NT corresponds to not treatment. ECAR was determined by using the Seahorse XF-24 Extracellular Flux Analyzer after the following sequential injections: rotenone (1 μM), glucose (30 mM), and 2-DG (100 mM). From the XF glycolysis stress test profile (a) basal ECAR, glycolysis, glycolytic capacity and glycolytic reserves (b) were calculated. All data shown were the mean ± SD of three independent experiments. Different superscripts letter for each column indicated significant differences ($p < 0.05$).

Moreover, the activity of glycolysis was reduced to 4.12 ± 0.87 mpH/ min per 3×10^4 after 5-FU, 7.51 ± 0.47 mpH/ min per 3×10^4 after MH and 8.49 ± 2.83 mpH/ min per 3×10^4 after STH treatments, while the combination treatment of MH+5-FU and STH+5-FU reduced it to 5.06 ± 1.33 and 4.09 ± 0.96 mpH/ min per 3×10^4 (Figure 3.63).

Finally, the glycolytic capacity and glycolytic reserve were decreased to 9.34 ± 0.38 and 5.23 ± 0.49 mpH/ min per 3×10^4 after 5-FU,14.86 ± 1.41and 7.36 ± 0.89 mpH/ min per

3×10^4 after MH and 16.63 ± 4.24 and 8.14 ± 1.41 mpH/ min per 3×10^4 after STH treatment (Figure 3.63), compared to the control. Furthermore, in the presence of MH and STH, 5-FU decreased the activity up to 9.48 ± 1.58 and 4.48 ± 0.25 mpH/ min per 3×10^4, and 6.88 ± 1.30 and 2.79 ± 0.34 / min per 3×10^4, correspondingly compared to control (Figure 3.63).

3.3.8.3. Effect of 5-FU in a combination of MH and STH on AMPK signaling pathway on HCT-116 and LoVo cells

We also assesed the role of 5-FU alone and in combination with MH or STH on AMPK signaling on HCT-116 and LoVo cells. As shown in Figure 3.64, the expression of p-AMPK/AMPK was decreased 0.65 fold after 5-FU treatment, 0.33 fold after MH treatment and 0.51 fold after STH treatment, respectively in HCT-116 cells, while both combination induced largest decreased 0.44 fold and 0.27 fold compared to control. Subsequently, the expression of PGC1α and SIRT1 also decreased by 5-FU (0.41 fold and 0.36 fold), MH (0.39 fold and 0.41 fold) and STH (0.49 fold and 0.46 fold) treatments, while the combination treatment of MH+5-FU (0.49 fold and 0.39 fold) was slightly less effective and STH+5-FU (0.39 fold and 0.30 fold) was more effective compared compared to 5-FU alone (Figure 3.64).

On the other hand, in LoVo cells the 5-FU treatment alone was less effective compared to MH+5-FU and STH+5-FU (Figure 3.65). The expressions of p-AMPK/AMPK, PGC1α and SIRT1 were 0.62 fold, 0.73 fold and 0.70 fold after 5-FU treatment, 0.64 fold, 0.59 fold and 0.63 fold after MH treatment and 0.75 fold, 0.56 fold and 0.64 fold after STH treatment. While after the treatment of MH+5-FU the expression was 0.61 fold, 0.47 fold and 0.55 fold and STH+5-FU the expression was 0.71 fold, 0.41 fold and 0.65 fold, respectively (Figure 3.65).

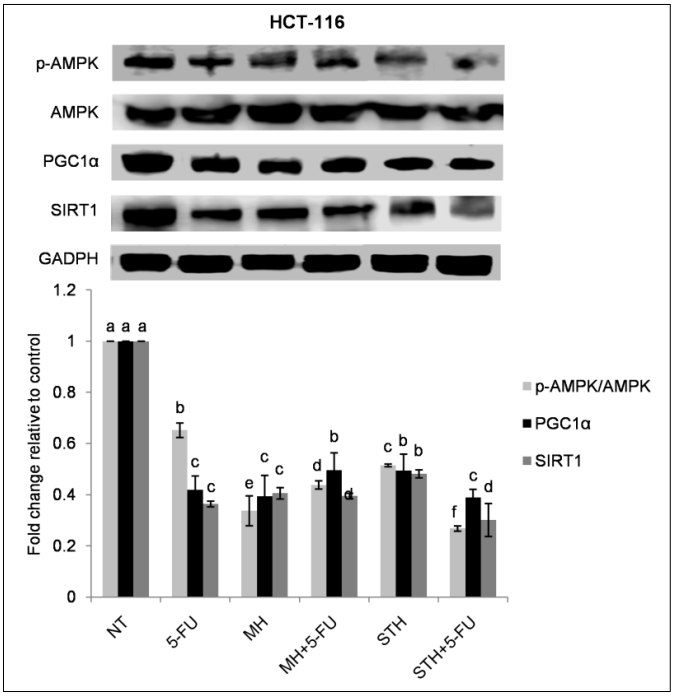

Figure 3.64. Effect of 5-FU and/or MH and STH on AMPK pathway in HCT-116 cells. After 24 h incubation, HCT-116 cells were exposed to IC_{50} doses of 5-FU, MH, STH, MH+5-FU and STH+5-FU for 48 h. The NT corresponds to not treatment.The protein expressions of p-AMPK, AMPK, PGC1α and SIRT1 were determined by western blotting analysis. GADPH was used as a loading control. All data shown were the mean ± SD of three independent experiments. Different superscripts letter for each column indicated significant differences ($p < 0.05$).

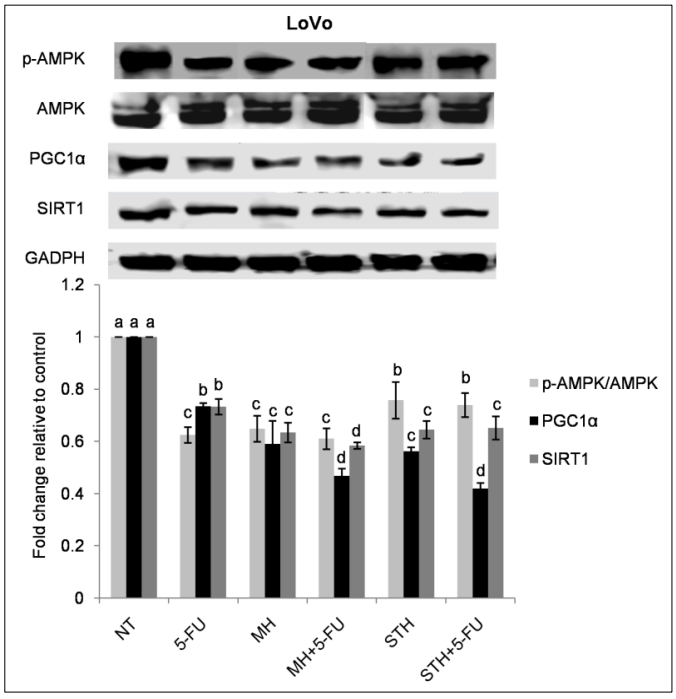

Figure 3.65. Effect of 5-FU and/or MH and STH on AMPK pathway in LoVo cells. After 24 h incubation, LoVo cells were exposed to IC_{50} doses of 5-FU, MH, STH, MH+5-FU and STH+5-FU for 48 h. The NT corresponds to not treatment. The protein expressions of p-AMPK, AMPK, PGC1α and SIRT1 were determined by western blotting analysis. GADPH was used as a loading control. All data shown were the mean ± SD of three independent experiments. Different superscripts letter for each column indicated significant differences ($p < 0.05$).

3.2.9. Effect of MH and STH on metastasis activity on HCT-116 and LoVo cells

3.2.9.1. Effect of MH and STH on the migration and invasion ability of HCT-116 and Lovo cells

The migration ability of HCT-116 and LoVo cells was observed after 5-FU and MH+5-FU or STH+5-FU treatments. The migration ability of HCT-116 cells decreased up to 60% after 5-FU treatment, 70% after MH treatment and 44% after STH treatment; in the presence of MH and STH the inhibitory activity of 5-FU increased up to 64% and 69% compared to control 16% (Figure 3.66).

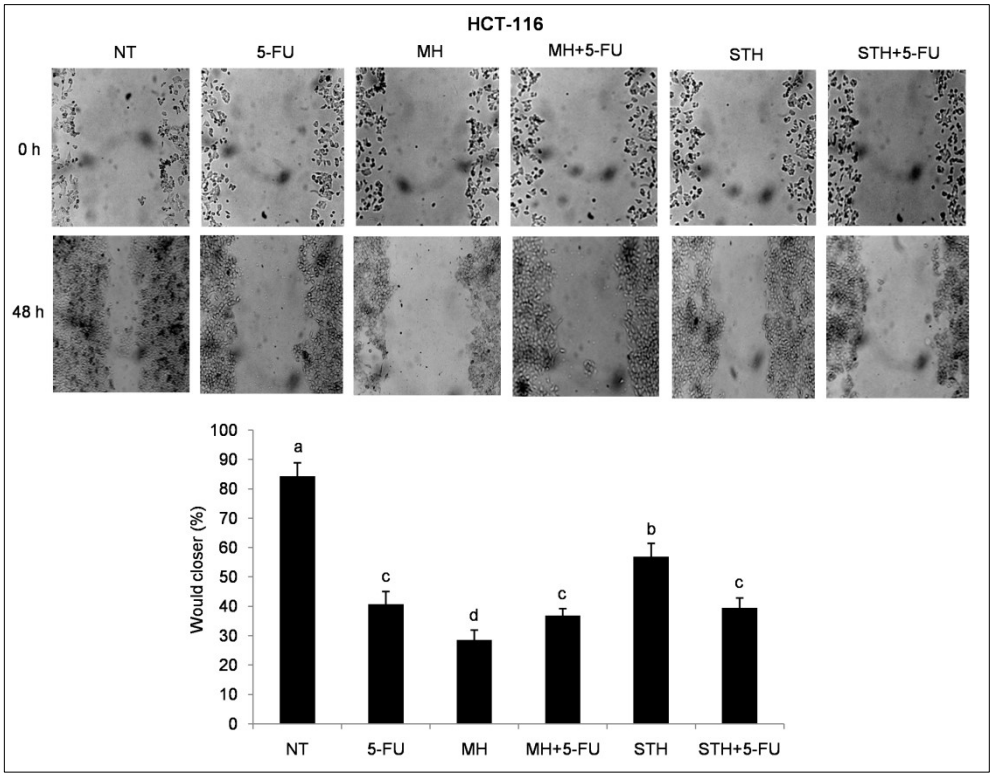

Figure 3.66. Effect of 5-FU and/or MH and STH on migration ability of HCT-116 cells by wound healing assay. After 24 h incubation, HCT-116 cells were exposed to IC_{50} doses of 5-FU, MH, STH, MH+5-FU and STH+5-FU for 48 h. The NT corresponds to not treatment. The wound closure percentages were analyzed by Image J software. All data shown were the mean ± SD of three independent experiments. Different superscripts letter for each column indicated significant differences ($p < 0.05$).

Similarly, in LoVo cells the exposure to 5-FU inhibited the migration ability 57% and similarly MH and STH inhibited the migration 51% and 60% compared to control 18% (Figure 3.67). Interestingly, both combination inhibited the migration ability up to 68% (Figure 3.67).

All these results suggested that the migration ability of 5-FU enhanced when it used with MH and STH in both cell lines.

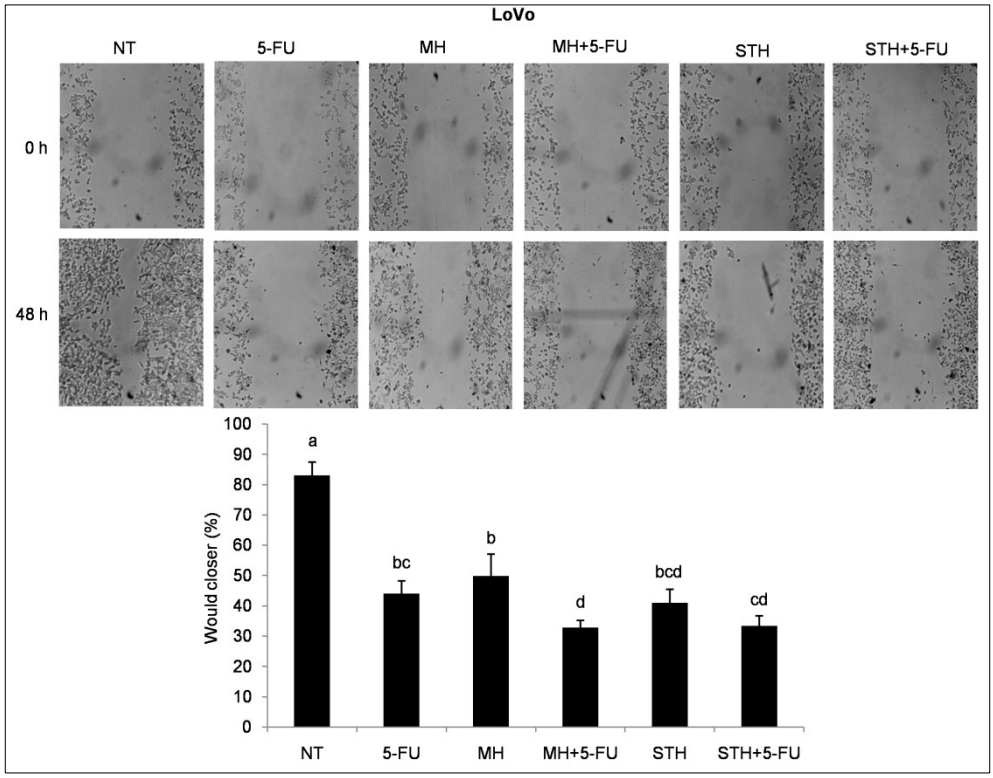

Figure 3.67. Effect of 5-FU and/or MH and STH on migration ability of LoVo cells by wound healing assay. After 24 h incubation, LoVo cells were exposed to IC_{50} doses of 5-FU, MH, STH, MH+5-FU and STH+5-FU for 48 h.The NT corresponds to not treatment. The wound closure percentages were analyzed by Image J software. All data shown were the mean ± SD of three independent experiments. Different superscripts letter for each column indicated significant differences ($p < 0.05$).

The invasion ability after 5-FU and MH+5-FU or STH+5-FU treatment was observed by the expression of MMP-2 and MMP-9 proteins in both CRC cell lines. In HCT-116 cells, the expression of MMP-2 and MMP-9 was 0.48 fold and 0.50 fold after 5-FU treatment, 0.69 fold and 0.49 fold after MH treatment and 0.70 fold and 0.54 fold after STH treatment, compared to control (Figure 3.68a). Both proteins decreased up to 0.40 fold and 0.38 fold after the treatment of MH+5-FU and 0.35 fold and 0.50 fold after STH+5-FU treatment, respectively (Figure 3.68a). A similar trend was also observed in LoVo cells (Figure 3.68b). The MMP-2 and MMP-9 expression was decreased 0.45 fold and 0.42 fold after exposure to 5-FU, 0.50 fold and 0.52 fold after exposure to MH and 0.51 fold and 0.57 fold after exposure to STH. At the same time, 5-FU decreased the expression of

MMP-2 and MMP-9 up to 0.31 fold and 0.25 fold in the presence of MH and 0.26 fold and 0.46 fold in the presence of STH, respectively (Figure 3.68b).

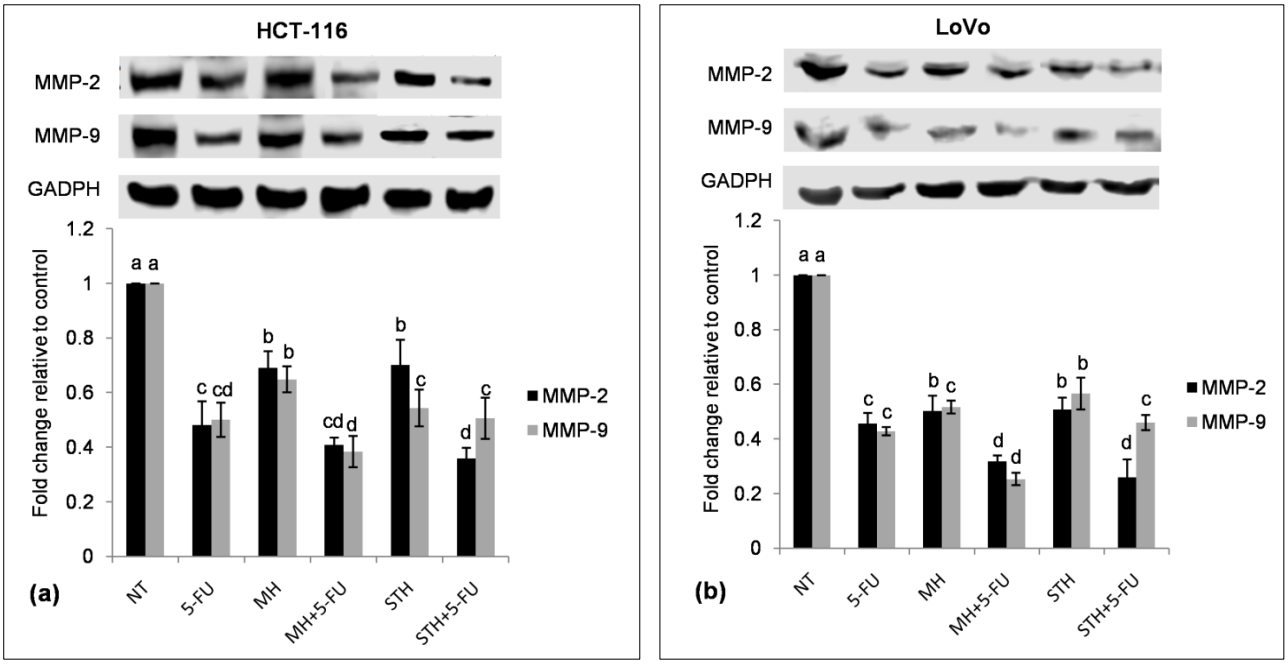

Figure 3.68. Effect of 5-FU and/or MH and STH on the expression of MMP-2 and MMP-9. After 24 h incubation, HCT-116 (a) and LoVo (b) cells were exposed to IC_{50} doses of 5-FU, MH, STH, MH+5-FU and STH+5-FU for 48 h. The NT corresponds to not treatment. The protein expressions of MMP-2 and MMP-9 were determined by western blotting analysis. GADPH was used as a loading control. All data shown were the mean ± SD of three independent experiments. Different superscripts letter for each column indicated significant differences ($p < 0.05$).

3.2.9.2. Effect of 5-FU in a combination of MH and STH on the colony formation of HCT-116 and LoVo cells

A colonogenic assay was used to evaluate the effect of 5-FU alone or combining with MH and STH in HCT-116 and LoVo cells. In HCT-116 cells, chronic exposure to 5-FU, MH and STH significantly decreased colony formation up to 82%, 52% and 60% compared with control (10%) (Figure 3.69a). In addition of MH and STH with less concentration of 5-FU, the colony formation decreased up to 72% and 78%, respectively (Figure 3.69a).

Furthermore, in LoVo cells, chronic exposure to 5-FU, MH and STH significantly decreased colony formation up to 80%, 62% and 65% compared with control (10%) (Figure 3.69b). In addition of MH and STH with less concentration of 5-FU, the colony formation was decreased up to 83% and 75%, respectively (Figure 3.69b).

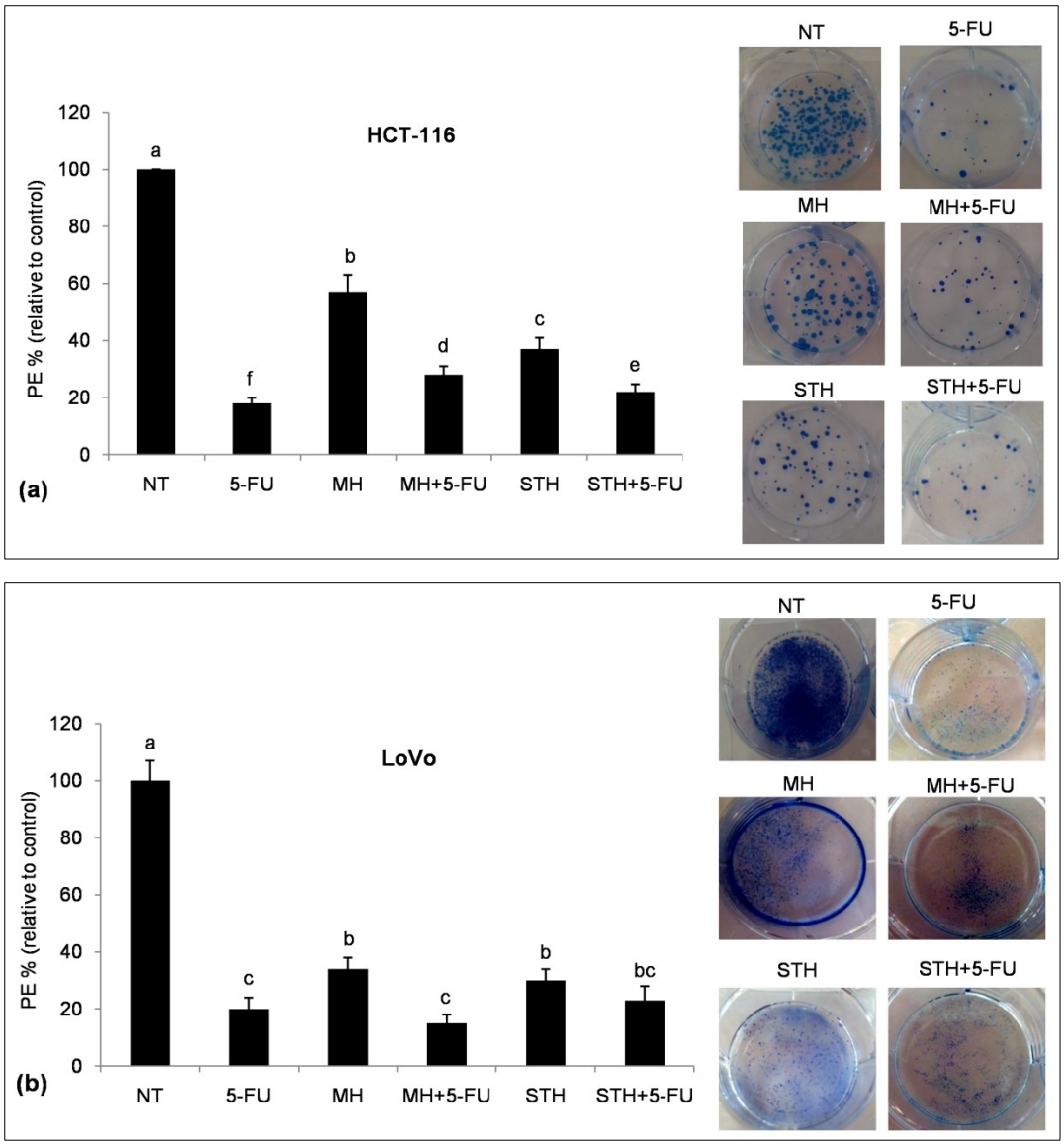

Figure 3.69. Effects of 5-FU and/or MH and STH in HCT-116 (a) and LoVo (b) cells colony formation. Representative images of the colony wells. Cells were seeded at low density in McCoy's 5A and F-12K media supplement with IC_{50} doses of 5-FU, MH, STH, MH+5-FU and STH+5-FU for 12 days. The NT corresponds to not treatment. The colonies were subsequently fixed with 70% ethanol and stained with methylene blue for analysis of colony formation. Quantitative image analysis of colonies in cultured HCT-116 cells. All data shown were the mean ± SD of three independent experiments. Different superscripts letter for each column indicated significant differences ($p < 0.05$).

3.2.9.3. Effect of MH and STH on the expressions of EMT-related genes in HCT-116 and LoVo cells

The expression of EMT related markers of E-cadherin, N-cadherin and β-catenin was evaluated in colon cancer HCT-116 and LoVo cells after the treatment with 5-FU and MH+5-FU or STH+5-FU. In HCT-116 cells, E-cadherin levels were increased up to 1.70 fold after the treatment of 5-FU, up to 1.64 fold after the treatment of MH and up to 1.57 fold after the treatment of STH, respectively compared to control (Figure 3.70). The expression of the same proteins was increased up to 1.87 fold and 2.00 fold, when it combined with MH and STH (Figure 3.70). Furthermore, N-cadherin and β-catenin were suppressed 0.62 fold and 0.34 fold after the treatment of 5-FU, 0.72 fold and 0.50 fold after the treatment of MH and 0.50 fold and 0.58 fold after the treatment of STH, correspondingly (Figure 3.70). Moreover, when 5-FU was combined with MH and STH the expression was almost similar like 5-FU (Figure 3.70).

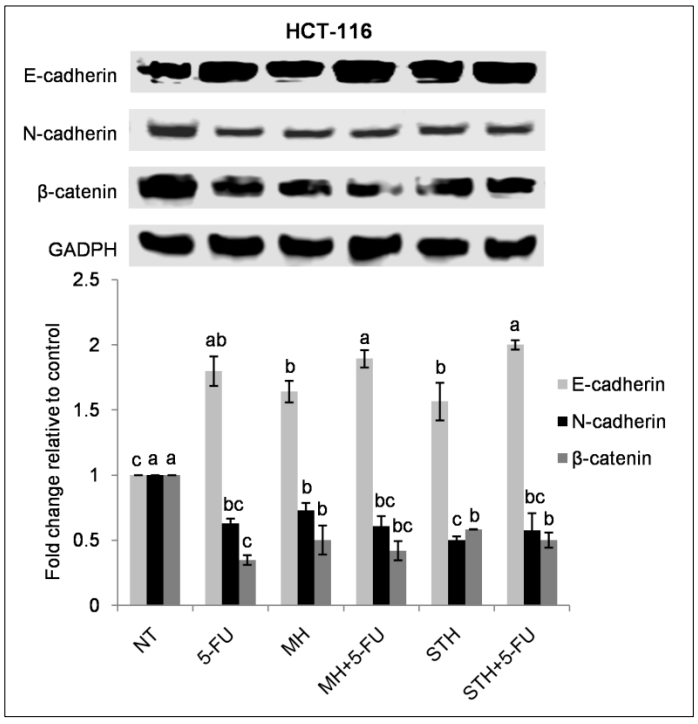

Figure 3.70. Effect of 5-FU and/or MH and STH on the EMT related gene. After 24 h incubation, HCT-116 cells were exposed toIC_{50} doses of 5-FU, MH, STH, MH+5-FU and STH+5-FU for 48 h. The NT corresponds to not treatment. The protein expressions of E-cadherin, N-cadherin and β-catenin were determined by western blotting analysis. GADPH was used as a loading control. All data shown were the mean ± SD of three independent experiments. Different superscripts letter for each column indicated significant differences ($p < 0.05$).

In LoVo cells, 5-FU elevated the levels of E-cadherin 2.18 fold, while MH and STH elevated up to 1.83 fold and 2.00 fold, respectively compared to control (Figure 3.71). The combination treatment of MH+5-FU elevated the levels 2.28 fold and STH+5-FU elevated 2.02 fold (Figure 3.71). The expression levels of N-cadherin and β-catenin were reduced 0.52 fold and 0.38 fold after 5-FU treatment, 0.45 fold and 0.51 fold after MH treatment and 0.46 fold and 0.40 fold after STH treatment. Moreover, when 5-FU combined with MH and STH, the expression of N-cadherin was decreased 0.48 fold and 0.38 fold and the expression of β-catenin was decreased 0.38 fold and 0.42 fold, correspondingly compared to control (Figure 3.71).

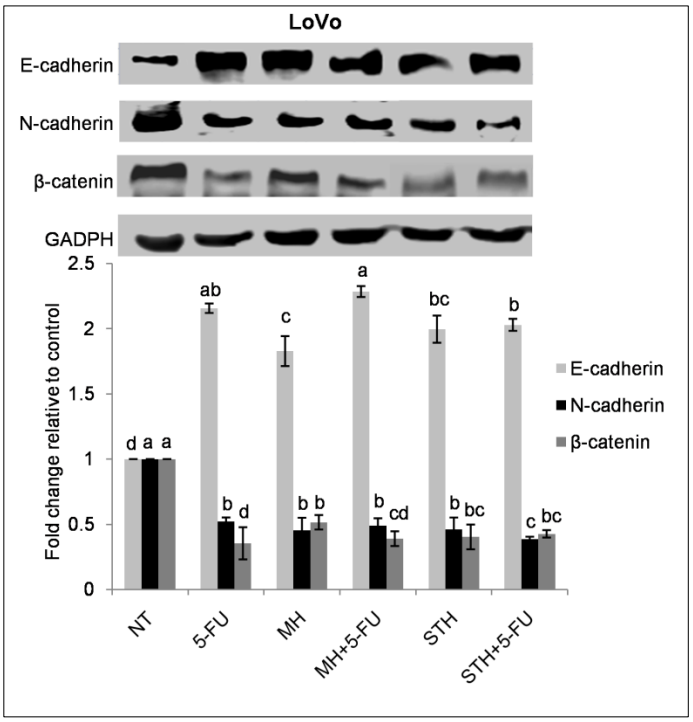

Figure 3.71. Effect of 5-FU and/or MH and STH on the EMT related gene. After 24 h incubation, LoVo cells were exposed toIC_{50} doses of 5-FU, MH, STH, MH+5-FU and STH+5-FU for 48 h. The NT corresponds to not treatment. The protein expressions of E-cadherin, N-cadherin and β-catenin were determined by western blotting analysis. GADPH was used as a loading control. All data shown were the mean ± SD of three independent experiments. Different superscripts letter for each column indicated significant differences ($p < 0.05$).

3.2.9.4. Effect of MH and STH on the metastasis promoting factor expression CXCR4 and NFκB in Lovo cells

The expression of tumor metastasis promoting factor CXCR4 and NFκB was examined in the presence of 5-FU and MH+5-FU or STH+5-FU on metastatic colon cancer LoVo cells. As shown in Figure 3.72, the expression of both proteins significantly was decreased ($p < 0.05$) 0.35 fold and 0.62 fold after 5-FU treatment, 0.55 fold and 0.60 fold after MH treatment and 0.58 fold and 0.63 fold after STH treatment compared to control. Moreover, in the presence of MH, 5-FU reduced the expression of CXCR4 0.36 fold and NFκB 0.50 fold. Similarly, in the presence of STH, 5-FU decreased the expression of both proteins 0.52 fold and 0.58 fold (Figure 3.72). Taken together, in metastatic LoVo cells, the effect of 5-FU was enhanced more in the presence of MH compared to STH.

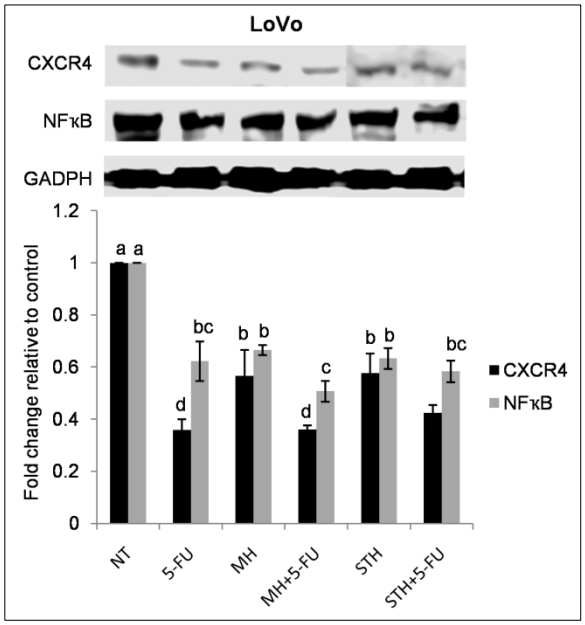

Figure 3.72. Effect of 5-FU and/or MH and STH on the expression of tumor metastasis promoting factor CXCR4 and NFκB on metastasis colon cancer LoVo cells. After 24 h incubation, LoVo cells were exposed to IC_{50} doses of 5-FU, MH, STH, MH+5-FU and STH+5-FU for 48 h. The NT corresponds to not treatment. The protein expressions of CXCR4 and NFκB were determined by western blotting analysis. GADPH was used as a loading control. All data shown were the mean ± SD of three independent experiments. Different superscripts letter for each column indicated significant differences ($p < 0.05$).

DISCUSSION: PART III

The last aim of my PhD project was to evaluate the contribution of honey as an adjunct to chemotherapeutic drugs. To the best of our knowledge, this is the first report to demonstrate the chemopreventive effects against colon cancer HCT-116 and LoVo cells by using the combination of MH and STH with 5-FU at IC_{50} doses for all the treatments.

Chemotherapy extends the overall survival rate in CRC patients. From the last four decades, 5-FU stands as the first choice for treatment of CRC but unfortunately only 10 to 15% CRC patients respond to this monotherapy drug, while the response rates enhances 50% when it combined with other anticancer agents (González-Vallinas et al., 2013b). Therefore, the development of new approaches to increase the effectiveness of 5-FU combining with other polyphenol or polyphenol containing foods is vitally required to overcome the cancer cell resistance and reduce the severity of adverse toxicity. In the second part of my results, we evaluated the preventive effects of MH and STH in colon adenocarcinoma (HCT-116) and metastatic (LoVo) cell line by focusing different molecular targets. In this part, we observed that honey potentiates the anticancer effects of 5-FU chemotherapy on human colon cancer cells.

A few numbers of investigations have demonstrated that honey increases the anti-cancer effects of chemotherapy and reduces the cytotoxic side effects in several in *in vit*ro and *in vivo* cancer model. In a rat model of melanoma cancer, MH decreased the toxic effects of paclitaxel and increased the anti-tumor activity of the drug (Fernandez-Cabezudo et al., 2013). In colon cancer HCT-116 cells, 5-FU treatment inhibited the cellular proliferation, but the inhibitory effects are significantly increased even at lower concentration of 5-FU when it combined with Gelam honey (Hakim et al., 2013). In another one, Tualang honey increased the anticancer activity of Tamoxifen drug in a breast cancer MCF-7 cells at less concentration and additionally it protected the healthy cells from the toxic effects of the drug (Yaacob et al., 2013). In our present work, in HCT-116 cells, the IC_{50} value of 5-FU alone was 20 µM (Figure 3.40) but when it was combined with MH (10 mg/mL) and STH (5 mg/mL,) the IC_{50} value of 5-FU was 10 µM. So at 2 fold lower concentration we observed the similar effects (Figure 3.41 and Figure 3.42). In the case of LoVo cells, the IC_{50} value of 5-FU alone was 50 µM (Figure 3.40) but when it combined with MH (20 mg/mL) and STH (10 mg/mL) the IC_{50} value of 5-FU was 20 µM (Figure 3.41 and Figure 3.42). In both cell lines we needed less concentration of STH compared to MH for potentiates the 5-FU effects.

Previous studies reported that the arresting ability of 5-FU increased on cancer cell cycle when it was combined with other natural compounds at very low concentration (González-Sarrías et al., 2015). In colon cancer Caco-2, HT-29 and SW-480 cells, urolithin A increased the treatment efficacy of 5-FU in a dose dependent manner and the combination treatment arrested the cell cycle at S and G_2/M phase with slightly increased apoptotic effects (González-Sarrías et al., 2015). Furthermore, the combination of curcumin and 5-FU arrested the cell cycle at S phase and increased apoptosis in CRC cells compared to treatment with the single agents (Shakibaei et al., 2015). In agreement with previous studies, we also observed similar effects in our present works. Cell cycle analysis of HCT-116 cells showed that 5-FU treatment arrested the cell cycle at S-phase and induced apoptosis by increasing the cells at the Sub-G_1 phase and at the same time it decreased the cell at G_0/G_1 and G_2/M phase (Figure 3.43). The combination data indicated that the MH+5-FU induced almost similar effects like 5-FU alone and STH+5-FU induced few less effects compared to 5-FU at IC_{50} doses (Figure 3.43). The increasing amount of cells at Sub-G_1 phase was similar after all the treatments and both combinations decreased more amount of cells at G_2/M phase compared to 5-FU alone (Figure 3.43). Furthermore, in LoVo cells, 5-FU arrested the cell cycle at G_2/M phase, while the combination treatment also induced similar effects like 5-FU (Figure 3.43). Both combinations decreased more amounts of cells at G_0/G_1 phase compared to 5-FU alone but a number of cells at Sub-G_1 phase was more in 5-FU compared to the combination. It suggested that the when 5-FU was combined with MH and STH it induced similar effect at a lower concentration of 5-FU IC_{50}.

Furthermore, we observed the apoptotic effect of 5-FU alone or in co-treatment with MH and STH in both cell lines. According to the flow cytometry analysis, 5-FU treatment significantly increased the apoptotic effect in HCT-116 and LoVo cells but the combination with MH and STH was less effective compared to 5-FU alone (Figure 3.45 and Figure 3.46). These findings were similar of those presented in a previous report by Kao et al., who observed that ellagic acid synergistically enhanced the chemosensitivity of 5-FU by apoptosis induction in colon cancer HT-29, Colo 320DM and SW480 cells but not in LoVo cells (Kao et al., 2012). In another study, MH increased the number of caspase-3 positive cells in a tumor bearing mice after combining with paclitaxel (Fernandez-Cabezudo et al., 2013). The combination of curcumin with 5-FU also induced more apoptotic effects by increasing the expression of caspase-3, -8, -9, Bax and PARP

compared to a single agent in colon cancer HCT-116 cells (Shakibaei et al., 2013). Additionally, quercetin increased 5-FU induced apoptotic effects by increasing the expression of caspase-3, -9, c-PARP and p53 in microsatellite instability CRC cells (Xavier et al., 2011). In our work, we observed that in HCT-116 cells, the effect of 5-FU and MH+5-FU was almost similar for the p53 and caspase-3 expression but less effect was observed when it combined with STH+5-FU (Figure 3.45). In LoVo cells, p53 and caspase-3 expressed more after 5-FU treatment compared to the combination treatment but the expression of caspase-3 was similar after the treatment of 5-FU and MH+5-FU and it was less effective after STH+5-FU treatment (Figure 3.46).

The anti-inflammatory effects of 5-FU significantly ($p < 0.05$) increased when it was combined with MH and STH (Figure 3.48). In HCT-116 cells, 5-FU treatment suppressed the expression of NFκB, IL-6, iNOS and TNF-α, while the combination of MH+5-FU and STH+5-FU was most effective compared to 5-FU alone (Figure 3.48). In a previous report, oral administration of crude honey decreased the cytotoxicity of chemotherapeutic drug cisplatin by suppression of NFκB activation (Hamad et al., 2015). Furthermore, curcumin enhanced the 5-FU chemotherapic activity, by inhibiting the expression NFκB in a chemoresistance CRC cells (Shakibaei et al., 2015).

It has previously been reported that chemotherapeutic drug induced DNA damage causes apoptosis activating the MAPK pathway (Bragado et al., 2007). Similarly, in our present work, we also observed that the 5-FU induced p-p38MAPK and p-Erk1/2 activation for inducing apoptosis (Figure 3.49). Subsequently, we observed the combination effect of MH+5-FU and STH+5-FU on p-p38MAPK and p-Erk1/2 pathways in HCT-116 and LoVo cells. We observed that the both combination was slightly less effective in inducing the expression of p-p38MAPK, but the expression of p-Erk/12 was most effective compared to 5-FU alone in HCT-116 cells (Figure 3.49a). Furthermore, in LoVo cells, the combination of STH+5-FU was most effective for increasing the expression of p-p38MAPK and p-Erk1/2 compared to 5-FU alone or MH+5-FU treatments (Figure 3.49b). Mohapatra et al. explained that the combination of resveratrol and 5-RU induced apoptosis through activating p-p38MAPK and p-JNK and the expression of p-Erk1/2 was unchanged in human colon cancer HCT-116 cells (Mohapatra et al., 2011). Furthermore, green tea polyphenols dramatically increased the expression of p-p38MAPK and p-Erk1/2 in lung cancer cells when they were added together with celecoxib (Suganuma et al., 2006). In another study, the combination of two plants derived drugs triptolide and

hydroxycamptothecin enhanced the expression of p-p38MAPK and p-Erk1/2 for increasing apoptosis in lung adenocarcinoma cells (Meng et al., 2015).

Next, we observed the effect of 5-FU alone or combined with MH and STH in EGFR pathways. In both cell lines, the combination treatments suppressed more the expression of EGFR compared to 5-FU alone (Figure 3.50). Similarly, the expression of HER2 was more suppressed after STH+5-FU treatment compared to 5-FU or MH+5-FU in HCT-116 cells. In the case of LoVo cells, HER2 was suppressed more in both combinations compared to 5-FU alone (Figure 3.50). The expression of p-Akt was suppressed more or similarly in combination treatments in both cell lines compared to 5-FU alone (Figure 3.50). A similar effect was also observed when curcumin enhanced the treatment efficacy of the chemotherapeutic drug by suppressing the expression of p-EGFR, p-HER2, p-IGR-1R and p-Akt in colon cancer HCT-116 cells (Patel et al., 2010). Furthermore, the combination of green tea polyphenols and tamoxifen suppressed the expression of EGFR, p-EGFR and p-Akt expression both in *in vitro* and *in vivo* breast cancer model (Scandlyn et al., 2008).

In our present investigation, we also observed the oxidative stress inducing death of HCT-116 and LoVo cells in response to co-treatments of MH+5-FU and STH+5-FU. The intracellular ROS production was increased after 5-FU treatment in HCT-116 and LoVo cells (Figure 3.51 and Figure 3.52). Moreover, in the presence of MH and STH, ROS production was significantly increased compared to single dose of 5-FU in both cell lines (Figure 3.51 and Figure 3.52). Previous investigations by other researchers also confirmed that the natural compounds have the ability to enhance the ROS production ability of 5-FU compared to a single agent in different types of cancer cells including colon cancer (Kong et al., 2015; Li et al., 2014; Liu et al., 2016).

On the other hand, in order to confirm the oxidative stress induced cell death we also observed the effects of this combination treatment on the biomarkers of lipid, protein and DNA damage. In our results, we found that in HCT-116 cells, the TBARS levels and protein carbonyl content were increased after 5-FU treatment but in the presence of MH and STH similar effects like 5-FU alone were noted (Figure 3.53a). Furthermore, in LoVo cells, both combination enhanced the levels of TBARS and protein carbonyl content compared to 5-FU alone, in particular the STH+5-FU was most effective (Figure 3.53b). In the case of DNA damage, 5-FU and the combination treatments of STH+5-FU were most effective and induced similar effects, while MH+5-FU was less effective in both cell lines (Figure 3.54). Additionally, we observed the pro-oxidative effects of 5-FU in the presence

of MH and STH in HCT-116 and LoVo cells. The activities of antioxidant enzymes, such as GPx, GST, GR, SOD and catalase, distinctly decreased by the combination treatment compared to 5-FU alone in both cell lines (Figure 3.55 and Figure 3.56). These results provide the possibility that MH and STH inside the cells could cause accumulation of ROS, which oxidized intracellular antioxidant agents thus sensitizing the cancer cells to 5-FU provoked oxidative stress inducing cell death. In a previous report Fan et al. found that the selenium enhanced the 5-FU induced human melanoma cancer cell death by triggering oxidative stress through increasing ROS mediated DNA damage and inhibited antioxidant enzyme activities (Fan et al., 2013a).

There is an increasing amount of evidence in the literature that the upregulation of Nrf2 and HO-1 expression by epigenetic modification is associated with resistance of 5-FU in CRC (Kang et al., 2014; Kang et al., 2016; Zhao et al., 2015). In our present work, we evaluated the expression of Nrf2 and HO-1, in addition with SOD and catalase in HCT-116 and LoVo cells after the successive treatments. All the treatments suppressed the expression of all the enzymes, while the combination treatment was most effective compared to 5-FU alone in both cell lines (Figure 3.57 and Figure 3.58). The pro-oxidative effects of 5-FU was enhanced in the presence of MH and STH. Furthermore, some investigations observed the synergistic effects of the natural compound and chemotherapeutic drug in the Nrf2 pathway. For example, chrysin and apigenin enhanced the therapeutic efficacy of anticancer drug doxorubicin by suppressing the mRNA and protein levels of Nrf2 in hepatocellular carcinoma cells (Gao et al., 2013a; Gao et al., 2013b). Similarly, nobiletin increased the anticancer effects of several chemotherapeutic drugs through inhibiting the expression of Akt and Nrf2 in multidrug resistant ovarian cancer cells (Ma et al., 2015).

Additionally, we observed the combination treatments in ER stress related biomarkers of ATF6 and XBP1 expression in both CRC cell lines. In HCT-116 cells, both combinations increased the ATF6 and XBP1 expression similar like 5-FU alone at less concentration, but in LoVo cells the combination treatments were less effective compared to 5-FU alone (Figure 3.59). Up to date, there are no data on the ATF6 and XBP1 expression of the combination of honey or other bioactive compounds and chemotherapeutic drugs.

Recently, several evidence addressed that the dysregulated metabolism is associated with therapeutic resistance (Zhao et al., 2013), a vastly clinical applicable area in cancer metabolism research which has not been purposely addressed. To overcome the therapeutic

resistance and improve the therapeutic efficacy, it is an urgent need to use combination chemotherapeutic agents with targeted disruption of dysregulated cancer cell metabolism. Higher aerobic glycolysis was observed in drug resistant cancer cells to more quick ATP production to survive under stress condition (Zhou et al., 2012). 5-FU resistance colon cancer cells are able to survive due to make addiction of OXPHOS (Denise et al., 2015) and resistant cells maintain the SRC and MRC through upregulating the OXPHOS for using ATP under stress condition or enhanced energy demand for proliferation (Dranka et al., 2010; Hill et al., 2012).

To the best of our knowledge, this is the first time that the effects of 5-FU in the presence of MH and STH in colon cancer cell metabolism, targeting mitochondrial respiration and glycolysis function, were evaluated. All the parameters of mitochondrial respiration, such as basal OCR, ATP production, proton link, SRC and MRC were decreased after all the treatments; particularly, the combination of MH+5-FU and 5-FU induced almost similar effects and STH+5-FU was most effective in HCT-116 and LoVo cells (Figure 3.60 and Figure 3.61). Furthermore, we observed the ECAR values as an indicator of glycolysis, glycolytic capacity and glycolytic reserve. Here we also evaluated the same trends like OCR. In both cell lines, the combination of STH+5-FU was most effective treatment for reducing the glycolysis function compared to 5-FU and MH+5-FU (Figure 3.62 and Figure 3.63).

Based on the recent evidence, AMPK activation is required to improve cancer cell proliferation in metabolic stress microenvironment (Chaube et al., 2015; Jeon, 2016; Li et al., 2015), SIRT1-PGC1-α stimulate the mitochondrial biogenesis and OXPHOS, increase metastasis activity and correlate with chemoresistance in malignant cancer phenotype (LeBleu et al., 2014; Vellinga et al., 2015). In our works, we evaluated the effect of p-AMPK/AMPK, SITR1 and PGC1-α expression in colon cancer HCT-116 and LoVo cells after the treatment with 5-FU and MH+5-FU or STH+5-FU. In HCT-116 cells, both combinations decreased the expression of p-AMPK/AMPK and SIRT1 compared to 5-FU alone; the STH+5-FU was most effective (Figure 3.64). Moreover, the expression of PGC1-α was decreased after all the treatments but 5-FU and STH+5-FU induced similar effects, while MH+5-FU were less effective (Figure 3.64). In the case of LoVo cells, the expression of p-AMPK/AMPK was suppressed after all the treatments, while 5-FU and MH+5-FU induced similar effects but STH+5-FU was less effective (Figure 3.65). The

expressions of PGC1-α and SIRT1 were also suppressed after all the treatments but both combination treatments were most effective compared to 5-FU single dose (Figure 3.65).

The anti-metastatic effects of 5-FU in the combination with MH and STH were observed in HCT-116 and LoVo cells according to different aspects. The anti-migration effects of 5-FU increased when it was combined with MH and STH in both cell lines (Figure 3.66 and Figure 3.67) at a lower concentration of 5-FU. Similar effects were observed by other natural compounds when they were combined with 5-FU in colon cancer HCT-116 cells (Mohapatra et al., 2011; Shakibaei et al., 2015). Additionally, the expression of MMP-2 and MMP-9 was suppressed more in both cell lines after MH+5-FU treatments compared to 5-FU alone (Figure 3.68). In the case of STH+5-FU treatments, the expression of MMP-2 was more suppressed compared to 5-FU and MMP-9 was suppressed similarly like 5-FU (Figure 3.68). To date, only one study explains that the curcumin potentiates 5-FU to inhibit the expression of MMP-9 in colon cancer HCT-116 cells (Shakibaei et al., 2015).

Furthermore, most of the natural compounds increased the colony inhibiting ability of the chemotherapeutic drug compared to a single dose in the different types of *in vitro* cancer model (He et al., 2017; Nagaraju et al., 2014; Shakibaei et al., 2015). However, in our results, we observed that the combination treatment was slightly less effective compared to 5-FU treatment for reducing the HCT-116 cells colony formation ability at IC_{50} doses for all the treatments (Figure 3.69a). Interestingly, in our previous chapter, we observed that at the highest concentration of MH and STH alone reduced the colony formation ability similarly or slightly more compared to 5-FU treatment alone (Figure 3.12). Moreover, in LoVo cells the combination treatment was more effective compared to 5-FU treatment for reducing the LoVo cells colony formation ability at IC_{50} doses for all the treatments (Figure 3.69b).

The expression of EMT related markers, E-cadherin, N-cadherin and β-catenin were also modulated after the combination treatment of MH+5-FU and STH+5-FU in both cell lines (Figure 3.70 and Figure 3.71). The expression of E-cadherin was significantly ($p < 0.05$) increased after the combination treatments in both cell lines (Figure 3.70 and Figure 3.71). A similar effect was also observed in HCT-116 cells by the co-treatment of curcumin and 5-FU by Buhrmann et al. (Buhrmann et al., 2014). Additionally, we also observed the expression of N-cadherin and β-catenin after the similar treatments. In HCT-116 cells, we observed similar effects after all the treatments for N-cadherin expression (Figure 3.70) while in LoVo cells; the expression of N-cadherin was most effective compared to 5-FU

and MH+5-FU (Figure 3.71). The expression of β-catenin was less effective in the combination treatment compared to 5-FU in both cell lines (Figure 3.70 and Figure 3.71).

Finally, we observed the expression of tumor metastasis promoting factor CXCR4 and NFκB in LoVo cells. The expression of CXCR4 was similar after 5-FU and MH+5-FU treatment, while the STH+5-FU was slightly less effective. The expression of NFκB was suppressed more after the both combination treatment compared to 5-FU alone (Figure 3.72). Shakibaei et al. also examined the effects of curcumin and 5-FU in a metastatic and chemoresistance colon cancer cells (Shakibaei et al., 2015). The group evaluated that the combination treatments suppressed the expression of CXCR4, MMP-9 and NFκB more effectively than a single 5-FU (Shakibaei et al., 2015).

CONCLUSIONS

Based on the results obtained in the evaluation of the anticancer potential of MH and STH on *in vitro* colon cancer models, the following conclusions can be drawn:

1. Both varities of honey used in the present work possesed high content of total polyphenol, flavonoids and antioxidant capacity; the bioactive compounds of honey depend on its floral sources, geographical origins, seasonal and environmental factors which have a significant impact on the anti-proliferative potential.

2. Evidence indicated that MH and STH induced cytotoxic effects in HCT-116 and LoVo cells by suppressing inflammation through decreasing the expression of NFκB, p-IκBα and inflammatory cytokines, arresting cell cycle at S and G_2/M phase, activating apoptosis through increasing the expression of p53, caspase-3 and c-PARP and inducing oxidative stress by generating ROS, reducing antioxidant enzyme activity and inducing DNA, protein and lipid damage. In addition, exposure to both kinds of honey increased ER stress associated HCT-116 and LoVo cells death by elevating ATF6 and XBP1 expression. Similarly, the expression of p-p38MAPK and p-Erk1/2 pathway was increased while the EGFR, HER2 and p-Akt pathway were decreased after the treatment of MH and STH. Both honey varieties act as a regulator of energy metabolism of HCT-116 and LoVo cells both in anaerobic and aerobic pathways and indicate an alternative strategy for treatment of cancer. Interestingly, MH and STH can suppress the AMPK pathway which plays an important role in mitochondrial biogenesis in cancer cells to promote metabolism under glucose limiting condition. These findings provide fundamental insights into the molecular mechanism of MH and STH induced cell death. Both types of honey show good promise and merits to be further evaluated as a potential therapeutic agent for the treatment of human colon carcinoma.

3. This works also provides new evidence to support the anti-metastatic effect of MH and STH against adenocarcinoma and metastatic CRC cells. Our results show that both honeys inhibited the migration and colony formation ability, as well as suppressed invasion abilities, observed by decreasing MMP-2 and MMP-9 expression and regulating the expression of EMT-related genes, including E- cadherin, N-cadherin and β-catenin. Based on these results, we conclude that MH and STH may serve as an effective therapeutic agent for colorectal metastasis treatment.

4. The development of new approaches to increase the effectiveness of 5-fluorouracil combining with polyphenol containing foods is vitally required: (i) to increase the effectiveness of conventional chemotherapy, (ii) to overcome the cancer cell resistance, and (iii) to reduce the severity of adverse toxicity. The anti-inflammation, anti-proliferation, apoptosis induction, and increased ROS production were significantly ($p < 0.05$) enhanced after co-treatment of 5-fluorouracil in the presence of MH or STH compared to single doses of 5-fluorouracil. Moreover, the anti-metastasis effects of 5-fluorouracil also increased when it was combined with MH and STH by decreasing the migration ability, as well as suppressing the expression of MMP-2, MMP-9, E-cadherin, NFκB and CXCR4 proteins.

These interesting and promising results encourage our knowledge about chemopreventive effects honey and could be useful for further studies to highlight the phenolic compounds of MH or STH and the possible molecular mechanisms as well as *in vivo* studies against colon cancer.

REFERENCE

Abreu MT. 2010. Toll-like receptor signalling in the intestinal epithelium: how bacterial recognition shapes intestinal function. *Nat. Rev. Immunol.* 10, 131.

Aebi H. 1984. Catalase in vitro. *Methods Enzymol.* 105, 121-126.

Afrin S, Forbes-Hernandez TY, Gasparrini M, Bompadre S, Quiles JL, Sanna G, Spano N, Giampieri F, and Battino M. 2017. Strawberry-tree honey induces growth inhibition of human colon cancer cells and increases ROS generation: a comparison with Manuka honey. *Int. J. Mol. Sci.* 18, 613.

Afrin S, Giampieri F, Gasparrini M, Forbes-Hernandez TY, Varela-López A, Quiles JL, Mezzetti B, and Battino M. 2016. Chemopreventive and therapeutic effects of edible berries: A focus on colon cancer prevention and treatment. *Molecules* 21, 169.

Afroz R, Tanvir EM, Karim N, Hossain MS, Alam N, Gan SH, and Khalil MI. 2016. Sundarban honey confers protection against isoproterenol-induced myocardial infarction in wistar rats. *BioMed Res. Int.* 2016, Article ID 6437641, 1-10.

Aggarwal BB. 2004. Nuclear factor-κB: the enemy within. *Cancer cell* 6, 203-208.

Ahmed AYBH, Wabaidur SM, Siddiqui MR, Alothman ZA, Obeid MS, Khan MR, and Al-tamrah SA. 2016. Simultaneous determination of twenty-five polyphenols in multifloral and cactus honeys using solid-phase extraction and high-performance liquid chromatography with photodiode array detection. *European Food Res. Technol.* 242, 943-952.

Ahmed FE, Ahmed NC, Vos PW, Bonnerup C, Atkins JN, Casey M, Nuovo GJ, Naziri W, Wiley JE, and Mota H. 2013. Diagnostic microRNA markers to screen for sporadic human colon cancer in stool: I. Proof of principle. *Cancer Genomics Proteomics* 10, 93-113.

Ahmed S, and Othman NH. 2013. Honey as a potential natural anticancer agent: a review of its mechanisms. *Evid. Based Complement. Alternat. Med.* 2013, 1-7.

Aliyu M, Odunola OA, Farooq AD, Mesaik AM, Choudhary MI, Fatima B, Qureshi TA, and Erukainure OL. 2012. Acacia honey modulates cell cycle progression, pro-inflammatory cytokines and calcium ions secretion in PC-3 cell line. *J. Cancer Sci. Ther.* 4, 401-407.

Alvarez-Suarez JM, Gasparrini M, Forbes-Hernández TY, Mazzoni L, and Giampieri F. 2014. The composition and biological activity of honey: A focus on Manuka honey. *Foods* 3, 420-432.

Alvarez-Suarez JM, Giampieri F, and Battino M. 2013. Honey as a source of dietary antioxidants: structures, bioavailability and evidence of protective effects against human chronic diseases. *Curr. Med. Chem.* 20, 621-638.

Alvarez-Suarez JM, Giampieri F, Cordero M, Gasparrini M, Forbes-Hernández TY, Mazzoni L, Afrin S, Beltrán-Ayala P, González-Paramás AM, and Santos-Buelga C. 2016. Activation of AMPK/Nrf2 signalling by Manuka honey protects human dermal fibroblasts against oxidative damage by improving antioxidant response and mitochondrial function promoting wound healing. *J. Funct. Foods* 25, 38-49.

Alvarez-Suarez JM, Tulipani S, Díaz D, Estevez Y, Romandini S, Giampieri F, Damiani E, Astolfi P, Bompadre S, and Battino M. 2010a. Antioxidant and antimicrobial capacity of several monofloral Cuban honeys and their correlation with color, polyphenol content and other chemical compounds. *Food Chem. Toxicol.* 48, 2490-2499.

Alvarez-Suarez JM, Tulipani S, Romandini S, Bertoli E, and Battino M. 2010b. Contribution of honey in nutrition and human health: a review. *Med. J. Nutrition. Metab.* 3, 15-23.

Alzahrani HA, Alsabehi R, Boukraâ L, Abdellah F, Bellik Y, and Bakhotmah BA. 2012. Antibacterial and antioxidant potency of floral honeys from different botanical and geographical origins. *Molecules* 17, 10540-10549.

Atrott J, and Henle T. 2009. Methylglyoxal in Manuka honey – correlation with antibacterial properties. *Czech J. Food Sci.* 27, S163-S165.

Badolato M, Carullo G, Cione E, Aiello F, and Caroleo MC. 2017. From the hive: Honey, a novel weapon against cancer. *European J. Med. Chem.* , Doi: https://doi.org/10.1016/j.ejmech.2017.07.064.

Batumalaie K, Zaman Safi S, Mohd Yusof K, Shah Ismail I, Devi Sekaran S, and Qvist R. 2013. Effect of gelam honey on the oxidative stress-induced signaling pathways in pancreatic hamster cells. *Int. J. Endocrinol.* 2013, 1-10.

Benzie IFF, and Strain JJ. 1996. The ferric reducing ability of plasma (FRAP) as a measure of "antioxidant power". *Anal. Biochem.* 239, 70-76.

Bhardwaj M, Kim N-H, Paul S, Jakhar R, Han J, and Kang SC. 2016. 5-Hydroxy-7-Methoxyflavone Triggers Mitochondrial-Associated Cell Death via Reactive

Oxygen Species Signaling in Human Colon Carcinoma Cells. *PloS one* 11, e0154525.

Bischofberger AS, Dart CM, Horadagoda N, Perkins NR, Jeffcott LB, Little CB, and Dart AJ. 2016. Effect of Manuka honey gel on the transforming growth factor β1 and β3 concentrations, bacterial counts and histomorphology of contaminated full-thickness skin wounds in equine distal limbs. *Aust. Vet. J.* 94, 27-34.

Bogdanov S, Jurendic T, Sieber R, and Gallmann P. 2008. Honey for nutrition and health: a review. *J. Am. Coll. Nutr.* 27, 677-689.

Boland CR, and Goel A. 2010. Microsatellite instability in colorectal cancer. *Gastroenterology* 138, 2073-2087. e3.

Bouzaiene NN, Jaziri SK, Kovacic H, Chekir-Ghedira L, Ghedira K, and Luis J. 2015. The effects of caffeic, coumaric and ferulic acids on proliferation, superoxide production, adhesion and migration of human tumor cells *in vitro*. *Eur. J. Pharmacol.* 766, 99-105.

Boyer B, and Thiery JP. 1993. Epithelium-mesenchyme interconversion as example of epithelial plasticity. *Apmis* 101, 257-268.

Boyle P, and Langman JS. 2000. ABC of colorectal cancer: Epidemiology. *BMJ* 321, 805.

Bradford MM. 1976. A rapid and sensitive method for the quantitation of microgram quantities of protein utilizing the principle of protein-dye binding. *Anal. Biochem.* 72, 248-254.

Bragado P, Armesilla A, Silva A, and Porras A. 2007. Apoptosis by cisplatin requires p53 mediated p38α MAPK activation through ROS generation. *Apoptosis* 12, 1733-1742.

Brunk UT, and Terman A. 2002. The mitochondrial-lysosomal axis theory of aging. *FEBS J.* 269, 1996-2002.

Buhrmann C, Kraehe P, Lueders C, Shayan P, Goel A, and Shakibaei M. 2014. Curcumin suppresses crosstalk between colon cancer stem cells and stromal fibroblasts in the tumor microenvironment: potential role of EMT. *PLoS One* 9, e107514.

Cabras P, Angioni A, Tuberoso C, Floris I, Reniero F, Guillou C, and Ghelli S. 1999. Homogentisic acid: a phenolic acid as a marker of strawberry-tree (*Arbutus unedo*) honey. *J. Agri. Food Chem.* 47, 4064-4067.

Cao H, Xu E, Liu H, Wan L, and Lai M. 2015. Epithelial–mesenchymal transition in colorectal cancer metastasis: A system review. *Pathol. Res. Pract.* 211, 557-569.

Cao SS, and Kaufman RJ. 2014. Endoplasmic reticulum stress and oxidative stress in cell fate decision and human disease. *Antioxid. Redox Signal.* 21, 396-413.

Carlberg I, and Mannervik B. 1985. Glutathione reductase. *Methods Enzymol.* 113, 484-490.

Carter DA, Blair SE, Cokcetin NN, Bouzo D, Brooks P, Schothauer R, and Harry EJ. 2016. Therapeutic manuka honey: no longer so alternative. *Front. Microbiol.* 7, 1-11.

Castro-Vázquez L, Díaz-Maroto MC, and Pérez-Coello MS. 2007. Aroma composition and new chemical markers of Spanish citrus honeys. *Food Chem.* 103, 601-606.

Chalkiadaki A, and Guarente L. 2015. The multifaceted functions of sirtuins in cancer. *Nat. Rev. Cancer* 15, 608.

Chan CW, Deadman BJ, Manley-Harris M, Wilkins AL, Alber DG, and Harry E. 2013. Analysis of the flavonoid component of bioactive New Zealand Manuka (Leptospermum scoparium) honey and the isolation, characterisation and synthesis of an unusual pyrrole. *Food Chem.* 141, 1772-1781.

Chaube B, Malvi P, Singh SV, Mohammad N, Viollet B, and Bhat MK. 2015. AMPK maintains energy homeostasis and survival in cancer cells via regulating p38/PGC-1α-mediated mitochondrial biogenesis. *Cell Death Dis.* 1, 1-11.

Chen RZ, Pettersson U, Beard C, Jackson-Grusby L, and Jaenisch R. 1998. DNA hypomethylation leads to elevated mutation rates. *Nature* 395, 89.

Chen X, Sun K, Jiao S, Cai N, Zhao X, Zou H, Xie Y, Wang Z, Zhong M, and Wei L. 2014. High levels of SIRT1 expression enhance tumorigenesis and associate with a poor prognosis of colorectal carcinoma patients. *Sci. Rep.* 4, 7481.

Chen Y-J, Lin K-N, Jhang L-M, Huang C-H, Lee Y-C, and Chang L-S. 2016. Gallic acid abolishes the EGFR/Src/Akt/Erk-mediated expression of matrix metalloproteinase-9 in MCF-7 breast cancer cells. *Chem Biol. Interact.* 252, 131-140.

Cheng Y-W, Pincas H, Bacolod MD, Schemmann G, Giardina SF, Huang J, Barral S, Idrees K, Khan SA, and Zeng Z. 2008. CpG island methylator phenotype associates with low-degree chromosomal abnormalities in colorectal cancer. *Clin. Cancer Res.* 14, 6005-6013.

Cherchi A, Spanedda L, Tuberoso C, and Cabras P. 1994. Solid-phase extraction and high-performance liquid chromatographic determination of organic acids in honey. *J. Chromatogr. A* 669, 59-64.

Chidambaram M, Manavalan R, and Kathiresan K. 2011. Nanotherapeutics to overcome conventional cancer chemotherapy limitations. *J. Pharm. Pharm. Sci.* 14, 67-77.

Chou T-C. 2006. Theoretical basis, experimental design, and computerized simulation of synergism and antagonism in drug combination studies. *Pharmacol. Rev.* 58, 621-681.

Ciulu M, Spano N, Pilo MI, and Sanna G. 2016. Recent Advances in the Analysis of Phenolic Compounds in Unifloral Honeys. *Molecules* 21, 451.

Clevers H. 2004. At the crossroads of inflammation and cancer. *Cell* 118, 671-674.

Cunningham D, Humblet Y, Siena S, Khayat D, Bleiberg H, Santoro A, Bets D, Mueser M, Harstrick A, and Verslype C. 2004. Cetuximab monotherapy and cetuximab plus irinotecan in irinotecan-refractory metastatic colorectal cancer. *N. Engl. J. Med.* 351, 337-345.

Custodio A, and Feliu J. 2013. Prognostic and predictive biomarkers for epidermal growth factor receptor-targeted therapy in colorectal cancer: beyond KRAS mutations. *Crit. Rev. Oncol. Hematol.* 85, 45-81.

da Silva PM, Gauche C, Gonzaga LV, Costa ACO, and Fett R. 2016. Honey: Chemical composition, stability and authenticity. *Food Chem.* 196, 309-323.

Davies M, Barraclough DL, Stewart C, Joyce KA, Eccles RM, Barraclough R, Rudland PS, and Sibson DR. 2008. Expression and splicing of the unfolded protein response gene XBP-1 are significantly associated with clinical outcome of endocrine-treated breast cancer. *Int. J. Cancer* 123, 85-88.

Deiana V, Tuberoso C, Satta A, Pinna C, Camarda I, Spano N, Ciulu M, and Floris I. 2015. Relationship between markers of botanical origin in nectar and honey of the strawberry tree (*Arbutus unedo*) throughout flowering periods in different years and in different geographical areas. *J. Apic. Res.* 54, 342-349.

Denise C, Paoli P, Calvani M, Taddei ML, Giannoni E, Kopetz S, Kazmi SMA, Pia MM, Pettazzoni P, and Sacco E. 2015. 5-Fluorouracil resistant colon cancer cells are addicted to OXPHOS to survive and enhance stem-like traits. *Oncotarget* 6, 41706.

Derry MM, Raina K, Agarwal C, and Agarwal R. 2013. Identifying molecular targets of lifestyle modifications in colon cancer prevention. *Front. Oncol.* 3, 1-20.

Dhillon AS, Hagan S, Rath O, and Kolch W. 2007. MAP kinase signalling pathways in cancer. *Oncogene* 26, 3279-3290.

Dimitrova B, Gevrenova R, and Anklam E. 2007. Analysis of phenolic acids in honeys of different floral origin by solid-pase extraction and high-performance liquid chromatography. *Phytochem. Anal.* 18, 24-32.

Doi E, Shibata D, and Matoba T. 1981. Modified colorimetric ninhydrin methods for peptidase assay. *Anal. Biochem.* 118, 173-184.

Dranka BP, Hill BG, and Darley-Usmar VM. 2010. Mitochondrial reserve capacity in endothelial cells: The impact of nitric oxide and reactive oxygen species. *Free Radic. Biol. Med.* 48, 905-914.

Dziedzic A, Kubina R, Kabała-Dzik A, Wojtyczka RD, Morawiec T, and Bułdak RJ. 2014. Caffeic acid reduces the viability and migration rate of oral carcinoma cells (SCC-25) exposed to low concentrations of ethanol. *Int. J. Mol. Sci.* 15, 18725-18741.

Elmore S. 2007. Apoptosis: a review of programmed cell death. *Toxicol. Pathol.* 35, 495-516.

Enayat S, Ceyhan MŞ, Taşkopara B, Stefek M, and Banerjee S. 2016. CHNQ, a novel 2-Chloro-1, 4-naphthoquinone derivative of quercetin, induces oxidative stress and autophagy both in vitro and in vivo. *Arch. Biochem. Biophys.* 596, 84-98.

Erejuwa OO, Sulaiman SA, and Wahab MSA. 2014. Effects of honey and its mechanisms of action on the development and progression of cancer. *Molecules* 19, 2497-2522.

Escuredo O, Dobre I, Fernández-González M, and Seijo MC. 2014. Contribution of botanical origin and sugar composition of honeys on the crystallization phenomenon. *Food Chem.* 149, 84-90.

Fan C, Chen J, Wang Y, Wong Y-S, Zhang Y, Zheng W, Cao W, and Chen T. 2013a. Selenocystine potentiates cancer cell apoptosis induced by 5-fluorouracil by triggering reactive oxygen species-mediated DNA damage and inactivation of the ERK pathway. *Free Radic. Biol. Med.* 65, 305-316.

Fan Y, Mao R, and Yang J. 2013b. NF-κB and STAT3 signaling pathways collaboratively link inflammation to cancer. *Protein & cell* 4, 176-185.

FAOSTAT. 2014. Production quantity of honey, natural for 2014: Livestock Primary from pick lists for Data/Regions/Elements/Production Quantity". United Nations, Food and Agriculture Organization, Statistics Division. Retrieved 24 May 2017. Internet: http://www.fao.org/faostat/en/#data/QL.

Fauzi AN, Norazmi MN, and Yaacob NS. 2011. Tualang honey induces apoptosis and disrupts the mitochondrial membrane potential of human breast and cervical cancer cell lines. *Food Chem. Toxicol.* 49, 871-878.

Fearon ER, and Vogelstein B. 1990. A genetic model for colorectal tumorigenesis. *Cell* 61, 759-767.

Ferlay J, Soerjomataram I, Dikshit R, Eser S, Mathers C, Rebelo M, Parkin DM, Forman D, and Bray F. 2015. Cancer incidence and mortality worldwide: sources, methods and major patterns in GLOBOCAN 2012. *Int. J. Cancer* 136, E359-E386.

Ferlay J, Soerjomataram I, Ervik M, Dikshit R, Eser S, Mathers C, Rebelo M, Parkin DM, Forman D, and Bray F. 2013. GLOBOCAN 2012 v1.0, Cancer incidence and mortality worldwide: IARC Cancer Base No. 11. Lyon, France: International agency for research on cancer. Available online: http://globocan.iarc.fr

Fernandez-Cabezudo MJ, El-Kharrag R, Torab F, Bashir G, George JA, El-Taji H, and Al-Ramadi BK. 2013. Intravenous administration of manuka honey inhibits tumor growth and improves host survival when used in combination with chemotherapy in a melanoma mouse model. *PLoS One* 8, e55993.

Ferreira ICFR, Aires E, Barreira JCM, and Estevinho LM. 2009. Antioxidant activity of Portuguese honey samples: Different contributions of the entire honey and phenolic extract. *Food Chem.* 114, 1438-1443.

Foran E, Garrity-Park MM, Mureau C, Newell J, Smyrk TC, Limburg PJ, and Egan LJ. 2010. Upregulation of DNA Methyltransferase–Mediated Gene Silencing, Anchorage-Independent Growth, and Migration of Colon Cancer Cells by Interleukin-6. *Mol. Cancer Res.* 8, 471-481.

Fraga MF, Ballestar E, Villar-Garea A, Boix-Chornet M, Espada J, Schotta G, Bonaldi T, Haydon C, Ropero S, and Petrie K. 2005. Loss of acetylation at Lys16 and trimethylation at Lys20 of histone H4 is a common hallmark of human cancer. *Nat. Genet.* 37, 391-400.

Fraser SP, Hemsley F, and Djamgoz MBA. 2016. Caffeic acid phenethyl ester: Inhibition of metastatic cell behaviours via voltage-gated sodium channel in human breast cancer in vitro. *Int. J. Biochem. Cell Biol.* 71, 111-118.

Fukuyama R, Ng KP, Cicek M, Kelleher C, Niculaita R, Casey G, and Sizemore N. 2007. Role of IKK and oscillatory NFκB kinetics in MMP-9 gene expression and chemoresistance to 5-fluorouracil in RKO colorectal cancer cells. *Mol. Carcinog.* 46, 402-413.

Gao A-M, Ke Z-P, Shi F, Sun G-C, and Chen H. 2013a. Chrysin enhances sensitivity of BEL-7402/ADM cells to doxorubicin by suppressing PI3K/Akt/Nrf2 and ERK/Nrf2 pathway. *Chem. Biol. Interact.* 206, 100-108.

Gao A-M, Ke Z-P, Wang J-N, Yang J-Y, Chen S-Y, and Chen H. 2013b. Apigenin sensitizes doxorubicin-resistant hepatocellular carcinoma BEL-7402/ADM cells to doxorubicin via inhibiting PI3K/Akt/Nrf2 pathway. *Carcinogenesis* 34, 1806-1814.

Gao Z, Guo B, Gao R, Zhu Q, and Qin H. 2015. Microbiota disbiosis is associated with colorectal cancer. *Front. Microbiol.* 6, 1-9.

Ghashm AA, Othman NH, Khattak MN, Ismail NM, and Saini R. 2010. Antiproliferative effect of Tualang honey on oral squamous cell carcinoma and osteosarcoma cell lines. *BMC Complement. Altern. Med.* 10, 49.

Goldberg JE, and L Schwertfeger K. 2010. Proinflammatory cytokines in breast cancer: mechanisms of action and potential targets for therapeutics. *Curr. Drug Targets* 11, 1133-1146.

Goldstein NS, and Armin M. 2001. Epidermal growth factor receptor immunohistochemical reactivity in patients with American Joint Committee on cancer stage IV colon adenocarcinoma. *Cancer* 92, 1331-1346.

Gonzalez-Donquiles C, Alonso-Molero J, Fernandez-Villa T, Vilorio-Marqués L, Molina AJ, and Martín V. 2017. The NRF2 transcription factor plays a dual role in colorectal cancer: A systematic review. *PloS One* 12, e0177549.

González-Sarrías A, Tomé-Carneiro J, Bellesia A, Tomás-Barberán FA, and Espín JC. 2015. The ellagic acid-derived gut microbiota metabolite, urolithin A, potentiates the anticancer effects of 5-fluorouracil chemotherapy on human colon cancer cells. *Food & function* 6, 1460-1469.

González-Vallinas M, González-Castejón M, Rodríguez-Casado A, and Ramírez de Molina A. 2013a. Dietary phytochemicals in cancer prevention and therapy: a complementary approach with promising perspectives. *Nutr. Rev.* 71, 585-599.

González-Vallinas M, Molina S, Vicente G, de la Cueva A, Vargas T, Santoyo S, García-Risco MR, Fornari T, Reglero G, and de Molina AR. 2013b. Antitumor effect of 5-fluorouracil is enhanced by rosemary extract in both drug sensitive and resistant colon cancer cells. *Pharmacol. Res.* 72, 61-68.

Grossi V, Peserico A, Tezil T, and Simone C. 2014. p38α MAPK pathway: A key factor in colorectal cancer therapy and chemoresistance. *World J. Gastroenterol.* 20, 9744.

Grune T, Merker K, Sandig G, and Davies KJA. 2003. Selective degradation of oxidatively modified protein substrates by the proteasome. *Biochem. Biophys. Res. Commun.* 305, 709-718.

Gunasekaran S, Venkatachalam K, and Namasivayam N. 2015. p-Methoxycinnamic acid, an active phenylpropanoid induces mitochondrial mediated apoptosis in HCT-116 human colon adenocarcinoma cell line. *Environ. Toxicol. Phamacol.* 40, 966-974.

Guo W, Wang N, and Feng Y. 2017. Recent Progress on the Molecular Mechanisms of Anti-invasive and Metastatic Chinese Medicines for Cancer Therapy. *In* "Unique Aspects of Anti-cancer Drug Development", pp. 115-135. InTech.

Gupta GP, and Massagué J. 2006. Cancer metastasis: building a framework. *Cell* 127, 679-695.

Gupta J, del Barco Barrantes I, Igea A, Sakellariou S, Pateras IS, Gorgoulis VG, and Nebreda AR. 2014. Dual function of p38α MAPK in colon cancer: suppression of colitis-associated tumor initiation but requirement for cancer cell survival. *Cancer Cell* 25, 484-500.

Habig WH, Pabst MJ, and Jakoby WB. 1974. Glutathione S-transferases the first enzymatic step in mercapturic acid formation. *J. Biol. Chem.* 249, 7130-7139.

Hakim L, Alias E, Makpol S, Ngah WZ, Morad NA, and Yusof YA. 2013. Gelam honey and ginger potentiate the anti cancer effect of 5-FU against HCT 116 colorectal cancer cells. *Asian Pac. J. Cancer Prev.* 15, 4651-4657.

Hamad R, Jayakumar C, Ranganathan P, Mohamed R, El-Hamamy MMI, Dessouki AA, Ibrahim A, and Ramesh G. 2015. Honey feeding protects kidney against cisplatin nephrotoxicity through suppression of inflammation. *Clin. Exp. Pharmacol. Physiol.* 42, 843-848.

Hampel H, Frankel WL, Martin E, Arnold M, Khanduja K, Kuebler P, Nakagawa H, Sotamaa K, Prior TW, and Westman J. 2005. Screening for the Lynch syndrome (hereditary nonpolyposis colorectal cancer). *N Engl J Med* 352, 1851-1860.

Hardie DG. 2011. AMP-activated protein kinase—an energy sensor that regulates all aspects of cell function. *Genes & development* 25, 1895-1908.

He B, Wei W, Liu J, Xu Y, and Zhao G. 2017. Synergistic anticancer effect of curcumin and chemotherapy regimen FP in human gastric cancer MGC-803 cells. *Oncol. Lett.* 14, 3387-3394.

Henderson T, Nigam PS, and Owusu-Apenten RK. 2015. A universally calibrated microplate ferric reducing antioxidant power (FRAP) assay for foods and applications to Manuka honey. *Food Chem.* 174, 119-123.

Herman JG, and Baylin SB. 2003. Gene silencing in cancer in association with promoter hypermethylation. *N Engl J Med* 349, 2042-2054.

Hermosín I, Chicón RM, and Cabezudo MD. 2003. Free amino acid composition and botanical origin of honey. *Food Chem.* 83, 263-268.

Hill BG, Benavides GA, Lancaster JR, Ballinger S, Dell'Italia L, Zhang J, and Darley-Usmar VM. 2012. Integration of cellular bioenergetics with mitochondrial quality control and autophagy. *Biol. Chem.* 393, 1485-1512.

Ho H-H, Chang C-S, Ho W-C, Liao S-Y, Wu C-H, and Wang C-J. 2010. Anti-metastasis effects of gallic acid on gastric cancer cells involves inhibition of NF-κB activity and downregulation of PI3K/AKT/small GTPase signals. *Food Chem. Toxicol.* 48, 2508-2516.

Huang XF, and Chen JZ. 2009. Obesity, the PI3K/Akt signal pathway and colon cancer. *Obes. Rev.* 10, 610-616.

Hussein SZ, Mohd Yusoff K, Makpol S, and Mohd Yusof YA. 2012. Gelam honey inhibits the production of proinflammatory, mediators NO, PGE2, TNF-α, and IL-6 in carrageenan-induced acute paw edema in rats. *Evid. Based Complement. Alternat. Med.* 2012, 1-13.

Hussein SZ, Yusoff KM, Makpol S, and Yusof YAM. 2013. Gelam honey attenuates carrageenan-induced rat paw inflammation via NF-κB pathway. *PloS one* 8, e72365.

Iglesias MT, de Lorenzo C, Polo MdC, Martín-Álvarez PJ, and Pueyo E. 2004. Usefulness of amino acid composition to discriminate between honeydew and floral honeys. Application to honeys from a small geographic area. *J. Agri. Food Chem.* 52, 84-89.

Islam A, Khalil I, Islam N, Moniruzzaman M, Mottalib A, Sulaiman SA, and Gan SH. 2012. Physicochemical and antioxidant properties of Bangladeshi honeys stored for more than one year. *BMC Complement. Alter. Med.* 12, 1.

Islam MS, Giampieri F, Janjusevic M, Gasparrini M, Forbes-Hernandez TY, Mazzoni L, Greco S, Giannubilo SR, Ciavattini A, and Mezzetti B. 2017. An anthocyanin rich strawberry extract induces apoptosis and ROS while decreases glycolysis and fibrosis in human uterine leiomyoma cells. *Oncotarget* 8, 23575.

Jackson-Thompson J, Ahmed F, German RR, Lai S-M, and Friedman C. 2006. Descriptive epidemiology of colorectal cancer in the United States, 1998–2001. *Cancer* 107, 1103-1111.

Jaganathan SK, Balaji A, Vignesh Vellayappan M, Kumar Asokan M, Priyadharshni Subramanian A, Aruna John A, Supriyanto E, Izwan Abd Razak S, and Marvibaigi

M. 2015. A review on antiproliferative and apoptotic activities of natural honey. *Anticancer Agents Med. Chem.* 15, 48-56.

Jaganathan SK, and Mandal M. 2009a. Antiproliferative effects of honey and of its polyphenols: a review. *BioMed Res. Int.* 2009, 1-13.

Jaganathan SK, and Mandal M. 2009b. Honey constituents and their apoptotic effect in colon cancer cells. *J. Apiprod. Apimed. Sci.* 1, 29-36.

Jaganathan SK, and Mandal M. 2010. Involvement of non-protein thiols, mitochondrial dysfunction, reactive oxygen species and p53 in honey-induced apoptosis. *Invest. New Drugs* 28, 624-633.

Jaganathan SK, Supriyanto E, and Mandal M. 2013. Events associated with apoptotic effect of p-coumaric acid in HCT-15 colon cancer cells. *World J. Gastroenterol.* 19, 7726-7734.

Jass JR, and Smith M. 1992. Sialic acid and epithelial differentiation in colorectal polyps and cancer–a morphological, mucin and lectin histochemical study. *Pathology* 24, 233-242.

Jenkinson F, and Steele RJC. 2010. Colorectal cancer screening–methodology. *Surgeon* 8, 164-171.

Jeon HK, Choi Su, and Jung NP. 2005. Association of the ERK1/2 and p38 kinase pathways with nitric oxide-induced apoptosis and cell cycle arrest in colon cancer cells. *Cell Biol. Toxicol.* 21, 115-125.

Jeon S-M. 2016. Regulation and function of AMPK in physiology and diseases. *Exp. Mol. Med.* 48, e245.

Jeon S-M, Chandel NS, and Hay N. 2012. AMPK regulates NADPH homeostasis to promote tumour cell survival during energy stress. *Nature* 485, 661.

Jin D, Fang Y, Li Z, Chen Z, and Xiang J. 2015. Epithelial-mesenchymal transition-associated microRNAs in colorectal cancer and drug-targeted therapies. *Oncol. Rep.* 33, 515-525.

Johnson JJ, and Mukhtar H. 2007. Curcumin for chemoprevention of colon cancer. *Cancer Lett.* 255, 170-181.

Jones AWE, Yao Z, Vicencio JM, Karkucinska-Wieckowska A, and Szabadkai G. 2012. PGC-1 family coactivators and cell fate: Roles in cancer, neurodegeneration, cardiovascular disease and retrograde mitochondria–nucleus signalling. *Mitochondrion* 12, 86-99.

Jubri Z, Narayanan NNN, Karim NA, and Ngah WZW. 2012. Antiproliferative activity and apoptosis induction by gelam honey on liver cancer cell line. *Int. J. Appl. Sci. Technol.* 2, 135-141.

Kakkar P, Das B, and Viswanathan PN. 1984. A modified spectrophotometric assay of superoxide dismutase.

Kamal MA, and Klein P. 2011. Determination of sugars in honey by liquid chromatography. *Saudi J. Biol. Sci.* 18, 17-21.

Kaneuchi M, Sasaki M, Tanaka Y, Sakuragi N, Fujimoto S, and Dahiya R. 2003. Quercetin regulates growth of Ishikawa cells through the suppression of EGF and cyclin D1. *Int. J. Oncol.* 22, 159-164.

Kang KA, Piao MJ, Kim KC, Kang HK, Chang WY, Park IC, Keum YS, Surh YJ, and Hyun JW. 2014. Epigenetic modification of Nrf2 in 5-fluorouracil-resistant colon cancer cells: involvement of TET-dependent DNA demethylation. *Cell Death Dis.* 5, e1183.

Kang KA, Piao MJ, Ryu YS, Kang HK, Chang WY, Keum YS, and Hyun JW. 2016. Interaction of DNA demethylase and histone methyltransferase upregulates Nrf2 in 5-fluorouracil-resistant colon cancer cells. *Oncotarget* 7, 40594.

Kao T-Y, Chung Y-C, Hou Y-C, Tsai Y-W, Chen C-H, Chang H-P, Chou J-L, and Hsu C-P. 2012. Effects of ellagic acid on chemosensitivity to 5-fluorouracil in colorectal carcinoma cells. *Anticancer Res.* 32, 4413-4418.

Kasala ER, Bodduluru LN, Madana RM, Gogoi R, and Barua CC. 2015. Chemopreventive and therapeutic potential of chrysin in cancer: mechanistic perspectives. *Toxicol. Lett.* 233, 214-225.

Kee J-Y, Han Y-H, Kim D-S, Mun J-G, Park J, Jeong M-Y, Um J-Y, and Hong S-H. 2016. Inhibitory effect of quercetin on colorectal lung metastasis through inducing apoptosis, and suppression of metastatic ability. *Phytomedicine* 23, 1680-1690.

Khalil MI, Moniruzzaman M, BoukraÃ¢ Ld, Benhanifia M, Islam MA, Islam MN, Sulaiman SA, and Gan SH. 2012. Physicochemical and antioxidant properties of Algerian honey. *Molecules* 17, 11199-11215.

Khalil ML, and Sulaiman SA. 2010. The potential role of honey and its polyphenols in preventing heart disease: a review. *Afr. J. Tradit. Complement. Alternat. Med.* 7, 315-321.

Khan I, Paul S, Jakhar R, Bhardwaj M, Han J, and Kang SC. 2016. Novel quercetin derivative TEF induces ER stress and mitochondria-mediated apoptosis in human colon cancer HCT-116 cells. *Biomed. Pharmacother.* 84, 789-799.

Khan MS, Devaraj H, and Devaraj N. 2011. Chrysin abrogates early hepatocarcinogenesis and induces apoptosis in N-nitrosodiethylamine-induced preneoplastic nodules in rats. *Toxicolo. Appl. Pharmacol.* 251, 85-94.

Kim H-S, Hwang J-T, Yun H, Chi S-G, Lee S-J, Kang I, Yoon K-S, Choe W-J, Kim S-S, and Ha J. 2008a. Inhibition of AMP-activated protein kinase sensitizes cancer cells to cisplatin-induced apoptosis via hyper-induction of p53. *J. Biol. Chem.* 283, 3731-3742.

Kim H-S, Wannatung T, Lee S, Yang WK, Chung SH, Lim J-S, Choe W, Kang I, Kim S-S, and Ha J. 2012. Quercetin enhances hypoxia-mediated apoptosis via direct inhibition of AMPK activity in HCT116 colon cancer. *Apoptosis* 17, 938-949.

Kim I, Xu W, and Reed JC. 2008b. Cell death and endoplasmic reticulum stress: disease relevance and therapeutic opportunities. *Nat. Rev. Drug Discov.* 7, 1013.

Kishore RK, Halim AS, Syazana MSN, and Sirajudeen KNS. 2011. Tualang honey has higher phenolic content and greater radical scavenging activity compared with other honey sources. *Nutr. Res.* 31, 322-325.

Klampfer L. 2011. Cytokines, inflammation and colon cancer. *Curr. Cancer Drug Targets* 11, 451-464.

Kojima M, Morisaki T, Sasaki N, Nakano K, Mibu R, Tanaka M, and Katano M. 2004. Increased nuclear factor-kB activation in human colorectal carcinoma and its correlation with tumor progression. *Anticancer Res.* 24, 675-682.

Kong L, Wang X, Zhang K, Yuan W, Yang Q, Fan J, Wang P, and Liu Q. 2015. Gypenosides synergistically enhances the anti-tumor effect of 5-fluorouracil on colorectal cancer in vitro and in vivo: a role for oxidative stress-mediated DNA damage and p53 activation. *PLoS One* 10, e0137888.

Kryczka J, Stasiak M, Dziki L, Mik M, Dziki A, and Cierniewski C. 2012. Matrix metalloproteinase-2 cleavage of the β1 integrin ectodomain facilitates colon cancer cell motility. *J. Biol. Chem.* 287, 36556-36566.

Kuipers EJ, Grady WM, Lieberman D, Seufferlein T, Sung JJ, Boelens PG, van de Velde CJH, and Watanabe T. 2015. Colorectal cancer. *Nat. Rev. Dis. Primers.* 1, 1-25.

Laplante M, and Sabatini DM. 2012. mTOR signaling in growth control and disease. *Cell* 149, 274-293.

LeBleu VS, O'Connell JT, Herrera KNG, Wikman-Kocher H, Pantel K, Haigis MC, De Carvalho FM, Damascena A, Chinen LTD, and Rocha RM. 2014. PGC-1α mediates mitochondrial biogenesis and oxidative phosphorylation to promote metastasis. *Nat. Cell Biol.* 16, 992.

Lee HS, Cho HJ, Yu R, Lee KW, Chun HS, and Park JHY. 2014. Mechanisms underlying apoptosis-inducing effects of Kaempferol in HT-29 human colon cancer cells. *Int. J. Mol. Sci.* 15, 2722-2737.

Lee KW, Bode AM, and Dong Z. 2011. Molecular targets of phytochemicals for cancer prevention. *Nat. Rev. Cancer* 11, 211.

Lengauer C, Kinzler KW, and Vogelstein B. 1998. Genetic instabilities in human cancers. *Nature* 396, 643.

Levine R. 1990. "Determination of carbonyl content in oxidatively modified proteins/Levine RL, Garland D., Oliver CN, Amici A., Climent I., Lenz A.-G., Ahn B.-W., Shaltiel S., Stadtman ER. Methods in Enzymolology–1990–186–P:465–478.."

Li N, Huang D, Lu N, and Luo L. 2015. Role of the LKB1/AMPK pathway in tumor invasion and metastasis of cancer cells. *Oncol. Rep.* 34, 2821-2826.

Li N, Sun C, Zhou B, Xing H, Ma D, Chen G, and Weng D. 2014. Low concentration of quercetin antagonizes the cytotoxic effects of anti-neoplastic drugs in ovarian cancer. *PLoS One* 9, e100314.

Li SKH, and Martin A. 2016. Mismatch repair and colon cancer: mechanisms and therapies explored. *Trends Mol. Med.* 22, 274-289.

Liang C-C, Park AY, and Guan J-L. 2007. In vitro scratch assay: a convenient and inexpensive method for analysis of cell migration in vitro. *Nat. Protoc.* 2, 329-333.

Liao C-L, Lai K-C, Huang A-C, Yang J-S, Lin J-J, Wu S-H, Wood WG, Lin J-G, and Chung J-G. 2012. Gallic acid inhibits migration and invasion in human osteosarcoma U-2 OS cells through suppressing the matrix metalloproteinase-2/-9, protein kinase B (PKB) and PKC signaling pathways. *Food Chem. Toxicol.* 50, 1734-1740.

Liao JC, Lee KT, You BJ, Lee CL, Chang WT, Wu YC, and Lee H-Z. 2015. Raf/ERK/Nrf2 signaling pathway and MMP-7 expression involvement in the trigonelline-mediated inhibition of hepatocarcinoma cell migration. *Food Nutr. Res.* 59, 29884.

Liu Y, Bi T, Dai W, Wang G, Qian L, Gao Q, and Shen G. 2016. Oxymatrine synergistically enhances the inhibitory effect of 5-fluorouracil on hepatocellular carcinoma in vitro and in vivo. *Tumor Biol.* 37, 7589-7597.

Liu Y, Lang T, Jin B, Chen F, Zhang Y, Beuerman RW, Zhou L, and Zhang Z. 2017. Luteolin inhibits colorectal cancer cell epithelial-to-mesenchymal transition by suppressing CREB1 expression revealed by comparative proteomics study. *J. Proteomics* 161, 1-10.

Lou C, Zhang F, Yang M, Zhao J, Zeng W, Fang X, Zhang Y, Zhang C, and Liang W. 2012. Naringenin decreases invasiveness and metastasis by inhibiting TGF-β-induced epithelial to mesenchymal transition in pancreatic cancer cells. *PloS One* 7, e50956.

Ma W, Feng S, Yao X, Yuan Z, Liu L, and Xie Y. 2015. Nobiletin enhances the efficacy of chemotherapeutic agents in ABCB1 overexpression cancer cells. *Sci. Rep.* 5, 18789.

Manach C, Scalbert A, Morand C, Rémésy C, and Jiménez, Liliana. 2004. Polyphenols: food sources and bioavailability. *Am. J. Clin. Nutr.* 79, 727-747.

Manach C, Williamson G, Morand C, Scalbert A, and Rémésy C. 2005. Bioavailability and bioefficacy of polyphenols in humans. I. Review of 97 bioavailability studies. *Am. J. Clin. Nutr.* 81, 230S-242S.

Mantovani A. 2009. Cancer: inflaming metastasis. *Nature* 457, 36-37.

Manzanares AB, García ZH, Galdón BR, Rodríguez ER, and Romero CD. 2014 Physicochemical characteristics of minor monofloral honeys from Tenerife, Spain. *LWT Food Sci. Nutr.* 55, 572-578.

Mariotto AB, Robin Yabroff K, Shao Y, Feuer EJ, and Brown ML. 2011. Projections of the cost of cancer care in the United States: 2010–2020. *J. Natl. Cancer Inst.* 103, 117-128.

Mármol I, Sánchez-de-Diego C, Pradilla Dieste A, Cerrada E, and Rodriguez Yoldi MJ. 2017. Colorectal carcinoma: a general overview and future perspectives in colorectal cancer. *Int. J. Mol. Sci.* 18, 197.

Marnett LJ. 1999. Lipid peroxidation—DNA damage by malondialdehyde. *Mutat. Res.* 424, 83-95.

Marshall SM, Schneider KR, Cisneros KV, and Gu L. 2014. Determination of antioxidant capacities, α-dicarbonyls, and phenolic phytochemicals in florida varietal honeys using HPLCDAD-ESI-MSn. *J. Agri. Food Chem.* 62, 8623-8631.

Mavric E, Wittmann S, Barth G, and Henle T. 2008. Identification and quantification of methylglyoxal as the dominant antibacterial constituent of Manuka (*Leptospermum scoparium*) honeys from New Zealand. *Mol. Nutr. Food Res.* 52, 483-489.

Meda A, Lamien CE, Romito M, Millogo J, and Nacoulma OG. 2005. Determination of the total phenolic, flavonoid and proline contents in Burkina Fasan honey, as well as their radical scavenging activity. *Food Chem.* 91, 571-577.

Mena S, Ortega A, and Estrela JM. 2009. Oxidative stress in environmental-induced carcinogenesis. *Mutat. Res. Genet. Toxicol. Environ. Mutagen.* 674, 36-44.

Mendel J. 2004. Evidenced based medicine. Benefits, limitations and issues for complementary and alternative medicine. *Aust. J. Holist. Nurs.* 11, 21-29.

Mendelsohn J, and Baselga J. 2000. The EGF receptor family as targets for cancer therapy. *Oncogene* 19, 6550.

Menegon S, Columbano A, and Giordano S. 2016. The dual roles of NRF2 in cancer. *Trends Mol. Med.* 22, 578-593.

Meng G, Wang W, Chai K, Yang S, Li F, and Jiang K. 2015. Combination treatment with triptolide and hydroxycamptothecin synergistically enhances apoptosis in A549 lung adenocarcinoma cells through PP2A-regulated ERK, p38 MAPKs and Akt signaling pathways. *Int. J. Oncol.* 46, 1007-1017.

Meyerhardt JA, Catalano PJ, Haller DG, Mayer RJ, Macdonald JS, Benson Iii AB, and Fuchs CS. 2003. Impact of diabetes mellitus on outcomes in patients with colon cancer. *J. Clin. Oncol.* 21, 433-440.

Miguel MG, Antunes MD, and Faleiro ML. 2017. Honey as a Complementary Medicine. *Integrative medicine insights* 12, doi: 10.1177/1178633717702869.

Mihaylova MM, and Shaw RJ. 2011. The AMP-activated protein kinase (AMPK) signaling pathway coordinates cell growth, autophagy, & metabolism. *Nat. Cell Biol.* 13, 1016.

Miyaki M, Konishi M, Kikuchi-Yanoshita R, Enomoto M, Igari T, Tanaka K, Muraoka M, Takahashi H, Amada Y, and Fukayama M. 1994. Characteristics of somatic mutation of the adenomatous polyposis coli gene in colorectal tumors. *Cancer Res.* 54, 3011-3020.

Mohamed M, Sirajudeen KNS, Swamy M, Yaacob M, and Sulaiman S. 2010. Studies on the antioxidant properties of Tualang honey of Malaysia. *Afr. J. Tradit. Complement. Altern. Med.* 7, 59-63.

Mohapatra P, Preet R, Choudhuri M, Choudhuri T, and Kundu CN. 2011. 5-fluorouracil increases the chemopreventive potentials of resveratrol through DNA damage and MAPK signaling pathway in human colorectal cancer cells. *Oncol. Res.* 19, 311-321.

Moniruzzaman M, Sulaiman SA, Khalil MI, and Gan SH. 2013. Evaluation of physicochemical and antioxidant properties of sourwood and other Malaysian honeys: a comparison with manuka honey. *Chem. Cent. J.* 7, 1.

Mook ORF, Frederiks WM, and Van Noorden CJF. 2004. The role of gelatinases in colorectal cancer progression and metastasis. *Biochim. Biophys. Acta* 1705, 69-89.

Moskwa J, Borawska MH, Markiewicz-Zukowska R, Puscion-Jakubik A, Naliwajko SK, Socha K, and Soroczynska J. 2014. Polish natural bee honeys are anti-proliferative and anti-metastatic agents in human *Glioblastoma multiforme* U87MG cell line. *PloS one* 9, e90533.

Mu C, Jia P, Yan Z, Liu X, Li X, and Liu H. 2007. Quercetin induces cell cycle G1 arrest through elevating Cdk inhibitors p2l and p27 in human hepatoma cell line (HepG2). *Methods Find. Exp. Clin. Pharmacol.* 29, 179-184.

Munkholm P. 2003. The incidence and prevalence of colorectal cancer in inflammatory bowel disease. *Aliment. Pharmacol. Ther.* 18, 1-5.

Murakami T, Kawada K, Iwamoto M, Akagami M, Hida K, Nakanishi Y, Kanda K, Kawada M, Seno H, and Taketo MM. 2013. The role of CXCR3 and CXCR4 in colorectal cancer metastasis. *Int. J. Cancer* 132, 276-287.

Nabeshima K, Inoue T, Shimao Y, and Sameshima T. 2002. Matrix metalloproteinases in tumor invasion: role for cell migration. *Pathol. Int.* 52, 255-264.

Nagaraju GP, Alese OB, Landry J, Diaz R, and El-Rayes BF. 2014. HSP90 inhibition downregulates thymidylate synthase and sensitizes colorectal cancer cell lines to the effect of 5FU-based chemotherapy. *Oncotarget* 5, 9980.

Najdi R, Holcombe RF, and Waterman ML. 2011. Wnt signaling and colon carcinogenesis: beyond APC. *J. Carcinog.* 10.

Nogueira V, and Hay N. 2013. Molecular pathways: reactive oxygen species homeostasis in cancer cells and implications for cancer therapy. *Clin. Cancer Res.* 19, 4309-4314.

Núñez-Sánchez MA, González-Sarrías A, Romo-Vaquero M, García-Villalba R, Selma MV, Tomás-Barberán FA, García-Conesa M-T, and Espín JC. 2015. Dietary phenolics against colorectal cancer—From promising preclinical results to poor

translation into clinical trials: Pitfalls and future needs. *Mol. Nutr. Food Res.* 59, 1274-1291.

Nutakul W, Sobers HS, Qiu P, Dong P, Decker EA, McClements DJ, and Xiao H. 2011. Inhibitory effects of resveratrol and pterostilbene on human colon cancer cells: a side-by-side comparison. *J. Agri. Food Chem.* 59, 10964-10970.

Ogino S, Nosho K, Kirkner GJ, Kawasaki T, Meyerhardt JA, Loda M, Giovannucci EL, and Fuchs CS. 2009. CpG island methylator phenotype, microsatellite instability, BRAF mutation and clinical outcome in colon cancer. *Gut* 58, 90-96.

Ogunwobi OO, and Beales ILP. 2007. The anti-apoptotic and growth stimulatory actions of leptin in human colon cancer cells involves activation of JNK mitogen activated protein kinase, JAK2 and PI3 kinase/Akt. *Int. J. Colorectal Dis.* 22, 401-409.

Ohkawa H, Ohishi N, and Yagi K. 1979. Assay for lipid peroxides in animal tissues by thiobarbituric acid reaction. *Anal. Biochem.* 95, 351-358.

Ohta T, Takahashi M, and Ochiai A. 2006. Increased protein expression of both inducible nitric oxide synthase and cyclooxygenase-2 in human colon cancers. *Cancer Lett.* 239, 246-253.

Okugawa Y, Grady WM, and Goel A. 2015. Epigenetic alterations in colorectal cancer: emerging biomarkers. *Gastroenterology* 149, 1204-1225. e12.

Okuma E, Saeki K, Shimura M, Ishizaka Y, Yasugi E, and Yuo A. 2000. Induction of apoptosis in human hematopoietic U937 cells by granulocyte-macrophage colony-stimulating factor: possible existence of caspase 3-like pathway. *Leukemia* 14, 612.

Pandurangan AK, Mohebali N, Esa NM, Looi CY, Ismail S, and Saadatdoust Z. 2015. Gallic acid suppresses inflammation in dextran sodium sulfate-induced colitis in mice: possible mechanisms. *Int. Immunopharmacol.* 28, 1034-1043.

Pasupuleti VR, Sammugam L, Ramesh N, and Gan SH. 2017. Honey, propolis, and royal jelly: a comprehensive review of their biological actions and health benefits. *Oxid. Med. Cell. Longev.* 2017.

Patel BB, Gupta D, Elliott AA, Sengupta V, Yu Y, and Majumdar APN. 2010. Curcumin targets FOLFOX-surviving colon cancer cells via inhibition of EGFRs and IGF-1R. *Anticancer Res.* 30, 319-325.

Petretto GL, Cossu M, and Alamanni MC. 2015. Phenolic content, antioxidant and physico-chemical properties of Sardinian monofloral honeys. *Int. J. Food Sci. Technol.* 50, 482-491.

Phang C-W, Karsani SA, Sethi G, and Malek SNA. 2016. Flavokawain C inhibits cell cycle and promotes apoptosis, associated with endoplasmic reticulum stress and regulation of MAPKs and Akt signaling pathways in HCT 116 human colon carcinoma cells. *PloS One* 11, e0148775.

Pichichero E, Cicconi R, Mattei M, Muzi MG, and Canini A. 2010. Acacia honey and chrysin reduce proliferation of melanoma cells through alterations in cell cycle progression. *Int. J. Oncol.* 37, 973-981.

Pino MS, and Chung DC. 2010. The chromosomal instability pathway in colon cancer. *Gastroenterology* 138, 2059-2072.

Porcza LM, Simms C, and Chopra M. 2016. Honey and cancer: current status and future directions. *Diseases* 4, 30.

Poynter JN, Siegmund KD, Weisenberger DJ, Long TI, Thibodeau SN, and Lindor N. 2008. Colon Cancer Family Registry Investigators. Molecular characterization of MSI-H colorectal cancer by MLHI promoter methylation, immunohistochemistry, and mismatch repair germline mutation screening. *Cancer Epidemiol. Biomarkers Prev.* 17, 3208-15.

Priyadarsini RV, Murugan RS, Maitreyi S, Ramalingam K, Karunagaran D, and Nagini S. 2010. The flavonoid quercetin induces cell cycle arrest and mitochondria-mediated apoptosis in human cervical cancer (HeLa) cells through p53 induction and NF-κB inhibition. *Eur. J. Pharmacol.* 649, 84-91.

Ramamoorthi G, and Sivalingam N. 2014. Molecular mechanism of TGF-β signaling pathway in colon carcinogenesis and status of curcumin as chemopreventive strategy. *Tumor Biol.* 35, 7295-7305.

Re R, Pellegrini N, Proteggente A, Pannala A, Yang M, and Rice-Evans C. 1999. Antioxidant activity applying an improved ABTS radical cation decolorization assay. *Free Radic. Biol. Med.* 26, 1231-1237.

Rodrigues NR, Rowan A, Smith ME, Kerr IB, Bodmer WF, Gannon JV, and Lane DP. 1990. p53 mutations in colorectal cancer. *Proc. Natl. Acad. Sci. U.S.A.* 87, 7555-7559.

Rosa A, Tuberoso CIG, Atzeri A, Melis MP, Bifulco E, and Dessì MA. 2011. Antioxidant profile of strawberry tree honey and its marker homogentisic acid in several models of oxidative stress. *Food Chem.* 129, 1045-1053.

Rosivatz E, Becker I, Bamba M, Schott C, Diebold J, Mayr D, Höfler H, and Becker K-F. 2004. Neoexpression of N-cadherin in E-cadherin positive colon cancers. *Int. J. Cancer* 111, 711-719.

Ryu MJ, and Chung HS. 2015. [10]-Gingerol induces mitochondrial apoptosis through activation of MAPK pathway in HCT116 human colon cancer cells. *In Vitro Cell. Dev. Biol. Anim.* 51, 92-101.

Ryu S, Lim W, Bazer FW, and Song G. 2017. Chrysin induces death of prostate cancer cells by inducing ROS and ER stress. *J. Cell. Physiol.* 232, 3786–3797.

Safi SZ, Batumalaie K, Qvist R, Mohd Yusof K, and Ismail IS. 2016. Gelam honey attenuates the oxidative stress-induced inflammatory pathways in pancreatic hamster cells. *Evid. Based Complement. Alternat. Med.* 2016, 1-13.

Sah JF, Balasubramanian S, Eckert RL, and Rorke EA. 2004. Epigallocatechin-3-gallate inhibits epidermal growth factor receptor signaling pathway evidence for direct inhibition of ERK1/2 and AKT kinases. *J. Biol. Chem.* 279, 12755-12762.

Said AH, Raufman J-P, and Xie G. 2014. The role of matrix metalloproteinases in colorectal cancer. *Cancers* 6, 366-375.

Sakamoto K, Maeda S, Hikiba Y, Nakagawa H, Hayakawa Y, Shibata W, Yanai A, Ogura K, and Omata M. 2009. Constitutive NF-κB activation in colorectal carcinoma plays a key role in angiogenesis, promoting tumor growth. *Clin. Cancer Res.* 15, 2248-2258.

Saletti P, Molinari F, De Dosso S, and Frattini M. 2015. EGFR signaling in colorectal cancer: a clinical perspective. *Gastrointest Cancer* 5, 21-38.

Samowitz WS, Albertsen H, Herrick J, Levin TR, Sweeney C, Murtaugh MA, Wolff RK, and Slattery ML. 2005. Evaluation of a large, population-based sample supports a CpG island methylator phenotype in colon cancer. *Gastroenterology* 129, 837-845.

Sano R, and Reed JC. 2013. ER stress-induced cell death mechanisms. *Biochim. Biophys. Acta* 1833, 3460-3470.

Santandreu FM, Valle A, Oliver J, and Roca P. 2011. Resveratrol potentiates the cytotoxic oxidative stress induced by chemotherapy in human colon cancer cells. *Cell. Physiol. Biochem.* 28, 219-228.

Santos BL, Oliveira MN, Coelho PLC, Pitanga BPS, da Silva AB, Adelita T, Silva VDgA, de Fd Costa M, El-Bachá RS, and Tardy M. 2015. Flavonoids suppress human glioblastoma cell growth by inhibiting cell metabolism, migration, and by

regulating extracellular matrix proteins and metalloproteinases expression. *Chem. Biol. Interact.* 242, 123-138.

Saxena S, Gautam S, and Sharma A. 2010. Physical, biochemical and antioxidant properties of some Indian honeys. *Food Chem.* 118, 391-397.

Scandlyn MJ, Stuart EC, Somers-Edgar TJ, Menzies AR, and Rosengren RJ. 2008. A new role for tamoxifen in oestrogen receptor-negative breast cancer when it is combined with epigallocatechin gallate. *Br. J. Cancer* 99, 1056.

Scanu R, Spano N, Panzanelli A, Pilo MI, Piu PC, Sanna G, and Tapparo A. 2005. Direct chromatographic methods for the rapid determination of homogentisic acid in strawberry tree (Arbutus unedo L.) honey. *J. Chromatogr. A* 1090, 76-80.

Schetter AJ, Okayama H, and Harris CC. 2012. The role of microRNAs in colorectal cancer. *Cancer J.* 18, 244.

Schmoll HJ, Van Cutsem E, Stein A, Valentini V, Glimelius B, Haustermans K, Nordlinger B, Van de Velde CJ, Balmana J, and Regula J. 2012. ESMO Consensus Guidelines for management of patients with colon and rectal cancer. a personalized approach to clinical decision making. *Ann. Oncol.* 23, 2479-2516.

Schramm DD, Karim M, Schrader HR, Holt RR, Cardetti M, and Keen CL. 2003. Honey with high levels of antioxidants can provide protection to healthy human subjects. *J. Agri. Food Chem.* 51, 1732-1735.

Schroeter EH, Kisslinger JA, and Kopan R. 1998. Notch-1 signalling requires ligand-induced proteolytic release of intracellular domain. *Nature* 393, 382.

Shadkam MN, Mozaffari-Khosravi H, and Mozayan MR. 2010. A comparison of the effect of honey, dextromethorphan, and diphenhydramine on nightly cough and sleep quality in children and their parents. *J. Alter. Complement. Med.* 16, 787-793.

Shakibaei M, Kraehe P, Popper B, Shayan P, Goel A, and Buhrmann C. 2015. Curcumin potentiates antitumor activity of 5-fluorouracil in a 3D alginate tumor microenvironment of colorectal cancer. *BMC Cancer* 15, 250.

Shakibaei M, Mobasheri A, Lueders C, Busch F, Shayan P, and Goel A. 2013. Curcumin enhances the effect of chemotherapy against colorectal cancer cells by inhibition of NF-κB and Src protein kinase signaling pathways. *PloS One* 8, e57218.

Shen L, Toyota M, Kondo Y, Lin E, Zhang L, Guo Y, Hernandez NS, Chen X, Ahmed S, and Konishi K. 2007. Integrated genetic and epigenetic analysis identifies three different subclasses of colon cancer. *Proc. Natl. Acad. Sci. U.S.A.* 104, 18654-18659.

Shen Y, Yang J, Li J, Shi X, Ouyang L, Tian Y, and Lu J. 2014. Carnosine inhibits the proliferation of human gastric cancer SGC-7901 cells through both of the mitochondrial respiration and glycolysis pathways. *PLoS One* 9, e104632.

Sherr CJ. 1994. G1 phase progression: cycling on cue. *Cell* 79, 551-555.

Siegel R, DeSantis C, Virgo K, Stein K, Mariotto A, Smith T, Cooper D, Gansler T, Lerro C, and Fedewa S. 2012. Cancer treatment and survivorship statistics, 2012. *CA Cancer J. Clin.* 62, 220-241.

Siegel RL, Miller KD, Fedewa SA, Ahnen DJ, Meester RGS, Barzi A, and Jemal A. 2017a. Colorectal cancer statistics, 2017. *CA Cancer J. Clin.* 67, 177-193.

Siegel RL, Miller KD, and Jemal A. 2016. Cancer statistics, 2016. *CA Cancer J. Clin.* 66, 7-30.

Siegel RL, Miller KD, and Jemal. A. 2017b. Cancer statistics, 2017. *CA Cancer J. Clin.* 67, 7-30.

Sies H, Koch OR, Martino E, and Boveris A. 1979. Increased biliary glutathione disulfide release in chronically ethanol-treated rats. *FEBS Lett.* 103, 287-290.

Simon K. 2016. Colorectal cancer development and advances in screening. *Clin. Interv. Aging* 11, 967.

Sinicrope FA, Rego RL, Halling KC, Foster N, Sargent DJ, La Plant B, French AJ, Laurie JA, Goldberg RM, and Thibodeau SN. 2006. Prognostic impact of microsatellite instability and DNA ploidy in human colon carcinoma patients. *Gastroenterology* 131, 729-737.

Sivagami G, Vinothkumar R, Preethy CP, Riyasdeen A, Akbarsha MA, Menon VP, and Nalini N. 2012. Role of hesperetin (a natural flavonoid) and its analogue on apoptosis in HT-29 human colon adenocarcinoma cell line–A comparative study. *Food Chem. Toxicol.* 50, 660-671.

Slattery ML, Lundgreen A, Kadlubar SA, Bondurant KL, and Wolff RK. 2013. JAK/STAT/SOCS-signaling pathway and colon and rectal cancer. *Mol. Carcinog.* 52, 155-166.

Soldatkin OO, Peshkova VM, Saiapina OY, Kucherenko IS, Dudchenko OY, Melnyk VG, Vasylenko OD, Semenycheva LM, Soldatkin AP, and Dzyadevych SV. 2013. Development of conductometric biosensor array for simultaneous determination of maltose, lactose, sucrose and glucose. *Talanta* 115, 200-207.

Song M, Garrett WS, and Chan AT. 2015. Nutrients, foods, and colorectal cancer prevention. *Gastroenterology* 148, 1244-1260. e16.

Song W, Dang Q, Xu D, Chen Y, Zhu G, Wu K, Zeng J, Long Q, Wang X, and He D. 2014. Kaempferol induces cell cycle arrest and apoptosis in renal cell carcinoma through EGFR/p38 signaling. *Oncol. Rep.* 31, 1350-1356.

Spano N, Casula L, Panzanelli A, Pilo MI, Piu PC, Scanu R, Tapparo A, and Sanna G. 2006. An RP-HPLC determination of 5-hydroxymethylfurfural in honey: the case of strawberry tree honey. *Talanta* 68, 1390-1395.

Spano N, Ciulu M, Floris I, Panzanelli A, Pilo MI, Piu PC, Salis S, and Sanna G. 2009a. A direct RP-HPLC method for the determination of furanic aldehydes and acids in honey. *Talanta* 78, 310-314.

Spano N, Piras I, Ciulu M, Floris I, Panzanelli A, Pilo MI, Piu PC, and Sanna G. 2009b. Reversed-phase liquid chromatographic profile of free amino acids in strawberry-tree (Arbutus unedo L.) honey. *J. AOAC Int.* 92, S1145-S1156.

Stoffel EM, and Kastrinos F. 2014. Familial colorectal cancer, beyond Lynch syndrome. *Clin. Gastroenterol. Hepatol.* 12, 1059-1068.

Subramanian AP, John AA, Vellayappan MV, Balaji A, Jaganathan SK, Mandal M, and Supriyanto E. 2016. Honey and its phytochemicals: Plausible agents in combating colon cancer through its diversified actions. *J. Food Biochem.* 40, 613-629.

Suganuma M, Kurusu M, Suzuki K, Tasaki E, and Fujiki H. 2006. Green tea polyphenol stimulates cancer preventive effects of celecoxib in human lung cancer cells by upregulation of GADD153 gene. *Int. J. Cancer* 119, 33-40.

Suman S, Das TP, Ankem MK, and Damodaran C. 2014. Targeting Notch signaling in colorectal cancer. *Curr. Colorectal Cancer Rep.* 10, 411-416.

Sun C, Tan H, Zhang Y, and Zhang H. 2016. Phenolics and abscisic acid identified in acacia honey comparing different SPE cartridges coupled with HPLC-PDA. *Food Comp. Anal. Biochem.* 53, 91-101.

Swellam T, Miyanaga N, Onozawa M, Hattori K, Kawai K, Shimazui T, and Akaza H. 2003. Antineoplastic activity of honey in an experimental bladder cancer implantation model: *in vivo* and *in vitro* studies. *Int. J. Urol.* 10, 213-219.

Tahir AA, Sani NFA, Murad NA, Makpol S, Ngah WZW, and Yusof YAM. 2015. Combined ginger extract & Gelam honey modulate Ras/ERK and PI3K/AKT pathway genes in colon cancer HT29 cells. *Nutr. J.* 14, 1-10.

Tamagawa H, Oshima T, Shiozawa M, Morinaga S, Nakamura Y, Yoshihara M, Sakuma Y, Kameda Y, Akaike M, and Masuda M. 2012. The global histone modification

pattern correlates with overall survival in metachronous liver metastasis of colorectal cancer. *Oncol. Rep.* 27, 637-642.

Terzić J, Grivennikov S, Karin E, and Karin M. 2010. Inflammation and colon cancer. *Gastroenterology* 138, 2101-2114. e5.

Thiery JP, and Sleeman JP. 2006. Complex networks orchestrate epithelial–mesenchymal transitions. *Nat. Rev. Mol. Cell Biol.* 7, 131-142.

Toyota M, Ahuja N, Ohe-Toyota M, Herman JG, Baylin SB, and Issa J-PJ. 1999. CpG island methylator phenotype in colorectal cancer. *Proc. Natl. Acad. Sci. U.S.A.* 96, 8681-8686.

Toyota M, Ohe-Toyota M, Ahuja N, and Issa J-PJ. 2000. Distinct genetic profiles in colorectal tumors with or without the CpG island methylator phenotype. *Proc. Natl. Acad. Sci. U.S.A.* 97, 710-715.

Truzzi C, Annibaldi A, Illuminati S, Finale C, and Scarponi G. 2014. Determination of proline in honey: Comparison between official methods, optimization and validation of the analytical methodology. *Food Chem.* 150, 477-481.

Tuberoso CIG, Bifulco E, Caboni P, Cottiglia F, Cabras P, and Floris I. 2009. Floral markers of strawberry tree (*Arbutus unedo* L.) honey. *J. Agri. Food Chem.* 58, 384-389.

Tuberoso CIG, Boban M, Bifulco E, Budimir D, and Pirisi FM. 2013. Antioxidant capacity and vasodilatory properties of Mediterranean food: the case of Cannonau wine, myrtle berries liqueur and strawberry-tree honey. *Food Chem.* 140, 686-691.

Ullman TA, and Itzkowitz SH. 2011. Intestinal inflammation and cancer. *Gastroenterology* 140, 1807-1816. e1.

Ulloa PA, Maia M, and Brigas AF. 2015. Physicochemical Parameters and Bioactive Compounds of Strawberry Tree (*Arbutus unedo* L.) Honey. *J. Chem.* 2015, 1-10.

Umesalma S, Nagendraprabhu P, and Sudhandiran G. 2015. Ellagic acid inhibits proliferation and induced apoptosis via the Akt signaling pathway in HCT-15 colon adenocarcinoma cells. *Mol. Cell. Biochem.* 399, 303-313.

Urosevic J, Nebreda AR, and Gomis RR. 2014. MAPK signaling control of colon cancer metastasis. *Cell Cycle* 13, 2641-2642.

USDA. 2015a. Agricultural Research Service, Nutrient Data Laboratory. USDA National Nutrient Database for Standard Reference, Release 28. Version Current: September 2015. Internet: http://www.ars.usda.gov/nea/bhnrc/ndl. 2015.

USDA. 2015b. Full Report (All Nutrients): 19296, Honey. National Nutrient Database, Agricultural Research Service, Release 28. 2015. Retrieved 30 October 2015. Internet: https://ndb.nal.usda.gov/ndb/foods/show/6287.

Valko M, Rhodes C, Moncol J, Izakovic MM, and Mazur M. 2006. Free radicals, metals and antioxidants in oxidative stress-induced cancer. *Chem. Biol. Interact.* 160, 1-40.

Van Cutsem E, Cervantes A, Nordlinger B, and Arnold D. 2014. Metastatic colorectal cancer: ESMO Clinical Practice Guidelines for diagnosis, treatment and follow-up. *Ann. Oncol.* 25, iii1-iii9.

Vandamme L, Heyneman A, Hoeksema H, Verbelen J, and Monstrey S. 2013. Honey in modern wound care: a systematic review. *Burns* 39, 1514-1525.

Vellinga TT, Borovski T, de Boer VCJ, Fatrai S, van Schelven S, Trumpi K, Verheem A, Snoeren N, Emmink BL, and Koster J. 2015. SIRT1/PGC1α dependent increase in oxidative phosphorylation supports chemotherapy resistance of colon cancer. *Clin. Cancer Res.* 21, 2870-2879.

Viuda-Martos M, Ruiz-Navajas Y, Fernández-López J, and Pérez-Álvarez JA. 2008. Functional properties of honey, propolis, and royal jelly. *J. Food Sci.* 73, 117-124.

Vogelstein B, Fearon ER, Hamilton SR, Kern SE, Preisinger AC, Leppert M, Smits AMM, and Bos JL. 1988. Genetic alterations during colorectal-tumor development. *N. Engl. J. Med.* 319, 525-532.

Vucenik I, and Stains JP. 2012. Obesity and cancer risk: evidence, mechanisms, and recommendations. *Ann. N. Y. Acad. Sci.* 1271, 37-43.

Waghela BN, Sharma A, Dhumale S, Pandey SM, and Pathak C. 2015. Curcumin conjugated with PLGA potentiates sustainability, anti-proliferative activity and apoptosis in human colon carcinoma cells. *PloS One* 10, e0117526.

Wagner EF, and Nebreda ÃnR. 2009. Signal integration by JNK and p38 MAPK pathways in cancer development. *Nat. Rev. Cancer* 9, 537-549.

Wang S-W, and Sun Y-M. 2014. The IL-6/JAK/STAT3 pathway: potential therapeutic strategies in treating colorectal cancer. *Int. J. Oncol.* 44, 1032-1040.

Wang X-H, Andrae L, and Engeseth NJ. 2002. Antimutagenic effect of various honeys and sugars against Trp-p-1. *J. Agri. Food Chem.* 50, 6923-6928.

Wee LH, Morad NA, Aan GJ, Makpol S, Ngah WZW, and Yusof YAM. 2015. Mechanism of chemoprevention against colon cancer cells using combined Gelam honey and

Ginger extract via mTOR and Wnt/β-catenin pathways. *Asian Pac. J. Cancer Prev.* 16, 6549-6556.

Weisenberger DJ, Siegmund KD, Campan M, Young J, Long TI, Faasse MA, Kang GH, Widschwendter M, Weener D, and Buchanan D. 2006. CpG island methylator phenotype underlies sporadic microsatellite instability and is tightly associated with BRAF mutation in colorectal cancer. *Nat. Genet.* 38, 787.

Wen CTP, Hussein SZ, Abdullah S, Karim NA, Makpol S, and Yusof YAM. 2012. Gelam and Nenas honeys inhibit proliferation of HT 29 colon cancer cells by inducing DNA damage and apoptosis while suppressing inflammation. *Asian Pac. J. Cancer Prev.* 13, 1605-1610.

Weston RJ, Mitchell KR, and Allen KL. 1999. Antibacterial phenolic components of New Zealand manuka honey. *Food Chem.* 64, 295-301.

Williams GH, and Stoeber K. 2012. The cell cycle and cancer. *J. Pathol.* 226, 352-364.

Winzer BM, Whiteman DC, Reeves MM, and Paratz JD. 2011. Physical activity and cancer prevention: a systematic review of clinical trials. *Cancer Causes Control* 22, 811-826.

Won S-R, Lee D-C, Ko SH, Kim J-W, and Rhee H-I. 2008. Honey major protein characterization and its application to adulteration detection. *Food Res. Int.* 41, 952-956.

Wu J, Omene C, Karkoszka J, Bosland M, Eckard J, Klein CB, and Frenkel K. 2011. Caffeic acid phenethyl ester (CAPE), derived from a honeybee product propolis, exhibits a diversity of anti-tumor effects in pre-clinical models of human breast cancer. *Cancer Lett.* 308, 43-53.

Wu M, Neilson A, Swift AL, Moran R, Tamagnine J, Parslow D, Armistead S, Lemire K, Orrell J, and Teich J. 2007. Multiparameter metabolic analysis reveals a close link between attenuated mitochondrial bioenergetic function and enhanced glycolysis dependency in human tumor cells. *Am. J. Physiol., Cell Physiol.* 292, C125-C136.

Xavier CPR, Lima CF, Rohde M, and Pereira-Wilson C. 2011. Quercetin enhances 5-fluorouracil-induced apoptosis in MSI colorectal cancer cells through p53 modulation. *Cancer Chemother. Pharmacol.* 68, 1449-1457.

Xia Y, Lian S, Khoi PN, Yoon HJ, Joo YE, Chay KO, Kim KK, and Do Jung Y. 2015. Chrysin inhibits tumor promoter-induced MMP-9 expression by blocking AP-1 via suppression of ERK and JNK pathways in gastric cancer cells. *PloS One* 10, e0124007.

Xu D, Jin J, Yu H, Zhao Z, Ma D, Zhang C, and Jiang H. 2017. Chrysin inhibited tumor glycolysis and induced apoptosis in hepatocellular carcinoma by targeting hexokinase-2. *J. Exp. Clin. Cancer Res.* 36, 44.

Yaacob NS, Nengsih A, and Norazmi MN. 2013. Tualang honey promotes apoptotic cell death induced by tamoxifen in breast cancer cell lines. *Evid. Based Complement. Alternat. Med.* 2013, 1-9.

Yadav RK, Chae S-W, Kim H-R, and Chae HJ. 2014. Endoplasmic reticulum stress and cancer. *J. Cancer Prev.* 19, 75.

Yang B, Huang J, Xiang T, Yin X, Luo X, Huang J, Luo F, Li H, Li H, and Ren G. 2014. Chrysin inhibits metastatic potential of human triple-negative breast cancer cells by modulating matrix metalloproteinase-10, epithelial to mesenchymal transition, and PI3K/Akt signaling pathway. *J. Appl. Toxicol.* 34, 105-112.

Zhang L, Zhou F, and ten Dijke P. 2013a. Signaling interplay between transforming growth factor-β receptor and PI3K/AKT pathways in cancer. *Trends Biochem. Sci.* 38, 612-620.

Zhang Q, Zhao X-H, and Wang Z-J. 2008. Flavones and flavonols exert cytotoxic effects on a human oesophageal adenocarcinoma cell line (OE33) by causing G2/M arrest and inducing apoptosis. *Food Chem. Toxicol.* 46, 2042-2053.

Zhang R, Chung Y, Kim HS, Kim DH, Kim HS, Chang WY, and Hyun JW. 2013b. 20-O-(β-D-glucopyranosyl)-20 (S)-protopanaxadiol induces apoptosis via induction of endoplasmic reticulum stress in human colon cancer cells. *Oncol. Rep.* 29, 1365-1370.

Zhang W, and Liu HT. 2002. MAPK signal pathways in the regulation of cell proliferation in mammalian cells. *Cell Res.* 12, 9.

Zhao X-Q, Zhang Y-F, Xia Y-F, Zhou Z-M, and Cao Y-Q. 2015. Promoter demethylation of nuclear factor-erythroid 2-related factor 2 gene in drug-resistant colon cancer cells. *Oncol. Lett.* 10, 1287-1292.

Zhao Y, Butler EB, and Tan M. 2013. Targeting cellular metabolism to improve cancer therapeutics. *Cell Death Dis.* 4, e532.

Zhou Y, Tozzi F, Chen J, Fan F, Xia L, Wang J, Gao G, Zhang A, Xia X, and Brasher H. 2012. Intracellular ATP levels are a pivotal determinant of chemoresistance in colon cancer cells. *Cancer Res.* 72, 304-314.

ACKNOWLEDGMENTS

Firstly, all of my praises be to Allah alone, the creator, the supreme authority of the universe for bestowing me the good health, strength and perseverance needed to accomplish this piece of work.

I would like to express my sincere acknowledgement and deepest appreciation to my tutor, Prof. Maurizio Battino for his supervision and tremendous support over the past three years of my PhD. The most needed, he provided me unflinching encouragement in various ways and providing me with an excellent atmosphere for doing research. He sacrifices many of his precious hours and extensive preoccupation with professional and academic responsibilities. Special thanks to him again, without his cordial help I could not complete this work or become a research scientist I wanted to be.

I would also like to give special thanks to Dr. Francesca Giampieri for her constant guidance, encouragement, discussions and suggestions in day-to-day life in the lab. Also she helped me in many ways outside of the lab that made my way of life smooth in Ancona. I truly respect and admire her for her modesty, diligence and her enthusiasm for science. I have learned a lot from her in all these years especially the importance of hard work and commitment to be a successful scientist.

Special thanks to Dr. Tamara Y. Forbes-Hernandez for her continuing guidance, generous technical support and suggestions in the course of all matters pertaining to laboratory experiment and studies of this work. I always felt peace when she told me “Don’t worry” throughout this study.

I would also like to acknowledge Dr. Massimiliano Gasparrini since it was a great privilege for me to get his suggestions/advice to carry out my research work. In particular, he ordered all the laboratory accessories in time for making my experiments very smooth.

I am particularly grateful to Dr. Patricia Reboredo-Rodriguez for having done the HPLC analysis for me. I would always remember you for your care and sensibility for me.

I am very thankful to Danila Cianciosi (PhD student) who as a good friends, were always willing to help and give her best accompany. It would have been a lonely lab without you.

I am sincerely grateful to Prof. Gavino Sanna and Dr Nadia Spano who provided us the Strawberry tree honey samples from different area of Sardinia, Italy.

I would like to express my gratitude to dear friend, Dr Md Soriful Islam and Dr. Most Mauluda Akhtar, with whom I shared pleasantly, most of my free-time, for their sweetness and amazing friendship.

I would like to thank the most amazing person in my life, my husband. His love, patience, support, understanding and faith in me have been my greatest source of motivation. Last but most importantly, I want to thank from core of my heart to my parents, sister and brother as well as my father and mother in law, for their endless love, well-wishes and support that always stimulate me to do something best.

Ancona, November 27, 2017